HETEROCYCLIC SCHIFF BASES OF AMINOPHENOLS AND THEIR TRANSITION METAL COMPLEXES: A VERSATILE PHARMACOPHORE

Thesis submitted to
Cochin University of Science and Technology
in partial fulfillment of the requirements for the degree of

Doctor of Philosophy

in

Chemistry

under the Faculty of Science

By

Shanty A. A.

DEPARTMENT OF APPLIED CHEMISTRY
COCHIN UNIVERSITY OF SCIENCE AND TECHNOLOGY
KOCHI – 682 022

July 2017

Heterocyclic Schiff Bases of Aminophenols and Their Transition Metal Complexes: A Versatile Pharmacophore

Ph.D. Thesis under the Faculty of Science

Author

Shanty A.A
Research Scholar
Department of Applied Chemistry
Cochin University of Science and Technology
Kochi 682022
Kerala, India
Email id: shanty.sheen@gmail.com

Supervising Guide

Dr. P.V. Mohanan
Asst. Professor
Department of Applied Chemistry
Cochin University of Science and Technology
Kochi 682022
Kerala, India
Email id: pvmohanan@gmail.com

Department of Applied Chemistry
Cochin University of Science and Technology
Kochi 682022
Kerala, India

July 2017

"God himself will provide you with everything you need, according to his riches, and show you his generosity in Christ Jesus."

(Holy Bible- Philippians 4/19)

Dedicated to my beloved Jesus Christ

Department of Applied Chemistry
Cochin University of Science and Technology
Kochi – 682 022

Dr. P.V. Mohanan
Asst. Professor

Certificate

This is to certify that the thesis entitled ***"Heterocyclic Schiff bases of aminophenols and their transition metal complexes: A Versatile Pharmacophore"*** *is an authentic record of research work carried out by* ***Mrs. Shanty A.A.*** *under my supervision in partial fulfillment of the requirements for the degree of Doctor of Philosophy in Chemistry under the Faculty of Science of Cochin University of Science and Technology and further that no part thereof has been presented before for any other degree. All the relevant corrections and modifications suggested by the audience and recommended by the doctoral committee of the candidate during the presynopsis seminar have been incorporated in the thesis.*

.

Kochi
Date: 27/07/2017

Dr. P.V. Mohanan
Asst. Professor
Department of Applied Chemistry
Cochin University of Science and Technology
Kochi-682 022

Declaration

I hereby declare that the thesis entitled ***"Heterocyclic Schiff bases of aminophenols and their transition metal complexes: A Versatile Pharmacophore"*** *submitted for the award of Ph.D. Degree, is the result of investigations carried out by me at Department of Applied Chemistry, Cochin University of Science and Technology under the guidance of* ***Dr. P .V. Mohanan****, Asst. Professor and further that it has not previously formed the basis for the award of any other degree.*

Kochi-22
Date: 27/07/2017

Shanty A. A.

Acknowledgement

"When you want something,
all the
Universe ***conspires*** *in helping you to achieve it"*

Paulo Coelho (The Alchemist)

First and above all, praises and thanks to God, the Almighty, for showers of blessings throughout my life and for providing me this opportunity and granting me the capability to proceed successfully. Thank God for blessing me much more than I deserve.

This thesis appears in its current form due to the assistance and guidance of several people. I would therefore like to offer my sincere thanks to all of them.

I would like to express my deep and sincere gratitude to my research supervisor, Dr P.V. Mohanan for his excellent guidance, care, patience, and providing me freedom with an excellent atmosphere for doing research. Under his guidance I could successfully overcome many difficulties and I learned a lot. He has inspired me to become an independent researcher and helped me to realize the power of critical reasoning. Thank you dear Sir, for the constructive comments during the writing of the manuscripts and thesis.

I would like to express my deep gratitude and heartfelt thanks to Prof. K. Girish Kumar, Head, Department of Applied Chemistry for providing the necessary advice, facilities and opportunity for carrying out my research. He is also my doctoral committee member and M.phil project guide. He is a true role model teacher who makes learning an enlightening experience. Thanks to Girish sir, for considering me as his own student even after my M.Phil. course.

I am very thankful to Dr. K. Sreekumar, former H.O.D, Dept. of Chemistry for his valuable suggestions and clearing many of my doubts regarding my research work.

I express my sincere thanks to Prof. M. R. Prathapachandra Kurup, former H.O.D, Dept. of Chemistry for helping me to refine crystal structure and also for his guidance, support and concern.

I am also truly grateful to Dr. N. Manoj, former H.O.D, Dept. of Chemistry, Prof. S. Sugunan, Prof. K. K. Mohammed Yusuff, Dr. S. Prathapan, Dr. P. A. Unnikrishnan and Dr. P. M. Sabura Begum for their immense help during the various stages of my research. I am very much thankful to all non teaching staff for all help and support.

Most of the results described in this thesis would not have been obtained without a close collaboration with few Institutions. I am extremely indebted to Dr. K. G. Raghu, CSIR-NIIST, Trivandrum; Dr. Rajkamal Tripathi, Central Drug Research Institute, Lucknow, Dr. Sarita G. Bhat, Department of biotechnology and Robert Philip, senior technical officer, CSIR-NIIST, Trivandrum for providing necessary infrastructure and resources to accomplish my research work. My warm appreciation to Preethi (Niist, TVM), Tina and Bindhya (Department of biotechnology) for helping me during my work.

I am happy to acknowledge the services of SAIF at STIC, CUSAT; CDRI, Lucknow; and IIT, Mumbai for the help in sample analyses. I thank Shyam, Indu photos, who provided all the technical support and helped me to bring out the thesis in its final form.

I wish to extend my gratitude to Dr. S. Balachandran, M. G. College, Trivandrum for his thoughtful and detailed comments.

I thank my lab mates with whom I spend most of my time and was very helpful in doing my works and preparing my thesis. Their friendship and talks made the lab an interesting place to work. Once again I am grateful to all my lab mates, especially to Dr. Priya, Dr. Navya, Jessica, Bindu, Sneha, Maria, Divya, Geetha and Savitha. A special thanks to Bindu for being with me in all seminars and other activities.

A special thanks to analytical labmates where I can enter like going to my own home and all of them considered me as one among them. I gratefully recall happy memories of my M.phil lab mates, Dr. Theresa, Dr. Divya, Dr. Anuja, Sreejith, Soumya and Zafna, They helped me right when I needed help most. Special words of thanks to Jesny chechi who was always available for clearing my doubts and was really motivating. A special mention to Shalini, who never said no to me for the helps I asked her even in her busy schedule. I appreciate Shalini for her help and suggestion in the entire thesis.

I am grateful to Ambili and Mridula who became my good friends and helped in correcting my thesis. I also thank Sneha, Ammu and Anjaly for thesis correction.

I am thankful to polymer lab mates, our neighbors, whose help and friendship has added colors to these years. I thank Sherly miss, Jisha, Dr. Jibi … the list is endless…thanks to one and all. I would also like to thank all my physical, inorganic and organic lab friends for their love and affection.

I am extremely grateful to my Appachan and Ammachi for their love, prayers, care and sacrifices in educating and preparing me for my future. My father and mother in laws deserve big thanks for they left their home to stay with us and took care of our children. They were a part of our daily lives when we were going through the most difficult situation. Their help was invaluable. My sincere thanks to my brother, sister, brother in laws, sister in laws and their children for their prayers and moral support at times of tension, tiredness. I consider myself the luckiest to have such a lovely and caring family, standing beside me with their love and unconditional support.

I thank to a very special person, my husband, Sheen Mathew for his continued and unfailing love, support and understanding during my pursuit of Ph. D. degree. He was always around at times I thought that it was impossible to continue, he helped me to keep things in perspective. I greatly value his contribution and deeply appreciate his belief in me. All the good that comes from this book I look

forward to sharing with him! He is my Buddy and my Hero! I Love him Always & Forever. There are lots of things that he has done for me. I cannot count all these but I can simply explain them in two words THANK YOU for everything.

I also dedicate this Ph.D. thesis to my two lovely children, Angelo and Joann who are the pride and joy of my life. I love you more than anything and I appreciate all your patience and support during mamma's Ph.D. studies.

Finally, my thanks go to all the people who have supported me to complete the research work directly or indirectly.

Shanty

Preface

Medicinal inorganic chemistry is a rapidly developing field with enormous potential applications and offers new possibilities to the pharmaceutical industry. Metal-based complexes seem to be the one of the best therapeutic approaches to treat and diagnose the diseases. The use of transition metal complexes as therapeutic compounds has become more and more pronounced. Development of transition metal complexes as drugs is not an easy task; considerable effort is required to get a compound of interest. Beside all these limitations and side effects, transition metal complexes are still the most widely used chemotherapeutic agents. Copper exhibits considerable biochemical action either as an essential trace metal or as a constituent of various exogenously administered compounds in humans. Current interest in copper, zinc, and nickel complexes is stemming from their potential use as antimicrobial, antiviral, anti-inflammatory, antitumor agents, enzyme inhibitors or chemical nucleases. In addition, the study and development of these complexes could be helpful in the design and production of antiviral and antibacterial materials, able to deactivate HIV and H1N1 viruses.

The thesis entitled **"Heterocyclic Schiff bases of aminophenols and their transition metal complexes: A Versatile Pharmacophore"** is divided into ten chapters.

Chapter 1 outlines an introduction to Schiff bases and their transition metal complexes. It also provides a brief review of various biological application of Schiff bases and their metal complexes and highlights biological studies like antioxidant, enzyme activity and DNA binding.

Chapter 2 discusses synthesis and characterizations of Schiff bases and gives a brief sketch of the materials used for the synthesis. The

physicochemical methods used for the studies are also mentioned in this chapter.

Chapter 3 describes synthesis and characterizations of Ni(II), Cu(II) and Zn(II) complexes of synthesized Schiff bases.

Chapter 4 deals with antioxidant activity, solvent effect, structure activity relationship and mechanism of action of heterocyclic Schiff bases.

Chapter 5 describes DNA binding properties of Schiff bases and its metal complexes. Techniques such as UV-Vis spectroscopy, Cyclic Voltammetry (CV) and Circular Dichroism (CD) were used to probe the mode of binding of complexes to DNA.

Chapter 6 gives a brief introduction about Human Immunodeficiency Virus Type-1(HIV-1). HIV-RT inhibitory activity studies of synthesized Schiff bases and their Ni (II), Cu (II) and Zn (II) complexes are also discussed in this chapter.

Chapter 7 discusses antibacterial activity of Schiff bases and its metal complexes. The antibacterial activity of synthesized Schiff bases as well as their metal complexes was tested by using disc diffusion method. Minimum inhibitory concentration (MIC) was also evaluated.

Chapter 8 deals with α-amylase activity studies of heterocyclic Schiff bases and their Ni(II), Cu(II) and Zn(II) Complexes

Chapter 9 discusses the cytotoxicity of Schiff bases and their metal complexes .Cytotoxicty has been evaluated by MTT assay against normal 3T3L1 cells.

Chapter 10 gives the summary and conclusion of the work presented in the thesis. Future outlook of the work are also presented.

Contents

Chapter 1

BIOLOGICAL IMPORTANCE OF SCHIFF BASES AND THEIR TRANSITION METAL COMPLEXES

Contents

In coordination chemistry, one of the most fascinating areas is the interaction of metal ions with biological molecules. All metals will form coordination compounds. The structure of metal complexes consists of a central metal atom, bonded to a surrounding array of molecules or anions [1]. The role of coordination compounds in nature is very important. Most of the metal ions are essential to maintain human homeostasis and also play crucial roles in many biological processes by acting as cofactors in the proteins function thereby resulting in the stabilization, regulation and completion courses of cellular functions [2-5]. Chlorophyll, hemoglobin and vitamin B_{12} are some examples for such metal complexes. Inorganic medicinal chemistry and metal-based complexes seem to be one of the best therapeutic approaches to treat and diagnose the diseases [6-8]. On reviewing the literature, it is confirmed that metal complex exhibits greater biological property than that of free organic compounds [9-11]. Medici *et al.* reviewed historical development and amazing broad uses of metals, and the importance of their complexes in the medical area [12].

Compared to purely organic molecules, metal complexes have several advantages as a result of their varied reactivity pattern, structural diversity, and unique photo and electrochemical properties. To exploit these advantages, it is crucial to select good performing chelators with coordinating properties suitable for the proper stabilization of a given metal core [13-15]. Inorganic compounds mainly transition metals have played an important role in the development of new metal based drugs [16]. Transition metals exhibit various coordination geometry, oxidation states, spectral and magnetic properties and they can interact with large number of negatively charged molecules. This property of transition metals led to the recent development of drugs which are based on metals and are regarded to be potential candidates for pharmacological and therapeutic applications [17-20].

1.1 Schiff bases

Schiff bases are versatile ligands having imine or azomethine (–C=N–) functional group. They were first described by Hugo Schiff, German Chemist in1864 and hence they are named so [21]. Schiff bases are the backbone of large number of organic compounds and have enormous applications in many fields including analytical, biological, and inorganic chemistry [22]. Schiff bases are well known for their wide range of applications and are useful intermediates in organic synthesis [23]. These compounds have intrinsic biological activities including anticancer [24-26], anti-inflammatory [27-28], antitubercular [29-30], antioxidant [31-32], antibacterial [33-35], analgesic [36-37], antifungal and antifertility [38], herbicidal [39-40], anticonvulsant [41], anthelmintic [42] and antiproliferative [43]. Moreover, Schiff bases also exhibit fluorescence [44], photoluminescence [45], a potentiometric cation caring [46] and aggregation [47] properties.

1.1.1 Structure and properties of Schiff base

The functional group of Schiff base contain a carbon-nitrogen double bond with nitrogen atom connected to an alkyl, aryl, cyclo alkyl or heterocyclic groups which may be variously substituted, other than with hydrogen [48]. Scheme 1 shows the general formula of azomethine group which is the most common structural feature of Schiff bases.

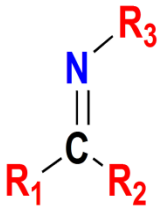

Scheme 1. General formula of Schiff base having azomethine linkage (R is an organic side chain)

Schiff bases are weak bases and are easily hydrolysed by dilute mineral acids, but not by aqueous alkali. They also form insoluble salts with strong acids through coordination of the electrons on nitrogen atom of azomethine group [49]. Most of the Schiff bases are stable in alkaline solutions. Aromatic aldehydes especially with an effective conjugation system, form stable Schiff bases, where as those from aliphatic aldehydes are found to be less stable. Aliphatic Schiff bases have a tendency to polymerize and are difficult to isolate [50]. Aldehydes can form Schiff base ligands more readily than ketones. This is because the reaction centres of aldehydes are sterically less hindered than ketones and the additional carbon of ketone contributes more electron density to the azomethine carbon making them less electrophilic compared to aldehydes [51].

The classical synthesis of Schiff bases reported by Schiff involves the condensation of primary amines and active carbonyl groups under azeotropic distillation [52]. The water thus formed in the system is removed using molecular sieves [53]. In the 1990s, an in *situ* method was developed for water elimination. Dehydrating solvents such as tetramethyl orthosilicate or trimethyl orthoformate were used for this purpose [54-55]. In 2004, Chakraborti *et al.* reported that the efficiency of these methods is dependent on the use of highly electrophilic carbonyl compounds and strongly nucleophilic amines. They also reported the use of substances that function as Lewis acids or Bronsted-Lowry to activate the carbonyl group of aldehydes (or ketones) catalyze the nucleophilic attack by amines, and dehydrate the system, eliminating water as the final step [56]. In the past thirteen years, a number of innovations and new techniques have been reported including solvent-free/clay/microwave irradiation [57-60]. Scheme 2 shows the general method for synthesis of Schiff bases.

Scheme 2: Synthesis of Schiff base

Mechanistically, two steps are involved in the formation of Schiff base (Scheme 3). In the first step, the azomethine nitrogen acts as a nucleophile, attacking the electrophilic carbonyl carbon of aldehydes or ketones. In the second step the nitrogen is deprotonated, and the electrons from this N-H bond push the oxygen off the carbon, leaving a compound with a C=N bond (an imine) and a water molecule is displaced [61-63].

Scheme 3: Mechanism of Schiff base (imine) formation

Several studies revealed that the chemical and biological importance of Schiff base is due to the presence of a lone pair of electrons in sp^2 hybridized orbital of nitrogen atom of the azomethine group. Ease of preparation, synthetic flexibility and the special characteristic property of C=N group makes Schiff base an excellent chelating agent [64]. The Schiff bases with functional group like (–OH), (–SH), ($–NO_2$) are considered as useful chelating agents. Schiff bases are insoluble in water and some of them are readily hydrolyzed back to amine and aldehyde [65]. Schiff bases can act as bidentate, tridentate, tetradentate or polydentate ligands (Figure 1.1) [66-68].

Figure 1.1 Examples for bidendate and tridendate Schiff base ligands.

Schiff base macrocycles formed by the self condensation reaction of appropriate formyl- or keto- and primary amine precursors (Figure 1.2) have many applications in the field of macrocycles and supramolecular chemistry [69].

Figure 1.2 Example for Schiff base macrocycle.

1.2 Importance of heterocyclic Schiff's base transition metal complexes

Schiff bases derived from heterocyclic scaffolds mainly sulfur, nitrogen and oxygen atom have great significance in many areas like biological, clinical, medicinal, analytical and pharmacological field [70]. Schiff base transition metal complexes obtained from heterocyclic molecules have been known to possess a wide range of biological and pharmacological activities. In recent years, they have received significant interest from many researchers in the area of drug research and development owing to their broad bioactivities such as antibacterial, antifungal, anti-inflammatory, anticonvulsant, antiviral and anticancer activities [71]. Heterocyclic Schiff-base metal complexes are

considered to be among the most important stereochemical models in main group and transition metal coordination chemistry due to their ease of preparation and structural variety [72].

Schiff base ligands are able to coordinate many metals and to stabilize them in different oxidation states. Multidentate Schiff bases ligands have been widely used, as they can form highly stable coordination compounds on coordination with metal ions [73]. Schiff base transition metal complexes exhibit well-defined coordination geometries and are attractive moieties for reversible recognition of nucleic acids research. Besides these, they often show distinct photophysical or electrochemical properties, thereby increasing the functionality of the binding agent. These properties of Schiff base transition metal complexes stimulated large interest for their noteworthy contributions to single molecule-based magnetism, material science [74], catalysis of many reactions like hydroformylation, carbonylation, reduction, oxidation, epoxidation [75] and their industrial applications [76] in the past two decades. Recently metal complexes with stable d^{10} electronic configuration have received a lot of attention in the field of bioinorganic and environmental chemistry [77].

The treatment of Schiff base ligands with metal salts gives metal complexes of Schiff base under suitable experimental conditions. Cozzi reported different synthetic routes (Figure1.3) for the preparation of metal complexes [78]. In route 1, metal complexes are prepared by refluxing Schiff bases with the corresponding metal acetate. Route 2 employs synthesis of metal alkoxides ($M(OR)_n$). The transition metal (M = Ti, Zr) bearing alkoxides can be easily handled and is commercially available. It is

difficult to use other alkoxide derivatives, especially in the case of highly moisture sensitive lanthanide derivatives. Metal alkyl Schiff base complexes are synthesized through route 3. The route 4 represents a schematic outline for the preparation of salen-type metal complexes. It is a two-step reaction based on deprotonation of the Schiff bases and then upon reaction with halides of metal. For deprotonation in coordinating solvents, sodium hydride NaH or potassium hydride KH is used and excess of hydrides can be eliminated by filtration. Deprotonation is a rapid step and refluxing of hot reaction mixture does not cause any decomposition. Metal amides $M(NMe_2)_4$ (M = Ti, Zr) are also employed as precursors for the synthesis of Schiff base metal complexes (Route 5).

Figure 1.3 Different synthetic routes for the preparation of metal complexes.

1.2.1 Applications of Schiff base and their transition metal complexes

Schiff bases are used as starting material in the synthesis of industrial and biological compounds such as lactams, used in the construction of poly vinyl chloride powder (PVC) based membrane selective sensors and also as ionophore in metal ion-selective electrodes [79--81]. Schiff bases contain phenyl or substituted phenyl group are sometimes called azo dyes. Many Schiff base transition metal complexes from this kind have been synthesized with metals such as, aluminum(III), iron(III), cobalt(II), nickel(II) and copper(II) complexes [82]. Schiff bases have been used in the preparation of a number of industrial and biologically active compounds like formazans, 4-thiazolidinines, benzoxazines, *via* ring closure, cyclo addition, and replacement reactions [83]. Schiff bases are very important compounds because of their wide spectrum of biological activities. Some examples for bioactive Schiff bases are shown in Figure1.4 [84].

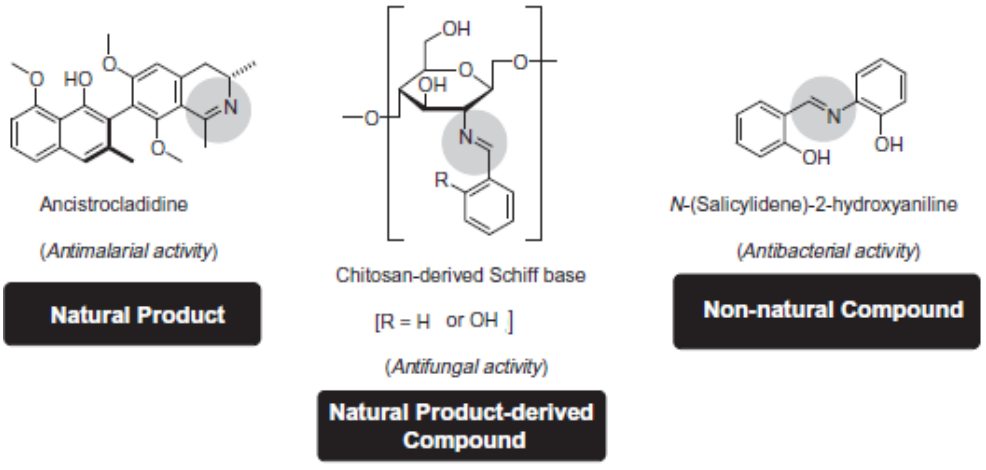

Figure 1.4 Examples of bioactive Schiff bases [Ref.84]

Many transition metal Schiff base complexes exhibit high catalytic activity and play a significant role in various reactions so to enhance their yield and product selectivity. The convenient route of preparation and thermal stability of Schiff base ligands have contributed significantly as metal complexes for their possible applications in catalysis [85].

The catalytic activity of metal complexes has been reported in various reactions as given below [86-90].

- Polymerization reaction
- Reduction of thionyl chloride
- Oxidation of organic compounds
- Reduction reaction of ketones
- Aldol reaction
- Epoxidation of alkenes
- Henry reaction

1.3 Biological activities of Schiff bases and their metal complexes

Schiff bases are important compounds in medicinal and pharmaceutical fields because of their wide spectrum of biological activities. The activity of these compounds is usually increased upon complex formation with transition metals.

1.3.1 Schiff base as antioxidant

Schiff base and their metal complexes are identified as having high capacity in scavenging free radicals [91-95]. Free radicals are causative agents of several oxidative damages such as cancer, liver cirrhosis, diabetes,

atherosclerosis and ageing [96]. Antioxidants are compounds which slow down or defense against free radical damage. The need of antioxidants become even more critical with increased exposure to free radicals pollution caused by drugs, cigarette smoke, stress, illness and even exercise can increase free radical production. Mruthyunjayaswamy *et al.* evaluated the antioxidant capacity of a new Schiff base ligand N-(4-phenylthiazol-2-yl)-2-(thiophen-2-ylmethylene) hydrazinecarboxamide and its Cu(II), Co(II), Ni(II) and Zn(II) complexes by DPPH method. The Schiff base ligand and its Cu(II), Co(II) complexes have exhibited a good antioxidant activity, whereas Ni(II) and Zn(II) complexes have shown moderate activity. The scavenging activity is concentration dependent [97].

Antioxidant property of (3E)-3-[(2-{(E)-[1(2,4dihydroxyphenyl) ethylidene]amino}ethyl)imino]-1-phenylbutan-1- one (DEPH2) and its metal [Co(II), Ni(II), Zn(II), Cu(II)] complexes [Figure 1.5] were screened by Ikechukwu *et al.* using DPPH and ABTS method. Compared to free Schiff base DEPH2, metal complexes showed higher antioxidant activity. The increased antioxidant activity of the metal complexes can be attributed to the electron withdrawing effect of the metal ions which facilitates the release of hydrogen to reduce the DPPH radical. The order of radical scavenging activity is Vitamin C > Cu (DEP) > Ni(DEP) = Rutin > Co(DEP) > Zn(DEP) > Schiff base (DEPH2) and that of the ABTS radical is: BHT > DEPH2 > Cu(DEP) > Zn(DEP) > Rutin > Ni(DEP) > Co(DEP). All the compounds exhibited moderate to higher % inhibition scavenging activity than the standard BHT and rutin at the lowest concentration (100 μg/mL). Cu(DEP) possessing the highest potency (IC_{50} = 2.11 + 1.69 μM). Schiff base and their metal complexes can be used as therapeutic agents for the treatment of pathological diseases and conditions caused as a result of excessive radicals or stress [98].

Figure 1.5 Example for Schiff base metal complexes showing antioxidant activity [Ref. 98].

1.3.2 Antimicrobial activity of Schiff base and its metal complexes

Antimicrobial and antifungal activities of various Schiff bases and their transition metal complexes have been reported [99-102]. Thamarai Selvi *et al.* synthesized a new heterocyclic Schiff base ligands and their complexes from 4-aminoantipyrine, thiophene-2-carboxaldehyde and 2-aminobenzoic acid. Antibacterial and antifungal activity evaluation of the metal complexes against *Escherichia coli, Pseudomonas aeruginosa, Staphylococcus aureus, Salmonella typhi and Candida albicans* exhibited that the complexes have potent biological activity than the ligands [103] (Figure 1.6).

Figure 1.6 Example for Schiff base metal complexes showing antimicrobial activity [Ref.103].

El-Sonbati *et al.* reported synthesis, structure characterization, antimicrobial, antioxidant and antitumor activity of 3-[(2-hydroxy-3-methoxy-

benzylidene)-hydrazono]-1,3-dihydro-indol-2-one and its Cu(II), Co(II), Ni(II) and Cd(II) metal complexes. The ligand and its metal complexes showed antimicrobial activity against bacterial species, gram positive (*Staphylococcus aureus*), gram negative (*Escherichia coli*) bacteria and yeast (*Candida albicans*). The ligand exhibited higher activity than the complexes. Molecular docking studies was used to predict the binding between ligand and the receptors of crystal structure of *E. coli* (3T88), crystal structure of *S. aureus* (3q8u) and crystal structure of *C. albicans* [104].

1 3.3 Analgesic, Anti-inflammatory activity

Chinnasamy *et al.* reported the synthesis and analgesic activity of novel Schiff base Isatin 3-(4-(4-Hydroxy-3-methoxylbenzylideneamino) phenylamino) indoline-2-one [105]. Analgesic and anti-inflammatory activity of N-(acridin-9-yl)-4 (benzo[d]imidazol/oxazol-2-yl) benzamides Schiff base (Figure 1.7) was reported by Sondhi *et al.* [106]. Schiff bases derived from 2-[(2,6-dichloroanilino) phenyl] acetic acid (Diclofenac acid) was synthesized and studied for their anti-inflammatory, analgesic and ulcerogenic activities [107].

Figure 1.7 N-(acridin-9-yl)-4 (benzo[d]imidazol/oxazol-2-yl) benzamides Schiff bases [Ref.106].

1.3.4 Anticancer activity

Metal complexes of Schiff bases with heterocyclic compounds also find applications as potential anticancer drugs, due to the presence of multifunctional groups [108-111]. Zinc complex of Schiff base synthesised from 2-amino-4-phenyl-5-methyl thiazole (Figure 1.8) shows potent anticancer activity when studied against human tumour cells such as breast cancer MCF-7, liver cancer HepG2, lung carcinoma A549 and colorectal cancer HCT116 [112]. A series of sulfapyridine-polyhydroxyalkylidene (or arylidene)-imino derivatives have been prepared and reported for antitumor activity [113].

Figure 1.8 Example for Schiff base metal complexes showing anticancer activity [Ref. 112].

Synthesis and anticancer activity (on MDA-MB-231 breast cancer cells) of novel ternary Cu(II) complex (shown in Figure 1.9) with Schiff base derived from 2-amino-4-fluorobenzoic acid and salicylaldehyde have been reported by Xin Li and coworkers. They identified that the tumor proteasome is a target of the complex. They have shown that the inhibition of the proteasomal activity (especially, chymotrypsinlike activity) by the complex can strongly induce apoptosis in the cultured breast cancer MDA-MB-231 cells. Their study reinforces the idea that proteasome targeted copper complexes have great potential to be developed into novel anticancer drugs [114].

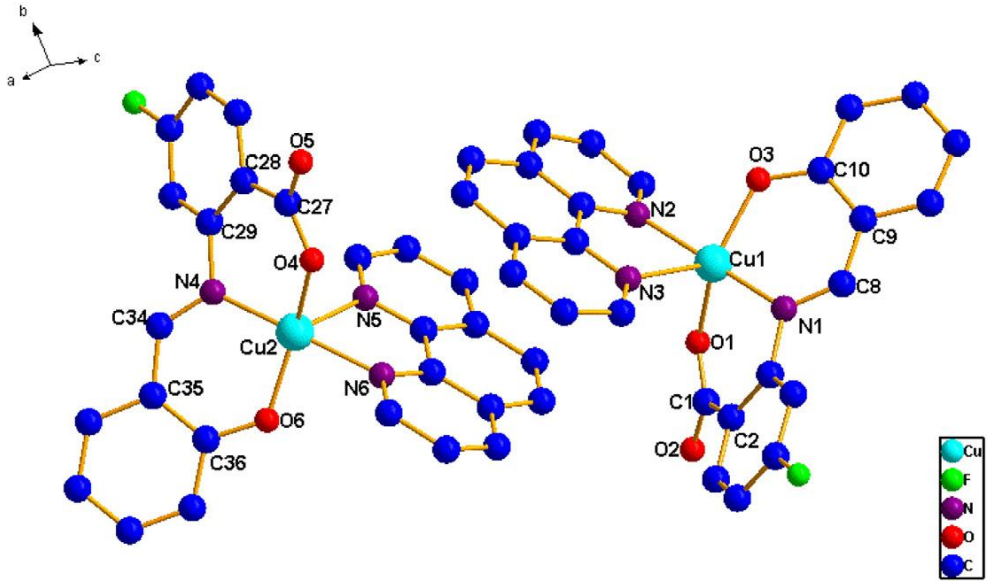

Figure 1.9 Crystal structure of $2Cu(C_{14}H_8NO_3F)(C_{12}H_8N_2)$ [anticancer] [Ref.114].

1.3.5 Antiviral activity

Schiff bases derived from salicylaldehyde and 1-amino-3-hydroxyguanidine tosylate can act as antiviral agents. Compound shown in (Figure 1.10) is very effective against mouse hepatitis virus [115]. A series of 3-(benzylideneamino)-2-phenylquinazoline-4(3H)-one was synthesized and evaluated for their cytotoxicity and antiviral activity [116]. Compounds having –OH group in 2nd position showed better antiviral activity. Thiazolines and azetidinones synthesized by the reaction of Schiff base wih thioglycolic acid and chloral acetyl chloride were evaluated for antibacterial and antiviral (against HIV-I) potential. All the compounds were found to be good HIV inhibitors except those with electro withdrawing group [117].

Figure 1.10 Example for Schiff base showing antiviral activity [Ref. 115].

Kumar *et al.* reported antiviral activity of new series of 3-(benzylideneamino)-2- phenylquinazoline-4(3H)-ones. These compounds were prepared through Schiff base formation of 3-amino-2-phenyl quinazoline-4(3H)-one with various substituted carbonyl compounds. Cytotoxicity and antiviral activity were screened against a series of virus including herpes simplex virus-1 (KOS), herpes simplex virus-2 (G), vaccinia virus, vesicular stomatitis virus, herpes simplex virus-1 TK-KOS ACVr, Sindbis virus, para influenza-3 virus, reovirus-1, Punta Toro virus, Coxsackie virus B4, feline corona virus (FIPV), feline herpes virus, respiratory syncytial virus, influenza A H1N1 subtype, influenza A H3N2 subtype, and influenza B virus [118].

1.3.6 Antimalarial Activity

Harpstrite *et al.* reported the mixed ligand complexes of Ni(II), Cu(II) and Fe(III) with Schiff-base-phenol and naphthalene-amine as anti-malarial agents [119]. In vitro activity of Schiff base-functionalised 5-nitroisoquinolines prepared by reacting 1-formyl-5-nitroisoquinoline with amines were investigated against an ACC Niger chloroquine resistant P. falciparum strain. Compound shown in Figure 1.11 was the most effective antimalarial agent.

Figure 1.11 Example for Schiff base as antimalarial agent [Ref. 119].

1.3.7 Anticonvulsant activity

Ragavendran *et al.* synthesized 4-aminobutyric acid (GABA) is the principal inhibitory neurotransmitter in the mammalian brain. GABA hydrazones were synthesized and evaluated for their anticonvulsant properties in different animal models [120]. Anti convulsing activity of new erindolylthiadiazoles and their thiazolidionones and formazans have been reported by Srivastava *et al.* [121]. A series of Schiff bases of phthalimide, 4-(1,3-dioxo-1,3-dihydro-2*H*-isoindol-2-yl)-*N*-(substitutedphenyl) methylene/ ethylidene benzohydrazide, was synthesized and evaluated for anticonvulsant and neurotoxic activities. All the compounds were found to be active and less toxic than phenytoin which was employed as a standard drug [122]. Schiff base of 3-aryl-4(3H)-quinazolinones-2-carboxaldehydes and thiosemicarbazone derivatives showed anticonvulsant potential due to thiosemicarbazone side chain at position ending with a free amino group and fluorine atom.

1.4 Antioxidant and its importance

1.4.1 Free radicals

A free radical may defined as a molecule or molecular fragments containing one or more unpaired electrons in its outermost atomic or molecular orbital and are capable of independent existence [123]. Free radicals are formed by the homolytic cleavage of a chemical bond. Once

formed these highly reactive radicals initiates a rapid destructive chain reaction [124]. The most commonly formed free radicals in biological system are superoxide ($O_2^{\bullet}$), hydroxyl ($OH^{\bullet}$), peroxyl ($RO_2^{\bullet}$), hydroperoxyl ($HO_2^{\bullet}$), alkoxyl ($RO^{\bullet}$), peroxyl ($ROO^{\bullet}$), nitric oxide ($NO^{\bullet}$), nitrogen dioxide ($NO_2^{\bullet}$) and lipid peroxyl ($LOO^{\bullet}$) [125-126]. Three important steps in free radical reaction are 1. Initiation step: Formation of radicals, 2. Propagation step: In this step, required free radical is regenerated repeatedly as a result of chain reaction, which would take the reaction to completion, 3.Termination step: Destruction of radicals [127].

Generation and sources of free radicals - Free radicals can be formed either endogenously or exogenously. Important sources of free radicals are [128]

Endogenous sources of free radicals

- Oxidative metabolic transformation
- Mitochondrial respiratory chain
- Oxygen burst (respiratory burst) during phagocytosis
- Eicosanoid synthesis
- Enzymatic reactions (oxygenases, oxidases)

Exogenous sources of free radicals

- Ionizing radiation
- Ultraviolet radiation, X-rays, gamma rays and microwave radiation
- Chemicals, tobacco smoke, etc.
- Oxygen free radicals in the atmosphere considered as pollutants

Free radical production occurs continuously in all cells as a part of cellular function. Excessive amounts of ROS may be harmful because they can initiate bimolecular oxidations which lead to cell injury and death, and

create oxidative damage or oxidative stress (refers to the situation of serious imbalance between production of reactive species and antioxidant defense) to biomolecules. Their presence in the biological system is very harmful and these free radical species are responsible for the damage of biomolecules such as nucleic acid, proteins, lipids, DNA and carbohydrates and this may cause many diseases such as cancer, atherosclerosis, ageing, hair loss, inflammation, immunosupresssion, diabetes and neurodegenerated disorders (such as Alzheimer's and Parkinson's diseases) (Figure 1.12)[129-130].

Figure 1.12 Sources and diseases of free radical

1.4.2 Antioxidants

Antioxidants are compounds which slow down or prevent the oxidation of other target molecules. They mop up free radicals and prevent them from causing cell damage. The human body uses an antioxidant

defense system to neutralize the excessive levels of reactive oxygen species. Major antioxidant defense enzymes are superoxide dismutase, catalase and gluatathion peroxidase [Figure 1.13].

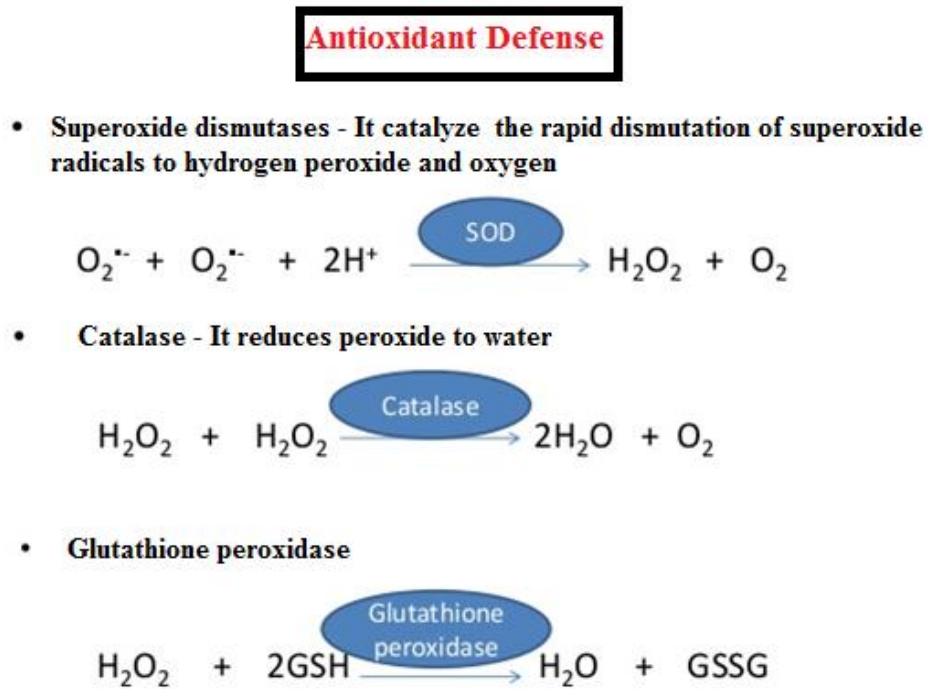

Figure 1.13 Antioxidant defense

Human antioxidant system is divided into enzymatic and non enzymatic antioxidants. They are further classified into different groups as shown in the Figure 1.14. Non enzymatic molecules include glutathione, tocopherol (vitamin E), vitamin C, β-carotene, and selenium [131-132].

Kinetically antioxidants are classified into different categories:

- Antioxidants that break chains by reacting with peroxyl radicals having weak O-H or N-H bonds: phenol, napthol, hydroquinone, aromatic amines and amino phenols.

- Antioxidants that break chains by reacting with alkyl radicals: quinones, nitrones, iminoquinones.
- Hydroperoxide decomposing antioxidants: sulphide, phosphide, thiophosphate.
- Metal deactivating antioxidants: diamines, hydroxyl acids and bifunctional compounds.
- Cyclic chain termination by antioxidants: aromatic amines, nitroxyl radical, variable valence metal compounds.
- Synergism of action of several antioxidants: phenol sulphide in which phenolic group reacts with peroxyl radical and sulphide group with hydro peroxide [133-134].

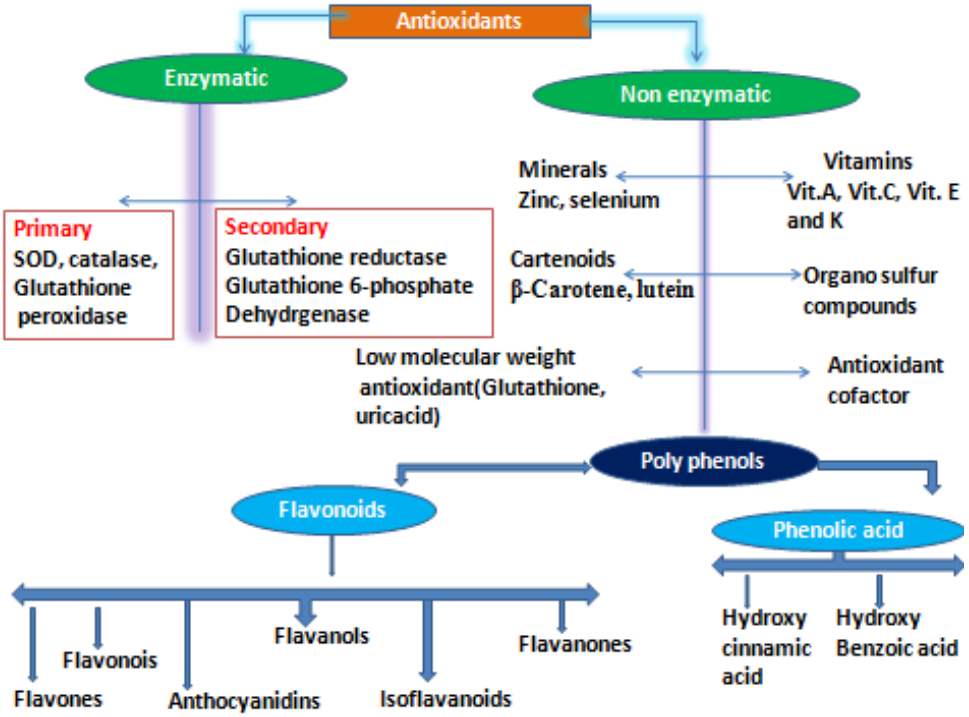

Figure 1.14 Classification of antioxidant.

The treatment with antioxidants is potentially a way to overcome the oxidative stress or oxidative damage. Antioxidant molecule can react with single free radicals and are capable of neutralizing free radicals by donating one of their own electrons (Figure1.15), ending the carbon-stealing reaction [135]. Because of this, there is a great interest in the discovery of natural and synthetic antioxidants that can serve as protective agents against diseases caused by free radicals.

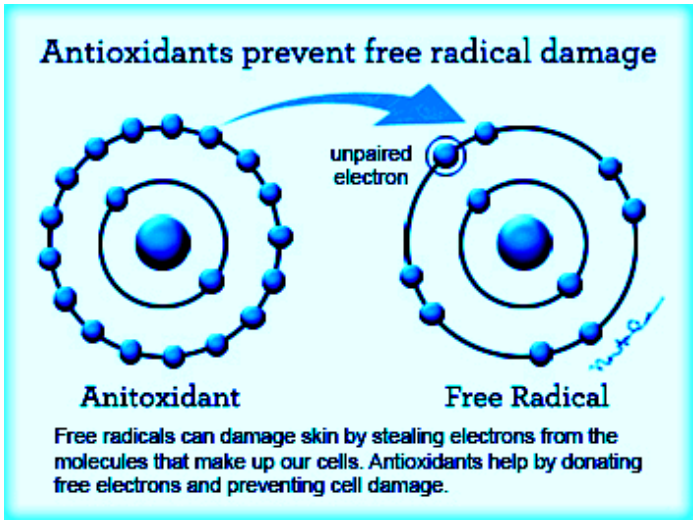

Figure1.15 Prevention of free radical damage by antioxidant

1.4.3 Natural and synthetic antioxidants

Based on the origin antioxidants are classified into natural, synthetic and nature-identical antioxidants. Natural antioxidants are synthesized by microorganisms, fungi, animals and plants. Antioxidants identical to natural antioxidants but synthesized in the industry are called nature identical antioxidants. Antioxidants synthesized or biosynthesized by human are called synthetic antioxidants. Synthetic antioxidants have been developed for the stabilization of bulk fats and oils or foods rich in lipids. They are substantially more efficient than α-tocopherol and other natural antioxidants

which are usually less liposoluble. Natural antioxidants are not pure substance as their active fraction is much lower than the actual addition while synthetic antioxidants are nearly 100 % pure. BHT (butylated hydroxyl toluene) and BHA (butylated hydroxyl anisole) are the most widely used synthetic antioxidants [136-138]. Examples for some synthetic antioxidants are given below.

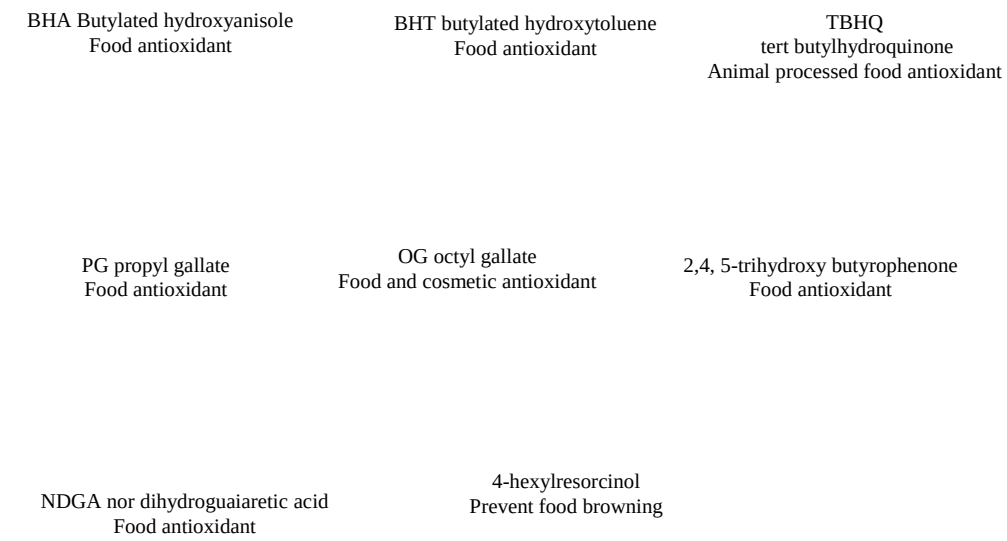

Figure 1.16 Synthetic antioxidants.

1.4.4 Phenolic antioxidants

Phenolic compounds are known as powerful chain breaking antioxidants. Radical scavenging activities of phenolic antioxidants are highly influenced by their chemical structure. Bond dissociation energy (BDE) of OH bond is one of the factors for the highest radical scavenging activity of phenolic antioxidants. Lower the BDE of OH bond, the more

active the antioxidant. Presence of intramolecular hydrogen bonding also stabilizes the radical and hence increases the radical scavenging activity [139-143]. Phenol acts as antioxidant by breaking the free radical chain reaction through the donation of its hydrogen atom to free radicals. Phenoxyl radical thus formed can be reduced to its parent compound by enzymatic or non-enzymatic reaction. The phenoxyl radical formed is stabilized by the delocalization of unpaired electron on the aromatic ring. Figure1.17 depicts the conjugated resonance stabilization of phenoxyl radicals [144-146].

Figure 1.17 Resonance stabilization of phenoxyl radical.

Antioxidant potential of phenolic compounds depends on the different substituent groups present and the extent of structure conjugation. Electron donating group enhances radical scavenging activity and electron withdrawing group reduces it. Structurally phenols may be divided into phenolic acid and flavonoids. Phenolic antioxidant, such as caffeic acid and its analogues showed antiviral and anti inflammatory property [147]. Resveratrol, a phenolic antioxidant is known for its anticancer and heart protecting effect [148]. Olive oil phenols inhibit human low density lipoprotein oxidation [149]. Some phenolic antioxidants are shown in Figure1.18.

Figure 1.18 Structures of some phenolic antioxidant.

1.5 DNA interactions

DNA, deoxyribonucleic acid is the critical therapeutic target of most antitumor drugs as well as many antiviral and antibacterial agents. In humans and almost all other organisms, the primary genetic material is double strand DNA. The important function of DNA is to store and transmit genetic information. To accomplish this function DNA must have two properties. Firstly, it must be chemically stable so as to reduce the possibility of damage. Secondly, DNA must also be capable of copying the information it contains. The two-stranded structure of DNA gives it both of these properties. Double helix structure of DNA molecule is proposed by Watson and Crick in 1953 [150].

DNA is made up of subunits called nucleotides. Each nucleotide is made up of 5-carbon sugar (deoxyribose), a phosphate and nitrogen containing heterocyclic base. Adenine, guanine, (purine) cytosine and thymine (pyrimidine) are the bases found in a DNA molecule [Figure 1.19]. The deoxyribose sugar of the DNA backbone has five carbons and three oxygens. The hydroxyl groups on the 5'- and 3'- carbons link to the phosphate groups to form the DNA backbone. In DNA double helix structure**,** the nucleotides connect the two strands through hydrogen bonds [Figure 1.20]. The nucleotide sequence contains the information found in DNA. As each nucleotide has a unique complimentary nucleotide, each strand contains all the information required to synthesize a new DNA molecule. The double stranded structure also makes the molecule more stable.

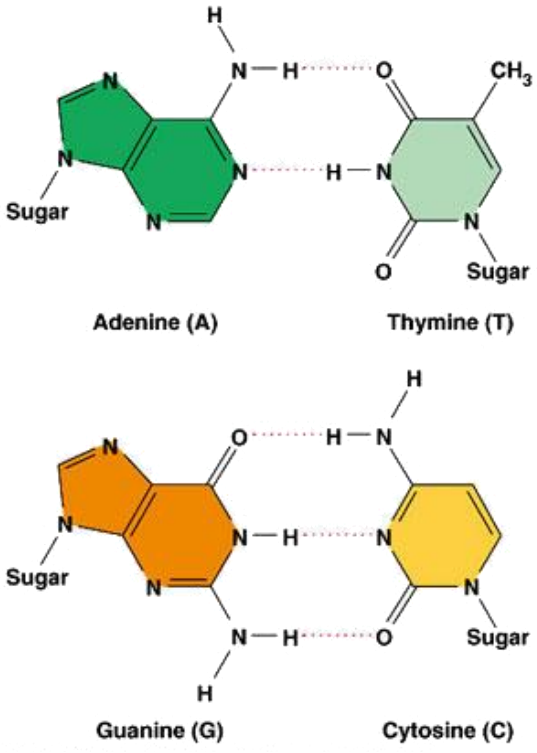

Figure 1.19 DNA bases.

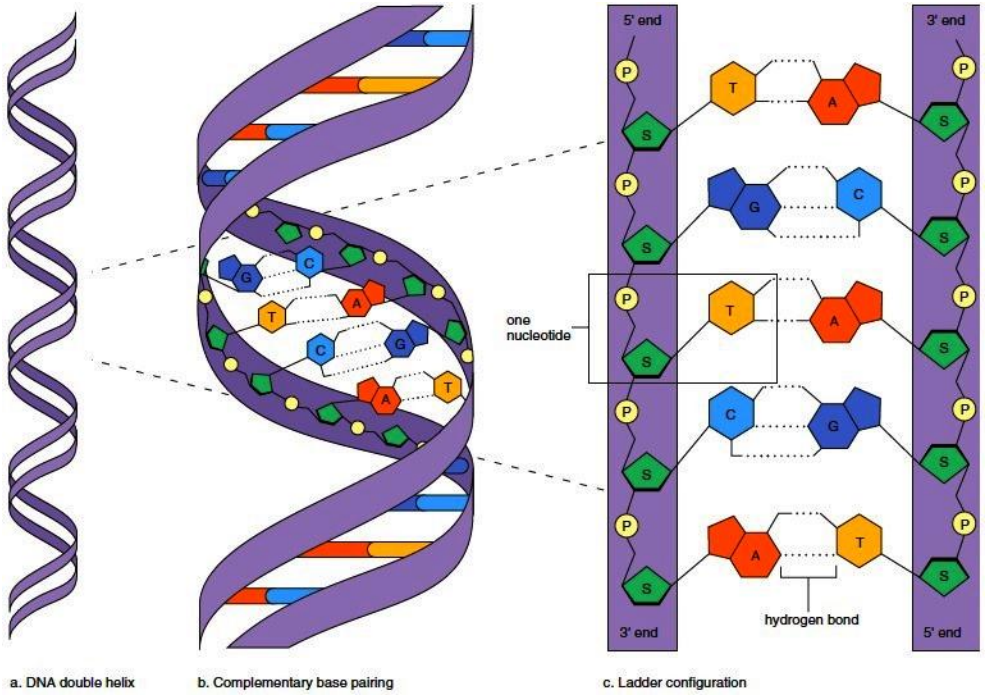

Figure 1.20 Double helix structure of DNA.

The three different forms of DNA double helix are A, B and Z. (Figure 1.21). These conformations are distinguished by the handedness of the helix, distance between consecutive bases, their pitch (the distance between base and the base obtained after a full 360° turn) and the number of nucleotides within one pitch [152]. A and B-DNA forms are right-handed while Z-DNA form is left-handed. DNA adopts mainly the B-conformation, with both forming right-handed helices. However, DNA double strands are able to take up the A-conformation in some protein-DNA complexes and under dehydrated conditions. Both B-helix and A-form helix have two grooves, the major and the minor grooves [153]. The major and minor groove differs in shape, size, hydration, electrostatic potential and position of hydrogen bonding sites [154]. In B form, two grooves differ in their

width but are equally deep. In contrast, the A-form helix possesses a small deep major groove, which is accessible only to water and metal ions. The term Z-DNA stems from the observed zig-zag conformation of the phosphate backbone of a left-handed helix taken up by alternating purine-pyrimidine DNA sequences (GC repeats) under high salt conditions. The distance between consecutive base-pairs and the degree of rotation of the helix per residue results from the changes in the sugar pucker from a C3′-endo to C2′-endo. Base pair sequence, relative humidity, and the presence of DNA-binding compounds influence the sugar puckering and conformation of DNA [155-156].

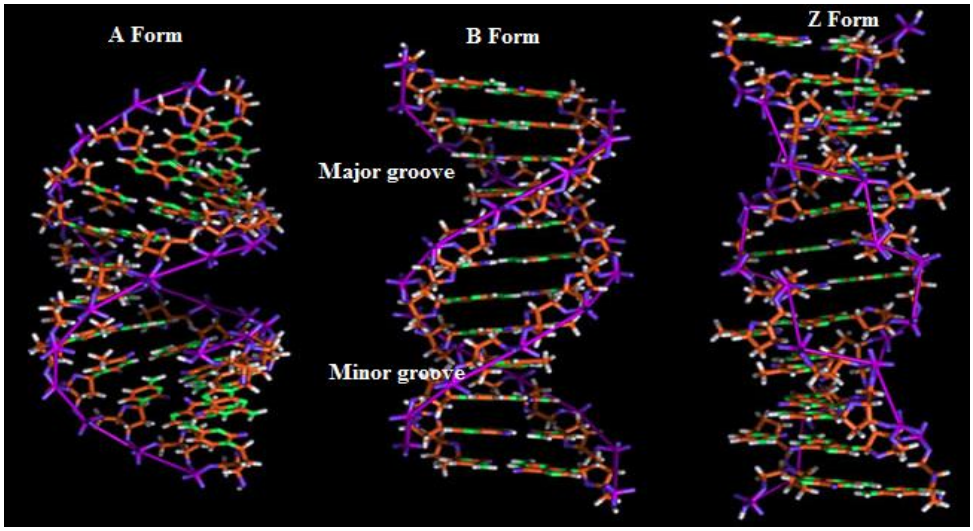

Figure 1.21 A, B and Z. form of DNA double helix.

1.5.1 Drug–DNA interactions

Transcription and replication are the major determinant of the gene expression that allows cells to proliferate, differentiate and maintain proper homeostasis. This also helps in the smooth functioning of all body processes [158]. Transcription machinery regulation is one of the ways to control gene expression. This has been achieved either at the transcription initiation stage

or at the elongation stage. DNA transcription or replication occurs only when DNA receives a signal in the form of a regulatory protein binding to a particular region of the DNA. DNA - small molecules interaction plays a significant role towards inhibition, modulation and activation of the transcription machinery. Thus synthetic/natural small molecule can act as therapeutic agents when activation or inhibition of DNA function is required to cure or control a disease [159].

Small molecules bind to double-stranded DNA either covalently or non-covalently (intercalation and groove binding, Figure 1.22).

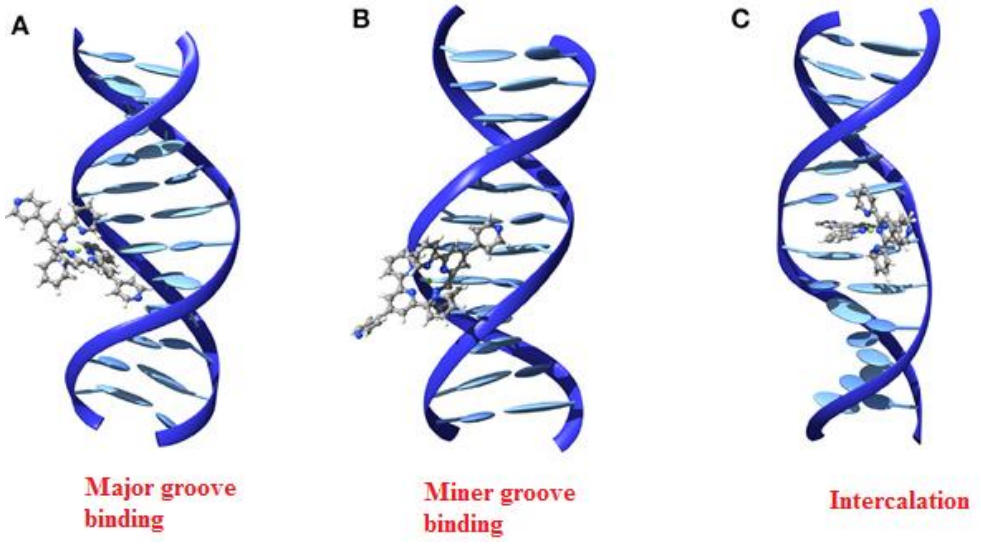

Figure 1.22 Modes of Binding in DNA.

Covalent binding is a common method of DNA interaction for anticancer drugs [160]. A major advantage of covalent binders is the high binding strength. Three modes of covalent binding to DNA are: Inter and intra-strand cross linking, replacement of nitrogenous bases, and alkylation of nitrogenous bases. Cisplatin is the most clinically successful DNA covalent binder that and makes an intra/interstrand cross-link through the

chloro groups with the nitrogen on the DNA bases (Figure 1.23) although it reacts with a diverse range of other biomolecules [161]. Such binding results in the unwinding of the double helix and subsequent inhibition of transcription, thereby resulting in subsequent cell death [162].

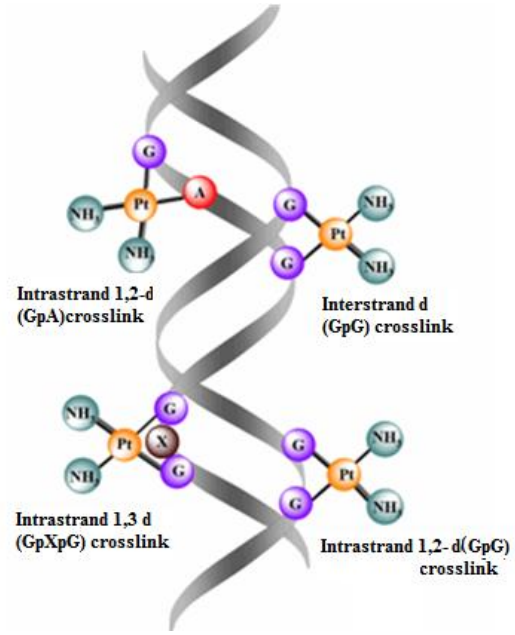

Figure 1.23 Inter and intra-strand cross linking of cisplatin.

1.5.2 Non covalent binding

Intercalation is defined as the insertion of a positively charged planar heterocyclic aromatic molecule between two adjacent base pairs of DNA double helix [163]. Intercalation stabilizes, lengthens, stiffens and unwinds the DNA double helix [164]. This effect dependent upon the "depth of insertion"[165]. Intercalation is reversible, and is stabilised by a combination of electrostatic, hydrogen bonding, entropic, van der waals and hydrophobic interactions. The two major types of intercalation-binding modes are: (1) classical intercalation and (2) threading intercalation. Binding by the classical mode is typified by the much-studied DNA stain

ethidium bromide and the antimalarial quinacrine [166]. Molecules that bind to double-stranded DNA (DNA) by intercalative mode have been significantly used as drugs. Intercalators can cause more significant distortion of the native conformations of DNA, indicating that intercalators produce strong structural perturbations in DNA.

Groove binding – Groove binders are another important class of small molecules with crescent shaped that bind to DNA and play major role in drug development [167]. In this type, molecules can bind to both the major and minor groove of DNA. These grooves are vastly different in size, shape and properties. The major groove is much wider than the minor groove and is the site for binding of many DNA interacting proteins [168-169]. Minor-groove binding usually involves greater binding affinity and higher sequence specificity than that of intercalator binding. Minor-groove binding has been demonstrated for neutral, mono-charged and multicharged ligands [170]. Netropsin is an example for minor groove binder. Major groove of DNA is an enthalpy-driven process, while minor groove interactions are dominated by entropic effects. Considerably small number of molecules is reported to bind to major groove. The reason for this probably lies in the fact that nitrogen and oxygen atoms in base pairs of wide and deep major groove are oriented towards the axis of the helix, making them accessible for proteins. Some antitumor agents with acridine carboxamide skeleton were reported as major groove binders [171]. Groove binding is based upon intermolecular interactions such as electrostatic and van der Waals attractions [172].

Several techniques have been employed to study the binding of small molecules to DNA including, UV-Visible spectroscopy, fluorescence spectroscopy, voltammetry, circular dichroism (CD)) and linear dichroism (LD).

DNA–small molecule interaction can be detected by UV-Vis absorption spectroscopy by measuring the changes in the absorption properties of the drug molecules or the DNA molecules. The UV–Vis absorption spectrum of DNA exhibits a broad band (200–350 nm) in the UV region with a maximum at 260 nm. This is a consequence of the chromophoric groups in pyrimidine and purine moieties responsible for the electronic transitions. Slight changes in the absorption maximum and the molar absorptivity can occur with the variations in pH or ionic strength of the media. DNA–drug interactions can be studied by comparison of UV–Vis absorption spectra of the free drug molecule and DNA–drug complexes, which are usually different. The binding with DNA through intercalation usually results in hypochromism and hypsochromism (blue shift) or bathochromism (red shift) [173-174].

Fluorescence spectroscopy is probably one of the most commonly used techniques to study interactions between small molecules (ligand and complexes) and DNA. The advantages of molecular fluorescence over other techniques are its high sensitivity, large linear concentration range and selectivity. The most intense and the most useful fluorescence are found in compounds containing aromatic functional groups with low-energy $\pi \rightarrow \pi$ transition levels. Compounds containing aliphatic and alicyclic carbonyl structures or highly conjugated double-bond structures may also show fluorescence, but the number of these transitions is small compared with those in aromatic systems [175].

CD and LD spectroscopies are useful techniques for the assessment of non-covalent drug-DNA interactions, which affect the electronic structure of the molecules. LD use polarized light and provides structural information in terms of the relative orientation between the bound drug molecule and the

DNA molecular long axis. LD spectroscopy involves measuring the difference in absorption of two linear polarizations of light, which usually are parallel and perpendicular to a sample orientation direction. In contrast to LD which depends only on the electric field vector, CD depends on both electric and magnetic interactions and provides additional structural information of DNA [176-177]. Electrochemical methods are another important techniques used to the study of metallointeraction and coordination of transition metal complexes to DNA [178].

1.6 Enzymes

Enzymes are very effective biological catalysts that accelerate or catalyze almost all metabolic reactions in living organisms. In other words, they either start chemical reactions or enhance the rate of reaction between biomolecules. Enzymes have two portions, a protein portion called the apoenzyme and a nonprotein portion, either a cofactor (inorganic) or coenzyme (organic). The proteins in enzymes are usually globular. The inter and intramolecular bonds holding proteins in their secondary and tertiary structures are disrupted by temperature and pH change. This causes structural changes indicating that the catalytic activity of an enzyme is pH and temperature sensitive. Enzymes are present in every cell in both plants and animals; and are responsible for regulating the biochemical reactions necessary to sustain life. Enzymes are highly specific, both in the substrate they affect, and in the reactions they catalyze. Enzymes are biodegradeable and work at low temperature and moderate pH. These are more stable catalysts than other chemicals or biological molecules, making them the most environment friendly solution for industrial manufacturing. Enzymes are classified according to the reactions they catalyze.

Six main groups of enzymes are hydrolases, ligases, isomerases, oxidoreductases, lyases, and transferases. hydrolases, oxidoreductases and transferases are the most numerous forms of enzymes, while the other enzymes are less common [179].

- Hydrolases break down carbohydrates, proteins, and fats such as during the process of digestion. This is achieved by adding a water molecule, thus the name hydrolases.
- By using an energy source, the ligases catalyze the formation of a bond between two substrate molecules.
- Isomerases catalyze the rearrangement of chemical groups within the same molecule.
- Oxidoreductases make oxidation-reduction.
- Lyases catalyze the formation of double bonds between atoms by adding or subtracting chemical groups.
- Transferases transfer chemical groups from one molecule to another.

1.6.1 Factors affecting catalytic activity of enzymes

- Temperature - As the temperature increases, reacting molecules gain more kinetic energy. This enhances the chances of a successful collision and so the rate of the reaction increases.
- pH- Each enzyme works within quite a small pH range. There is a pH at which enzyme activity is maximum (the optimal pH). pH change can make and break intra- and intermolecular bonds, changing the shape of the enzyme and, therefore, its effectiveness.

- Concentration of enzyme and substrate - concentrations of enzyme and substrate also affect the rate of an enzyme-catalysed reaction. As the concentration of either is increased the rate of reaction increases. For a given enzyme concentration, the rate of reaction increases with increasing substrate concentration up to a point, above which any further increase in substrate concentration produces no significant change in reaction rate. This is because the active sites of the enzyme molecules at any given point are virtually saturated with substrate.

Enzymes have a small region (typically only about 20 amino acids), known as the active site, that has the right shape and functional groups to bind to one of the reacting molecules. The reacting molecule that binds to the enzyme is called the substrate. The enzyme and substrate form a reaction intermediate (enzyme-substrate complex). This binding changes the distribution of electrons in the chemical bonds of the substrate(s), lowering the activation energy of the reaction and enabling generation of the final product [180].

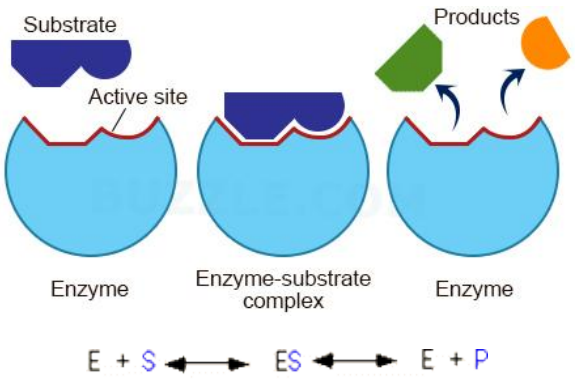

Enzyme controlled reactions are very fast compared to the reactions without any enzymes. In a chemical reaction large amount of heat energy is required to make the reaction occur at a faster rate and this is called activation energy. Enzymes are very efficient catalysts for biochemical

reactions. They speed up reactions by providing an alternative reaction pathway of lower activation energy. The half way point in a reaction is called as transition state and is represented as the top of the curve representing a chemical reaction (Figure1.24) [181].

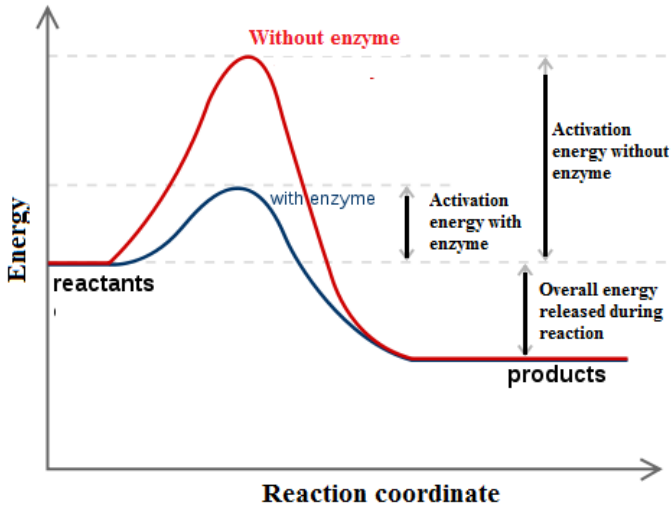

Figure 1.24 The energy variation as a function of reaction coordinate Enzyme kinetics**.**

Kinetic parameters: Michaelis-Menten constant (K_m) and the maximum reaction velocity (V_{max}) are two important enzyme parameters in a simple enzyme catalyzed reaction. The Lineweaver -Burk plot [182] depicting the enzyme kinetics is given as Figure1.25.

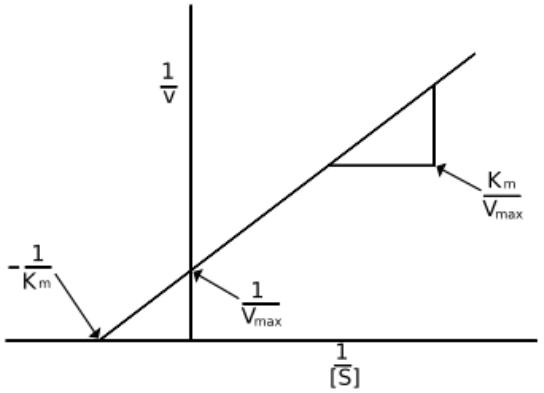

Figure 1.25 Lineweaver-Burk plot.

K_m is the substrate concentration, [S] at which half maximum velocity of reaction is observed under given set of conditions. Generally a lower K_m value signifies a higher affinity for the substrate. Value of K_m is dependent upon pH, temperature and other reaction conditions. V_{max} is the maximal activity of the enzyme when all of the active sites are saturated [183-184].

The Michaelis-Menten equation:

$$V = \frac{V_{max}[S]}{[S] + K_M}$$

To obtain V_{max} and K_m, the enzyme activity must be recorded and then plotted on a double reciprocal plot, a Lineweaver-Burk plot, and the Michaelis Menten equation is then rearranged to

$$\frac{1}{V} = \frac{K_M}{V_{max}} \frac{1}{[S]} + \frac{1}{V_{max}}$$

Enzyme Inhibitors and Activators

Enzyme inhibitors and activators that modulate the velocity of enzymatic reactions play an important role in the regulation of metabolism. Enzyme inhibitors act as a useful tool for the study of enzymatic reactions as well as for the design of new medicinal drugs. The enzyme inhibitors are low molecular weight chemical compounds. They can reduce or completely inhibit the enzyme catalytic activity either reversibly or permanently (irreversibly). Inhibitor can modify one amino acid, or several side chain(s) required in enzyme catalytic activity. Enzyme activators are chemical

compounds that increase a velocity of enzymatic reaction [185]. Their actions are opposite to the effect of enzyme inhibitors. Inhibitors can be split into the following categories:

- Irreversible Inhibitors: Molecules that permanently bind to the enzyme's active site or specific side chain,
- Competitive Inhibitors: These are competing molecules that will have a very similar structure to that of the natural substrate and thus will be complementary to the enzyme active site (Figure 1.26). In competitive inhibition, V_{max} remains the same but K_m increases. Competitive inhibition can be overcome by an increase in substrate concentration. They are therefore useful therapeutic agents and unlike irreversible inhibitors (like aspirin) their effect isn't long lasting [186].

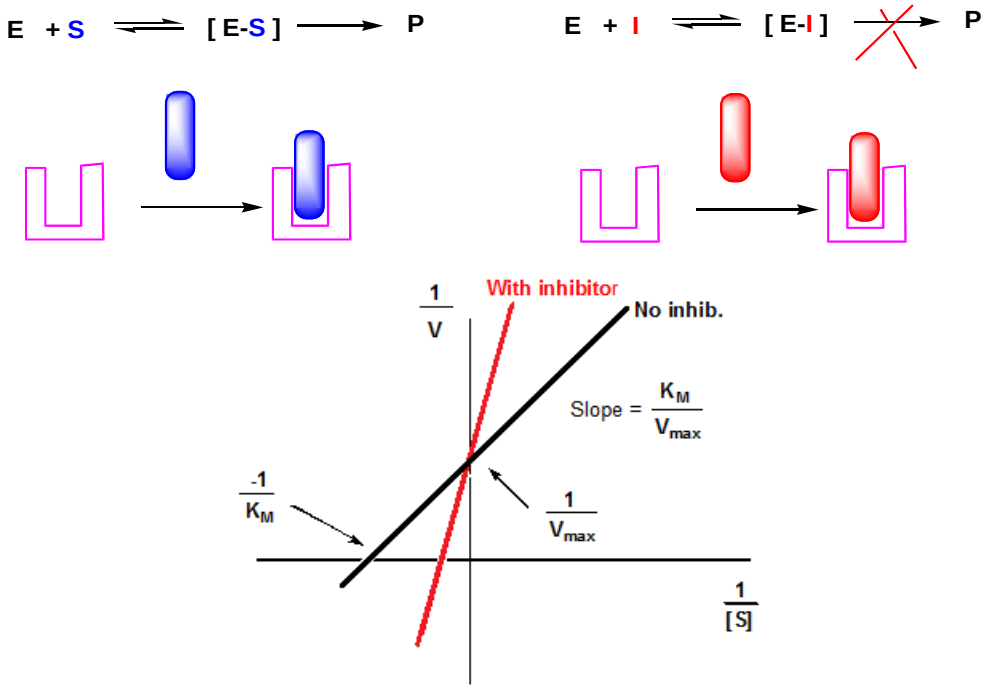

Figure 1.26 Equation and the effect of the competitive inhibitor on the double reciprocal plot of the substrate-reaction rate relationship.

Non-competitive inhibitors: This type of inhibitors bind to the allosteric site on the enzyme other than the active site, causing changes to enzyme shape resulting in disruption of the active site (Figure.1.27). This decreases the turnover number of the enzyme rather than preventing substrate binding- V_{max} decreases but k_m stays the same. This cannot be overcome with an increase in substrate concentration.

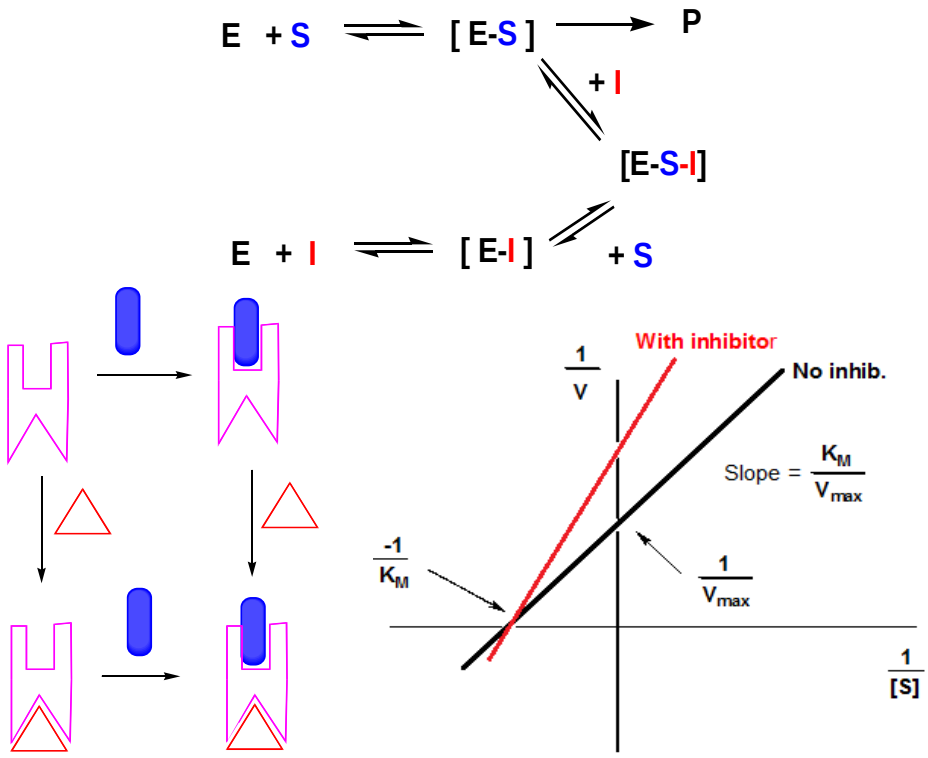

Figure 1.27 Equation and the effect of the non competitive inhibitor on the double reciprocal plot of the substrate-reaction rate relationship.

- Uncompetitive inhibitors only bind to an enzyme-substrate complex; so both K_m and V_{max} decrease as it takes longer for the substrate to leave the active site. This inhibition works when the concentration of enzyme-substrate complex is high.

1.7 Scope and objectives of the present study:

Biological activities of transition metal complexes derived from heterocyclic Schiff base ligands are one of the most exhaustively studied topic in coordination chemistry due to their enhanced activities compared to non Schiff base complexes. The complexes of Schiff bases have wide applications in food industry, dye industry, analytical chemistry, catalysis, fungicidal, agrochemical, anti-inflammable activity, antiradical activities and other biological activities. Metal chelates of Schiff bases hold exciting possibilities for the future, particularly in designing novel corrosion inhibitors, epoxy curing agents, semi conducting materials, catalytic systems, in formulating new synthetic routes and in developing new antifungal, antibacterial, antiviral, anticancer, antioxidant and antidiabetic agents. From the survey of existing literature, it appears that heterocyclic Schiff base and their complexes have a variety of applications in biological, clinical and analytical fields. Keeping the pronounced biological properties of Schiff bases and their transition metal complexes, it was thought worthwhile to synthesis some new heterocyclic Schiff base complexes and study their biological properties.

The main objectives of the work can be summarized as follows

- Synthesis and characterization of a new class of heterocyclic Schiff bases.
- Synthesis and characterization of Ni(II), Cu(II) and Zn(II) complexes of synthesised heterocyclic Schiff bases by spectroscopic data such as IR, UV-Visible, thermogravimetry, EPR, and elemental analysis.

- Biological studies of heterocyclic Schiff base and their Ni(II), Cu(II) and Zn(II) complexes. Present work has been focused on the following biological properties.
  - Anti-oxidant activity studies - solvent effect, structure activity relation and mechanism of action.
  - DNA binding studies
  - Anti-HIV studies
  - Anti-bacterial studies
  - Anti-Diabetics studies
  - Cytotoxicity studies

References

[1] P. A. Cox, Instant Notes Inorganic Chemistry. Ed. 2nd, BIOS Scientific Publishers, New York, USA, (2005).

[2] V. Mehmet, J. App. Pharm., (2016), doi:10.4172/1920-4159. 1000e 107.

[3] K. J. Waldron, J. C. Rutherford, D. Ford and N. J. Robinson, Nature, 460, (2009), 823 - 830.

[4] C. Andreini, I. Bertini, G. Cavallaro, G. L. Holliday and J. M. Hornton, J. Biol. Inorg. Chem., 13, (2008), 1205-1218.

[5] K. D. Mjos and C. Orvig, Chem. Rev., 114, (2014), 4540-4563.

[6] P. Aisen, C. Enns and M. Wessling-Resnick, Int. J. Biochem. Cell. Biol., 33, (2001), 940-959.

[7] M. Amina, M. Tariq, M. R. Elsegood and G. W. Weaver, J. Nucl. Med. Radiat.Ther., (2016), doi: 10.4172/2155-9619. 1000310.

[8] A. Z. Wail, Int. J. Org. Chem., 3, (2013), 75- 65.

[9] Y. Wang, H. Wang, H. Li and H. Sun Dalton Trans., 44, (2015), 437-447.

[10] S. Komeda and A. Casini, Current topics in med. chem., 12, (2012), 219-235.

[11] K. Hariprasath, B. Deepthi, Sudheer, I. Babu, P. Venkatesh, P. Sharfudeen and S. Soumya, J. Chem. Pharm. Res., 2, (2010), 496 - 499.

[12] S. Medici, M. Peana, V. M. Nurchi, J. I. Lachowicz and G. Crisponi and M. A. Zoroddu, Coord. Chem. Rev., 284, (2015), 329-350.

[13] A. Paulo, G. R. Morais, and J. L. Armando Pombeiro, Advances in Organometallic Chemistry and Catalysis, ed. 1st, John Wiley & Sons, (2014).

[14] G. R. Morais and A. Paulo, I. Santos, Organometallics, 31, (2012), 5693-5714

[15] A. A. Warra, J. Chem. Pharm. Res., 4, (2011), 951-958

[16] M. Selvaganapathy and N. Raman, J. Chem. Biol. Ther., 1, (2016), 108-121.

[17] K. D. Mjos and C. Orvig, Chem. Rev., 114, (2014), 4540- 4563.

[18] A. Bergamo and G. Sava, Chem. Soc. Rev. 44, (2015), 8818-8835.

[19] L. Zhang, R. Q. Liu, H. Peng, P. H. Li, Z. S. Xu and A. K. Whittaker, Nanoscale, 8, (2016), 1048-1049.

[20] J. R. Anacona and G. D. Silva, J. Chilean Chem. Soc., 2, (2010), 447- 450

[21] H. Zainab, Y. Emad, A. Ahmed and A. Altaie, Org. Med. Chem. Lett., (2014), 1- 4.

[22] A. A. Wasfi, T. M. Hassan and A. A. Hama, Int. J. Pharm., 6, (2015), 386-389.

[23] B. S. Sathe, E. Jaychandran, V. A. Jagtap, and G. M. Sreenivasa, Int. J. Pharmaceut. Res. Dev., 3, (2011), 164-169.

[24] B. S. Creaven, B. Duff, D. A. Egan, K. Kavanagh and G. Rosair, Inorg. Chem. Acta., 363, (2010), 4048-4058.

[25] S. M. M. Ali, K. M. Abul and M. Jesmin, Asian. Pac. J. Trop Biomed., 2, (2012), 438-442

[26] R. Miri, N. Razzaghi-asl, and M. K. Mohammadi, J. Mol. Modeling, 19, (2013), 727-735

[27] B. S. Sathe, E. Jaychandran, V. A. Jagtap, and G. M. Sreenivasa, Int. J. Pharmaceut. Res. Dev., 3, (2011), 164-169.

[28] S. M. Sondhi, N. Singh, A. Kumar, O. Lozach, and L. Meijer, Bioorg. Med. Chem., 14, (2006), 3758-3765.

[29] T. Aboul-Fadl, F. A. S. Bin-Jubair and O. Aboul-Wafa, Eur. J. Med. Chem., 45, (2010), 4578- 4586.

[30] T. Aboul-Fadl, F. A. Mohammed and E. A. Hassan, Archives of Pharmacal. Res., 26, (2003), 778-784.

[31] S. Zangade, A. Shinde, S. Chavan and Y. Vibhute, J .Chem., 7, (2015), 208-214.

[32] D. Wei, N. Li, G. Lu, and K. Yao, Sci. China B., 49, (2006), 225 - 229.

[33] S. Shinde, S. Zangade, Y. Chavan and Vibhute, Org. Comm., 7, (2014), 60-67.

[34] K. Mounika, B. Anupama, J. Pragathi, and C. Gyanakumari, J. Scientific Res., 2, (2010), 513-524.

[35] P. Venkatesh, Asian J. Pharmaceut. Health Sci., 1, (2011), 8-11.

[36] C. Chandramouli, M. R. Shivanand, T. B. Nayanbhai, B. Bheemachari and R. H. Udupi, J. Chem. Pharm. Res., 4, (2012), 1151-1159.

[37] R. P. Chinnasamy, R. Sundararajan, and S. Govindaraj, J. Adv. Pharm. Technol. Res., 1, (2010), 342- 347.

[38] M. M. Omar, G. G. Mohamed and A. M. M. Hindy, J. Therm. Anal. Cal., 86, (2006), 315-325.

[39] Y. Li, Z.Y. Yang and J. C. Wu, Eur. J. Med. Chem., 45, (2010), 5692-5701.

[40] G. H. Olie and S. Olive, Springer, Berlin, (1984), 152.

[41] A. K. Chaubey and S. N. Pandeya, Int. J. Pharm. Tech. Res., 4, (2012), 590-598.

[42] P. G. Avaji, C. H. Vinod Kumar, S. A. Patil, K. N. Shivananda and C. Nagaraju, Eur. J. Med. Chem., 44, (2009), 3552 - 3559.

[43] M. Hranjec, K. Starcevic, S. K. Pavelic, P. Lucin and K. Pavelic, Eur. J. Med. Chem., 46, (2011), 2274-2279.

[44] N. V. S. Rao, T. D. Choudhury, R. Deb, M. K. Paul, T. R. Rao and I. I. Smalyukh, Liq. Crys., 37, (2010), 1393-1410.

[45] A. Guha, J. Adhikary, T. Mondal and D. Das, Ind. J. Chem., 50, (2011), 1463-1468.

[46] M. A. Ashraf, A. Wajid, K. Mahmood, M. J. Maah and I. Yusoff, Int. J. Chem. Engg. Appl., 2, (2011), 252-255.

[47] G. Consiglio, S. Failla, P. Finocchiaro, I. P. Oliveri and S. D. Bella, Dalton. Trans., 41, (2012), 387-395.

[48] A. Bharat, N. Makwana, Pratik, Dave, B. Pratik and Timbadiya, Int. J. Sci. Tech. Manag. 4, (2015), 642-652.

[49] A. Xavier and N. Srividhya, J. Appl. Chem., 7, (2014), 6-15.

[50] P. Paul, Proc. Ind. Acad. Sci., 114, (2002), 269-276.

[51] L. A. Paquette, W. A. Benjamin, Principles of modern heterocyclic chemistry, Anybook Ltd., United Kingdom, (1968).

[52] R. B. Moffett and N. Rabjohn, organic synthesis, John Wiley and Sons, New York, USA, (1963).

[53] K. Taguchi and F. H. Westheimer, J. Org. Chem., 36, (1971), 1570-1572.

[54] B. E. Love and J. Ren, J. Org. Chem., 20, (1993), 5556-5557.

[55] G. C. Look, M. M. Murphy, D. A. Campbell and M. A. Gallop, Tetrahedron Lett., 17, (1995), 2937-2940.

[56] A. K. Chakraborti, S. Bhagat and S. Rudrawar, Tetrahedron Lett., 45, (2004), 7641-7644.

[57] M. Gopalakrishnan, P. Sureshkumar, V. Kanagarajan and J. Thanusu, Res. Chem. Intermed., 33, (2007), 541-548.

[58] M. Gopalakrishnan, P. Sureshkumar, V. Kanagarajan, J. Thanusu and R. Govindaraju, J. Chem. Res., 5, (2005), 299-303.

[59] K. H. Kapadnis, S. P. Jadhav, A. P. Patil and A. P. Hiray, World J. Pharm. Pharm. Sci., 5, (2010), 1055-1063.

[60] A. Xavier and N. Srividhya, J. Appl. Chem., 7, (2014), 6-15.

[61] P. Paul, Proc. Ind. Acad. Sci., 114, (2002), 269-276.

[62] L. A. Paquette and W. A. Benjamin, Principles of modern heterocyclic chemistry, Anybook Ltd., United Kingdom, (1968).

[63] F. A. Carey and R. A. Sundberg, Advanced Organic Chemistry. ed. 5th, New York, Springer, (2007).

[64] C. Price, M. R. J. Elsegood, W. Clegg and A. Houlton A, J. Chem. Soc. Chem. Commun., (1995), 2285-2286.

[65] Q. M. Saima, M. Najma, M. Arfana, S. Rubinaand M. Y. Khuhawar, Curr. Anal. Chem., 10, (2014), 393-417.

[66] K. B. Prasanta, H. Klaus and C. Shouvik, Polyhedron, 67, (2014), 181-190.

[67] S. Muthusamy and R. Natarajan, J. Chem. Biol. Ther., 1, (2016), 1-17.

[68] E. Mohammed, M. Gamall, A. Rifat, A. J. Baitul, A. I. Mohammad, P. Daniele, H. Howard, P. Gennaro and J. Christoph, Inorg. Chem., 53, (2016), 6449-6464.

[69] D. W. Young, Heterocyclic Chemistry, ed. 1st, London, Longman group Ltd., (1975).

[70] A. Kumar and R. Kumar, Int. Res. J. Pharm., 2, (2011), 11-12.

[71] H. Keypour, M. Rezaeivala, L. Valencia, P. Perez Lourido and H. RazaKhavasi, Polyhedron, 28, (2009), 3755-3756.

[72] K. Patick and K. E. Potts, Clin. Microbiol. Rev., 11, (1998), 614-627.

[73] M. M. T. Khan, S. B. Hulligudi, S. Shukla and Z. A. Shaikh, J. Mol. Catal., 57, (1990), 301-305.

[74] D. Bose, J. Banerjee, S. K. H. Rahaman, G. Mostafa, H. K. Fun, W. R. D. Bailey, M. J. Zaworotko and B. K. Ghosh, Polyhedron, 23, (2004), 2045-2053.

[75] H. A. El-Boraey, J. Therm. Anal. Calorim., 81, (2005), 339-346.

[76] B. K. Singh, P. Mishra, B. S. Garg, Spectrochim. Acta A., 69, (2008), 361-370.

[77] S. J. Swamy, S. Pola, Spectrochim. Acta. A., 70, (2008), 929-933.

[78] P. G. Cozzi, Chem. Soc. Rev., 33, (2004), 410-421.

[79] R. Ando, S. Mori, M. Hayashi, T. Yagyu and M. Maeda, Inorg. Chim. Acta., 357, (2004), 1177-1184.

[80] E. A. Taggi, M. A. Hafez, H. Wack, B. Young, D. Ferraris and T. Lectka, J. Am. Chem. Soc. 124, (2002), 6626-6635.

[81] M. H. Abu-Shawish and M. S. Saadeh, Anal. 44, (2007), 8-15.

[82] A. Maihub, M. El-Ajaily and S. Hudere, Asian J. Chem., 19, (2007), 1-4.

[83] K. Anu, B. Suman, K. Sunil, S. Neha and S. Vipin, J. Catalysts, 2, (2 013), 1-14.

[84] C. M. da Silva, D. L. da Silva, L. V. Modolo, R. B. Alves, M. A. de Resende, C.V.B. Martins and A. de Fatima, J. Adv. Res, 2, (2011), 21-8.

[85] K. C. Gupta and A. K. Sutar, Coord. Chem. Rev., 252, (2008), 1420-1450.

[86] A. Bilici, I. Kaya and F. Dogan, J. Polym. Sci. Part. A. Polym. Chem., 47, (2009), 2977-2984.

[87] T. Lin Che, Q. Chang Gao, J. She Zhao and G. Zhang G, Chin. J. Chem., 26, (2008), 1079-1084.

[88] Gonzalez-Riopedre G, M. I. Fernandez-Garc, F. Gomez, E. orneas and M. Maneiro, Catalysts, 3, (2013), 232-246.

[89] Y. Nishibayashi, I. Takei, S. Vemara and M. Hidai, Organometallics, 18, (1999), 2291-2293.

[90] X. H. Lu**,** Q. H. Xia**,** H. J. Zhan**,** H. X. Yuan**,** C. P. Ye and K. X. Su, J. Mol. Catal., 250, (2006), 62-69.

[91] A.Y. Wageeh, A. R. Noorsaadah, S. Omar, A. Azhar and B. A. H. Sharifah, Molecules, 21, (2016), 847-852.

[92] S. Zangade, A. Shinde, S. Chavan and Y. Vibhute, J. Chem., 7, (2015), 208-214.

[93] T. Nevin, B. Ercan, Ç. Naki and B. Kenan, J. Chem. Biochem., 3, (2015), 13-29.

[94] Ü. Yasemin, Ç. Fatih, D. Esra, B. Burak and S. Kemal, J. Med. Chem., 1, (2016), 1-5.

[95] H. Qi-Meige, F. Yan, Y. Xiao-Qiang, H. Dong-Cheng and L. Jia-Cheng, Polyhedron, 109, (2016), 75-80.

[96] P. Molyneux, J. Sci. Technol., 26, (2004), 211-219.

[97] B. H. M. Mruthyunjayaswamy, G. Y. Nagesh, M. Ramesh, B. Priyanka and B. Heena, Der. Pharm. Chem., 7, (2015), 556-562.

[98] P. E. Ikechukwu and A. A. Peter, Molecules, 20, (2015), 9788-9802.

[99] K. Richa, S. Brajraj, S. Swati, N. Kumari, K. Sunanda and Mandal, World J. Pharm. Sci., 4, (2015), 696-707.

[100] A. Bharat, Makwana, N. Pratik, Dave, B. Pratik and Timbadiya, Int. J. Sci. Tech. Manag., 4, (2015), 642-652.

[101] H. Qi-Meige, F. Yan, Y. Xiao-Qiang, H. Dong-Cheng and L. Jia-Cheng, Polyhedron, 109, (2016), 75-80.

[102] J. M. Anandakumaran, L. Sundararajan, T. Jeyakumar and N.U. Mohammad, J. Am. Chem. Sci., 11, (2016), 1-14.

[103] E. S. Thamarai and S. Mahalakshmi, Int. J. Adv. Res. Dev., 2, (2017), 51-56.

[104] A. Z. El-Sonbati, M. A. Diaba, A. A. El-Bindarya, M. I. Abou-Dobara and H. A. Seyama, J. Mol. Liq., 218, (2016), 434-456.

[105] R. P. Chinnasamy, R. Sundararajan and S. J. Govindraj, Adv. Pharm. Tech. Res., 3, (2010), 342-347.

[106] M. S. Sondhi, N. Singh, Kumar, O. Lozach and L. Meijer, Bioorg. Med. Chem., 14, (2006), 3758-3765.

[107] S. V. Bhandari, K. G. Bothara, M. K. Raut, A. A. Patil and A. P. Sarkate, Med. Chem., 16, (2008), 1822-1831.

[108] R. Wang, X. Zhang, H. Song, S. Zhou and S. Li, Bioorg. Med. Chem. Lett., 24, (2014), 4304-4307.

[109] J. Ma, D. Chen and K. Lu, Eur. J. Med. Chem., 86, (2014), 257-269.

[110] G. Y. Nagesh, K. M. Raj and B. H. M. Mruthyunjayaswamy, J. Mol. Struct., 1079, (2015), 423-432.

[111] A. Kellett, M. O'Connor, M. McCann, M. McNamara, P. Lynch and G. Rosair, Dalton Trans., 40, (2011), 1024-1027.

[112] M. M. Abd-Elzaher, A. A. Mousa, H. A. Moustafa, M. M Ali and A. A. EI-Rashedy, Beni-Suef Univ. J. Basic Appl. Sci., 5, (2016), 85-96.

[113] M. M. Kamel, H. I. Ali, M. M. Anwar, N. A. Mohamed and A. M. Soliman, Eur. J. Med. Chem., 45, (2010), 572-580.

[114] L. Xin, Cai-feng Bi, Yu-hua Fan, Z. Xia, Xiang-min Meng and Lian-sheng Cui, Inorg. Chem. Comms. 50, (2014), 35-41.

[115] P. H. Wang, J. G. Keck, E. J. Lien and M. M. C. Lai, J. Med. Chem, 33, (1990), 608-614.

[116] S. K Krishnan, S. Ganguly, R. Veerasamy and B. Jan, Eur. Rev. Med. Pharmacol. Sci., 15, (2011), 673-681.

[117] R. N. Patel, K. R. Desai, P.Y. Purohit, K. S. Nimavat and K. B. Vyas, Heterocyclic lett., 2 (2012), 99-105.

[118] K. S. Kumar, S. Ganguly, R. Veerasamy and E. De Clercq, Eur. J. Med.Chem., 45, (2010), 5474-5479.

[119] Harpstrite, E. Scott, Collins, D. Silvia, A. Oksman, Goldberg, E. Daniel, Sharma and Vijay, Med. Chem., 4, (2008), 392- 395.

[120] V. Ragavendran, D. Sriram, S. K. Patel, I. V. Reddy and N. Bharathwajan., Eur. J. Med. Chem., 42, (2007), 146-151.

[121] V. K. Archana Srivastava and A. Kumar, Ind. J. Pharm. Sci., 65, (2003), 358-362.

[122] M. A. Bhat and M. A Al-Omar**,** Acta poloniae. Pharmaceutica. 68, (2011), 375-380.

[123] B. Halliwell, J. M .C. Gutteridge, Free Radicals in Biology and Medicine, ed. 2nd, Clarendon Press, Oxford, (1999).

[124] T. Bahorun, M. A. Soobrattee, V. Luximon-Ramma and O. I. Aruoma, Int. J. Med., 1, (2006), 1-17.

[125] M. Valko, C. J. Rhodes, J. Moncola, M. Izakovic and M. Mazur, Chem. Biol. Interact., 160, (2006), 1-40.

[126] D. M. Miller, G. R. Buettner and S. D. Aust, Free Radic. Biol. Med., 8, (1990), 95-108.

[127] K. Manavalan and C. Ramasamy, Physical Pharmaceutics, ed. 2nd, Vignesh Publishers, Chennai, (2001).

[128] C. G. Nagendrappa , Resonance, 10, (2005), 65-73.

[129] C. Basu, S. Chowdhury, R. Banerjee, H. S. Evans and S. Mukherjee, Polyhedron, 26, (2007), 3617-3624.

[130] E. A. Shalaby, S. M. M. Shanab and V. J. Singh, Med. Plants Res., 24, (2010), 2622-2632.

[131] R. A. Jacob, Nutrition Res., 15, (1995), 755-766.

[132] A. S. Emad and M. M. S. Sanaa, Biochem. Anal. Biochem., 10, (2013), 528-539.

[133] S. J. S. Flora, Oxid. Med. Cell. Longev., 2, (2009), 191-206.

[134] M. Carocho and I. C .F. R. Ferreira, Food Chem. Toxicol., 51, (2013), 15-25.

[135] S. Saikat, C. Raja, C. Sridhar, Y. S. R. Reddy and D. Biplab, Int. J. Pharm. Sci. Rev. Res., 3, (2017), 91-100.

[136] B. J. F. Hudson, Appl. Sci., 317, (1990), 1-18.

[137] K. Omura, J. Am. Oil Chem. Soc., 72, (1993), 1505 -1509.

[138] H. V. Kumar and N. Naik, Eur. J. Med. Chem. 45, (2010), 2-10.

[139] O. Sawant, J. Kadam and R. Ghosh, J. Herbal Med. Toxicol. 3, (2009), 39-44.

[140] E. Bendary, R. R. Francis, H. M. G. Ali, M. I. Sarwat an S. El Hady, Ann. Agri. Sci., 2, (2013), 173-181.

[141] M. Mohammadpour, A. Sadeghi, A. Fassihi, L. Saghaei, A. Movahedian and M. Rostami, J. Res. Pharma. Scie., 3, (2012), 171-179.

[142] M. J. Ajitha, S. Mohanlal, C. H. Suresh and A. Jayalekshmy, J. Agric. Food. Chem., 60, (2012), 3693-3699.

[143] F. Shahidi, P. K. Janitha and P. D. Wanasundara, Crit. Rev. Food. Sci. Nutr., 32, (1992), 67-103.

[144] T. Sawa, M. Nakao, T. Akaike, K. Ono and H. Maeda, J. Agric. Food Chem.,47, (1999), 397-402.

[145] Y. Sakihama, M. F. Cohen, S. C. Grace and H. Yamasaki, 177, (2002), 67-80.

[146] C. Yohann, A. Felix and P. Roman, J. Am. Oil. Chem. Soc., 89, (2012), 55-66

[147] M. Nardini, M. D. Aquino, G. Tomassi, V. Gentill, M. D. Felice and C. Scaccini, Free Radic. Biol. Med., 19, (1995), 541-552.

[148] M. Jang, L. Cai, G.O. Udeani, K.V. Slowing, C.F. Thomas and C.W.W. Beecher, Sci., 275, (1997), 218-220.

[149] F. Visioli, G. Bellomo, G. Montedoro and C. Galli, Atherosclerosis., 117, (1995), 25-32.

[150] J. D. Watson and F. H. C. Crick, Nature, 171, (1953), 737-738.

[151] C. Ban, B. Ramakrishnan and M. Sundaralingam, J. Mol. Biol., 236, (1994), 275-285.

[152] R. E. Dickerson, Methods Enzymol., 211, (1992), 67-111.

[153] R. E. Dickerson, H. R. Drew, B. N. Conner, M. Wing, A. V. Fratini and M. L. Kopka, Science, 216, (1982), 475-485.

[154] C. Oguey, N. Foloppe and B. Hartmann, PLoS One, 5, (2010), 15931-15936.

[155] D. Svozil, J. Kalina, M. Omelka and B. Schneider, Nucleic Acids Res., 36, (2008), 3690-3706.

[156] X. Chen, B. Ramakrishnan and M.Sundaralingam, Nat. Struct. Biol., 2, (1995), 733-735.

[157] A. Rich and S. Zhang, Nat. Rev. Genet., 4, (2003), 566-572.

[158] P. J. Mitchell and R. Tjian, Science, 245, (1989), 371-378.

[159] M. Gottesfeld, L. Neely, J. W. Trauger, E. E. Baird and P. B. Dervan, Nature, 387, (1997), 202-205.

[160] Q. Lu, J. Med. Chem., 50, (2007), 2601-2604.

[161] D. B. Živadin, B. Jovana, P. Biljana, H. Stephanie and V. E. Rudi, Dalton Trans**.,** 41, (2012), 12329-12345.

[162] V. Cepeda, M. A. Fuertes, J. Castilla, C. Alonso, C. Quevedo and J. M. Perez, Anti-Cancer Agents Med. Chem., 7, (2007), 3-18.

[163] L. S. Lerman, J. Mol. Biol., 3, (1961), 18-30.

[164] Clement, B. and Jung, F., Drug Metab. Dispos., 22, (1994), 486-497.

[165] U. Pindur, M. Haber and K. Sattler, J. Chem. Educ., 70, (1993), 263-272.

[166] M. Ganeshpandian, R. Loganathan, E. Suresh, A. Riyasdeen, M. A. Akbarsha and M. Palaniandavar, Dalton Trans., 43, (2014), 1203-1219.

[167] S. K. Kim and B. Nordén, FEBS Lett., 315, (1993), 61-64.

[168] A. Goldman, ed. 2nd, vol. 2, Oxford University Press, New York, 2, (1996), 376-378.

[169] C. Bourdouxhe, P. Colson, C. Houssier, J. P. Henichart, M. J. Waring, W. A. Dennyand C. Bailly, Anticancer Drug Des., 10, (1995), 131-154.

[170] C. Bailly and J. B. Chaires, Bioconjugate Chem., 9, (1998), 513-538.

[171] S. Neidle, Principles of Nucleic Acid Structure, Elsevier, Amsterdam, (2008), 151-158.

[172] L. Privalov, A. I. Dragan, C. Crane-Robinson, K. J. Breslauer, D. P. Remeta and C. A. S. A. Minetti, J. Mol. Biol., 365, (2007), 1-9.

[173] M. Sirajuddin, S. Ali, A. Haider, N. A. Shah, A. Shah and M. R. Khan, Polyhedron, 40, (2012), 19-31.

[174] M. Sirajuddin, S. Ali, N. A. Shah, M. R. Khan and M. N. Tahir, Spectrochim. Acta A., 94, (2012), 134-142.

[175] J. R. Lakowicz, Principles of Fluorescence Spectroscopy, ed. 3rd, Springer, New York, USA, (2006).

[176] A. Rodger, Methods Mol. Biol., 613, (2010), 37-54.

[177] M. Eriksson, B. Nordén, Methods Enzymol., 340, (2001), 68-98.

[178] T. R. Ravikumar Naik and H. S. Bhojya Naik, Int. J. Electrochem. Science, 3, (2008), 409-415.

[179] T. P. Bennett and E. Frieden, Modern Topics in Biochemistry, Macmillan, London, (1969), 43-45.

[180] J. Holum, Elements of General and Biological Chemistry, ed. 2nd, Wiley, New York, (1968).

[181] M. F. Chaplin, C. Bucke, Enzyme Technology, Science Cambridge University press, Cambridge, (1990).

[182] R. Martinek, J. Am. Med. Tech., 31, (1969), 162-168.

[183] W. W. Cleland, CRC Crit. Rev. Biochem., 13, (1982), 385-428.

[184] R. Walsh, E. Martin and S. Darvesh, Integr. Biol., 3, (2011), 1197-1201.

[185] W. W. Cleland, Biochim. Biophys. Acta., 67, (1963), 173-187.

[186] S. J. Tseng and J. P. Hsu, J. Theor. Biol., 4, (1990), 457-64.

Chapter - 2

EXPERIMENTAL TECHNIQUES, SYNTHESIS AND CHARACTERIZATION OF HETEROCYCLIC SCHIFF BASE LIGANDS

Contents

2.1 Introduction

Schiff bases are the compounds containing azomethine group (-HC=N-) which were first reported by Hugo Schiff in 1864. It is formed by condensation of a primary amine with an active carbonyl compound, and generally takes place under acid, base catalysis or with heat [1]. Schiff bases are useful chelators because of their ease of preparation, structural varieties, varied denticities and subtle steric and electronic control on the framework [2]. Schiff bases have potential sites such as nitrogen and other donor atoms, which has attributed to their stability and applications in many fields [3]. They are considered as "privileged ligands" and are most widely used due to their ease of synthesis and good solubility in common solvents [4]. In azomethine derivatives, the C=N linkage has major role in their biological activity. The nitrogen atom of azomethine may be involved in the formation of constituents and interferes in normal cell processes.

Schiff bases are considered as very important scaffolds for inorganic chemists as these are widely used in medicinal inorganic chemistry due to their diverse biological, pharmacological and antitumor activities. Schiff bases have gained much importance in biomimetic modelling applications and in liquid crystals aspect [5]. Heterocyclic scaffolds containing an azole ring system and phenol derivatives have been known to possess a wide range of biological applications such as antifungal [6], antioxidant [7], antibacterial [8], antitumor [9], anti-inflammatory [10] and antipyretic applications [11]. Schiff bases are generally excellent chelating agents. Schiff bases are also used as catalysts, intermediates in organic synthesis, dyes [12], pigments, polymer stabilizers, and corrosion inhibitors [13]. Thiophene and pyrrole nucleus has been established as the potential entity in the largely growing chemical world of heterocyclic compounds possessing promising pharmacological characteristics.

This chapter is broadly divided into two sections. Part A provides details of the reagents used and various analytical and physico-chemical techniques employed in the characterization and biological studies of ligands and its complexes. Part B gives the details of the preparation and spectral characterization of Schiff base ligands used in the present study. Single crystal X-ray studies of the Schiff bases are also included in this part.

2.2 A) Materials and Methods

2.2.1 Chemicals

2-aminophenol, 2-amino-4-nitrophenol, 2-amino-4-methylphenol, thiophene-2-carboxaldehyde and pyrrole-2-carboxaldehyde were purchased from Aldrich. Metal salts used were $Zn(CH_3COO)_2.4H_2O$ (E. Merck, GR), $Ni(CH_3COO)_2.4H_2O$ (Merck, 98%), $Cu(CH_3COO)_2.H_2O$ (E. Merck, GR).

Solvents; methanol, chloroform, acetone, acetonitrile and ethyl acetate were obtained from Merck. All materials used were of the highest purity available and used without further purification. Solvents employed were either of 99% purity or purified by known laboratory procedures [14].

2.2.2 Physico-chemical methods

2.2.2.1 Elemental analyses

Carbon, hydrogen and nitrogen analyses of all synthesized compounds were carried out using a Vario EL III CHNS analyzer at Sophisticated Test and Instrumentation Centre (SAIF), Cochin University of Science and Technology, Kochi, India. The metal content of the complexes were determined by AAS after digestion with concentrated nitric acid. The analysis were done using Thermo Electron Corporation, M series Atomic Absorption Spectrophotometer.

2.2.2.2 Electronic spectra

Electronic spectra of the ligands and their complexes were recorded in DMSO on a Thermo electron Nicolet Evolution 300 UV-Vis. spectrophotometer.

2.2.2.3 FT-IR spectroscopy

Infrared spectra were recorded on a JASCO FT-IR-5300 Spectrometer in the range 4000–400 cm^{-1}using KBr pellets. IR spectra give valuable information about the structure of the complex and nature of functional group present. IR spectra also provide valuable information regarding the mode of coordination of the ligand to the metal ion.

2.2.2.4 Conductivity measurements

Molar conductivities of the complexes in DMSO solutions (10^{-3} M) at room temperature were measured using a Systronic model 303 direct reading conductivity meter.

2.2.2.5 Magnetic susceptibility measurements

The magnetic susceptibility measurements were done at room temperature on a Magway MSB Mk 1 Magnetic Susceptibility Balance [15].

The solid sample is tightly packed into weighed sample tube with a suitable length (*l*) and noted the sample weight (*m*). Then the packed sample tube was placed into tube guide of the balance and noted the reading (*R*). The mass susceptibility, χ_g, is calculated using:

$$\chi_g = C_{Bal} * l * R - R_0 / 10^{-9} m$$

Where l = the sample length (cm)

m = the sample mass (g)

R = the reading for the tube plus sample

R_0 = the empty tube reading

C_{Bal} = the balance calibration constant

Then molar susceptibility $\chi_m = \chi_g \times$ molecular formula of the complex. Molar susceptibility corrected for diamagnetism of all the atoms present in the complex using the Pascal's constants [16-17].

The effective magnetic moment, μ_{eff}, is then calculated using the following expression:

$$\mu_{eff} = 2.84(T * X_A)^{1/2}$$

Where T is the absolute temperature and X_A is the corrected molar susceptibility

2.2.2.6 TG -DTG

TG -DTG analysis of the complexes were carried out under air and nitrogen at a heating rate of 10°C min^{-1} using a Perkin Elmer Pyris Diamond TG analyser in the temperature range of 0-800°C at Sophisticated Test and Instrumentation Centre (SAIF), Cochin University of Science and Technology, Kochi, India.

2.2.2.7 EPR spectroscopy

EPR spectra of the complexes were recorded in the solid state at RT, solid state at LNT and in DMF at LNT using Varian E-112 X-band spectrometer using TCNE (g = 2.0028) as standard at the SAIF, IIT, Mumbai, India.

2.2.2.8 NMR spectroscopy

^{1}H NMR spectra were recorded in $CDCl_3$ on a Burker Advance DRX 300 FT-NMR spectrometer with TMS as the internal standard. The ^{1}H NMR spectrum gives some important information regarding the formation of Schiff base ligands. ^{1}H NMR spectrum provides useful information about the number of different types of hydrogen present in the molecule and their electronic environment.

2.2.2.9 Mass spectrometry

Mass spectrometry is the most accurate method for determining the molecular mass of a compound. In this technique molecules are bombarded with highly energetic electrons. The molecules are ionized and broken up into many fragments. Some of which are positive ions. Each kind of ion has

a particular mass to charge ratio (m/z). It is used to prove the identity of a compound and establish structure for a new compound. It helps to establish exact molecular mass and molecular formula. It can reveal the presence of certain structural units present in a molecule. The instrument used for mass spectrometry is Waters 3100 Mass Detector using ESI technique designed for routine LC-MS analysis was recorded at Department of Applied Chemistry, Cochin University of Science and Technology, Kochi, India.

2.2.2.10 Single crystal XRD

The single crystal X-ray diffraction studies were carried out using a Bruker AXS Kappa Apex 2 CCD diffractometer, with graphite monochromated Mo Kα radiation (λ = 0.71073Å). Unit cell dimensions and intensity data were recorded at 296K. The structure was solved with direct method using SIR 92 [18] and refinement was carried out by full-matrix least squares on F^2 using SHELXL-97 [19]. The program SAINT/XPREF was used for data reduction and APEX2/SAINT for cell refinement [20]. All non–hydrogen atoms were refined anisotropically. Structures were plotted by DIAMOND software version.

2.3.1 B) Synthesis of heterocyclic Schiff bases

Six heterocyclic Schiff bases were prepared. The synthesized compounds were crystalline, colored, non-hygroscopic, and insoluble in water, soluble in ethanol, acetone, chloroform, ethyl acetate, DMF and DMSO.

2.3.1.1 Synthesis of Schiff base derived from thiophene-2-carboxaldehyde and 2-aminophenol (TA)

Thiophene-2-carboxaldehyde (18.3 mmol) in methanol (20 mL) and 2-aminophenol (18.3 mmol) in methanol (20 mL) were mixed, boiled under

reflux for 8 h. The resulting solution was concentrated and cooled. The precipitate formed was collected and recrystallized from petroleum ether by slow evaporation. The yellow single crystals were collected. The yield and melting point of the product was determined.

Scheme 2.1 Preparation of TA

2.3.1.2 Synthesis of Schiff base derived from thiophene-2-carboxaldehyde and 2-amino-4-nitrophenol (TNA)

Thiophene-2-carboxaldehyde (12.1 mmol) in methanol (20 mL) and 2-amino-4-nitrophenol (12.1 mmol) in methanol (20 mL) were mixed, boiled under reflux for 9 h. The yellow precipitate formed was collected and washed with petroleum ether and dried. Yield and melting point of the product was determined.

Scheme 2.2 Preparation of TNA

2.3.1.3 Synthesis of Schiff base derived from thiophene-2-carboxaldehyde and 2-amino-4-methylphenol (TMA)

Thiophene-2-carboxaldehyde (8.13 mmol) in methanol (20 mL) and 2-amino-4-methylphenol (8.13 mmol) in methanol (20 mL) were mixed, boiled under reflux for 8 h. The resulting solution was concentrated and

cooled. The precipitate formed was collected and recrystallized from petroleum ether. The yellow single crystals were collected. The yield and melting point of the product was determined.

Scheme 2.3 Preparation of TMA

2.3.1.4 Synthesis of Schiff base derived from pyrole-2-carboxaldehyde and 2-aminophenol (PA)

To a solution of 2-aminophenol (9.2 mmol) in methanol (20 mL), pyrrole-2-carboxaldehyde (9.2 mmol) in methanol was added drop wise. The above mixture was refluxed for 6-7 h. After completion of the reaction, cooled to room temperature and solvent was evaporated slowly. The dark brown needle like crystals was separated out. It was washed with alcohol, ether and recrystallized from ethanol. The yield and melting point of the product was determined.

Scheme 2.4 Preparation of PA

2.3.1.5 Synthesis of Schiff base derived from pyrole-2-carboxaldehyde and 2-amino-4-nitro phenol (PNA)

Methanolic solution of 2-amino-4-nitrophenol (4.03 mmol) was added to a methanolic solution of pyrrole-2-carboxaldehyde (4.03 mmol).

The mixture was refluxed for 5-7 h. Solution was evaporated slowly and the orange colored crystalline compound separated washed with ethanol and ether. The yield and melting point of the product was determined.

Scheme 2.5 Preparation of PNA

2.3.1.6 Synthesis of Schiff base derived from pyrrole-2-carboxaldehyde and 2-amino-4-methylphenol (PMA)

Methanolic solution of 2-amino-4-methylphenol (8.2 mmol) was added to methanolic solutions of pyrrole-2-carboxaldehyde (8.2 mmol). The mixture was refluxed on a boiling water bath for 5-6 h. The solution was evaporated slowly. Crystalline product obtained was filtered, washed with water, methanol and ether and recrystallized from ethanol methanol (1:1) mixture. The yield and melting point of the product was determined.

Scheme 2.6 Preparation of PMA

2.3.2 Characterizations of the Heterocyclic Schiff bases.

The synthesized Schiff-bases were characterized by elemental analysis, IR, UV–Vis, Mass, ^{13}C and ^{1}H NMR spectra and single crystal XRD.

2.3.2.1 Elemental analyses

The analytical data for the TA, TNA, TMA, PA, PNA, and PMA are given in the Table 2.1. They are in good agreement with empirical formula.

Table 2.1 Analytical data of Schiff base ligands

Compound	Empirical formula	Formula weight	m.p ^{0}C	Color (yield %)	Calculated (found %)			
					C	H	N	S
TA	$C_{11}H_9NOS$	203.26	130	Yellow 70	65 (64.71)	4.46 (4.01)	6.89 (6.88)	15.78 15.91)
TNA	$C_{11}H_8N_2O_3S$	248.26	180	Yellow 80	53.22 (53.01)	3.25 (3.30)	11.28 (11.21)	12.92 12.53)
TMA	$C_{12}H_{11}NOS$	217.29	120	Yellow 80	66.33 (66.10)	5.10 (5.01)	6.45 (6.41)	14.76 (14.69)
PA	$C_{11}H_{10}N_2O$	186.21	137	Dark brown 75	70.95 (71.02)	5.41 (4.99)	15.04 (15.39)	-
PNA	$C_{11}H_9N_3O_3$	231.21	198	Orange 76	57.14 (57.01)	3.92 (3.91)	18.71 (18.01)	-
PMA	$C_{12}H_{12}N_2O$	200.24	135	Light Yellow 70	71.98 (71.67)	6.04 (6.01)	13.99 (13.51)	-

2.3.2.2 Mass spectra

The mass spectra of ligands having peaks at MS (m/z): (M+) 204, 248, 218, 187, 232 and 201 (TA, TNA, TMA, PA, PNA and PMA respectively) confirming purity of the ligands (Figures 2.1-.2.6)

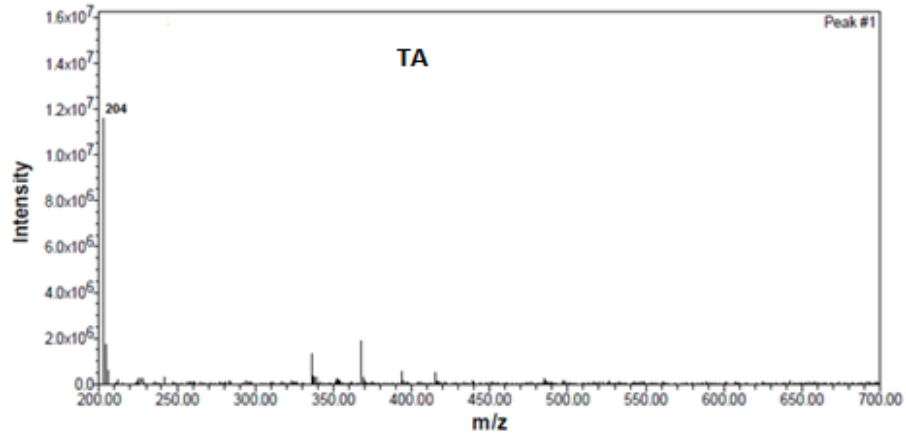

Figure 2.1 Mass Spectrum of TA.

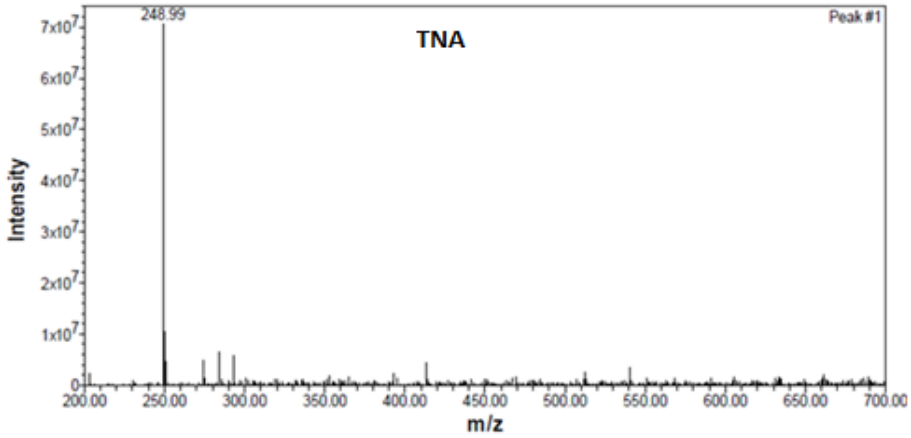

Figure 2.2 Mass Spectrum of TNA.

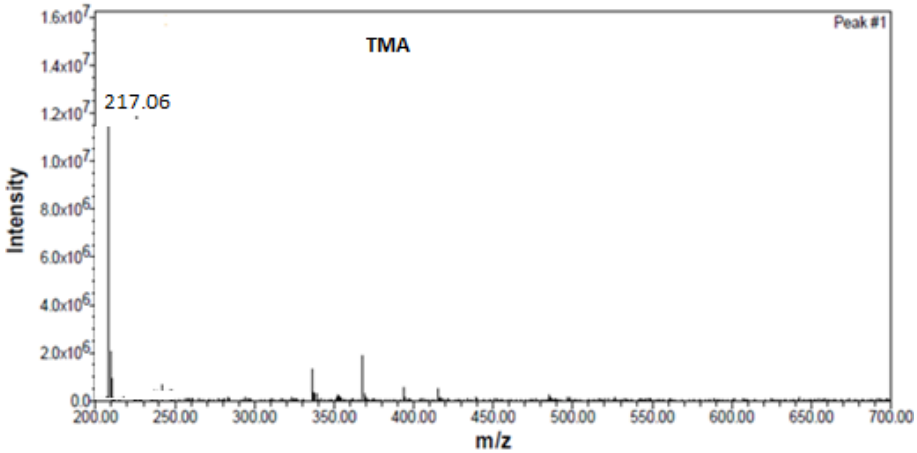

Figure 2.3 Mass Spectrum of TMA.

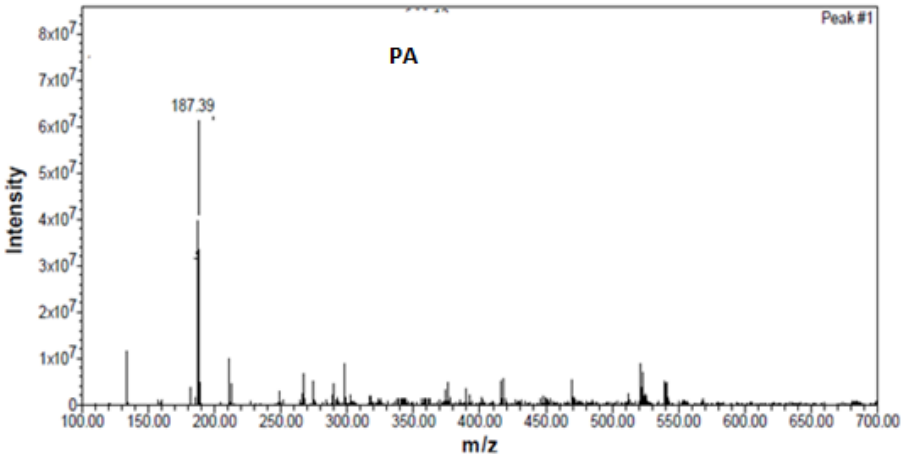

Figure 2.4 Mass Spectrum of PA.

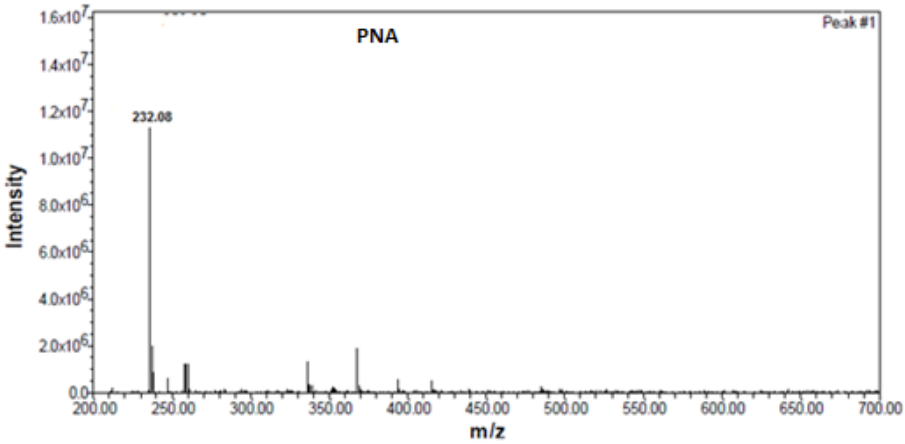

Figure 2.5 Mass Spectrum of PNA.

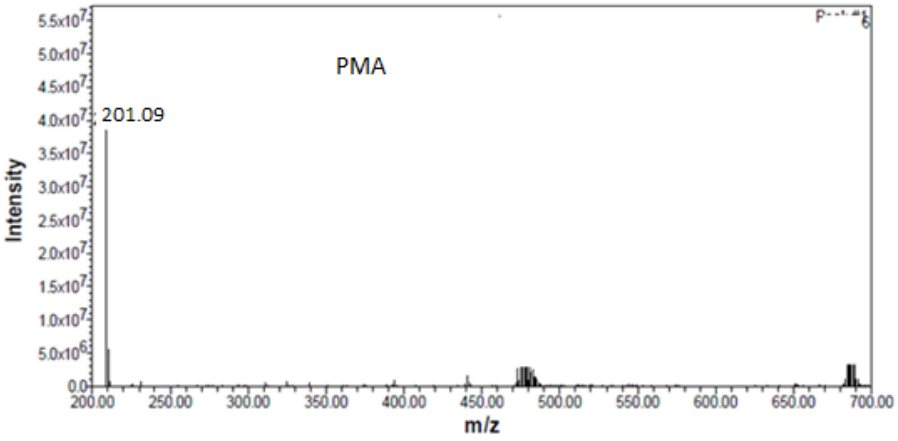

Figure 2.6 Mass Spectrum of PMA.

2.3.2.3 Infrared spectra

The IR spectra of Schiff bases (TA, TNA, TMA, PA, PNA and PMA) show strong band in the range 1659-1608cm^{-1} which can be attributed to azomethine *v*(HC=N) group [21]. The IR spectra of compounds show weak and broad band between 3450 and 3200 cm^{-1}range, which can be assigned to phenolic OH group [22]. In all three Schiff bases PA, PNA and PMA, N–H stretching frequency observed at 3377-3061cm^{-1}. In addition, the spectrum of TA, TNA and TMA showed a band resulting from C–S–C stretching of the thiophene moiety at 851 – 900 cm^{-1}[23]. Table 2.2 lists the FT-IR spectral bands of Schiff bases and corresponding spectra are given in Figures 2.7 to 2.12.

Table 2.2 Infrared spectral data of ligands (cm^{-1})

Compound	*v*(OH)	*v*(C=N)	*v*(C–S–C)	*v*(NH)
TA	3286	1608	865	-
TNA	3275	1615	876	-
TMA	3423	1625	851	-
PA	3304	1623	-	3019
PNA	3088	1650	-	3061
PMA	3320	1620	-	3078

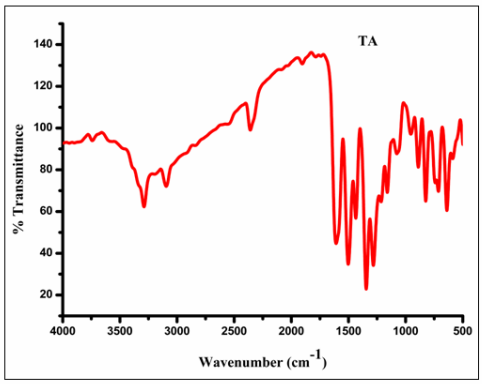

Figure 2.7 IR spectrum of TA.

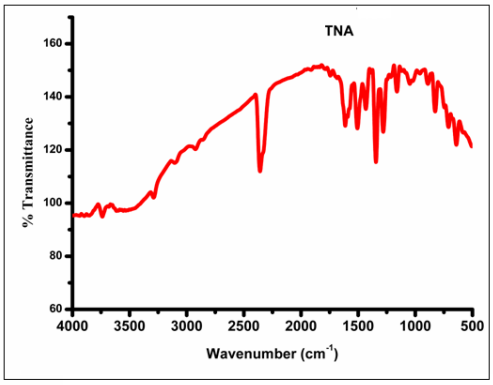

Figure 2.8 IR spectrum of TNA.

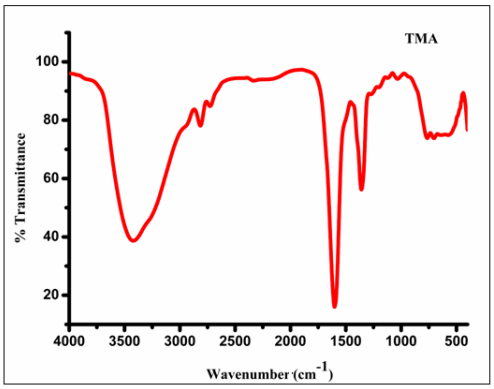

Figure 2.9 IR spectrum of TMA.

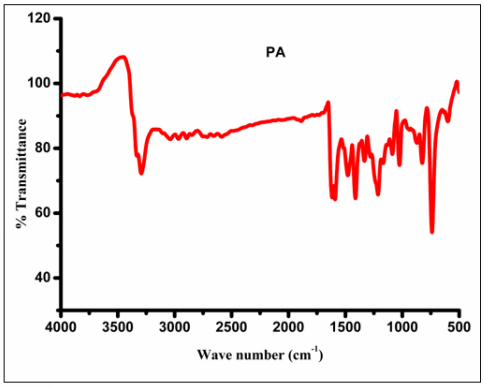

Figure 2.10 IR spectrum of PA.

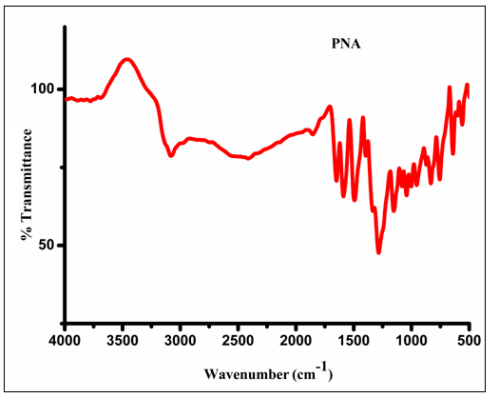

Figure 2.11 IR spectrum of PNA.

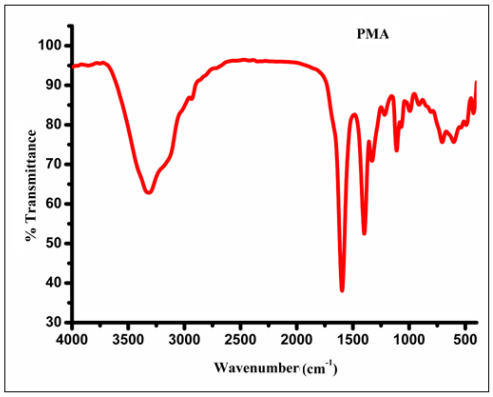

Figure 2.12 IR spectrum of PMA.

2.3.2.4 Electronic spectra

The electronic spectra of TA, TNA, TMA, PA, PNA, and PMA were taken in DMSO (10^{-5}mol L^{-1}) (Table 2.3 and Figures 2.13- 2.18). The UV–visible spectra of all the solid compounds showed two bands at 280-320 nm and 350-450 nm. The first band would be assigned to $\pi \rightarrow \pi^*$ transition within the aromatic ring. The second band would be due to $n \rightarrow \pi^*$ transition within the C=N group [24].

Table 2.3 Electronic spectral data of Schiff bases in DMSO (10^{-5} mol L^{-1})

Compound	π→ π* (nm)	n→ π* (nm)
TA	295	356
TNA	295	454
TMA	290	364
PA	299	359
PNA	302	356
PMA	269	363

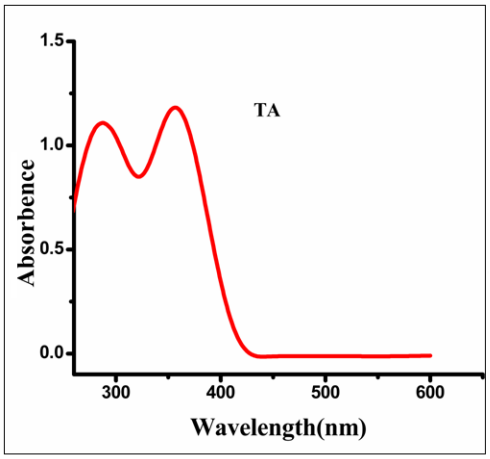

Figure 2.13 Electronic spectrum of TA.

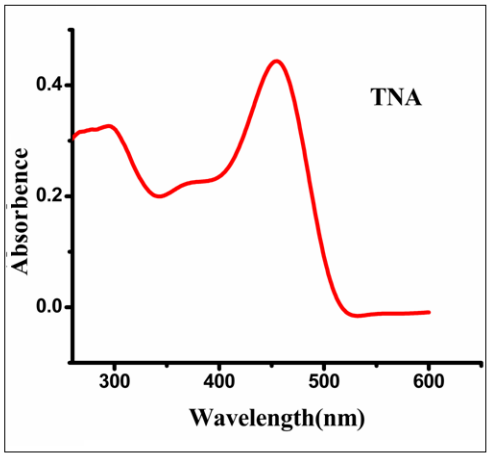

Figure 2.14 Electronic spectrum of TNA.

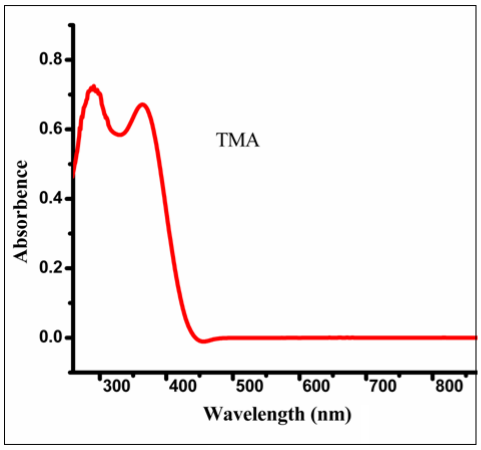

Figure 2.15 Electronic spectrum of TMA.

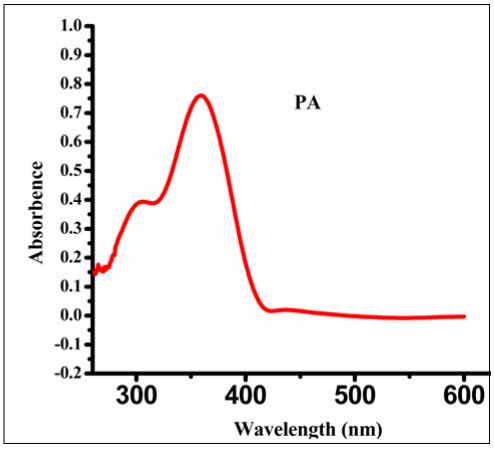

Figure 2.16 Electronic spectrum of PA.

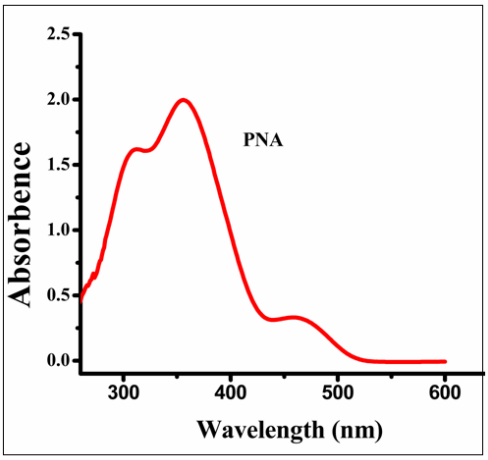

Figure 2.17 Electronic spectrum of PNA.

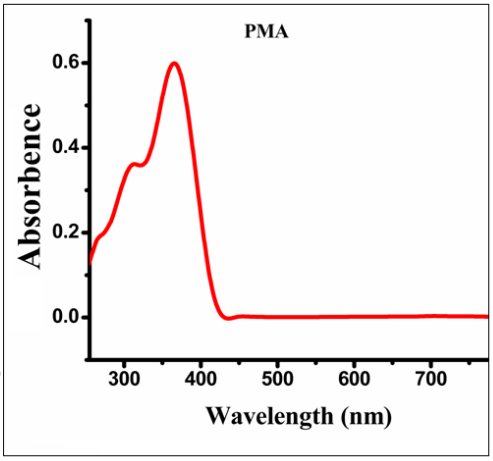

Figure 2.18 Electronic spectrum of PMA.

2.3.2.5 NMR spectra

In the ^{1}H NMR spectra, the formation of the Schiff base is supported by the presence of a singlet at δ (ppm) 8.75, 8.907, 8.74, 8.474, 8.694 and 8.430 (TA, TNA, TMA, PA, PNA and PMA respectively) corresponding to the azomethine proton (-CH=N-). Signal at 9.5-11ppm was attributed to the hydroxyl proton of the ortho-aminophenol moiety. The broadness of the signals was due to a strong hydrogen bonding between the imine N and the hydroxyl protons [25]. Aromatic protons were observed in the region 6.2 – 7.8 ppm. The ^{1}H NMR (Figures 2.19 - 2.24) and ^{13}C NMR (Figures 2.25 - 2.30) data of Schiff bases and their assignments are given in the Table 2.4.

Table 2.4 ^{1}H NMR and ^{13}C NMR spectral data of the Schiff bases

Compound	Assignments
TA	^{1}H NMR ($CDCl_3$ δppm); 6.8 (1H, q), 6.9 (1H, m), 8.7 (1H, s), 77.5 (5H, m), 10.5 (1H, broad); ^{13}C NMR (DMSO) 153 (C=N), 150 (COH), 142 (Thiophene C), 137 (ArC), 132 (Thiophene C), 130 (ArC), 128 (Thiophene C), 126 (Thiophene C), 120 (ArC), 119 (ArC), 116 (ArC).
TNA	^{1}H NMR ($CDCl_3$ δppm) ; 8.1 (1H, q), 8.2 (1H, m), 8.9 (1H, s), 7.62, 7.64 (2H, m), 7.0 (1H, d), 7.1 (1H, s) 7.2 (2H, m); ^{13}C NMR (DMSO) 158 (COH), 153 (C=N), 140 (Thiophene C), 137 (ArC), 128 (ArC), 124 (Thiophene C), 122 (Thiophene C), 119 (Thiophene C), 116 (ArC), 112 (ArC), 110 (ArC).
TMA	^{1}H NMR ($CDCl_3$ δ-ppm); 2.293 (3H, s, CH_3), 6.8-6.9 (2H, m), 7.71 (1H, m) 7.4-7.5 (3H, m), 8.7 (1H, s); ^{13}C NMR (DMSO) 158 (C=N), 152 (COH), 146 (Thiophene C), 141 (ArC), 138 (ArC), 136 (Thiophene C), 133 (ArC), 131 (Thiophene C), 128 (Thiophene C), 121 (ArC), 119 (ArC), 21 (Methyl C).
PA	^{1}H NMR ($CDCl_3$ δppm); 6.3 (1H, q); 6.7-6.9 (2H, m); 8.4 (1H, s) 77.2 (4H, m); 10.5-11 (1H, broad); ^{13}C NMR (DMSO) 152 (C=N), 146 (C-OH), 136 (Aromatic carbon (ArC)), 131 (Pyrrole C), 126 (ArC), 123 (Pyrrole C), 119 (Ar C), 116 (Ar C), 115 (Ar C), 115 (Pyrrole C), 109 (Pyrrole C).
PNA	^{1}H NMR ($CDCl_3$ δppm); 6.2 (1H, d), 6.7 (1H, d), 7(1H, d), 7.2 (1H, s), 7.9 (1H, q), 8.6 (1H, s), 8.1 (1H, d) ^{13}C NMR (DMSO) 158 (COH), 150 (C=N), 140 (ArC), 137 (ArC), 130 (Pyrrole C), 124 (ArC), 122 (Pyrrole C), 117 (ArC), 115 (ArC), 112 (Pyrrole C), 110 (Pyrrole C).
PMA	^{1}H NMR ($CDCl_3$ δ-ppm); 2.30 (3H, s, CH_3), 6.3 (1H, q), 6.9-7 (3H, m) 6.72-6.9 (2H, m), 8.4 (1H, s); ^{13}C NMR (DMSO) 158 (C=N), 146 (COH) 138 (ArC), 136 (ArC), 133 (Pyrole C), 128 (ArC), 124 (ArC), 121 (Pyrrole C) 119 (ArC), 115(Pyrrole C),111(Pyrrole C) 21(Methyl C)

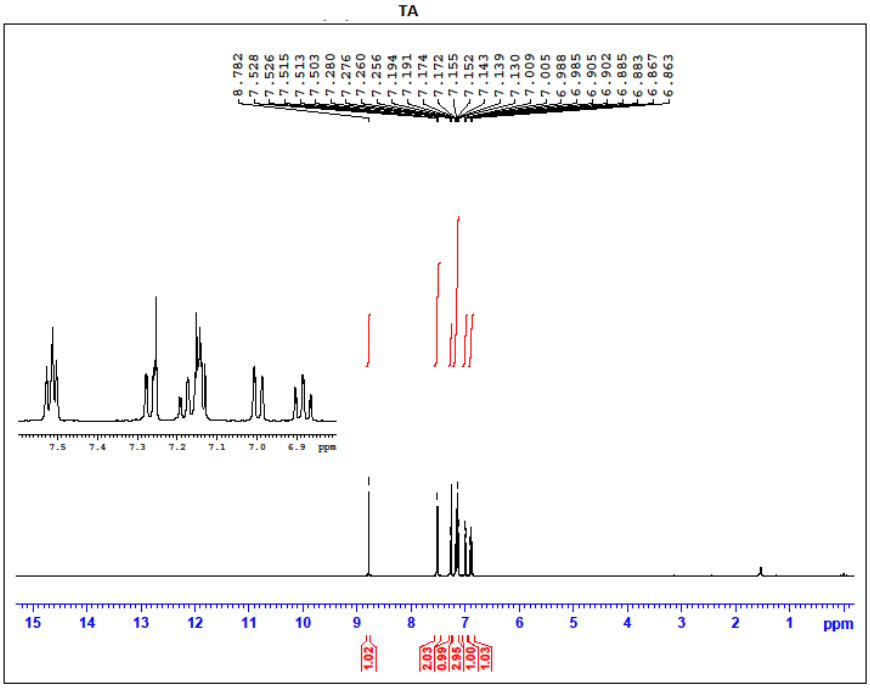

Figure 2.19 ^{1}H NMR spectrum of TA.

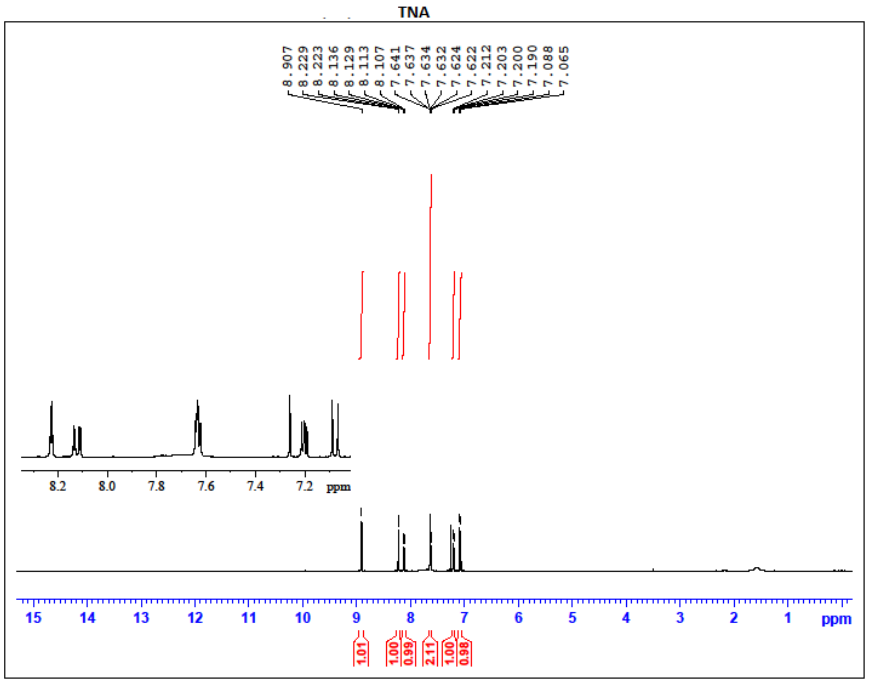

Figure 2.20 ^{1}H NMR spectrum of TNA.

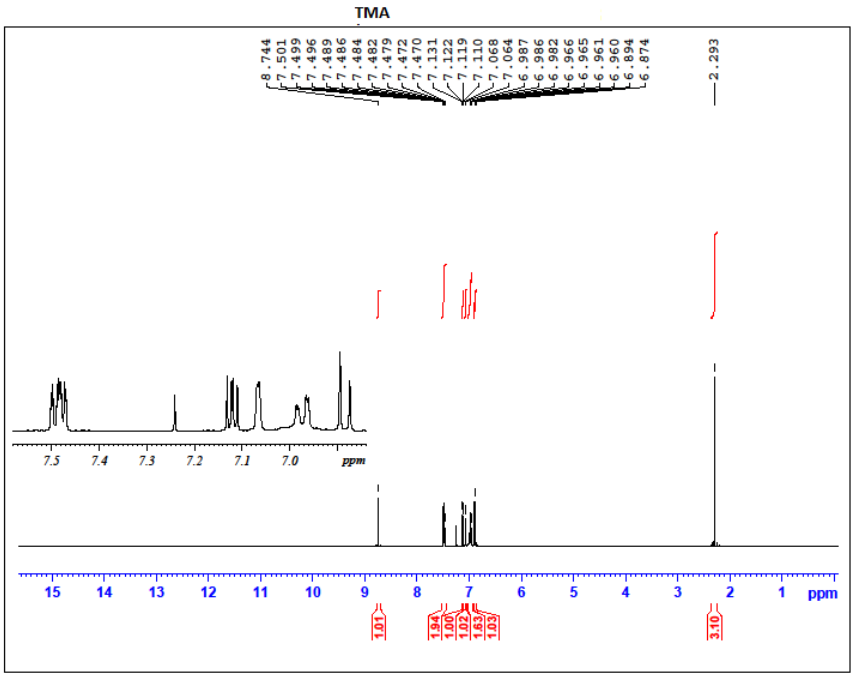

Figure 2.21 ^{1}H NMR spectrum of TMA.

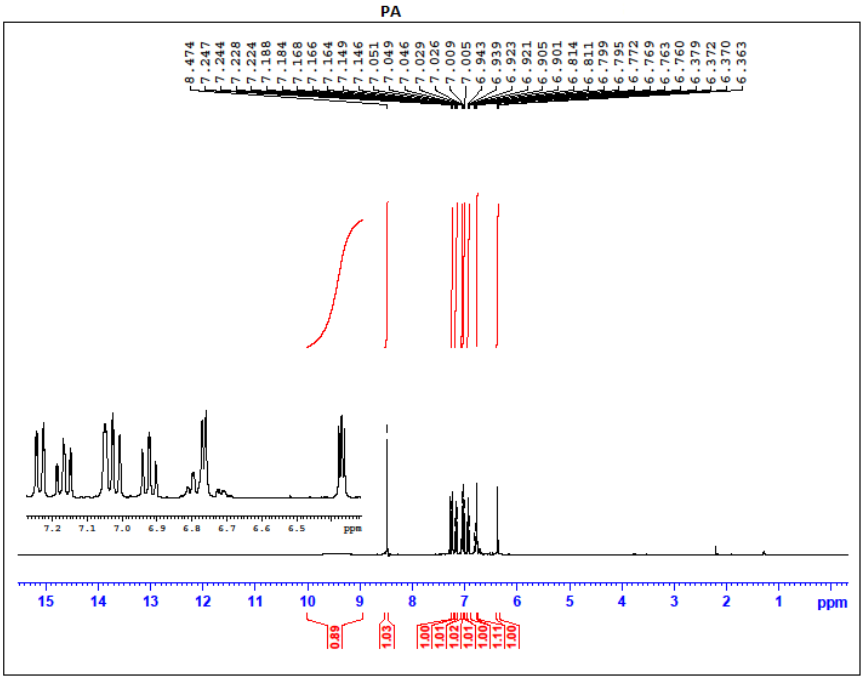

Figure 2.22 ^{1}H NMR spectrum of PA.

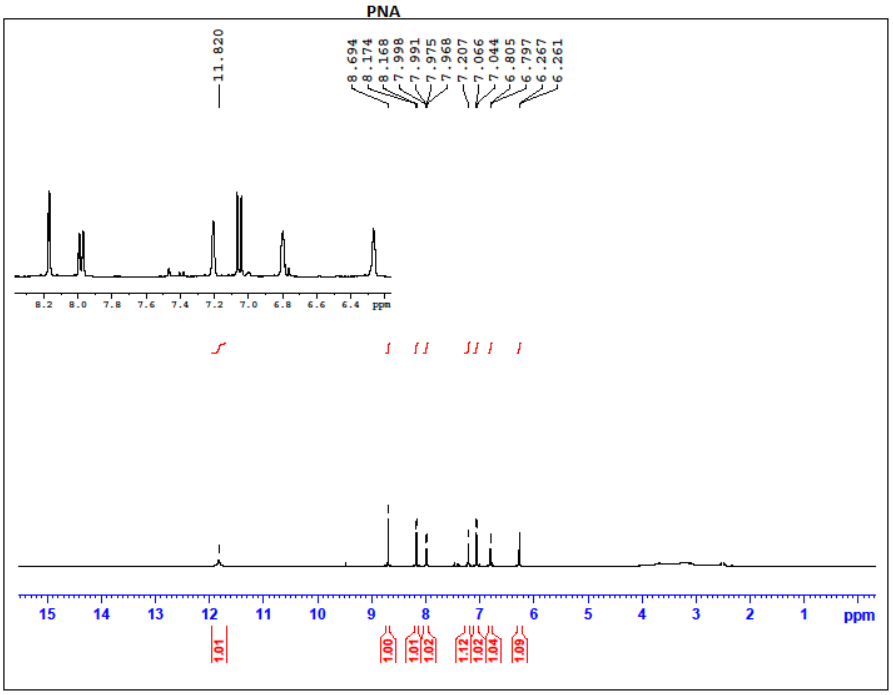

Figure 2.23 ^{1}H NMR spectrum of PNA.

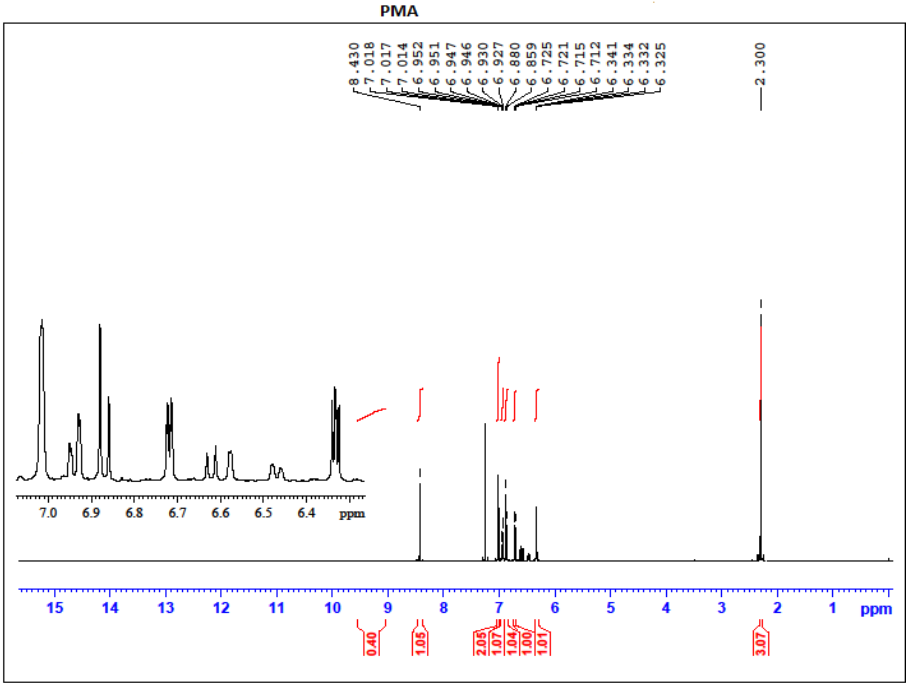

Figure 2.24 ^{1}H NMR spectrum of PMA.

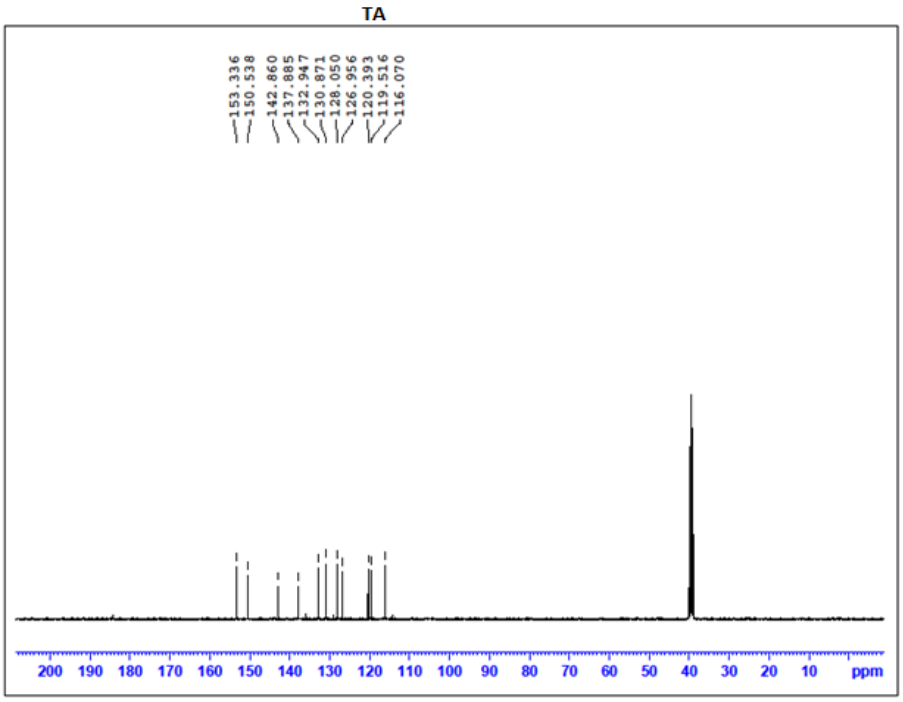

Figure 2.25 ^{13}C NMR spectrum of TA.

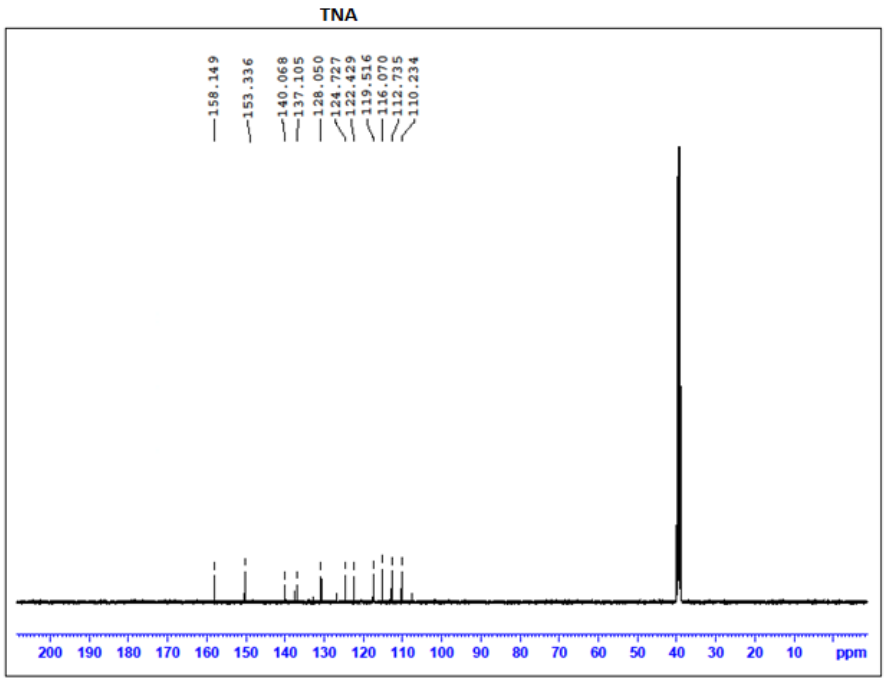

Figure 2.26 ^{13}C NMR spectrum of TNA.

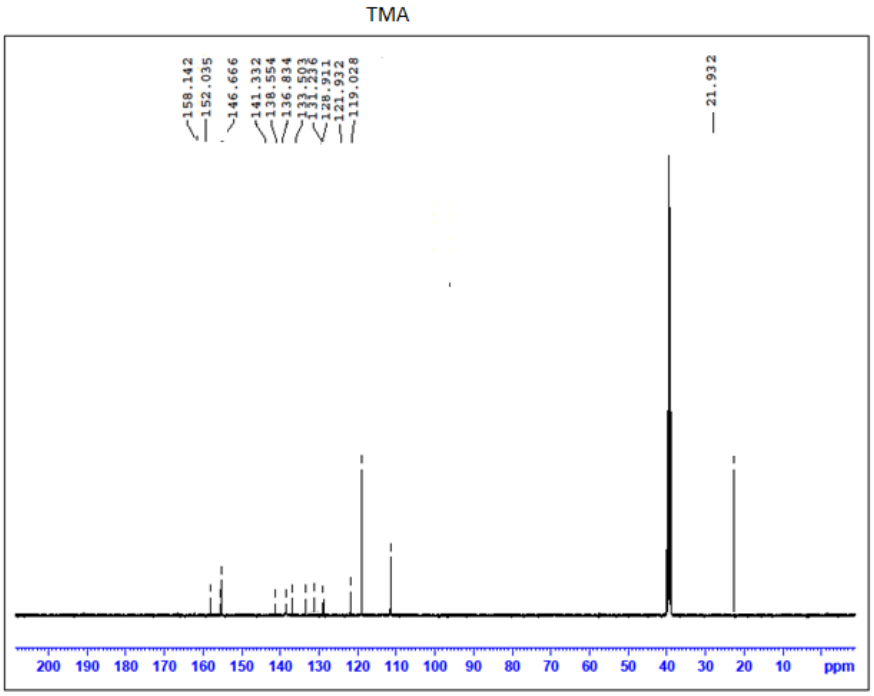

Figure 2.27 ^{13}C NMR spectrum of TMA.

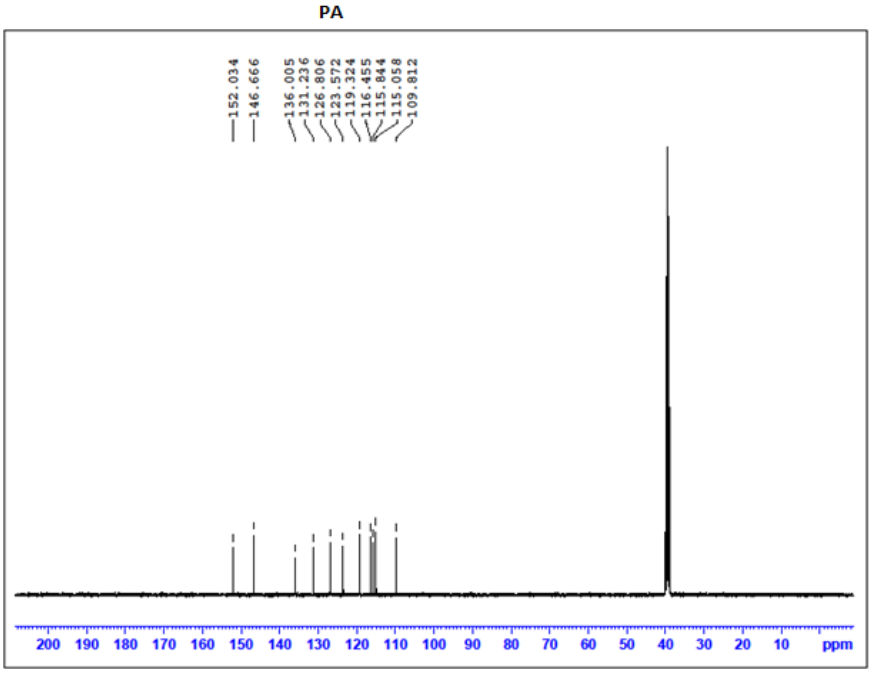

Figure 2.28 ^{13}C NMR spectrum of PA.

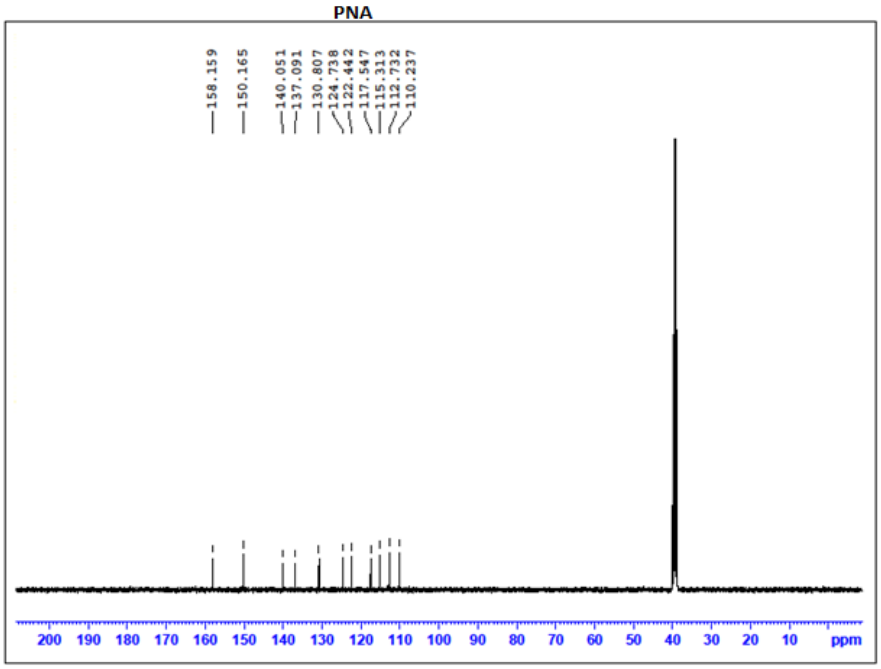

Figure 2.29 ^{13}C NMR spectrum of PNA.

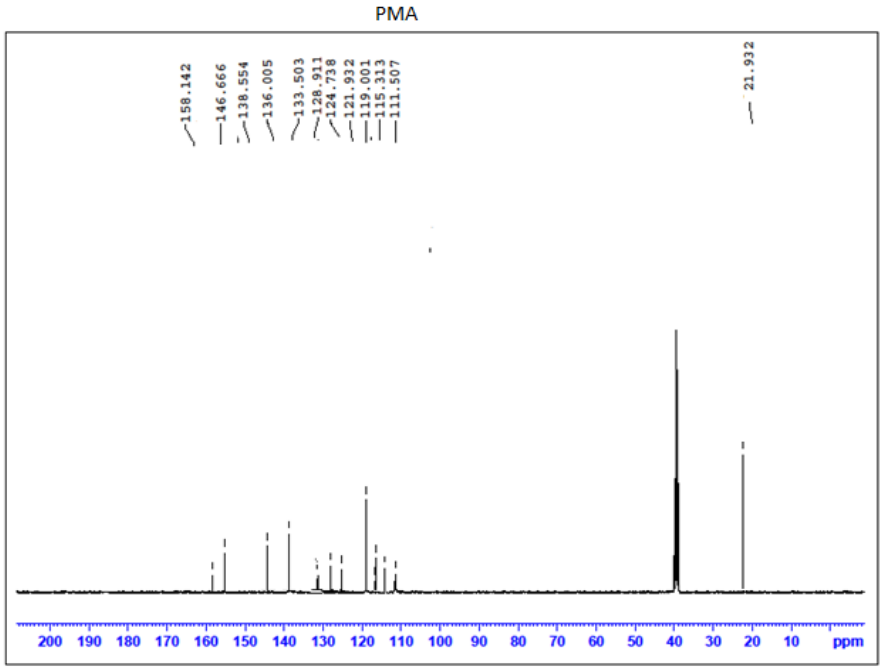

Figure 2.30 ^{13}C NMR spectrum of PMA.

2.4 Crystal structure Analysis

Two Schiff bases TA and TMA were obtained as single crystals. Slow evaporation of compounds TA and TMA which dissolved in petroleum ether at room temperature over 24 h afforded yellow color single crystals suitable for X-ray structure analysis. The technical details of data collection and some selected refinement parameters of compound TA are given in Table 2.5.

Table 2.5 Crystal data and structure refinement for TA

Empirical formula	: C_{11} H_9 N O S
Formula weight	: 203.26
Temperature	: 296(2) K
Wavelength	: 0.71073 A
Crystal system	: Orthorhombic
Space group	: *P b c a*
Unit cell dimensions	: a = 16.960(3) Å $\alpha = 90^0$
	: b = 13.429(2) Å $\beta = 90^0$
	: c = 17.576(3) Å $\gamma = 90^0$
Volume	: 4003.2(12) A^3
Z, Calculated density	: 16, 1.349 Mg/m^3
Absorption coefficient	: 0.286 mm^{-1}
F (000)	: 1696
Crystal size	: 0.35 x 0.25 x 0.25 mm
Theta range for data collection	: 2.25 to 24.20^0
Limiting indices	: $-17 \leq h \leq 19$, $-14 \leq k \leq 14$, $-20 \leq l \leq 11$
Reflections collected / unique	: 9346 / 3210 [R (int) = 0.0254]
Completeness to theta	: 24.20 87.4 %
Max. and min. transmission	: 0.9310 and 0.9180
Refinement method	: Full-matrix least-squares on F^2
Data / restraints / parameters	: 2805 / 2 / 261
Goodness-of-fit on F^2	: 1.033
Final R indices [I >2sigma(I)]	: R_1 = 0.0434, wR2 = 0.1174
R indices (all data)	: R_1 = 0.0710, wR2 = 0.1424
Largest diff. peak and hole	: 0.275 and -0.258 $e.A^{-3}$

2.4.1 Crystal structure of TA

The compound crystallizes in orthorhombic space group *Pbca*. The asymmetric unit of the ligand TA contains two independent molecules and shown in Figure 2.31. The molecules adopt the *E* conformation with respect to the azomethine C=N bond. The two crystallographically independent molecules present in the asymmetric unit of Schiff base TA possess same bond dimensions. Selected bond lengths (Å) and bond angles are shown in Table 2.6. Two intermolecular and one intramolecular hydrogen bonds (Figure 2.32) are present in the molecule (Table 2.7). The molecule also has two C–H ···π interaction with H···Cg distance of 2.92 and 2.85Å (Table 2.8).

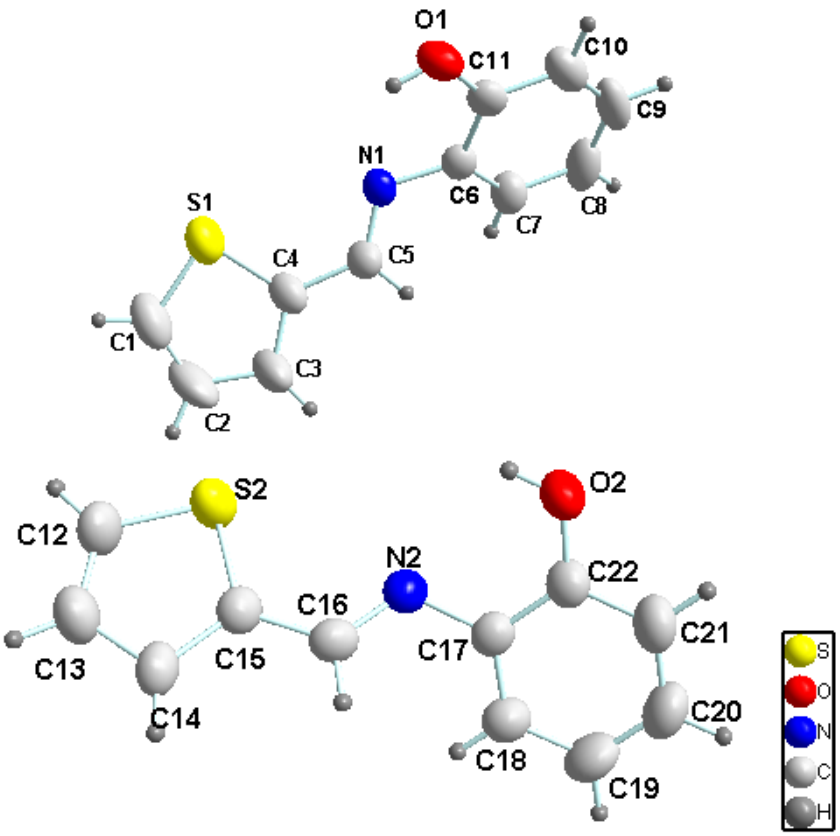

Figure 2.31 Asymmetric units of Schiff base TA.

Table 2.6 Important Bond lengths (Å) and angles (°) for TA

Bond Lengths		Bond Angles	
C16 – N2	1.275	N(2)–C(16)–C(15)	125.0
C5 – N1	1.271	N(2)–C(16)–H(16)	117.1
C15 –S2	1.719	C(13)–C(12)–S(2)	113.9
C4 – S1	1.708	S(2)–C(12)–H(12)	123.0
C11– O1	1.351	C(16)–N(2)–C(17)	118.2
C22– O2	1.352	N(1)–C(5)–H(4)	125.2

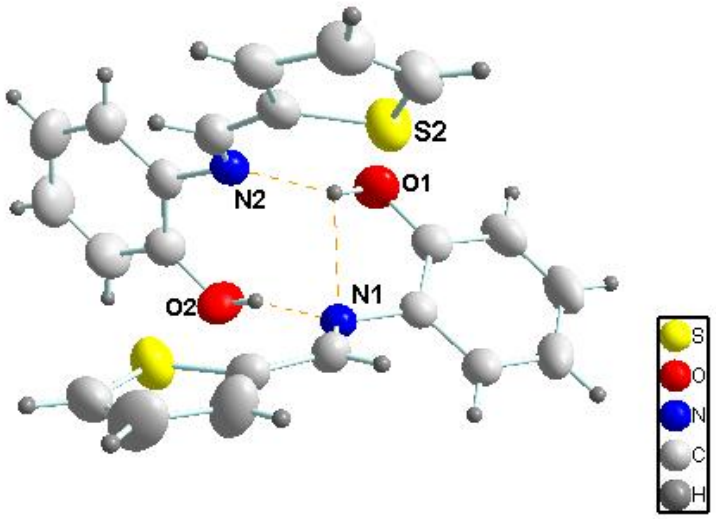

Figure 2.32 Hydrogen bonding in TA.

Table 2.7 Hydrogen bond geometry (Å)

D-H···A	d(D–H)	d(H···A)	d(D···A)	<(DHA)
O(2)–H(2') ···N(1)[a]	0.843(10)	2.820(3)	2.836(3)	168(4)
O(1)–H(1') ···N(1)	0.846(10)	2.41(4)	2.820(3)	111(3)
O(1)–H(1') ···N(2)[b]	0.846(10)	1.965(17)	2.776(4)	160(4)

Symmetry transformations used to generate equivalent atoms:

a x-1/2,-y+1/2,-z+1 b x+1/2,-y+1/2,-z+1

Table 2.8 C–H ···π interaction of TA

C–H··· π interaction	H···Cg (Å)	X···Cg (Å)
C(14) –H(14 ···Cg(2)[a]	2.92	3.766
C(21) –H(21)···Cg(2)[b]	2.85	3.711

Equivalent position code a =-1+x, y, z ; b = -1/2+x,y,1/2-z

2.4.2 Crystal structure of TMA

The technical details of data collection and some selected refinement parameters of compound TMA are given in Table 2.9

Table 2.9 Crystal data and structure refinement for TMA

Empirical formula	:	C_{12} H_{11} N O S
Formula weight	:	217.28
Temperature	:	296(2) K
Wavelength	:	0.71073 A
Crystal system	:	Triclinic
Space group	:	$P\bar{1}$
Unit cell dimensions	:	a = 8.535(7) Å α = 66.28(4)^0
	:	b = 11.358(13)Å β = 86.62(4)^0
	:	c = 13.677(17) Å γ = 69.03(3)^0
Volume	:	1128(2) A^3
Z, Calculated density	:	4, 1.279 Mg/m^3
Absorption coefficient	:	0.258 mm^{-1}
F (000)	:	456
Crystal size	:	0.50 x 0.40 x 0.20 mm
Theta range for data collection	:	2.66 to 22.00^0
Limiting indices	:	-8≤ h ≤ 7, -11≤ k ≤ 11, -14 ≤l ≤13
Reflections collected / unique	:	3392 /2763 [R (int) = 0.0202]
Completeness to theta	:	22.00 93.2 %
Max. and min. transmission	:	0.9501 and 0.8816
Refinement method	:	Full-matrix least-squares on F^2
Data / restraints / parameters	:	2574 / 2 / 281
Goodness-of-fit on F^2	:	1.035
Final R indices [I >2sigma(I)]	:	R1 = 0.0524, wR2 = 0.1278
R indices (all data)	:	R1 = 0.0744, wR2 = 0.1453
Largest diff. peak and hole	:	0.189 and -0.325 $e.A^{-3}$

The compound crystallizes in triclinic, space group $P\bar{1}$. The asymmetric units of the compound TMA along with atom numbering scheme is given in Figure 2.33. The two crystallographically independent molecules present in the asymmetric unit of Schiff base TMA possess same bond dimensions. Selected bond lengths (Å) and bond angles are shown in Table 2.10. Asymmetric unit of the compound TMA contain two independent molecules, both of which adopt the *E* conformation with respect to the azomethine C=N bond. One intermolecular and three intramolecular hydrogen bonds (Figure 2.34) are present in the molecule. (Table 2.11) The molecule also has one π···π interaction with Cg···Cg distance of 3.966 Å (Table 2.12).

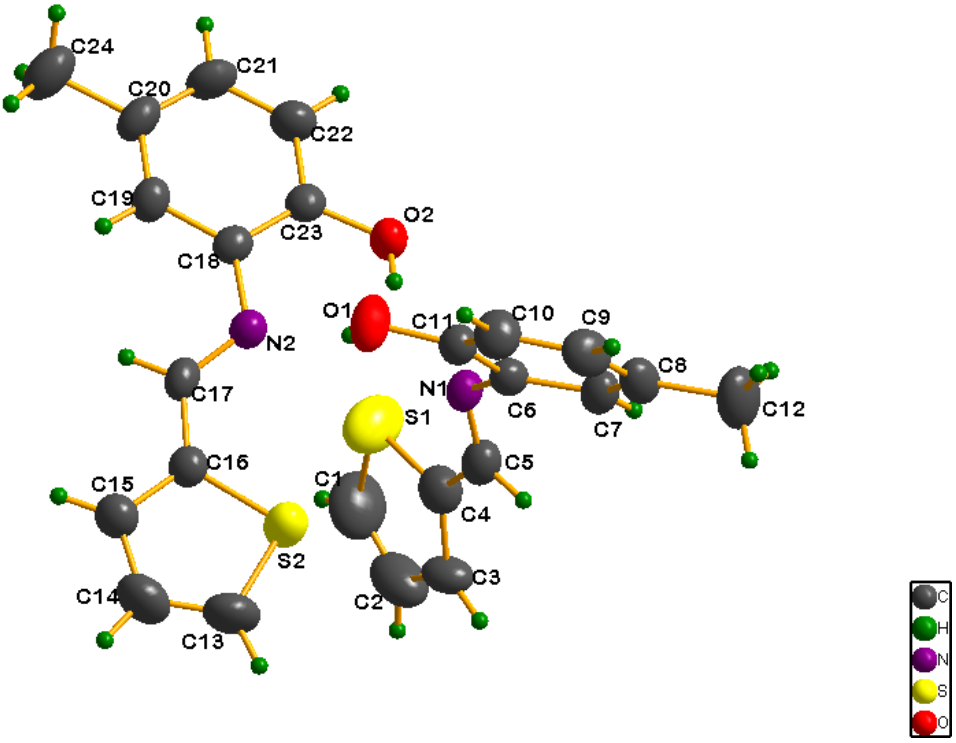

Figure 2.33 Asymmetric units of TMA with atom numbering scheme.

Table 2.10 Important Bond lengths (Å) and angles (°) for TMA

Bond Lengths		Bond Angles	
C17–N2	1.285	N(2)–C(17)–C(16)	125.0
C5 – N1	1.294	N(2)–C(17)–H(17)	117.5
C13 –S2	1.712	C(2)–C(1)–S(1)	113.2
C4 – S1	1.698	S(1)–C(1)–H(1)	123.4
C11– O1	1.377	N(1)–C(5)–H(4)	126.0
C23– O2	1.377	N(1)–C(5)–H(5)	117.0

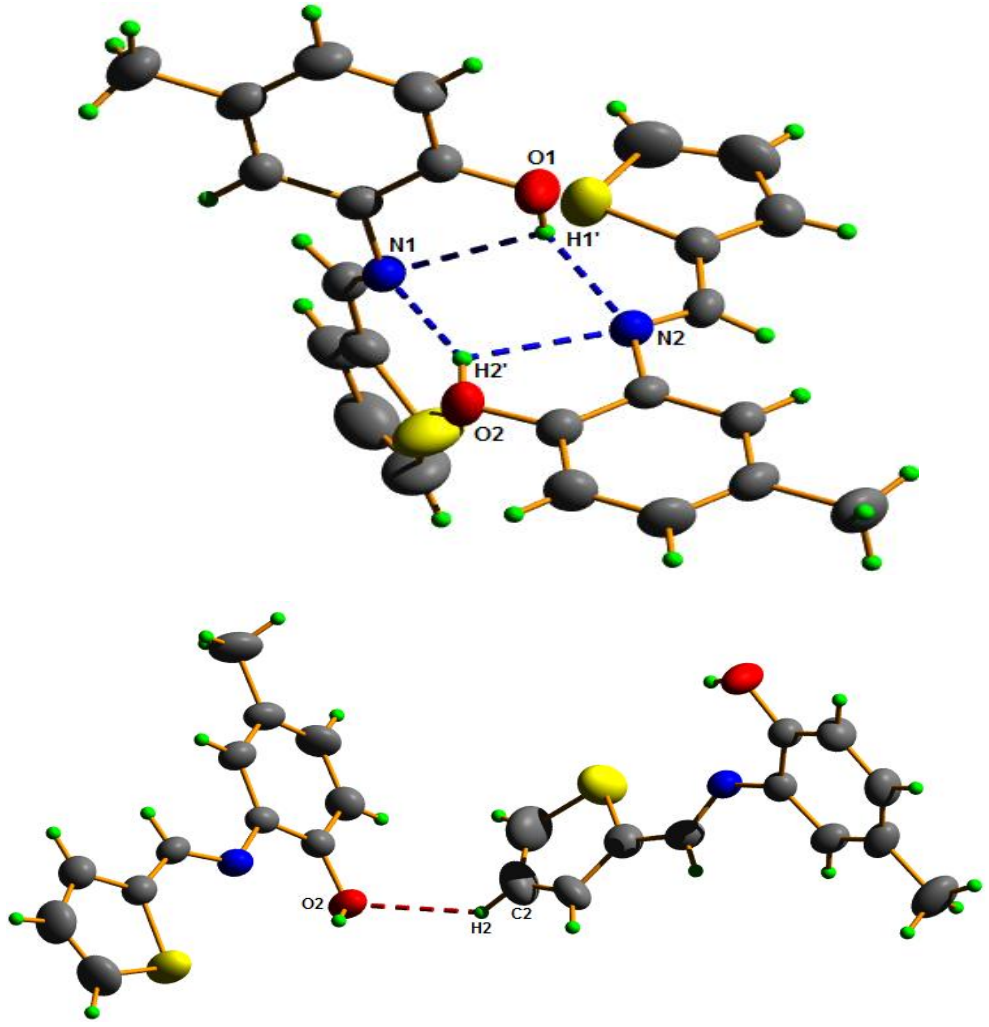

Figure 2.34 Hydrogen bonding in TMA.

Table 2.11 Hydrogen-bond geometry (Å) of TMA

D-H···A	d (D-H)	d(H···A)	d(D···A)	(D-H···A)
C(2)-H(2) ···O(2)[a]	0.93	2.64	3.355(7)	134.1
O(1)-H(1') ···N(1)	0.834(10)	2.43(4)	2.847(5)	112(3)
O(1)-H(1') ···N(2)	0.834(10)	2.09(2)	2.845(5)	150(4)
O(2)-H(2') ···N(1)	0.836(10)	2.08(3)	2.838(5)	151(6)

Symmetry transformations used to generate equivalent atoms: a x-1, y,

Table 2.12 π ···π interaction of TMA

π ···π interaction	Cg···Cg	A(Å)	B(Å)	γ(Å)
Cg(3)···Cg(4)	3.966(6)	8.2(2)	19.77	27.20

Symmetry code =1-x, 1-y, 1-z

2.5 Conclusion

This chapter deals with the details of various experimental and characterization techniques employed in the present work. Information about the synthesis and characterization of new Schiff bases derived from thiophene-2-carboxaldehyde and 2-aminophenol (TA), thiophene-2-carboxaldehyde and 2-amino-4-nitrophenol (TNA), thiophene-2-carboxaldehyde and 2-amino-4-methylphenol (TMA), pyrrole-2-carboxaldehyde and 2-aminophenol (PA), pyrrole-2-carboxaldehyde and 2-amino-4-nitro phenol (PNA), pyrrole-2-carboxaldehyde and 2-amino 4-methylphenol (PMA) was included in this chapter. The structure of TA and TMA were obtained from single crystal XRD studies. TA crystallizes in orthorhombic and TMA crystallize in triclinic. All synthesized Schiff bases were characterized by IR, UV–Visible, Mass, ^{1}H and ^{13}C NMR spectra. All these studies give good evidence for the structure of prepared compounds.

References

[1] A. Juan, P. Yaricruz, B. Alina and C. Juan, Med. Chem., 6, (2016), 467-473.

[2] T. S. Eman, Int. J. Curr. Res. Chem. Pharm. Science, 3, (2016), 118-123.

[3] A. K. Ahmad Sabry, F. Rabie Saad and M. A. Alaa El-Dine, A. J. A. C., 7, (2016), 233-245.

[4] M. R. Ummer, M. Dharmasivam, K. H. Azees, P. N. Rakesh, D. Mukesh and K. R Aziz, New J. Chem., 40, (2016), 2451-2465.

[5] M. Nath and P. K. Saini, Dalton. Trans., 40, (2011), 7077-7121.

[6] E. I. Grace, I. Terungwa, S. O. Olajire, S. Dooshima and K. Mabel Iyuana, I. J. I. S. R., 18, (2015), 117-121.

[7] M. A. Mokhles, A. L. Ammar, A. M. Hanan, A. M. Samia, M. A. Mamdouh and A. E. Ahmed, Beni-seufuniv. J. Appl. Sci., 5, (2016), 85-96.

[8] K. V. Shuvaev, L. N. Dawe and L. K. Thompson, Eur. J. Inorg. Chem., 29, (2010), 4583-4586.

[9] A. Pandey, D. S. Verma, A. Mishra and R. D. Dubey, Int. J. Chem. Tech. Res., 3, (2011), 178-184.

[10] C. Chandramouli, M. R. Shivanand, T. B. Nayanbhai, B. Bheemachari and R. H. Udupi, J. Chem. Pharm. Res., 4, (2012), 151-1159.

[11] R. P. Chinnasamy, R. Sundararajan and S. Govindaraj, J. Adv. Pharm. Technol. Res., 1, (2010), 342-347.

[12] K. M. Abuamer, A. A. Maihub, M. M. El-Ajaily, A. M. Etorki, M. M. Abou-Krisha and M. A. Almagani, Int. J. of Org. Chem., 4, (2014), 7-15.

[13] M. Sunitha, M. Padmaja, B. Anupama and C. Gyana Kumari, J. Fluoresc., 22, (2012), 1003-1012.

[14] Vogel's Textbook of Practical Organic Chemistry, ed. 5th, Longmans, London, (1989).

[15] B. N. Figgis and J. Lewis, Modern Coordination Chemistry, ed., J. Lewis and R. G. Wilkins, Interscience, New York, (1958).

[16] B. N. Figgis and J. Lewis, Progress in Inorganic Chemistry, ed. F. A. Cotton, Interscience, New York, (1964).

[17] P.W. Se1wood, Magnetochemistry, ed., 2nd, Interscience, New York, (1958).

[18] A. Altomare, M. Cascarano, C. Giacovazzo and A. Guagliardi, Appl. Crystallogr., 26, (1993), 343-345.

[19] G. M. Scheldrink, Acta Crystallogr. Sect. A, 64, (2008), 112-124.

[20] Bruker, SADABS, APEX2, SAINT, XPREP, BrukerAXS Inc., Madison, Wisconsin, USA, (2004).

[21] Y. Harinath, D. Harikishore Kumar Reddy, B. Naresh Kumar, Ch. Apparao and K. Seshaiah, Spectrochim. Acta Mol. Biomol. Spectrosc., 101, (2013), 264-272.

[22] K. S. Bibhesh, P. Anant, K. R. Hemant, B. Narendar and A. Devjani, Spectrochim. Acta Mol. Biomol. Spectrosc., 76, (2010), 376-382.

[23] R. P. Ajay, J. D. Kamini, S. R. Sambhaji, R. P. Vishwanath and S. L. Rama, J. chem. pharm. res., 4, (2012), 1413-1425.

[24] M. Shakir, A. Abbasi, M. Azam and A. U Khan, Spectrochim. Acta Mol. Biomol. Spectrosc., 79, (2011), 1866-1875.

[25] E. Akila, U. Markandan and R. Rajavel, Int. J. Pharm. Pharm. Sci., 5, (2013), 574-581.

Chapter - 3

SYNTHESIS AND CHARACTERIZATION OF Ni(II), Cu(II) AND Zn(II) HETEROCYCLIC SCHIFF BASE COMPLEXES

Contents

3.1 Introduction

The chemistry of Schiff base ligands and their metal complexes has expanded enormously and encompasses a vast area of organometallic compounds and various aspects of bioinorganic chemistry [1-3]. Schiff base ligands with heterocyclic molecule and/or containing hetero atoms such as N, O, and S show a broad biological activity and are of special interest because of the variety of ways in which they are interacted to transition metal ions [4-5]. Schiff base complexes incorporating phenolic group as chelating moieties in the ligand are considered as models for executing important biological reactions and mimic the catalytic activities of metallo enzymes [6-8]. The high stability potential of Schiff base complexes also exhibits antitumor or anti-HIV activity, to act as probes and model molecules of biochemical processes and have the ability to cleave DNA [9].

The first row transition elements play a vital role in the synthesis of several coordination complexes due to their different oxidation states which

facilitate their structural, stereo chemical, spectroscopic and electrochemical properties [10-12]. Among the various transition metals, the present study is focused on nickel, copper and zinc metal ions based on their widespread industrial and biological applications.

3.1.1 Importance of Ni(II), Cu(II) and Zn(II) complexes

Currently, the bioinorganic chemistry of nickel is a topic of increasing interest because the study of the interactions of Ni(II) with Schiff bases offers an opportunity to understand various properties of Ni(II). Since nickel compounds are present in the active sites of urease and are used extensively in the design and construction of new magnetic materials, the study of nickel compounds is of great interest in various aspects of chemistry [13-14].

Copper complexes with physiologically endogenous transition metal element centers showed various geometries, coordination numbers, various oxidation states, better solubility and higher affinity for the nucleobases [15]. Cu(II) complexes are regarded as the most promising alternatives to cisplatin as anticancer drugs [16]. The complexes of copper with Schiff bases have wide applications in food industry, dye industry, analytical chemistry, catalysis, fungicidal, agrochemical, anti-inflammable and antiradical activities [17- 18]. Copper complexes showed encouraging perspectives and displayed a significantly higher level of anticancer, antibacterial, antiproliferative and antimitotic activities for solid tumor metastases, and show general lower host toxicity than platinum compounds [19].

Zinc is an essential metal and one of the most bio-relevant transition-metal ions next to iron (human beings contain an average of approximately 2–3 g of zinc). Zn(II) cations, owing to their d^{10} electronic configuration, form

complexes with a flexible coordination environment and the geometries of these complexes can vary from tetrahedral to octahedral and severe distortions of the ideal polyhedra occur easily. Many features of zinc, such as its ability in assisting Lewis activation, nucleophile generation, fast ligand exchange, and leaving-group stabilization, make Zn(II) ideal for the catalysis of hydrolytic reactions, including DNA binding and DNA cleavage, which are important properties for use as anticancer agents [20-24].

The transition metal ions (Ni, Cu and Zn) attached to the donor atoms of the Schiff base ligand form stable metal ion complexes. Metal-based anticancer drugs exhibit enhanced selectivity and novel modes of DNA interaction, like non-covalent interactions that mimic the mode of interaction of biomolecules [25]. In recent years a number of research articles have been published on transition metal complexes of Cu(II), Ni(II) and Zn(II) with Schiff bases [26-30]. Cu(II), Ni(II) and Zn(II) complexes of Schiff-base ligand (E)-2-(5-methyl-4-phenylthiazol-2-yl)imino)methyl) phenol was synthesized and characterized. These compounds were investigated for inhibition against human TRK in vitro cytotoxicity for four human tumor cell lines. The Zn(II) complex showed potent inhibition against human TRK in the four cell lines (HepG2, MCF7, A549, HCT116) by the ratio 80, 70, 61 and 64% respectively as compared to the inhibition in the untreated cells in comparison with the reference drug (doxorubicin) [31].

New complexes of a *bis* Schiff base i.e. 3-(2-(2-hydroxy-3-methoxybenzylidene) hydrazono) indolin-2-one with Co^{2+}, Ni^{2+}, Cu^{2+} and Zn^{2+} were synthesized, characterized and were screened for their antimicrobial and antioxidant activities. It was found that for all of the complexes, the ligand coordinated with the metal center in a tridentate fashion. In the case of antimicrobial activity, the metal complexes were

found more potent than the ligand while for antioxidant activity the ligands showed more activity than the metal complexes [32].

Chaudhary and coworkers reported *in vitro* antibacterial studies of some transition metal complexes of Schiff base derived from 2-aminophenol and furan-2-carbaldehyde. The synthesized ligand, along with its metal complexes was screened for their in-vitro antibacterial activity against four bacterial pathogens (*E. coli*, *Bacillus subtilis*, *Staphylococcus aureus* and *P. vulgareous*). The results of these studies revealed that the free ligand and its metal complexes showed significant antibacterial potency [33].

3.2 Experimental

3.2.1 Materials

The details of materials used for the synthesis of Schiff base ligands and complexes have been given in Chapter2.

3.2.2 Synthesis of complexes

The transition metal complexes of heterocyclic Schiff bases were synthesized from the ligands TA, TNA, TMA, PA, PNA, and PMA which are described in Chapter 2. The following general procedure was followed to synthesize the complexes:

Methanolic solutions of the metal salts, nickel acetate (2.48 g, 0.01 mol), cupric acetate (1.99 g, 0.01 mol) and zinc acetate (2.19 g, 0.01 mol) are treated separately with each of the TA, TNA, TMA, PA, PNA and PMA (0.01 mol) in methanol. The solution was refluxed for three hours at 60°C. Ni(II) and Zn(II) complexes were precipitated in hot. While in the case of copper complexes, the precipitate was formed on slow evaporation

of the solvent. The product was washed with cold methanol and petroleum ether before drying over phosphorous pentoxide in a desiccator.

3.3 Results and discussion

The complexes formed are of fairly good stability and are found to be colored. All the complexes are insoluble in water and common organic solvents but are soluble in DMF and DMSO.

3.3.1 Elemental analysis

The analytical data of the Ni(II), Cu(II) and Zn(II) Schiff base complexes are presented in Table 3.1, 3.2 and 3.3. The analytical data of these complexes are in good agreement with the calculated values thus confirming the proposed composition for all the complexes.

Table 3.1 Analytical data of Ni(II) complexes

Complex	Formula weight	Color (yield %)	Element analysis Found (calc)%				% of metal found (calc)
			C	H	N	S	M
$[Ni(TA)_2(H_2O)_2]$	499.22	Dark Brown (70)	52.61 (52.93)	4.01 (4.04)	5.65 (5.61)	11.54 (11.76)	12.65 (12.80)
$[Ni(TNA)_2(H_2O)_2]\cdot 2H_2O$	625.01	Yellow (75)	42.04 (42.26)	3.21 (3.35)	8.94 (8.96)	10.06 (10.28)	9.21 (9.39)
$[Ni(TMA)_2]\cdot 3H_2O$	545.00	Yellow (69)	52.58 (52.86)	4.51 (4.81)	5.64 (5.45)	11.01 (11.06)	10.55 (10.05)
$[Ni(PA)_2]\cdot H_2O$	447.11	Dark green (70)	60.34 (59.10)	4.01 (4.51)	12.97 (12.53)	-	13.65 (13.13)
$[Ni(PNA)_2]\cdot 2H_2O$	555.12	Orange (75)	47.34 (47.60)	3.03 (3.63)	15.12 (15.14)	-	10.15 (10.57)
$[Ni(PMA)_2]$	457.15	Dark green (70)	62.85 (63.05)	4.55 (4.85)	12.17 (12.26)	-	12.42 (12.84)

Table 3.2 Analytical data of Cu(II) complexes

Complex	Formula weight	Color (yield %)	Element analysis Found (calc)%				% of metal found (calc)
			C	H	N	S	M
$[Cu(TA)_2H_2O]\cdot H_2O$	504.08	Dark brown (75)	52.01 (52.42)	3.88 (4.01)	5.76 (5.56)	11.77 (12.02)	12.88 (12.61)
$[Cu(TNA)_2]\cdot 2H_2O$	594.07	Dark brown (75)	44.01 (44.48)	2.99 (3.05)	9.58 (9.43)	9.65 (10.01)	10.50 (10.22)
$[Cu(TMA)_2]\cdot H_2O$	514.19	Dark brown (70)	56.35 (56.07)	3.94 (4.31)	5.50 (5.45)	11.92 (12.40)	12.01 (12.36)
$[Cu(PA)_2H_2O]\cdot 2H_2O$	487.99	Black (70)	53.94 (54.15)	4.51 (4.96)	11.21 (11.48)	-	12.89 (13.02)
$[Cu(PNA)_2]\cdot 3H_2O$	577.99	Black (70)	45.23 (45.72)	3.64 (3.84)	14.11 (14.54)	-	10.40 (10.99)
$[Cu(PMA)_2]\cdot H_2O$	480.00	Dark green (68)	58.86 (60.05)	4.78 (5.04)	11.96 (11.67)	-	13.70 (13.24)

Table 3.3 Analytical data and molar conductance data of Zn(II) complexes

Complex	Formula weight	Color (yield %)	Element analysis Found (calc)%				% of metal found (calc)	Molar conductance ($Ohm^{-1}\ cm^2\ mol^{-1}$)
			C	H	N	S	M	
$[Zn(TA)_2]$	469.93	Dark brown (70)	56.01 (56.23)	3.2 (3.43)	5.94 (5.96)	12.99 (13.93)	13.01 (13.93)	6.4
$[Zn(TNA)_2]$	559.91	Orange (75)	47.52 (47.19)	2.10 (2.52)	10.05 (10.01)	11.00 (11.45)	10.8 (11.02)	3.7
$[Zn(TMA)_2]$	497.97	Dark brown (68)	57.84 (57.89)	4.08 (4.05)	5.68 (5.63)	12.59 (12.88)	13.50 (13.10)	5.6
$[Zn(PA)_2]$	435.81	Yellow (70)	59.51 (60.63)	3.61 (4.16)	12.78 (12.86)	-	14.84 (15.01)	4.0
$[Zn(PNA)_2]$	525.83	Orange (70)	50.15 (50.25)	3.01 (3.07)	15.92 (15.98)	-	12.01 (12.44)	5.9
$[Zn(PMA)_2]$	463.86	Green (72)	61.90 (62.11)	4.78 (4.53)	12.03 (12.08)	-	13.90 (14.10)	3.5

3.3.2 Conductivity Measurements

The complexes were dissolved in DMSO and molar conductivities of 10^{-3} M of their solutions at room temperature were measured. The molar conductivity values are given in Table 3.4, 3.5 and 3.3 for the Ni(II), Cu(II) and Zn(II) complexes respectively. The conductance values for all complexes are in the range 3-20 $Ohm^{-1}cm^2$ mol^{-1} in DMSO and are in accordance with those reported for non-electrolytes in this solvent [34]. The molar conductivities show that ions are not present in the outer coordination sphere. Analytical data and molar conductance values for Zn^{2+} complex sufficiently supports the tetrahedral geometry for Zn^{2+} complex because it is well known that the Zn^{2+} generally forms tetrahedral complexes because of its d^{10} electronic configuration.

Table 3.4 Magnetic moment values and molar conductance data of Ni(II) complexes

Complex	Molar conductance ($ohm^{-1}cm^2mol^{-1}$)	μ_{eff} (B.M.)
$[Ni(TA)_2(H_2O)_2]$	7.0	2.96
$[Ni(TNA)_2(H_2O)_2]\cdot 2H_2O$	5.2	2.91
$[Ni(TMA)_2]\cdot 3H_2O$	3.3	3.69
$[Ni(PA)_2]\cdot H_2O$	4.6	3.66
$[Ni(PNA)_2]\cdot 2H_2O$	3.2	3.60
$[Ni(PMA)_2]$	20	3.57

Table 3.5 Magnetic moment values and molar conductance data of Cu(II) complexes

Complex	Molar conductance ($ohm^{-1}cm^2mol^{-1}$)	μ_{eff} (B.M.)
$[Cu(TA)_2H_2O]\cdot H_2O$	6	1.89
$[Cu(TNA)_2]\cdot 2H_2O$	11.1	1.88
$[Cu(TMA)_2]\cdot H_2O$	7.8	1.91
$[Cu(PA)_2H_2O]\cdot 2H_2O$	6.6	1.71
$[Cu(PNA)_2]\cdot 3H_2O$	18.4	1.87
$[Cu(PMA)_2]\cdot H_2O$	12.2	1.94

3.3.3 Magnetic susceptibility studies

For Ni(II), and Cu(II) complexes, the magnetic susceptibility measurements were carried out, and obtained data are presented in Table 3.4 and 3.5. From the results they were found to be paramagnetic in nature. In paramagnetic Ni(II) and Cu(II) complexes, often the magnetic moment (μ_{eff}) gives the spin only value [$s= (n(n+2))^{½}$ B.M.] corresponding to the number of unpaired electron. The variation from the spin only value is attributed to the orbital contribution and it varies with the nature of coordination and consequent delocalization [35]. Ni(II) has the electronic configuration $3d^8$ and should exhibit a magnetic moment higher than that expected for two unpaired electrons in octahedral (2.8 - 3.2 B.M.) and tetrahedral (3.4 - 4.2 B.M.) complexes, whereas its square planar complexes would be diamagnetic. The magnetic moment observed for the complexes $[Ni(TA)_2(H_2O)_2]$ and $[Ni(TNA)_2(H_2O)_2]\cdot 2H_2O$ were 2.96 and 2.91 B.M. which is consistent with the octahedral stereochemistry of the complex [36]. The magnetic moment of other Ni(II) complexes lies within the region 3.5 - 3.7 B.M. (Table 3.4) expected for tetrahedral complexes.

Magnetic moment (μ_{eff}) values of all copper(II) complexes were found to be in the range from 1.7 - 1.9 B.M. (Table 3.5) corresponding to one unpaired electron and this is an indication of monomeric compounds with square pyramidal or square planar geometry [37]. The copper(II) ion ($3d^9$) has one unpaired electron in the 3d shell, therefore its compounds were considered to have magnetic moments close to the spin-only value, 1.73 B.M. but due to spin orbit coupling, higher values are often observed [38] .

Due to completely filled 'd' shell as expected for Zn(II) ion, it exhibits diamagnetic nature. The present Zn(II) complexes are found to be diamagnetic in nature for tetrahedral geometry [39].

3.3.4 Infrared spectra

The infrared spectra for the present compounds taken in the range 4000-400 cm^{-1} help to indicate regions of absorption vibrations. The main stretching modes are for *ν*(OH)**,** *ν*(C=N), *ν*(C–O), *ν*(M–N) and *ν*(M–O). Comparison of the diagnostic bands in the infrared spectra of the ligands and its metal complexes adequately support the mode of coordination of the ligands with the metal ions [40]. The position and/or the intensities of these peaks are expected to change upon chelation. The infrared spectra of the complexes are given in Figures 3.1 - 3.18 and tentative assignments of these bands are given in Table 3.6, 3.7 and 3.8. Infrared spectrum of the ligands, (TA, TNA, TMA, PA, PNA and PMA) showed bands in the region 3450-3088 cm^{-1}, which can be attributed to phenolic OH group [41]. The involvement of deprotonated phenolic moiety in the complexation process is confirmed by the shift of *ν*(C–O) stretching band to a lower frequency to the extent 10-20 cm^{-1} [42]. The shift of *ν*(C–O) band at to a lower frequency suggests the weakening of *ν*(C–O) and formation of stronger M–O bond. A strong band at 1608, 1615, 1625, 1623,

1650 and 1620 cm^{-1} was assigned to the stretching vibration of azomethine *v*(C=N) for ligands TA, TNA, TMA, PA, PNA and PMA respectively [43]. On complex formation the band corresponding to *v*(C=N) shifted towards lower side (*v* - 20 cm^{-1}) indicating that the coordination takes place through azomethine nitrogen. Bands observed in Ni(II) and Cu(II) complexes in the region 3418-3304 cm^{-1} assigned for *v*(OH/H_2O) evidenced the presence of coordinated water molecules [44]. The existence of water of coordination in the spectra of the Ni(II) and Cu(II) complexes render it difficult to get conclusion from the *v*(OH) group of the ligands, which will be overlapped by those of the water molecules. But in the case of Zn(II) complexes, the band due to OH stretching vibration is absent.

Table 3.6 Characteristic infrared spectral bands (cm^{-1}) for Ni(II) complexes

Compound	***v*(OH)**	***v*(C=N)**	***v*(C–O)**
TA	3286	1608	1224
$[Ni(TA)_2 (H_2O)_2]$	3307	1588	1204
TNA	3275	1615	1277
$[Ni(TNA)_2(H_2O)_2]\cdot 2H_2O$	3402	1589	1193
TMA	3423	1625	1261
$[Ni(TMA)_2]\cdot 3H_2O$	3470	1595	1214
PA	3304	1623	1264
$[Ni(PA)_2]\cdot H_2O$	3436	1602	1247
PNA	3088	1650	1284
$[Ni(PNA)_2]\cdot 2H_2O$	3314	1595	1267
PMA	3320	1620	1280
$[Ni(PMA)_2]$	-	1602	1254

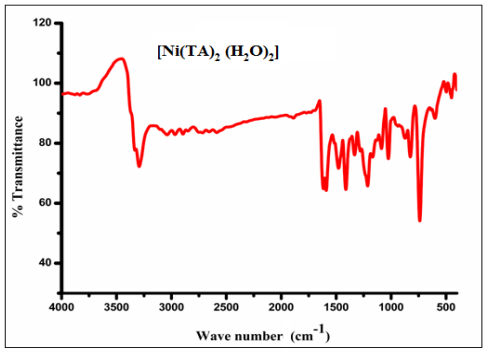

Figure 3.1 IR spectrum of $[Ni(TA)_2(H_2O)_2]$.

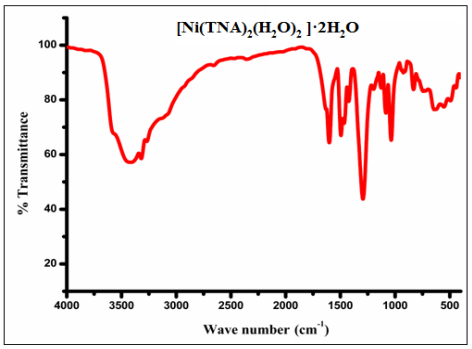

Figure 3.2 IR spectrum of $[Ni(TNA)_2(H_2O)_2]\cdot 2H_2O$..

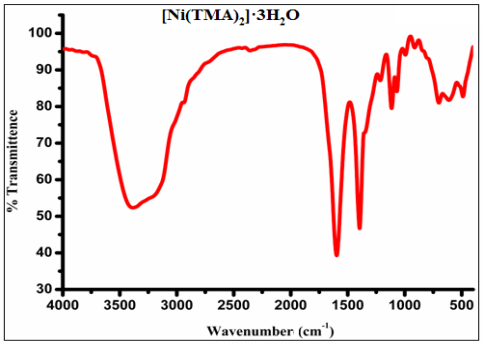

Figure 3.3 IR spectrum of $[Ni\ (TMA)_2]\cdot 3H_2O$.

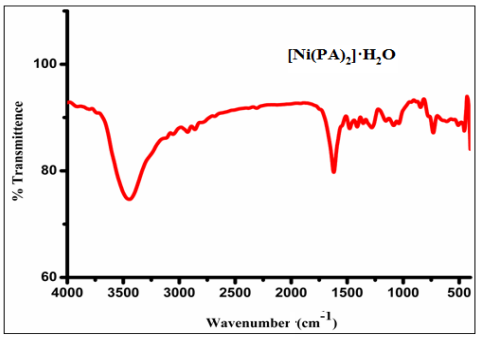

Figure 3.4 IR spectrum of $[Ni(PA)_2]\cdot H_2O$.

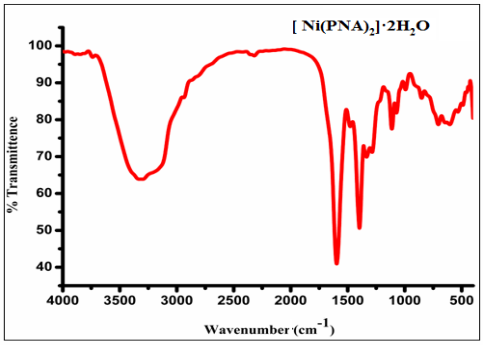

Figure 3.5 IR spectrum of $[Ni(PNA)_2]\cdot 2H_2O$.

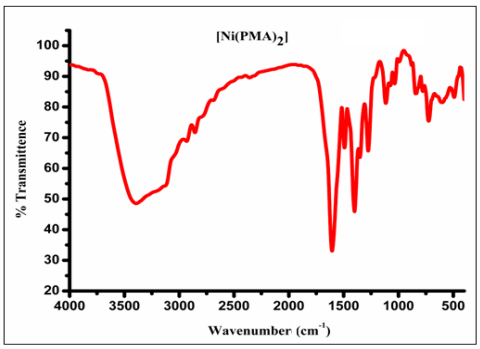

Figure 3.6 IR spectrum of $[Ni(PMA)_2]$.

Table 3.7 Characteristic infrared spectral bands (cm^{-1}) for Cu(II)complexes

Compound	*ν*(OH)	*ν*(C=N)	*ν*(C–O)
TA	3286	1608	1224
$[Cu(TA)_2.H_2O]\cdot H_2O$	3341	1568	1124
TNA	3275	1615	1277
$[Cu(TNA)_2]\cdot 2H_2O$	3429	1581	1227
TMA	3423	1625	1261
$[Cu(TMA)_2]\cdot H_2O$	3468	1574	1234
PA	3304	1623	1264
$[Cu(PA)_2H_2O]\cdot 2H_2O$	3354	1602	1213
PNA	3088	1650	1284
$[Cu(PNA)_2]\cdot 3H_2O$	3418	1594	1268
PMA	3320	1620	1280
$[Cu(PMA)_2]\cdot H_2O$	3382	1580	1224

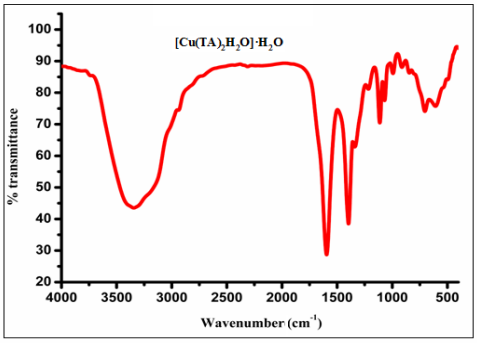

Figure 3.7 IR spectrum of $[Cu(TA)_2H_2O]\cdot H_2O$.

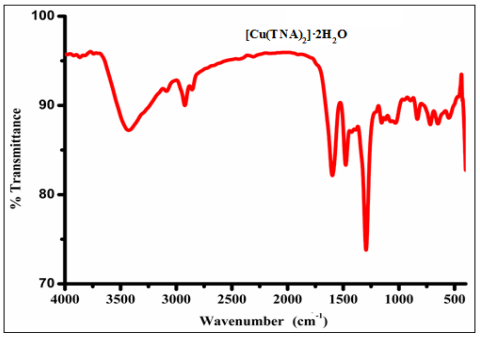

Figure 3.8 IR spectrum of $[Cu(TNA)_2]\cdot 2H_2O$.

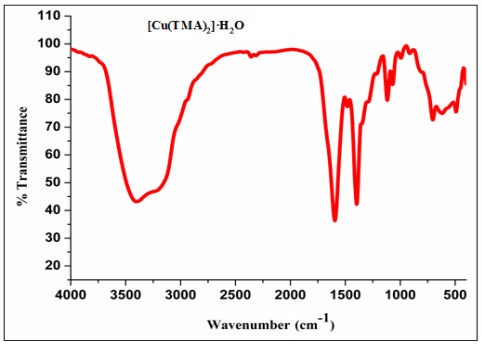

Figure 3.9 IR spectrum of $[Cu(TMA)_2]\cdot H_2O$.

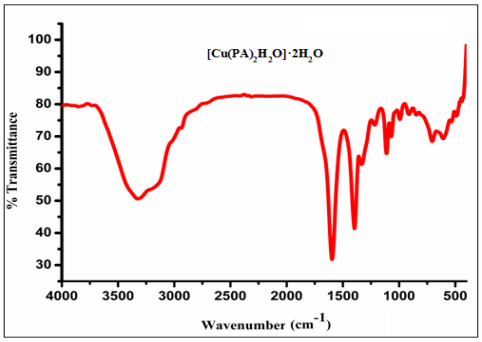

Figure 3.10 IR spectrum of $[Cu(PA)_2H_2O]\cdot 2H_2O$.

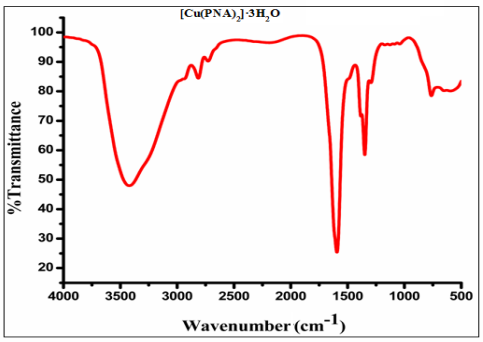

Figure 3.11 IR spectrum of $[Cu(PNA)_2]\cdot 3H_2O$.

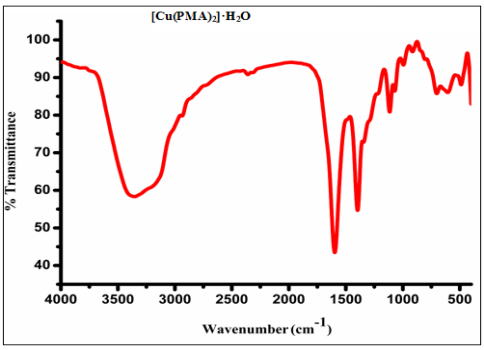

Figure 3.12 IR spectrum of $[Cu(PMA)_2]\cdot H_2O$.

Table 3.8 Characteristic infrared spectral bands (cm^{-1}) for Zn(II) complexes

Compound	*ν*(OH)	*ν*(C=N)	*ν*(C-O)
TA	3286	1608	1224
$[Zn(TA)_2]$	-	1598	1104
TNA	3275	1615	1277
$[Zn(TNA)_2]$	-	1582	1260
TMA	3423	1625	1261
$[Zn(TMA)_2]$	-	1594	1249
PA	3304	1623	1264
$[Zn(PA)_2]$	-	1609	1227
PNA	3088	1650	1284
$[Zn(PNA)_2]$	-	1581	1245
PMA	3320	1620	1280
$[Zn(PMA)_2]$	-	1602	1271

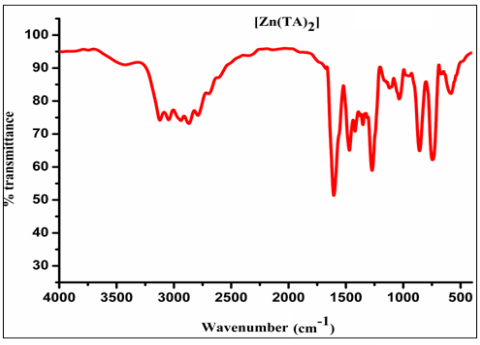

Figure 3.13 IR spectrum of $[Zn(TA)_2]$.

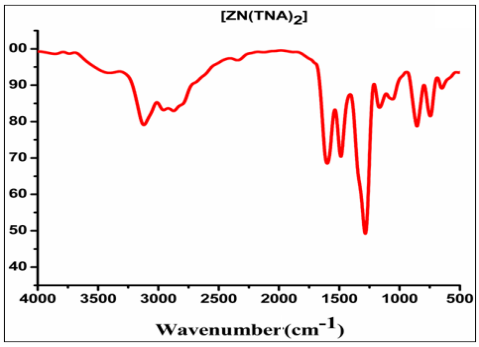

Figure 3.14 IR spectrum of $[Zn(TNA)_2]$.

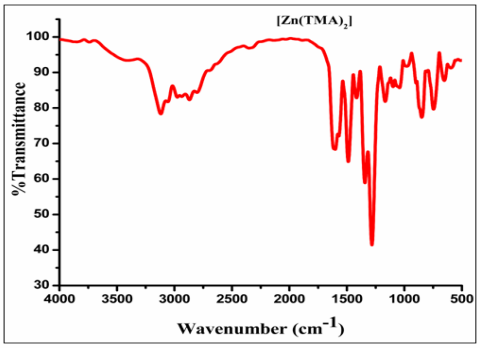

Figure 3.15 IR spectrum of $[Zn(TMA)_2]$.

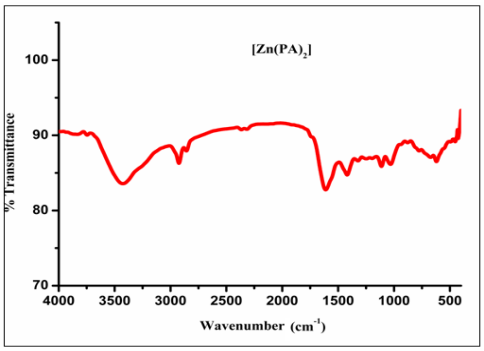

Figure 3.16 IR spectrum of $[Zn(PA)_2]$.

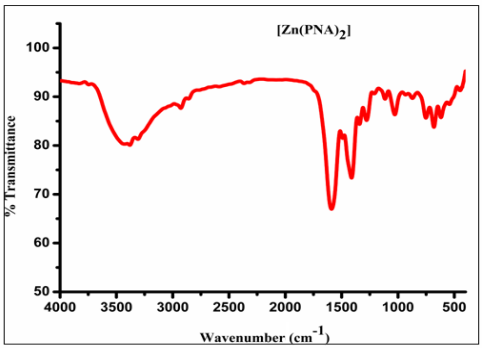

Figure 3.17 IR spectrum of $[Zn(PNA)_2]$.

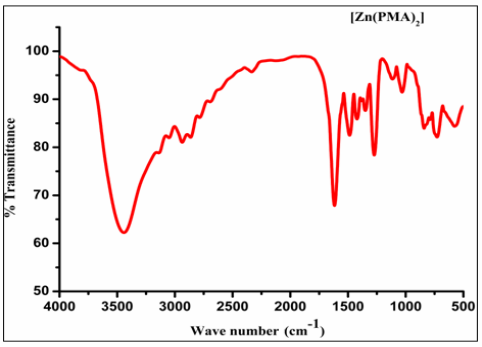

Figure 3.18 IR spectrum of $[Zn(PMA)_2]$.

3.3.5 Electronic spectra

The electronic spectra of all metal complexes were recorded in DMSO (10^{-4} and 10^{-2} M) in the range 45454 -11111 cm^{-1} (220-900 nm) and are given in Figures (3.19 - 3.36). The spectral bands and their assignments are listed in Tables 3.9, 3.10 and 3.11. The spectra of all metal complexes exhibit bands above 25000 cm^{-1} (400 nm) in addition to the $n \rightarrow \pi^*$ transition in the ligands. In absence of X-ray diffraction studies, the electronic spectra can be used for the determination of the structure of metal complexes as the number and position of spectral bands provide good insight in to the geometry of a metal complex [45- 47].

The electronic spectra of Ni(II) complexes display absorption bands in the range of 18450 - 15151 cm^{-1} and 20746 - 19493 cm^{-1}. These bands may be assigned to spin allowed transition $^3A_{2g}(F) \rightarrow {}^3T_{1g}(F)$ and $^3A_{2g}(F) \rightarrow {}^3T_{1g}(P)$. The position of bands suggest mostly of octahedral geometry for $[Ni(TA)_2(H_2O)_2]$ and $[Ni(TNA)_2(H_2O)_2]\cdot 2H_2O$ [48]. But for other nickel complexes, $[Ni(TMA)_2]\cdot 3H_2O$, $[Ni(PA)_2]\cdot H_2O$, $[Ni(PNA)_2]\cdot 2H_2O$ and $[Ni(PMA)_2]$ suggest tetrahedral geometry [49].

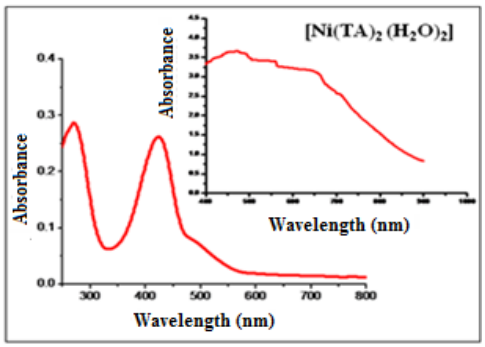

Figure 3.19 Electronic spectra of $[Ni(TA)_2(H_2O)_2]$.

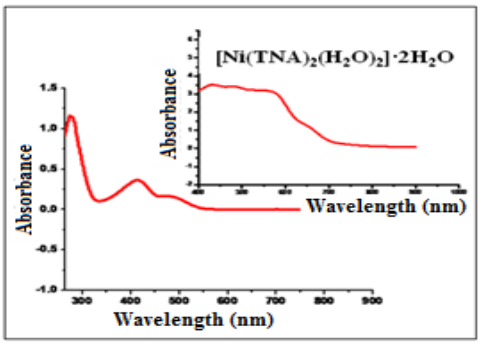

Figure 3.20 Electronic spectra of $[Ni(TNA)_2(H_2O)_2]\cdot 2H_2O$.

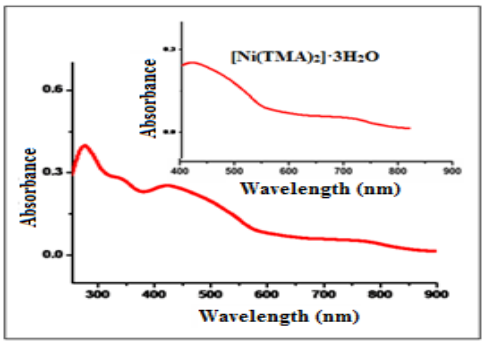

Figure 3.21 Electronic spectra of $[Ni(TMA)_2]\cdot 3H_2O$.

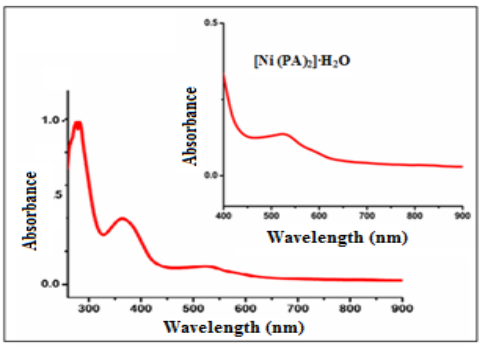

Figure 3.22 Electronic spectra of $[Ni(PA)_2]\cdot H_2O$.

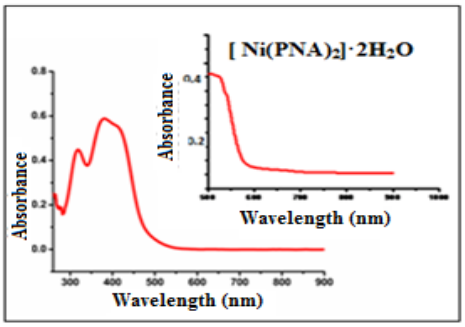

Figure 3.23 Electronic spectra of $[Ni(PNA)_2]\cdot 2H_2O$.

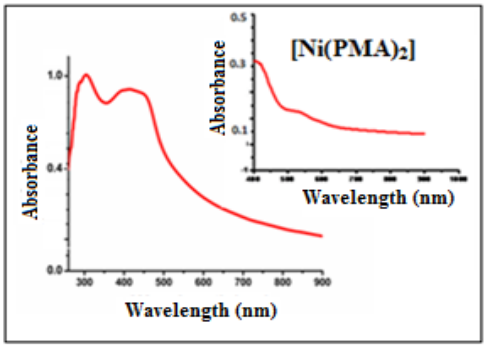

Figure 3.24 Electronic spectra of $[Ni(PMA)_2]$.

Table 3.9 Electronic spectral assignments for Ni(II) complexes

Complex	Electronic spectral bands :nm (cm^{-1})		log ε ($L\ mol^{-1}cm^{-1}$)	Band assignment
$[Ni(TA)_2\ (H_2O)_2]$	274	(36490)	3.46	Intra ligand transition
	424	(23580)	3.41	
	476	(21000)	1.72	CT
	558	(17920)	1.66	$^3A_{2g}(F)\rightarrow{}^3T_{1g}(p)$
	654	(15290)	1.59	$^3A_{2g}(F)\rightarrow{}^3T_{1g}(F)$
$[Ni(TNA)_2(H_2O)_2]\cdot 2H_2O$	276	(36230)	3.99	Intra ligand transition
	415	(24090)	3.57	
	482	(20740)	1.53	CT
	566	(17660)	1.49	$^3A_{2g}(F)\rightarrow{}^3T_{1g}$
	660	(15150)	1.41	$^3A_{2g}(F)\rightarrow{}^3T_{1g}(F)$
$[Ni(TMA)_2]\cdot 3H_2O$	278	(35970)	3.61	Intra ligand transition
	345	(28980)	3.45	
	469	(21320)	1.32	CT
	542	(18450)	1.18	$^3A_{2g}(F)\rightarrow{}^3T_{1g}(p)$
	752	(15150)	0.78	$^3A_{2g}(F)\rightarrow{}^3T_{1g}(F)$
$[Ni(PA)_2]\cdot H_2O$	286	(34960)	3.98	Intra ligand transition
	361	(27700)	3.65	
	524	(19080)	1.18	CT
	598	(16720)	0.98	$^3A_{2g}(F)\rightarrow{}^3T_{1g}(p)$
				$^3A_{2g}(F)\rightarrow{}^3T_{1g}(F)$
$[Ni(PNA)_2]\cdot 2H_2O$	319	(31340)	3.64	Intra ligand transition
	389	(25700)	3.76	
	513	(19490)	1.54	CT
				$^3A_{2g}(F)\rightarrow{}^3T_{1g}(p)$
$[Ni(PMA)_2]$	307	(32570)	4.00	Intra ligand transition
	420	(23810)	3.91	
	465	(21500)	1.48	CT
	550	(18180)	1.23	$^3A_{2g}(F)\rightarrow{}^3T_{1g}(p)$
				$^3A_{2g}(F)\rightarrow{}^3T_{1g}(F)$

The electronic spectra of all Cu(II) complexes $[Cu(TA)_2H_2O]\cdot H_2O$, $[Cu(TNA)_2]\cdot 2H_2O$, $[Cu(TMA)_2]\cdot H_2O$ $[Cu(PA)_2H_2O]\cdot 2H_2O$, $[Cu(PNA)_2]\cdot 3H_2O$ and $[Cu(PMA)_2]\cdot H_2O$ showed four major absorption bands around in the range 35842 cm^{-1}, 27548 cm^{-1}, 21929 cm^{-1}, and 14619 cm^{-1} (Table 3.10).The first band is assigned to $\pi\rightarrow\pi^*$ intra ligand transitions [50]. The band corresponding to azomethine showed a slight shift to longer wavelength on complexation, indicating coordination of ligands to metal through the azomethine moiety. The peak in the range 27548 - 21833 cm^{-1}could be due to Cu(II) → ligand charge transfer (MLCT) transitions. The band in the wavelength around in the range 21833 - 14619 cm^{-1}corresponds to d–d transitions [51]. $^2B_1g\rightarrow{}^2A_1g$ ($d_{x^2-y^2}$- d_{z^2}), $^2B_1g\rightarrow{}^2B_2g$ ($d_{x^2-y^2}$- d_{xy}) and $B_1g\rightarrow{}^2Eg$ ($d_{x^2-y^2}$- d_{xz}, d_{yz}) are the three possible spin allowed transitions for square planar or square pyramidal copper complexes with $d_{x^2-y^2}$ ground state. But these transitions are difficult to observe because of four lower orbital's are close together in energy. In the present work, these transitions are observed as shoulders in the range 20833 - 14619 cm^{-1} for all copper complexes [52].

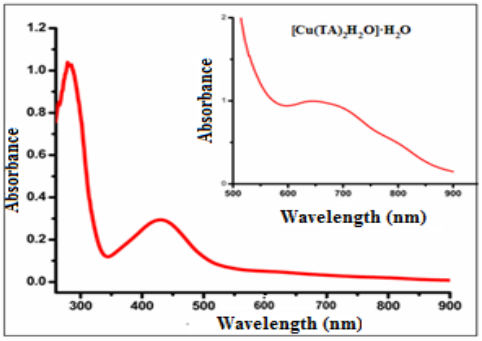

Figure 3.25 Electronic spectra of $[Cu(TA)_2H_2O]\cdot H_2O$.

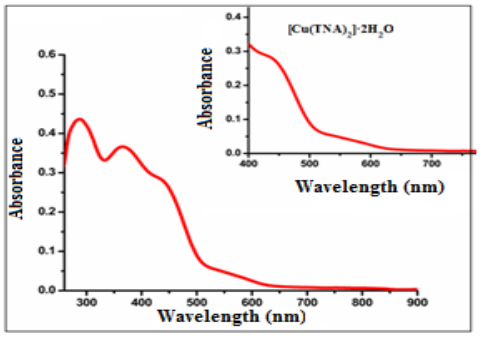

Figure 3.26 Electronic spectra of $[Cu(TNA)_2]\cdot 2H_2O$.

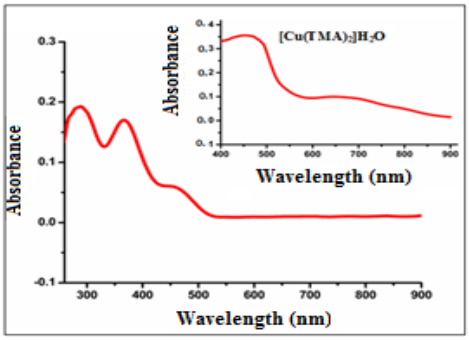

Figure 3.27 Electronic spectra of $[Cu(TMA)_2]\cdot H_2O$.

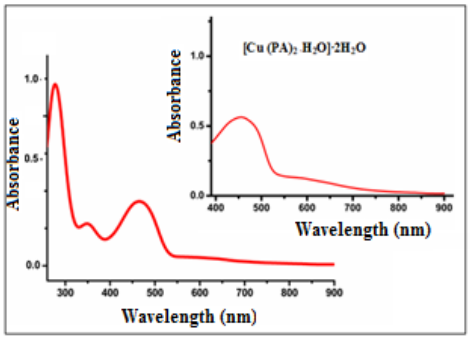

Figure 3.28 Electronic spectra of $[Cu(PA)_2H_2O]\cdot 2H_2O$.

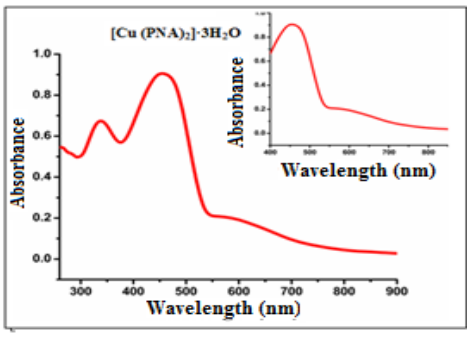

Figure 3.29 Electronic spectra of $[Cu(PNA)_2]\cdot 3H_2O$.

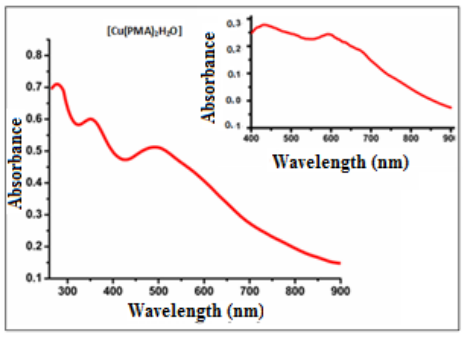

Figure 3.30 Electronic spectra of $[Cu(PMA)_2]\cdot H_2O$.

Table 3.10 Electronic spectral assignments for Cu(II) complexes

Complex	Electronic spectral bands :nm (cm^{-1})	log ε ($L\ mol^{-1}cm^{-1}$)	Band assignment
$[Cu(TA)_2H_2O]\cdot H_2O$	267 (37450)	3.92	Intra ligand transition
	283 (35330)	3.99	Intra ligand transition
	534 (18720)	1.3	$^2B_{1g} \rightarrow {}^2E_g$ ($d_{x^2-y^2} \rightarrow d_{xz}, d_{yz}$)
	665 (15030)	0.53	$^2B_{1g} \rightarrow {}^2B_{2g}$ ($d_{x^2-y^2} \rightarrow d$xy)
	790 (12650)	0.23	$^2B_{1g} \rightarrow {}^2A_{1g}$ ($d_{x^2-y^2} \rightarrow d_{z^2}$)
$[Cu(TNA)_2]\cdot 2H_2O$	290 (34480)	3.63	Intra ligand transition
	371 (26950)	3.57	Intra ligand transition
	445 (22470)	3.46	Intra ligand transition
	490 (20400)	0.92	$^2B_{1g} \rightarrow {}^2E_g$ ($d_{x^2-y^2} \rightarrow d_{xz}, d_{yz}$)
	570 (17540)	0.58	$^2B_{1g} \rightarrow {}^2B_2g$ ($d_{x^2-y^2} \rightarrow d_{xy}$)
$[Cu(TMA)_2]\cdot H_2O$	290 (34480)	3.28	Intra ligand transition
	365 (27390)	3.23	Intra ligand transition
	456 (21920)	2.77	Intra ligand transition
	475 (21050)	1.5	$^2B_{1g} \rightarrow {}^2E_g$ ($d_{x^2-y^2} \rightarrow d_{xz}, d_{yz}$)
	684 (14610)	1.0	$^2B_{1g} \rightarrow {}^2B_{2g}$ ($d_{x^2-y^2} \rightarrow d_{xy}$)
$[Cu(PA)_2H_2O]\cdot 2H_2O$	279 (35840)	3.99	Intra ligand transitions
	347 (28850)	3.43	Intra ligand transitions
	458 (21830)	1.64	$^2B_{1g} \rightarrow {}^2E_g$ ($d_{x^2-y^2} \rightarrow d_{xz}, d_{yz}$)
	604 (16550)	0.85	$^2B_{1g} \rightarrow {}^2B_{2g}$ ($d_{x^2-y^2} \rightarrow d_{xy}$)
$[Cu(PNA)_2]\cdot 3H_2O$	267 (37450)	3.72	Intra ligand transitions
	337 (29670)	3.82	Intra ligand transitions
	458 (21830)	1.9	$^2B_{1g} \rightarrow {}^2E_g$ ($d_{x^2-y^2} \rightarrow d_{xz}, d_{yz}$)
	609 (16420)	1.2	$^2B_{1g} \rightarrow {}^2B_{2g}$ ($d_{x^2-y^2} \rightarrow d_{xy}$)
$[Cu(PMA)_2]\cdot H_2O$	266 (37593)	3.85	Intra ligand transitions
	356 (28089)	3.78	Intra ligand transitions
	484 (20660)	1.7	$^2B_{1g} \rightarrow {}^2E_g$ ($d_{x^2-y^2} \rightarrow d_{xz}, d_{yz}$)
	595 (16800)	1.5	$^2B_{1g} \rightarrow {}^2B_{2g}$ ($d_{x^2-y^2} \rightarrow d_{xy}$)
	677 (14770)	1.4	$^2B_{1g} \rightarrow {}^2A_1g$ ($d_{x^2-y^2} \rightarrow d_{z^2}$)

The electronic spectrum of all Zn(II) complexes (Table 3.11) shows the absorption bands in the range 28490 $cm^{-1}$and 20534 cm^{-1} attributed to ligand to metal (M→L) charge transfer which is compactable with tetrahedral structure for all Zn(II) complexes, $[Zn(TA)_2]$, $[Zn(TNA)_2]$, $[Zn(TMA)_2]$, $[Zn(PA)_2]$, $[Zn(PNA)_2]$ and $[Zn(PMA)_2]$ [53-54]. There were no d-d transitions seen in the visible spectrum of the Zn^{2+} complexes and it was found to be diamagnetic in nature [55].

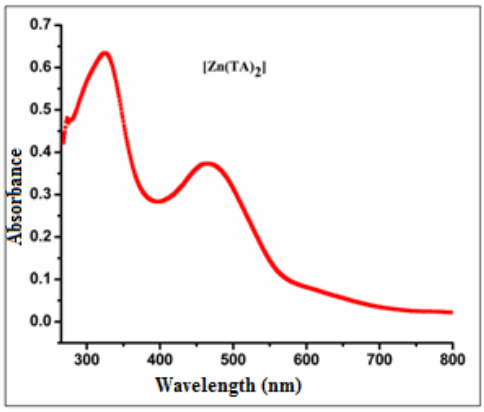

Figure 3.31 Electronic spectrum of $[Zn(TA)_2]$.

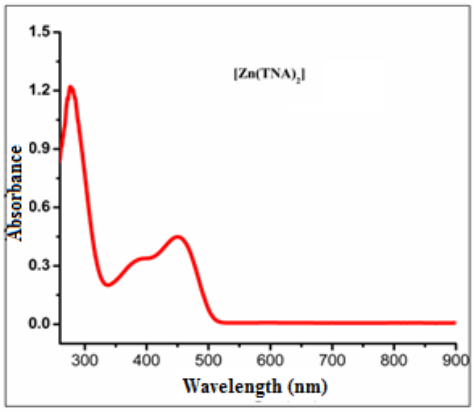

Figure 3.32 Electronic spectrum of $[Zn(TNA)_2]$.

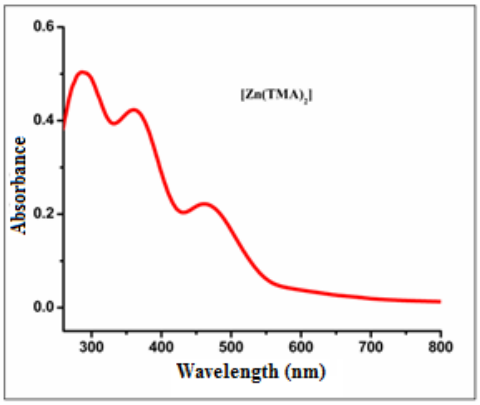

Figure 3.33 Electronic spectrum of $[Zn(TMA)_2]$.

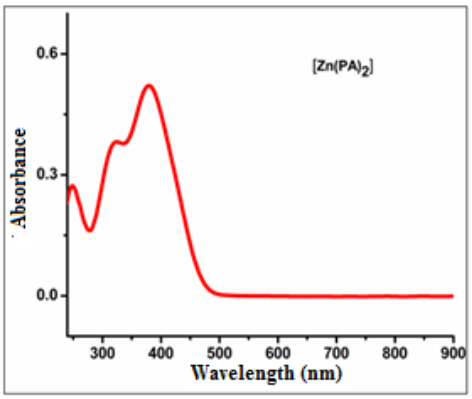

Figure 3.34 Electronic spectrum of $[Zn(PA)_2]$.

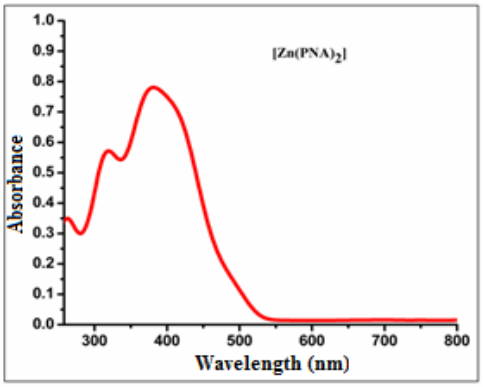

Figure 3.33 Electronic spectrum of $[Zn(PNA)_2]$.

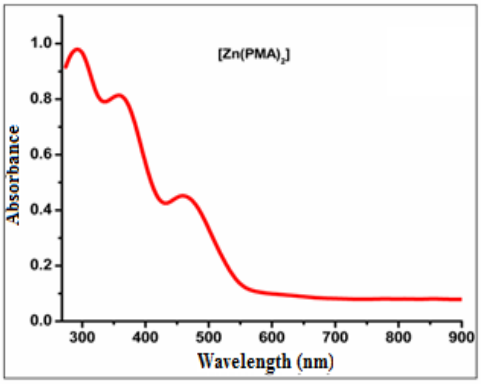

Figure 3.34 Electronic spectrum of $[Zn(PMA)_2]$.

Table 3.11 Electronic spectral assignments for Zn(II) complexes

Complex	Electronic spectral bands :nm (cm^{-1})	log ε ($L\ mol^{-1}cm^{-1}$)	Band assignment
$[Zn(TA)_2]$	293 (34120)	3.80	π→ π*
	430 (23250)	3.57	CT
$[Zn(TNA)_2]$	266 (37590)	4.00	π→ π*
	369 (27100)	3.50	CT
	454 (22020)	3.65	CT
$[Zn(TMA)_2]$	296 (33780)	3.71	π→ π*
	366 (27320)	3.62	CT
	474 (21090)	3.32	CT
$[Zn(PA)_2]$	260 (38460)	3.43	π→ π*
	321 (31150)	3.57	CT
	388 (25770)	3.72	CT
$[Zn(PNA)_2]$	269 (33550)	3.54	π→ π*
	317 (31540)	3.76	CT
	400 (25000)	3.89	CT
$[Zn(PMA)_2]$	298 (33550)	3.98	π→ π*
	366 (27320)	3.90	CT
	460 (21730)	3.64	CT

3.3.6 Electronic paramagnetic resonance spectra

The EPR spectra of the Cu(II) complexes in polycrystalline state at 298 K and in DMF at 77 K were recorded in the X-band, using 100-kHz modulation frequency and 9.1 GHz microwave frequency. The spectra of $[Cu(TA)_2H_2O]\cdot H_2O$ and $[Cu(TMA)_2]\cdot H_2O$ complexes shows an isotropic spectrum with g_{iso}= 2.10 and 2.12 respectively at room temperature (Figures 3.37 and 3.41). This spectrum consists of only one broad signal and hence only one *g* value due to dipolar broadening and enhanced spin lattice relaxation [56]. This type of spectra did not give any information about the electronic ground state of Cu(II) ion present in the complexes. All other

Cu(II) complexes $[Cu(TNA)_2]\cdot 2H_2O$, $[Cu(PA)_2H_2O]\cdot 2H_2O$, $[Cu(PNA)_2]\cdot 3H_2O$ and $[Cu(PMA)_2]\cdot H_2O$ (Figures 3.39, 3.43, 3.45 and 3.47) displayed axial spectra in the polycrystalline state at 298 K with $g_{\|}$ and $g\perp$ values. The variation in the $g_{\|}$ and $g\perp$ values indicates that in the solid state, the geometry of the compounds is affected by the nature of coordinating ligands [57]. These compounds with axial behavior in polycrystalline state show $g_{\|} > g\perp > 2.0023$, which is consistent with a $d_{x}^{2}{}_{-y}^{2}$ ground state in a square planar or square pyramidal geometry. For all these complexes, hyperfine splitting was not clear in both parallel and in perpendicular region.

The geometric parameter G, represents the exchange interaction between copper centers in the polycrystalline compound and is calculated for each complexes using the equation,

$$G = (g_{\|} - 2.0023) / (g\perp - 2.0023) \text{ for axial spectra [58].}$$

If G > 4, exchange interaction is negligible and if it less than 4, considerable exchange interaction is indicated in the solid complex. The calculated G values are less than 4 for complexes $[Cu(PA)_2H_2O]\cdot 2H_2O$ (3.73), $[Cu(PNA)_2]\cdot 3H_2O$ (3.76) and $[Cu(PMA)_2H_2O]$ (2.80) which indicate that considerable exchange interaction is present in the polycrystalline state of these complexes. G value for $[Cu(TNA)_2]\cdot 2H_2O$ is 4.29 which is greater than 4 and it indicates that there was negligible interaction.

The EPR spectra of all these complexes also recorded in frozen state at 77 K (Figures 3.38, 3.40, 3.42, 3.44, 3.46 and 3.48) and this gives more information about the geometry of the complexes [59]. For all the copper complexes $[Cu(TNA)_2]\cdot 2H_2O$ ($g_{\|}$ = 2.277 and $g\perp$ = 2.076), $[Cu(TMA)_2]\cdot H_2O$ ($g_{\|}$ = 2.298 and $g\perp$ = 2.065), $[Cu(PA)_2H_2O]\cdot 2H_2O$ ($g_{\|}$ = 2.24 and $g\perp$ = 2.065),

$[Cu(PNA)_2]\cdot 3H_2O$ ($g_{\|}$ = 2.25 and $g_{\perp}$ = 2.06) and $[Cu(PMA)_2]\cdot H_2O$ ($g_{\|}$ =2.22 and $g_{\perp}$ = 2.07), four well resolved hyperfine lines are observed in the parallel region due to coupling of the electron spin with the nuclear spin (^{63}Cu, I = 3/2) and the splitting are not well differentiable in the perpendicular region. In frozen DMF, $[Cu(TA)_2H_2O]\cdot H_2O$ reveals three sets of resonances at low, mid and high fields corresponding to g_x, g_y and g_z respectively. From the peak positions, the g values evaluated are g_x = 2.02, g_y = 2.07 and g_z = 2.39. Hyperfine structure was not resolved in both parallel and perpendicular regions. The calculated g values provide valuable information on the electronic ground state of the ion. If $g_z > g_y > g_z$, and the quantity of R {R = $(g_y - g_x)/(g_z - g_y)$} is greater than unity, the ground state is (d_z^2) and if R is less than unity, the ground state is (d_x^2-$_y^2$). For $[Cu(TA)_2H_2O]\cdot H_2O$ the value of 'R' (0.173) indicates d_x^2-$_y^2$ as ground state suggesting a rhombic structure. The EPR parameters of the Cu(II) complexes were presented in Table 3.12 and 3.13. The covalency of in-plane σ-bonds, in-plane π bonds and out-of- plane π-bonds was evaluated by using the bonding parameters α^2, β^2, γ^2. The EPR parameters $g_{\|}$, $g_{\perp}$, g_{av}, $A_{\|}$ and the energies of *d-d* transitions are used to evaluate these bonding parameters [60]. α^2, the value of in-plane sigma bonding parameter was estimated by using the expression

$$\alpha^2 = - A_{\|}/0.036 + (g_{\|} - 2.0023) + 3/7(g_{\perp} - 2.0023) + 0.04 \text{ [61]}$$

The bonding parameters $K^2_{\|} = \alpha^2\beta^2$ and $K^2_{\perp} = \alpha^2\gamma^2$ were calculated by using following expression

$$K^2_{\|} = (g_{\|} - 2.0023)\, E_{d\text{-}d}/8\lambda_0$$

$$K^2_{\perp} = (g_{\perp} - 2.0023)\, E_{d\text{-}d}/2\lambda_0$$

Where $K_{\|}$ and $K\perp$ are orbital reduction factors and λ_0 represents the one electron spin orbit coupling constant which equals -828 cm^{-1}. Hathaway [62] has pointed out that for pure sigma bonding $K_{\|} \approx K\perp \approx 0.77$, for in plane π-bonding $K_{\|} < K\perp$ for out-of-plane π-bonding, $K\perp < K_{\|}$. For $[Cu(TA)_2H_2O]\cdot H_2O$, $[Cu(TNA)_2]\cdot 2H_2O$, $[Cu(PA)_2H_2O]\cdot 2H_2O$, and $[Cu(PMA)_2]\cdot H_2O$ complexes, it is observed that $K_{\|} < K\perp$ which indicates the presence of significant in-plane π-bonding. In $[Cu(TNA)_2]\cdot 2H_2O$ and $[Cu(PNA)_2]\cdot 3H_2O$ complexes, out-of-plane π-bonding is significant. The nature of metal–ligand bond is evaluated by comparing the value of in-plane sigma bonding parameter α^2 i.e., if the M–L bond is purely ionic, the value of α^2 is unity and it is completely covalent, if $\alpha^2 = 0.5$. Here for all complexes, the value of $\alpha^2 < 1.0$ which indicate that the metal–ligand bonds in the complexes under investigation are partially ionic and partially covalent in nature.

Table 3.12 EPR spectral parameters of Cu(II) complexes in polycrystalline state at 298K

Polycrystalline at 298 K				
Compound	$g_{\|}$	$g\perp$	g_{iso}/g_{av}	**G**
$[Cu(TA)_2H_2O]\cdot H_2O$	0	0	0	0
$[Cu(TNA)_2]\cdot 2H_2O$	2.25	2.06	2.1233	4.2929
$[Cu(TMA)_2]\cdot H_2O$	0	0	0	0
$[Cu(PA)_2H_2O]\cdot 2HO$	2.255	2.07	2.1317	3.7326
$[Cu(PNA)_2]\cdot 3H_2O$	2.257	2.07	2.1323	3.7622
$[Cu(PMA)_2]\cdot H_2O$	2.15	2.055	2.0867	2.8027

Table 3.13: EPR spectral parameters of Cu(II) complexes in DMF solution at 77K

Solution at 77 K (DMF)													
Compound	$g_{\parallel}$	$g_{\perp}$	gz	α^2	$E_{d\text{-}d}$	$K_{\parallel}$ (Cu^{2+})	$K_{\perp}$ (Cu^{2+})	β^2 (Cu^{2+})	γ^2 (Cu^{2+})	$A_{\parallel}{}^{a}$	$A_{\perp}{}^{a}$	A_{av}	g_{av}
$[Cu(TA)_2H_2O]\cdot H_2O$	2.01	2.07	2.4	0.956	14706	0.1646	0.775	0.172	0.811	180	20	70	2.052
$[Cu(TNA)_2]\cdot 2H_2O$	2.28	2.08	0	0.894	17153	0.8434	0.874	0.943	0.976	190	0	70	2.143
$[Cu(TMA)_2]\cdot H_2O$	2.29	2.07	0	0.884	14620	0.8079	0.744	0.913	0.841	190	10	70	2.143
$[Cu(PA)_2H_2O]\cdot 2H_2O$	2.24	2.07	0	0.879	15848	0.7541	0.775	0.857	0.881	210	10	80	2.123
$[Cu(PNA)_2]\cdot 3H_2O$	2.25	2.06	0	0.895	16426	0.7836	0.756	0.875	0.845	210	20	80	2.123
$[Cu(PMA)_2]\cdot H_2O$	2.22	2.07	0	0.764	13889	0.6756	0.754	0.884	0.986	160	10	60	2.123

A is expressed in x 10^{-4} cm

a expressed in units of cm^{-1} multiplied by a factor of 10^{-4}

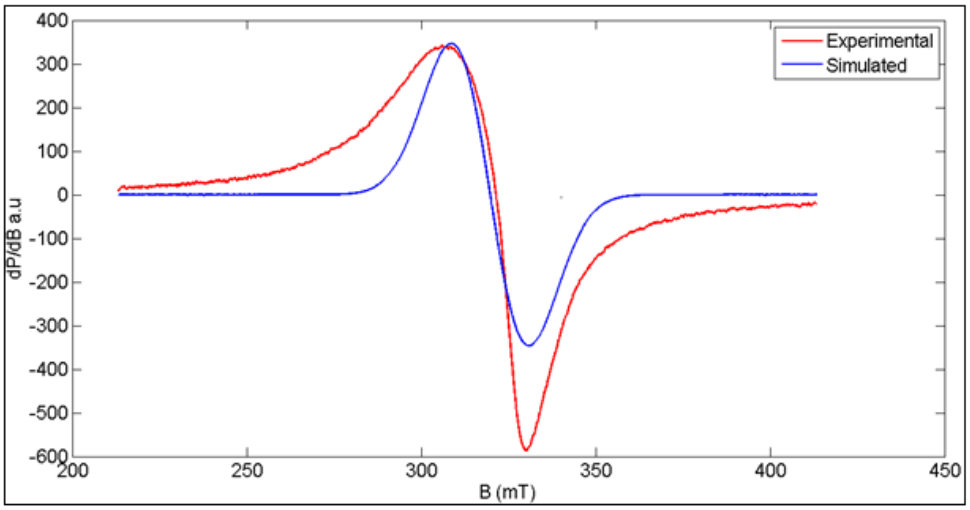

Figure 3.37 EPR spectrum of $[Cu(TA)_2H_2O]\cdot H_2O$ in polycrystalline state at 298 K.

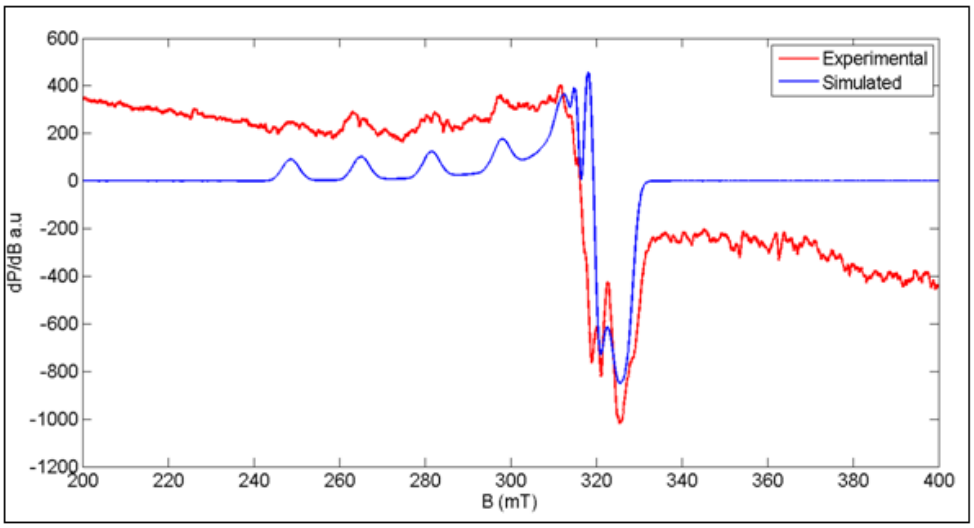

Figure 3.38 EPR spectrum of $[Cu(TA)_2H_2O]\cdot H_2O$ in DMF solution at 77 K.

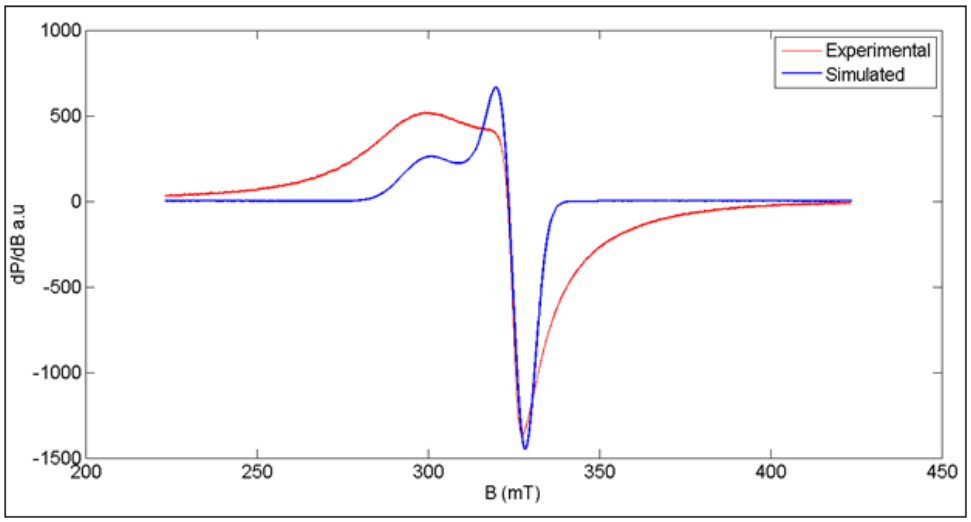

Figure 3.39 EPR spectrum of $[Cu(TNA)_2]\cdot 2H_2O$ in polycrystalline state at 298 K.

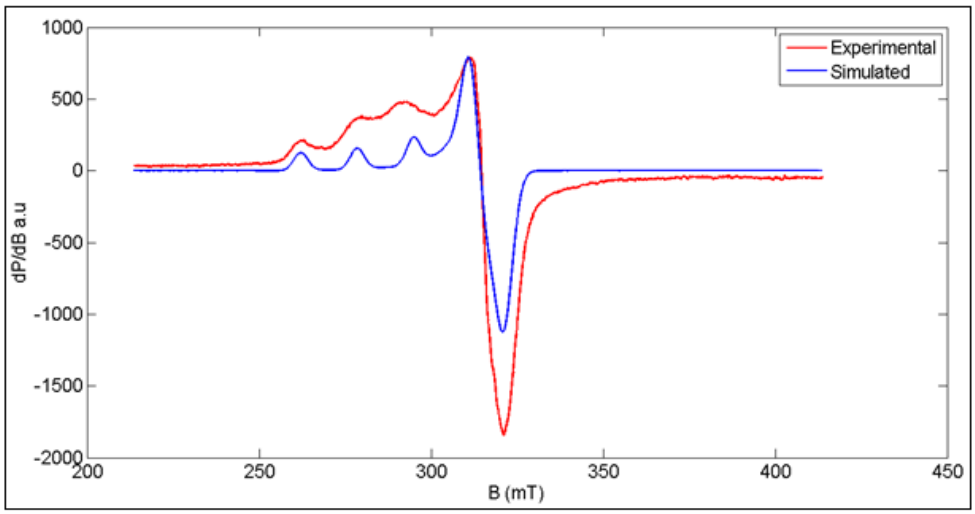

Figure 3.40 EPR spectrum of $[Cu(TNA)_2]\cdot 2H_2O$ in DMF solution at 77 K.

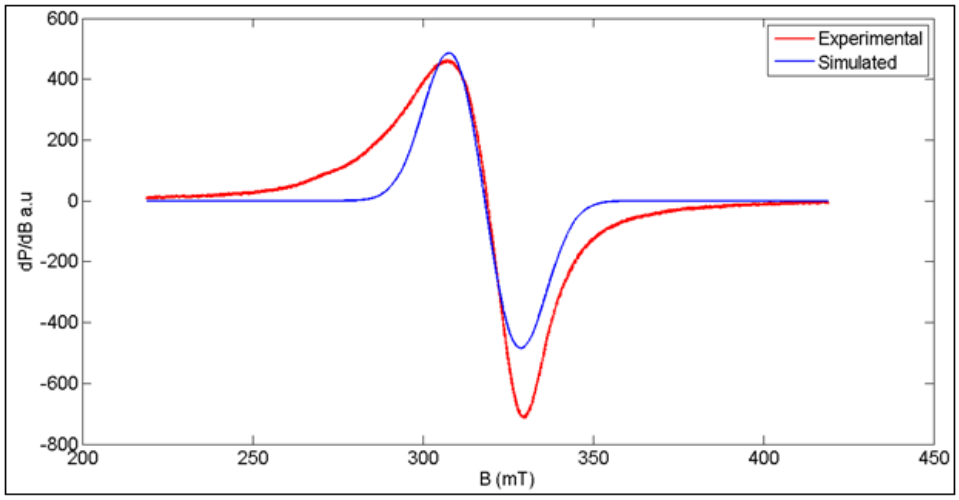

Figure 3.41 EPR spectrum of $[Cu(TMA)_2]\cdot H_2O$ in polycrystalline state at 298 K.

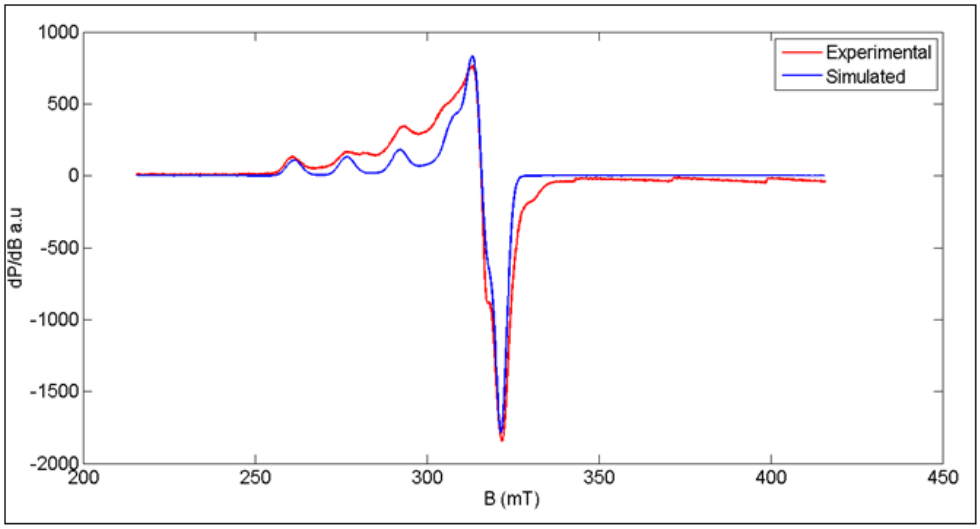

Figure 3.42 EPR spectrum of $[Cu(TMA)_2]\cdot H_2O$ in DMF solution at 77 K.

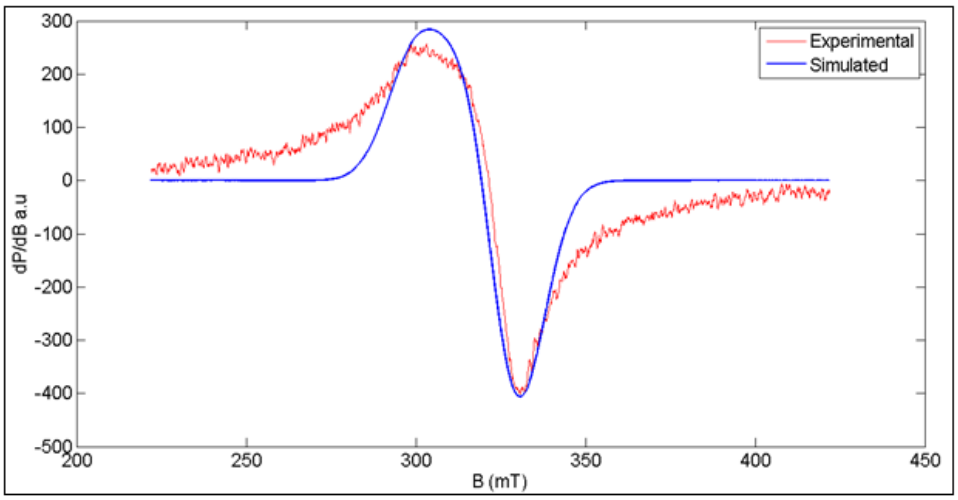

Figure 3.43 EPR spectrum of $[Cu(PA)_2H_2O]\cdot 2H_2O$ in polycrystalline state at 298K.

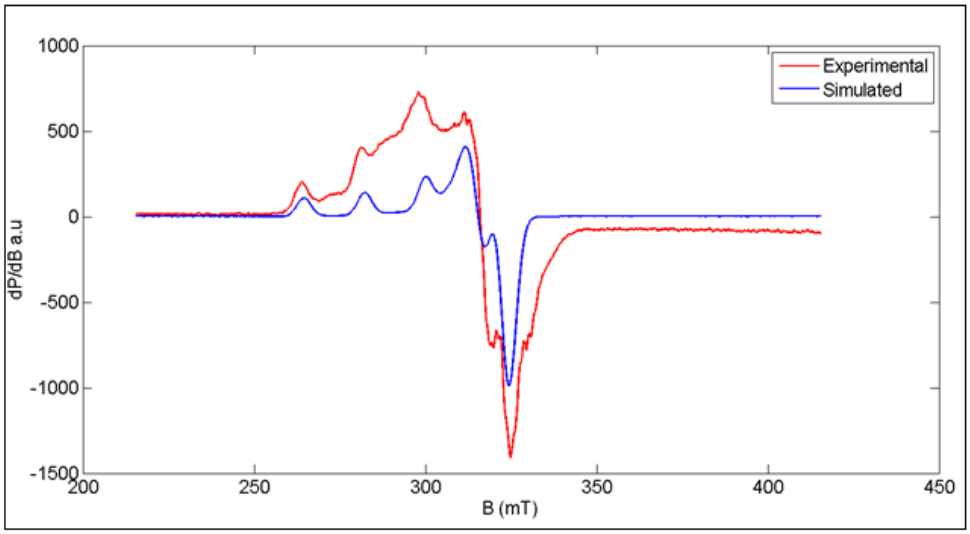

Figure 3.44 EPR spectrum of $[Cu(PA)_2H_2O]\cdot 2H_2O$ in DMF solution at 77 K.

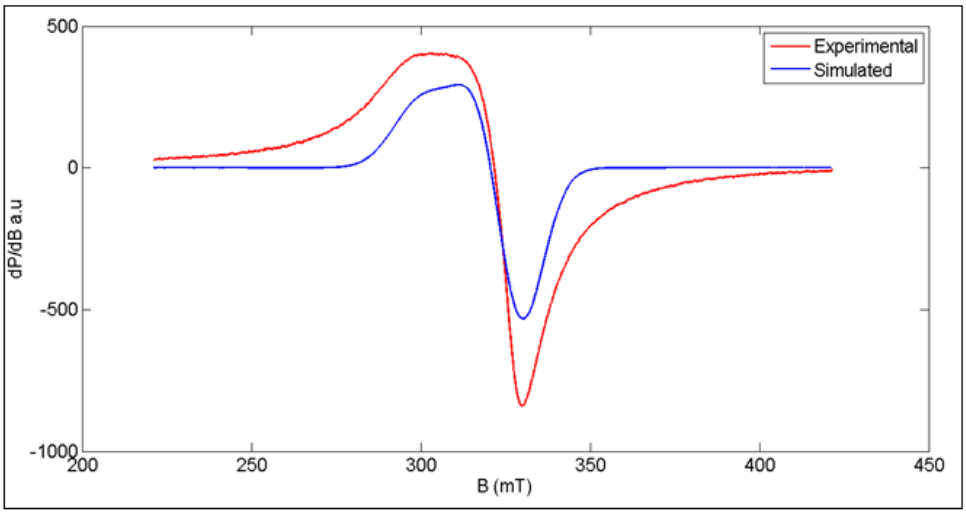

Figure 3.45 EPR spectrum of $[Cu(PNA)_2]\cdot 3H_2O$ in polycrystalline state at 298 K.

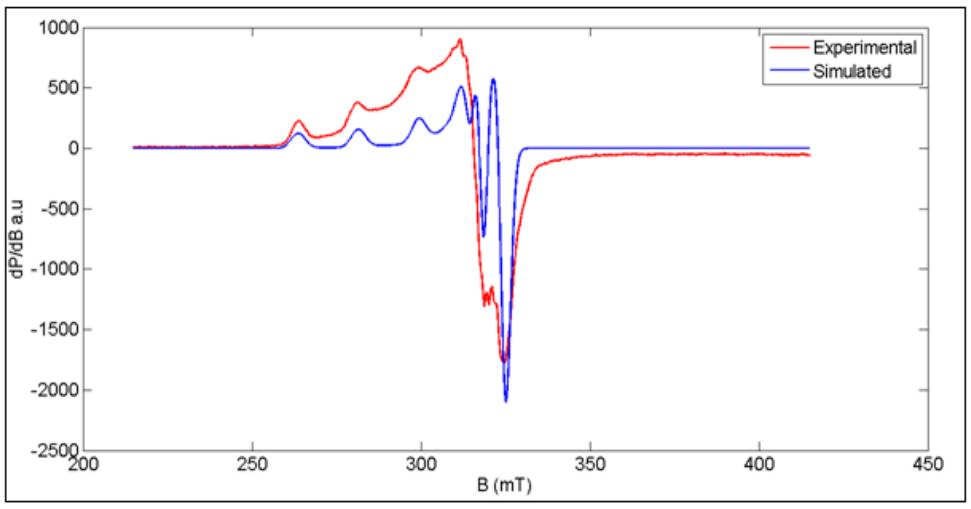

Figure 3.46 EPR spectrum of $[Cu(PNA)_2]\cdot 3H_2O$ in DMF solution at 77K.

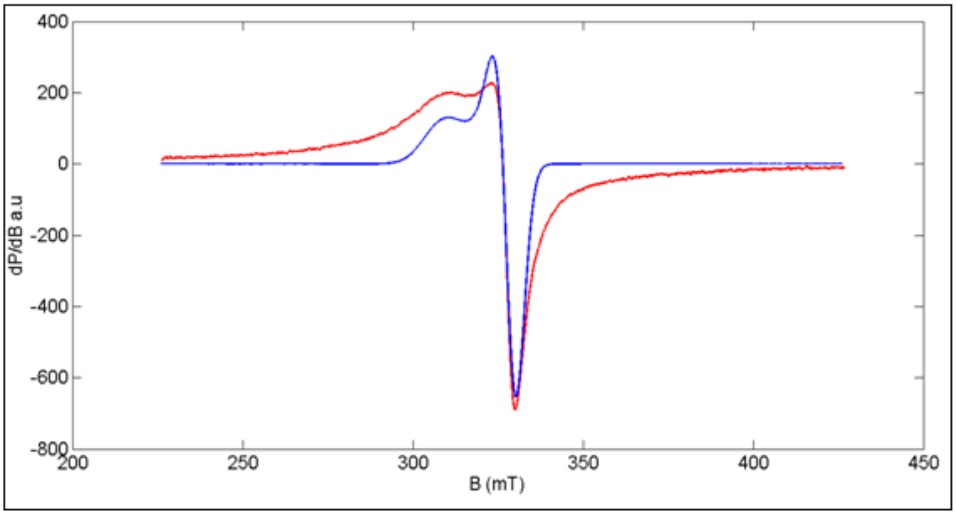

Figure 3.47 EPR spectrum of $[Cu(PMA)_2]\cdot H_2O$ in polycrystalline state at 298 K.

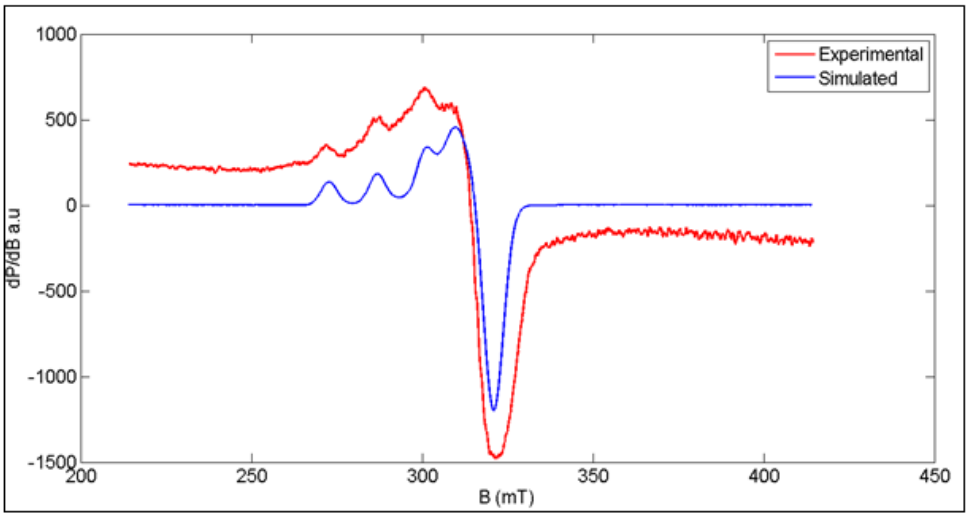

Figure 3.48 EPR spectrum of $[Cu(PMA)_2]\cdot H_2O$ in DMF solution at 77 K.

3.3.7 Thermogravimetric analysis

To determine the thermal stability and chemical composition of Ni(II), Cu(II) and Zn(II) complexes, thermogravimetric analysis has been performed in a temperature range of 0- 800 °C in nitrogen atmosphere at a heating rate of 10°C/min. The thermal analyses also help us to get valuable information regarding nature of water molecules in the complexes. For the complexes, the removal of water can proceed in one or two steps. Complexes lost hydrated water between 50 and 120°C, and then the coordinated water molecule was lost above ≥ 180°C. Most of the synthesized complexes show incomplete decomposition in TG-DTG plot [63]. The thermal stability data are listed in Table 3.14-3.16. The TGA curves of complexes are shown in Figures 3.49 - 3.66.

$[Ni(TA)_2(H_2O)_2]$, degraded in three steps. First step involved weight loss corresponding to the removal of two coordinated water molecules (temperature range 140 to 220 °C). Second step involved weight loss corresponding to removal of organic ligand (temperature range 220 to 385 °C). Third step resulted in weight loss corresponding to departure of remaining organic molecule (temperature range 385 to 630 °C). In the case of complexes $[Ni(TNA)_2(H_2O)_2]\cdot 2H_2O$, $[Ni(TMA)_2]\cdot 3H_2O$, $[Ni(PA)_2]\cdot H_2O$ and $[Ni(PNA)_2]\cdot 2H_2O$ mass loss in the temperature range 74-135 °C corresponds to the presence of lattice water molecules. After this temperature a gradual weight loss occurs due to the thermal degradation of organic moiety in one or two steps. $[Ni(PMA)_2]$ is stable up to 273 °C confirming that there is no coordinated water molecules present in the complex molecule [64].

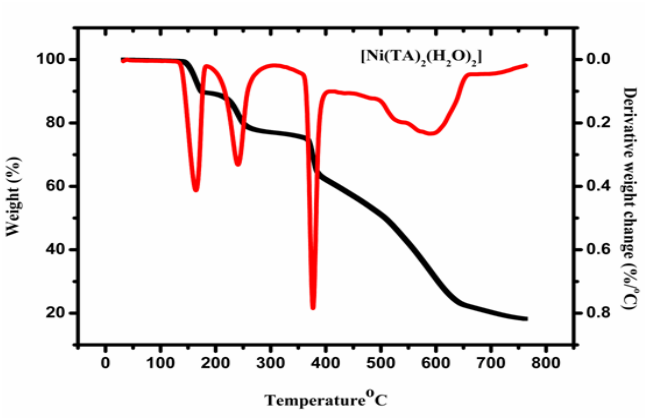

Figure 3.49 TG-DTG curves of $[Ni(TA)_2(H_2O)_2]$.

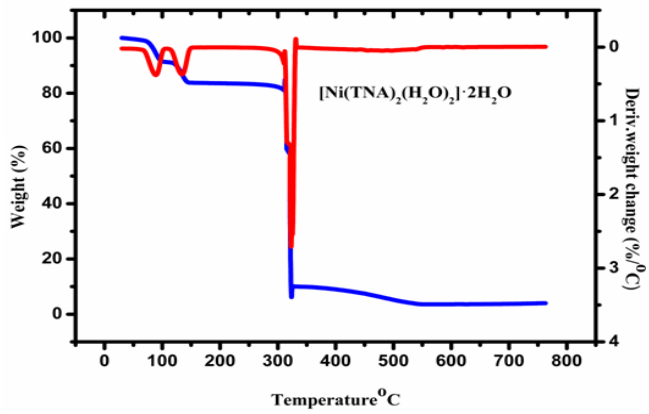

Figure 3.50 TG-DTG curves of $[Ni(TNA)_2(H_2O)_2]\cdot 2H_2O$.

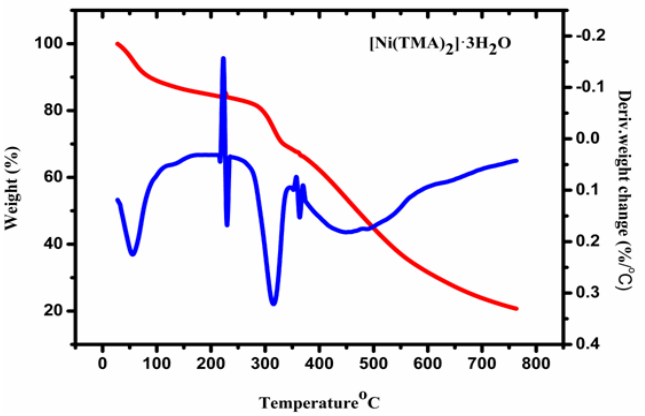

Figure 3.51 TG-DTG curves of $[Ni(TMA)_2]\cdot 3H_2O$.

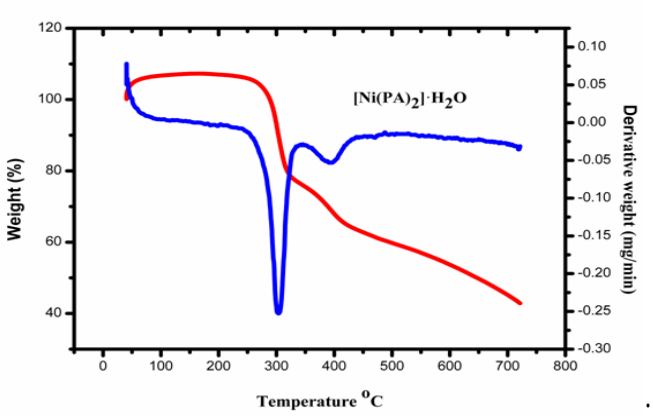

Figure 3.52 TG-DTG curves of $[Ni(PA)_2]\cdot H_2O$.

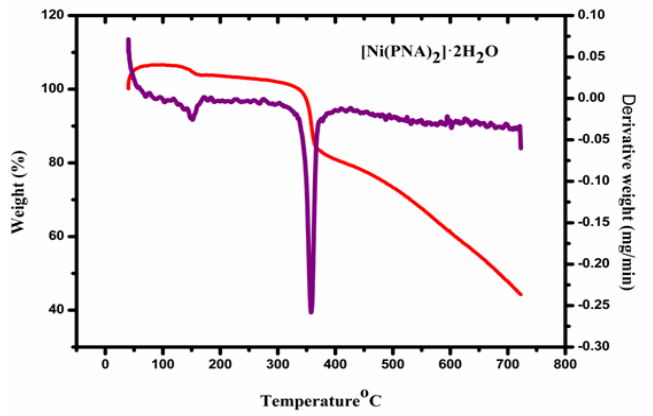

Figure 3. 53 TG-DTG curves of $[Ni(PNA)_2]\cdot 2H_2O$.

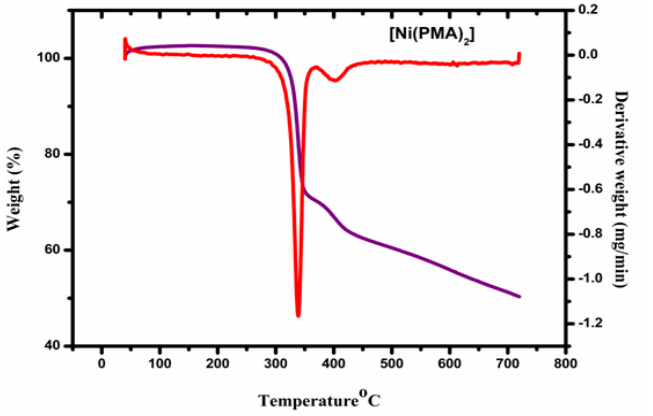

Figure 3.54 TG-DTG curves of $[Ni(PMA)_2]$.

Table 3.14: Data of the thermogravimetric analysis for Ni(II) complexes

Compound	Temperature (°C)	weight loss (%) Calc (found)	Assignments
$[Ni(TA)_2(H_2O)_2]$	140	7.24 (7.62)	Loss of coordinated water
	286	40.86 (41.34)	Elimination of one ligand molecule
	385	40.02 (39.76)	Decomposition of ligand molecule
$[Ni(TNA)_2(H_2O)_2]\cdot 2H_2O$	107	6.73 (6.56)	Loss of two lattice water
	143	6.02 (5.98)	Loss of coordinated water
	310	81.56 (80.98)	Decomposition of organic molecule
$[Ni(TMA)_2]\cdot 3H_2O$	83	10.80 (9.89)	Loss of lattice water
	221	37.55 (37.06)	Elimination of ligand molecule
	351	40.33 (39.82)	Decomposition of ligand molecule
$[Ni(PA)_2]\cdot H_2O$	95	4.02 (3.91)	Loss of lattice water
	283	40.01(39.86)	Decomposition of ligand molecule
$[Ni(PNA)_2]\cdot 2H_2O$	90	6.55 (6.10)	Loss of lattice water
	267	41.67 (41.34)	Decomposition of ligand molecule
$[Ni(PMA)_2]$	271	86.02 (85.84)	Decomposition of organic molecule

Copper complexes $[Cu(TA)_2H_2O]\cdot H_2O$ and $[Cu(PA)_2H_2O]\cdot 2H_2O$ decomposed in three stages. The first estimated mass loss observed in the temperature range of 80 -110 °C is due to the loss of lattice water molecules. The second mass loss in the temperature range 130−220 °C corresponds to the presence of one coordinated water molecules and third steps are found in the temperature range of 223–600 °C corresponding to the loss of organic molecules. All other copper complexes, $[Cu(TNA)_2]\cdot 2H_2O$, $[Cu(TMA)_2]H_2O$ $[Cu(PA)_2H_2O]\cdot 2H_2O$, $[Cu(PNA)_2]\cdot 3H_2O$, $[Cu(PMA)_2]\cdot H_2O$ showed mass loss in the temperature range 74-135 °C corresponds to the presence of lattice water molecules . Above this temperature, a gradual weight loss occurs due to decomposition of organic ligands.

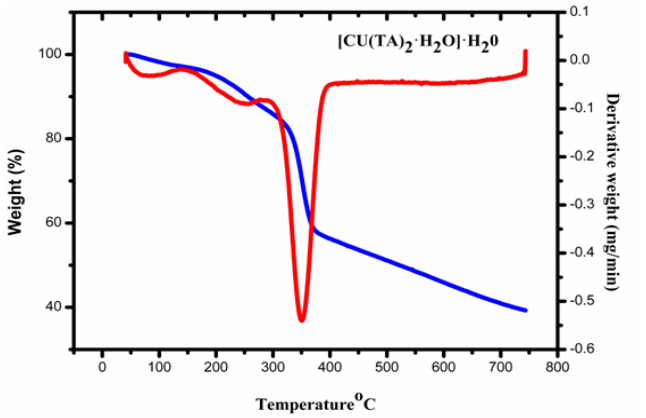

Figure 3.55 TG-DTG curves of $[Cu(TA)_2 \cdot H_2O] \cdot H_2O$.

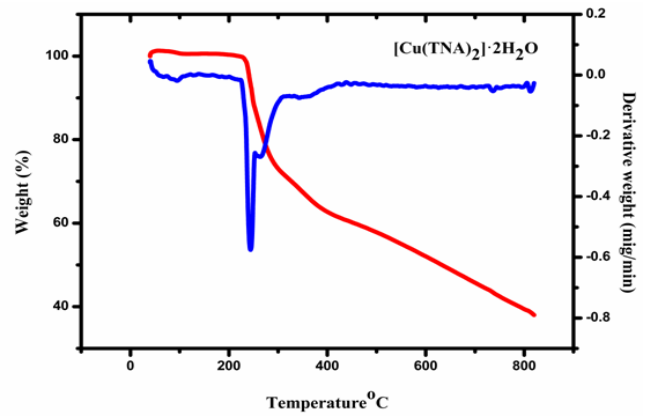

Figure 3.56 TG-DTG curves of $[Cu(TNA)_2] \cdot 2H_2O$.

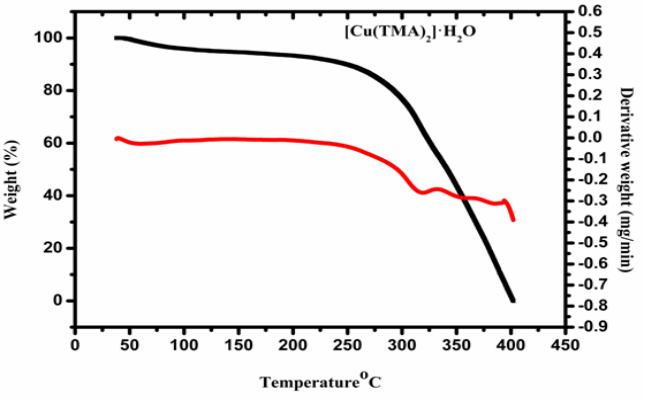

Figure 3.57 TG-DTG curves of $[Cu(TMA)_2] \cdot H_2O$.

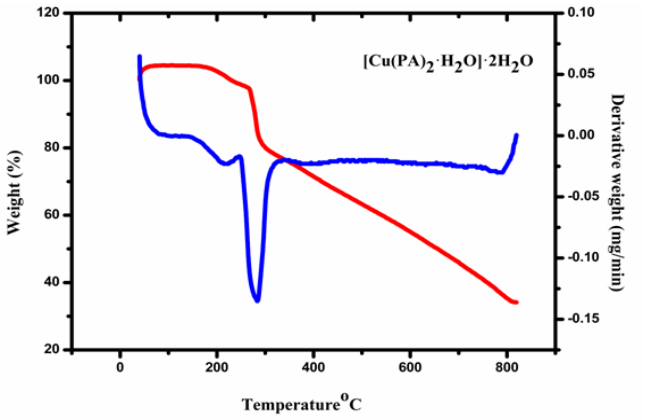

Figure 3.58 TG-DTG curves of $[Cu(PA)_2H_2O]\cdot 2H_2O$.

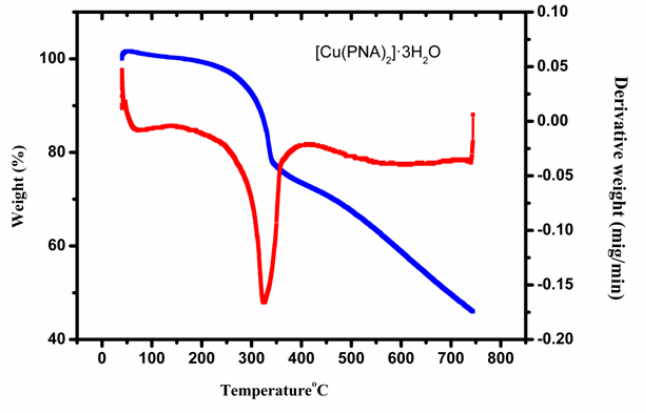

Figure 3.59 TG-DTG curves of $[Cu(PNA)_2]\cdot 3H_2O$.

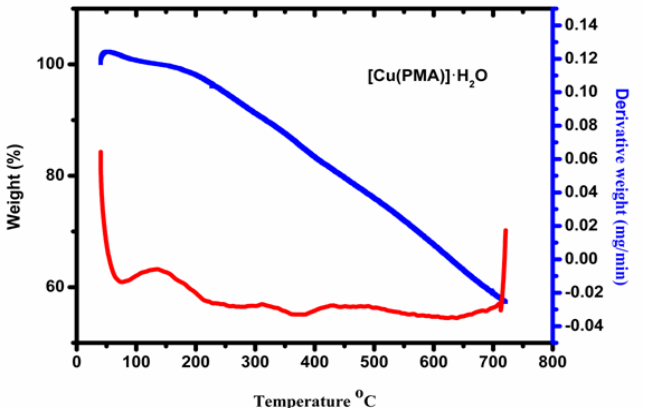

Figure 3.60 TG-DTG curves of $[Cu(PMA)_2]\cdot H_2O$.

Table 3.15 Data of the thermogravimetric analysis for Cu(II) complexes

Complex	Temperature (°C)	Weight loss (%) Calc (found)	Assignments
$[Cu(TA)_2H_2O]\cdot H_2O$	100	4.34 (4.81)	Loss of one lattice water
	150	4.67 (4.21)	Loss of one coordinated water
	288	40.45 (41.34)	Decomposition of ligand molecule
$[Cu(TNA)_2]\cdot 2H_2O$	95	6.04 (6.56)	Loss of two lattice water
	223	41.56 (41.98)	Decomposition of organic molecule
$[Cu(TMA)_2]\cdot H_2O$	81	3.80 (3.89)	Loss of one lattice water
	340	41.90 (42.06)	Decomposition of organic molecule
$[Cu(PA)_2H_2O]\cdot 2H_2O$	92	7.58 (7.21)	Loss of two lattice water
	147	3.42 (3.23)	Loss of one coordinated water
	283	40.45 (39.98)	Decomposition of organic molecule
$[Cu(PNA)_2]\cdot 3H_2O$	85	9.65 (9.23)	Loss of three lattice water
	325	40.77 (40.34)	Decomposition of organic molecule
$[Cu(PMA)_2]\cdot H_2O$	80	3.83 (3.81)	Loss of one lattice water
	240	41.66 (42.02)	Decomposition of organic molecule

The TGA curves of Zn(II) complexes show one or two step decomposition process. All the complexes, $[Zn(TA)_2]$, $[Zn(TNA)_2]$, $[Zn(TMA)_2]$, $[Zn(PA)_2]$, $[Zn(PNA)_2]$ and $[Zn(PMA)_2]$ are stable up to 250°C confirming that there is no coordinated or lattice water molecules present in the complex molecule. This is followed by the decomposition of the anhydrous complexes in two or three steps.

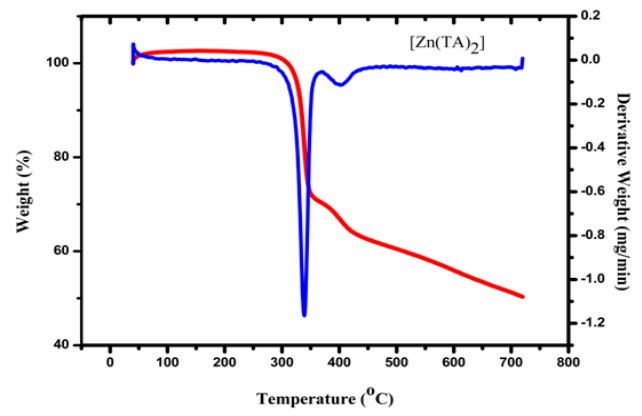

Figure 3.61 TG-DTG curves of $[Zn(TA)_2]$.

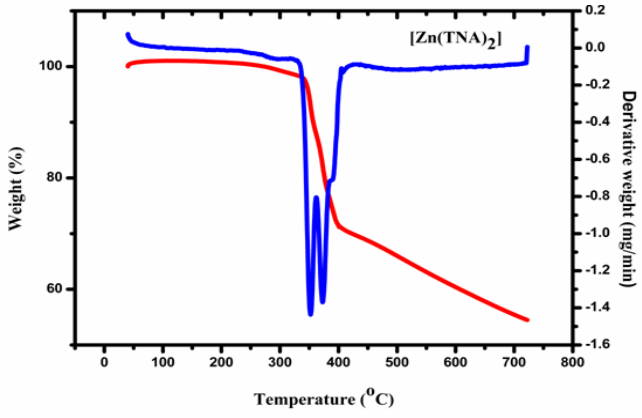

Figure 3.62 TG-DTG curves of $[Zn(TNA)_2]$.

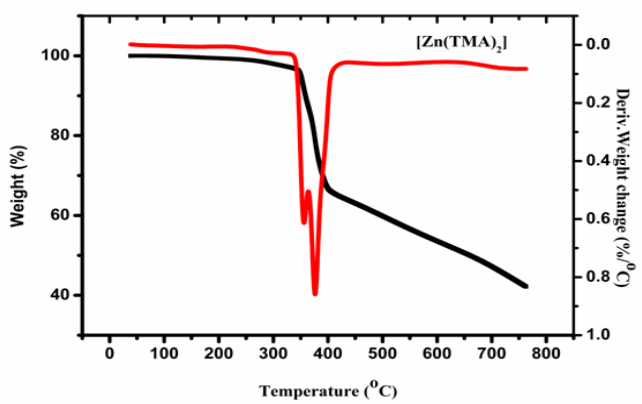

Figure 3.63 TG-DTG curves of $[Zn(TMA)_2]$

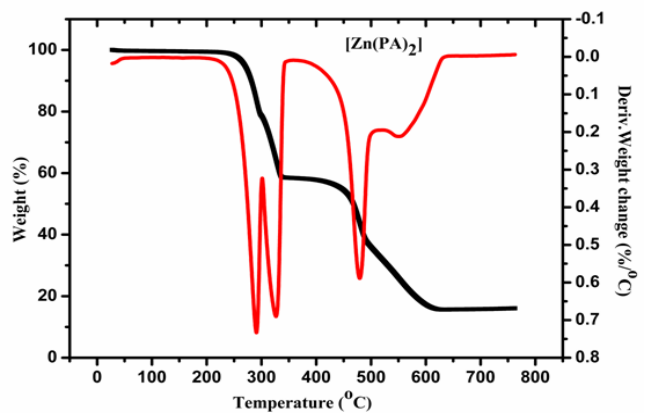

Figure 3.64 TG-DTG curves of $[Zn(PA)_2]$.

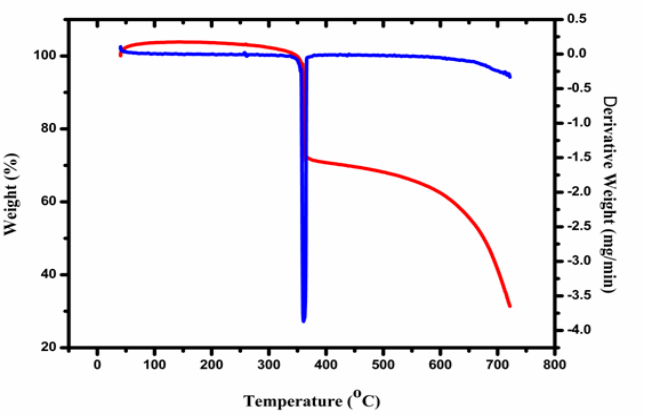

Figure 3.65 TG-DTG curves of $[Zn(PNA)_2]$.

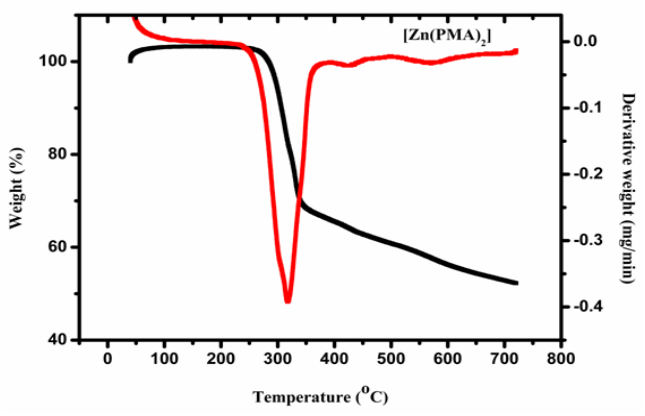

Figure 3.66 TG-DTG curves of $[Zn(PMA)_2]$.

Table 3.16 Data of the thermo gravimetric analysis for Zn(II) complexes

Complex	Temperature (°C)	Weight loss (%) Calc (found)	Assignments
$[Zn(TA)_2]$	303	43.45 (42.94)	Decomposition of ligand molecule
$[Zn(TNA)_2]$	345	40.56 (39.98)	Decomposition of ligand molecule
$[Zn(TMA)_2]$	349	41.70 (41.36)	Decomposition of ligand molecule
$[Zn(PA)_2]$	336	41.08 (41.22)	Elimination of ligand molecule
	496	40.03 (40.77)	Decomposition of ligand molecule
$[Zn(PNA)_2]$	353	40.77 (41.34)	Decomposition of ligand molecule
$[Zn(PMA)_2]$	254	41.66 (42.02)	Decomposition of ligand molecule

3.3.8 Geometry of the complexes

Based on the above results, following tentative structures are assigned for synthesized Ni(II), Cu(II) and Zn(II) heterocyclic Schiff base complexes (Figures 3.67-3.69).

Figure 3.67 Proposed structures of Ni(II) complexes

a = $[Ni(TA)_2(H_2O)_2]$, b =$[Ni(TNA)_2(H_2O)_2]\cdot 2H_2O$, c = $[Ni(TMA)_2]\cdot 3H_2O$,
d = $[Ni(PA)_2]\cdot H_2O$, e = $[Ni(PNA)_2]\cdot 2H_2O$, d =$[Ni(PMA)_2]$

Figure 3.68 Proposed structures of Cu(II) complexes

a = $[Cu(TA)_2H_2O]\cdot H_2O$, b = $[Cu(TNA)_2]\cdot 2H_2O$, c = $[Cu(TMA)_2]\cdot H_2O$
d = $[Cu(PA)_2H_2O]\cdot 2H_2O$, e = $[Cu(PNA)_2]\cdot 3H_2O$, f = $[Cu(PMA)_2]\cdot H_2O$

Figure 3.69 Proposed structures of Zn(II) complexes

a = $[Zn(TA)_2]$, b = $[Zn(TNA)_2]$, c = $[Zn(TMA)_2]$,
d = $[Zn(PA)_2]$, e = $[Zn(PNA)_2]$, f = $[Zn(PMA)_2]$

3.4 Conclusion

This chapter describes the synthesis and characterization of Ni(II), Cu(II) and Zn(II) complexes of Schiff bases TA, TNA, TMA, PA, PNA and PMA. The analytical data suggest that all Ni(II), Cu(II) and Zn(II) complexes are mononuclear. Low molar conductance values indicate that all Ni(II), Cu(II) and Zn(II) complexes are non electrolytic in nature. All the complexes are found to be thermally stable by thermogravimetric analysis. Magnetic moment values of $[Ni(TA)_2(H_2O)_2]$ (2.96 B.M.) and $[Ni(TNA)_2(H_2O)_2]\cdot 2H_2O$ (2.91 B.M.) suggest octahedral structure. The magnetic moment of other Ni(II) complexes $[Ni(TMA)_2]\cdot 3H_2O$, $[Ni(PA)_2]\cdot H_2O$, $[Ni(PNA)_2]\cdot 2H_2O$ and $[Ni(PMA)_2]$ lies within the range 3.5-3.7 B.M. that suggest tetrahedral structure. This was confirmed by electronic and IR spectral studies. Magnetic moment values of all copper complexes gives an indication of square pyramidal or square planar structure. UV-Vis, EPR and thermogravimetric data confirmed square pyramidal structure for $[Cu(TA)_2H_2O]\cdot H_2O$ and $[Cu(PA)_2H_2O]\cdot 2H_2O$ complexes and square planar structure for all other $[Cu(TNA)_2]\cdot 2H_2O$, $[Cu(TMA)_2]\cdot H_2O$, $[Cu(PNA)_2]\cdot 3H_2O$, $[Cu(PMA)_2]\cdot H_2O$ copper complexes. The physicochemical and spectral data reveals tetrahedral structure for all Zn(II) complexes.

References

[1] A. M. Abu-Diefaand and I. M. A. Mohamed, Beni-Suef Univ. J. Basic. Appl. Sci., 4, (2015), 119-133.

[2] N. Mala and K. S. Pramendra, Dalton Trans., 40, (2011), 7077-7121.

[3] K. S. Bibhesh, P. Anant, K. R. Hemant, B. Narendar and A. Devjani, Spectrochim. Acta. Mol. Biomol. Spectrosco., 76, (2010), 376-383.

[4] L. Shi, W. J. Mao, Y. Yang, and H. L. Zhu, 62, (2009), 3471-3477.

[5] J. Zhao, B. Zhao, J. Liu, W. Xu, and Z. Wang, Spectrochim. Acta. Mol. Biomol. Spectrosco., 57, (2001), 149-154.

[6] M. A. Karema, A. M. Abdussalam, M. Marei El-Ajaily, M. E. Abdunnaser, M. A. Mortaja Krisha and A. A. Majda, Int. J. Org. Chem., 4, (2014), 7-15.

[7] A. Muhammad, A. Itrat, A. Nighat, T. H. Muhammad, I. Lubna, H. Ajaz, I. Samina, H. B. Tanveer and K. Muhammad, Med. Chem. Drug Discovery, 2, (2012), 80-86.

[8] K. S. Bibhesh, P. Anant, K. R. Hemant, B. Narendar and A. Devjani, Spectrochim. Acta. Mol. Biomol. Spectrosco., 76, (2010), 376-383.

[9] E. Akila, M. Usharani and R. Rajavel, Int. J. Bioinorg. Chem., 2, (2011), 15-19.

[10] P. Rathi and D. P. Singh, Spectrochim. Acta A. Mol. Biomol. Spectrosc., 136, (2015), 381-387.

[11] L. Galluzzi, I. Vitale, J. Michels, C. Brenner, G. Szabadkai, A. Harel-Bellan, M. Catedo and G. Kroemer, Cell Death Diseases, 5, (2014), 1257-1259.

[12] S. Ghosh, S. Malik, B. Jain, and M. Gupta, J. Ind. Chem. Soc., 89, (2012), 471-478.

[13] X. Yi-Mei, L. Kuan, W. Yuhong, D. Wei and Y. Zi-Jian, Polymers., 9, (2017), 105, doi:10.3390/polym9030105.

[14] M. Pampa, B. Chaitali, G. B. D. Michael and G. Ashutosh, Polyhedron., 26, (2007), 3121-3128.

[15] A. Patra, T. K. Sen, A. Ghorai, G. T. Musie, S. K.Mandal, U. Ghosh and M. Bera, Inorg. Chem., 52, (2013), 2880-2890.

[16] R. R. Pulimamidi, S. Addla, R. Nomula and R. Pallepogu, J. Inorg. Biochem., 105, (2011), 1603-1612

[17] K. Rishu, K. Harpreet and K. K. Brij, Sci. Revs. Chem. Commun., 3, (2013), 1-15.

[18] S. Kannan, R. Ramesh and Y. Liu, J. Organomet. Chem., 692, (2007) 3380-3391.

[19] X.B. Yang, Q. Wang, Y. Huang, P. H. Fu, J. S. Zhang and R. Q. Zeng, Inorg. Chem. Commun., 25, (2012), 55-59.

[20] D. Dhananjay, K. Gurpreet, R. Anandan, G. Loganathan, C. Prateeti, A. Jaydeep, P. Jorge, D. Dharumadurai, R. C. Angshuman, A. A. Mohammad, K. Niranjan and B. Bhaskar, Eur. J. Inorg. Chem., (2014), 3350-3358.

[21] N. Vandna, S. Devender, K. S. Raman, T. Vijeta, K. Sonika, S. Ritu and S. K. Pratap, Cogent Chem., 1, (2015), 1079291.

[22] J. Chen, X. Wang, Y. Zhu, J. Lin, X. Yang, Y. Li, Y. Lu and Z. Guo, Inorg. Chem., 44, (2005), 3424-3430.

[23] B. Biswas, N. Kole, M. Patra, S. Dutta and M. Ganguly, J. Chem. Sci., 125, (2013), 1445-1453.

[24] H. Sakiyama, K. Ono, T. Suzuki, K. Tone, T. Ueno and Y. Nishida, Inorg. Chem. Commun., 8, (2005), 372-374.

[25] N. Nanjan, N. Ramaswamy, G. Steven, V. Krishnaswamy, N. Raju, D. B. Manickam and T. K. Pudupalayam, Polyhedron., 110, (2016), 203-220.

[26] S. R. Moamen, Y. Mohamed El-Sayed, M. Abdel and A. Adam, J. Mol. Struct., 1038, (2013), 62-72

[27] A. A. El-Sherif and T. M. A. Eldebss, Spectrochim. Acta Mol. Biomol. Spectrosc., 79, (2011), 1803-1814.

[28] A. M. Abu-Dief and L. A. E. Nassr, J. Iran. Chem. Soc., 12, (2015), 943-955.

[29] A. Z. Wail, Int. J. Org. Chem., 3, (2013), 73-95.

[30] R. Mithun and D. Biplab, Int. Res. J. Pure. Appl. Chem., 3, (2013), 232-249.

[31] M. A. Mokhles–Elzaher, A. L. Ammar, A. M. Hanan, A. M. Samia, A. M. Mamdouhand A. Ahmed El-Rashedyb J. Basic. Appl. Sci., 5, (2016), 85-96.

[32] K. Zahid, T. M. Zahida, A. K. T. Muhammad, M. K. Khalid, I. Lubna and L. Mehreen, J. Basic Appl. Sci., 11, (2015), 125-130.

[33] N. K. Chaudhary, Arch Appli Sci Res., 5, (2013), 227-231.

[34] E. Akila, M. Usharani and R. Rajavel, Int. J. Inorg. Bioinorg. Chem., 2, (2011), 15-19.

[35] B. I. Omar, A. M. Mahmoud and S. R. Moamen, Can. Chem. Trans., 2, (2014), 108-121.

[36] T. D. Priya and R. K. S. Hemakumar, J. Chem., 3, (2010), 266-270.

[37] S. T. Syed and K. Geetha, Indian J. Adv. Chem. Sci., 4, (2016), 40-48.

[38] S. N. Madhavan, A. Dasan and S. J. Raphael, J. Saudi Chem. Soc., 16, (2012), 83-88.

[39] R. J. Sachin and I. H. Seema, Orient. J. Chem., 3, (2014), 2231-5039.

[40] L. K.-Ahmadi and L. Shirmohammadzadeh, J. Nanostruct. Chem., 7, (2017), 179-190.

[41] S. Kiran, T. Ritu and K.Vikas, J. Basic. Appl. Res., 5, (2016), 21-30.

[42] K. Nakamoto, Infrared Spectra of Inorganic and Coordination Compounds, ed. 2nd, Wiley-Inter Science, (1963).

[43] A. Juan, P. Yaricruz, B. Alina and C. Juan, Med. Chem., 6, (2016), 467-473.

[44] S. Iran, T. Zainab and K. Moj, Int. J. Nano Dimens., 7, (2016), 127-136.

[45] B. Smita, G. Gajendra, D. Babulal and M. R. Kollipara, J. Organomet Chem., 695, (2010), 2098-2104.

[46] A. B. Hoda, A. M. A. Alaghaz and S. A. Mutlak, Int. J. Electrochem. Sci., 8, (2013), 9399 - 9413.

[47] M. Dinkar Malik, J. Pharma. Med. Res., 2, (2016), 36-38.

[48] T. D. Priya and R. K. S. Hemakumar, J. Chem., 3, (2010), 266-27

[49] P. Anant, P. G. Mukesh and K. K. Singh, J. Dev. Biol. Tissue Eng., 3, (2011), 13-19.

[50] N. H. Al-Shaalan, Molecules, 16, (2011), 8629-8645.

[51] B. Subhra, S. Soma, M. Samiran, C. Marschner and W. S. Sheldrick, Struct. Chem., 19, (2008), 115-121.

[52] M. K. Abdalla and M. M. Hadi, Int. J. Electrochem. Sci., 7, (2012), 10074 -10093.

[53] M. Y. Ali, American J. BioSci., 2, (2014), 22-34.

[54] A. P. Mishra and P. Gupta, J. Chem. Pharma. Res., 3, (2011), 150-161.

[55] K. Mohanan and B. Murukan, Metal Org. and Nano-Metal Chem., 35, (2005), 837-844.

[56] J. K. Roji, M. Sithambaresan, A. A. Ambili, N. Aiswarya and M. R. K. Prathapachandra kurup, Polyhedron, 113, (2016), 73-80.

[57] K. Jayakumar, M. Sithambaresan, N. Aiswarya and M. R. K. Prathapachandra Kurup, Spectrochim. Acta Mol. Biomol. Spectrosc., 139, (2015), 28-36.

[58] I. M. Procter, B. J. Hathaway and P. Nicholis, J. Chem. Soc., 0, (1968), 1678-1684.

[59] N. Aiswarya, M. Sithambaresan, S. S. Sreejith, and M. R. K. Prathapachandra Kurup, Inorg. Chim. Acta., 443, (2016), 251-266.

[60] K. Jayakumar, M. Sithambaresan, A. A. Ambili and M.R. K. Prathapachandra Kurup, Polyhedron., 75, (2014), 50-56

[61] B. N. Figgis, Introduction to Ligand fields, Interscience, New York, (1996).

[62] B. J. Hathaway, G. Wilkinson, R. D. Gillard and J. A. Mc Cleverty, Pergamon, 5, (1987), 533-537.

[63] N. Kavitha and P.V. Anantha Lakshmi , J. Saudi Chem. Soc., 21, (2017), 457-466.

Chapter - 4

ANTIOXIDANT ACTIVITY OF HETEROCYCLIC SCHIFF BASES - SOLVENT EFFECT, STRUCTURE ACTIVITY RELATIONSHIP AND MECHANISM OF ACTION

Contents

4.1 Introduction

Reactive oxygen species (ROS) such as hydroxyl radicals, superoxide radicals, singlet oxygen and hydrogen peroxide radical are constantly formed in our body as a result of normal organ functions or excessive oxidative stress [1]. Physical and mental stress, environmental pollution and the consumption of packed foods are increasing in day to day life which enhances the risks of generating free radicals. Over production of these radical can induce oxidative damage to biomolecules such as DNA, proteins, lipids and carbohydrates and this may accelerate cancer, Parkinsons disease, ageing etc. [2].

Blocking the generation of ROS and free radicals through the supplementation of antioxidants has a beneficial health effects. Many natural polyphenolic compounds and conjugated phenol derivatives are good antioxidants and can be used as food preservative to extend shelf life and to maintain quality of food. Synthetic phenolic antioxidants such as butylated hydroxyl toluene (BHT), butylated hydroxy anisole (BHA) and tertiary

butylated hydroxylquinine (TBHQ) are effective and cheaper than natural antioxidant. However synthetic antioxidants have been questioned due to their side effect for human health [3]. Synthetic antioxidants with low cytotoxicity values are thus suitable alternatives.

Hydroxyl-substituted Schiff bases with easily replaceable hydrogen atom of the OH groups attached to aromatic rings may be considered as effective antioxidants [4]. Imine bases containing heterocyclic scaffolds and phenol derivatives have been known to possess a wide range of biological application such as antifungal, antioxidant, antibacterial, antitumor, anti-inflammatory and antipyretic activities [5]. They are also well known as complexing agents [6] and powerful corrosion inhibitors [7]. Free radical scavenging capacity shown by this class of compounds make them potential drugs to prevent disease related to free radical damage [8].

In this chapter antioxidant activity of newly synthesized phenolic Schiff bases have been discussed. Radical scavenging activities of synthesized compounds were evaluated by using DPPH and ABTS radicals in polar and non polar solvents. BHA was used as standard. This chapter also describes mechanism of action and the relationship between the structure and antioxidant activity of few Schiff bases (Scheme 1)

Scheme 1 Antioxidant activity of heterocyclic Schiff bases

4.2 Experimental

4.2.1 Materials

All reagents used were of analytical grade. butylated hydroxyl anisole, 2,2'-Azinobis-3-ethylbenzothiazoline-6-sulfonic acid (ABTS), 2-Diphenyl-1-pikryl-hydrazyl (DPPH) were purchased from Aldrich. Solvents; methanol, chloroform, acetone, acetonitrile and ethyl acetate were obtained from Merck. The materials used for the preparation of phenolic Schiff base are presented in Chapter 2.

4.2.2 Methods

The Antioxidant assay- radical scavenging activity of the compounds (TA, TNA, TMA, PA, PNA and PMA) has been investigated using DPPH and ABTS radicals using BHA as the standard. The fixed reaction time and steady state measurement methods were used to find out antioxidant activity of these compounds in five different solvents (methanol, acetonitrile, acetone, ethyl acetate and chloroform) of varying polarity.

4.2.3 DPPH Free Radical Scavenging Activity

4.2.3.1 Fixed reaction time

The antioxidant activity of the compounds TA, TNA, TMA, PA, PNA and PMA was determined by the DPPH radical scavenging assay. The stock solution of the compounds was prepared by dissolving 1mg/mL in methanol. From the stock solution, appropriate amount was added to definite volume of DPPH (0.01 mmol) in methanol and made up to a final volume of 3 mL using methanol as solvent. After incubating for 30 min, the absorbance of the test compounds was taken at 517 nm using UV-Vis spectrophotometer. A system devoid of the compound was used as control. All determinations were performed in triplicate. Assay was also performed in different solvent. Percentage inhibition was calculated by the following equation.

% inhibition = [(Absorbance of control – Absorbance of test sample)/ Absorbance of control] x100

A graph was plotted with concentration against % inhibition. The concentration at which 50% fall in absorbance of DPPH values (IC_{50}) were calculated from the graph. IC_{50} is the concentration sufficient to obtain 50% of maximum scavenging activity [9].

4.2.3.2 Steady state measurement

In this method the decrease in absorbance was determined at each minute for duration of one hour. For each antioxidant, reaction kinetics was plotted. From these graph the percentage of DPPH radical remaining at the steady was determined and it was plotted against the molar ratio of antioxidant to DPPH radical.

$$\% \text{ DPPH radical remaining} = (C_f / C_0) \times 100$$

From the graph EC_{50} values were obtained. It was similar to IC_{50}. This parameter is defined as the efficient concentration required to decrease the initial DPPH concentration by 50%. The value of EC_{50} was expressed in terms of molar ratio of antioxidant to DPPH. Larger the $EC_{50,}$ the more efficient the antioxidant [10].

4.2.4 ABTS radical scavenging assay.

ABTS scavenging ability of the compounds was studied using the procedure reported in literature [11-12]. The working solution was prepared by mixing two stock solutions of 7 mM ABTS solution and 2.4 mM potassium persulfate solution in equal amounts (1:1). The mixture was allowed to react in the dark for 12 h at room temperature. The resulting solution was further diluted by mixing 1 mL ABTS solution to obtain an absorbance of 0.706 ± 0.001 units at 734 nm using the spectrophotometer. The ABTS scavenging capacity of the compounds were compared with that of BHA (standard drug). All tests and analyses were run in triplicate and the

results obtained were averaged. The percentage inhibition was calculated as ABTS radical scavenging activity using the following equation:

(%) Inhibition = [(Abs control – Abs sample) / Abs control] × 100

Where Abs control is the absorbance of ABTS radical + methanol and Abs sample is the absorbance of ABTS radical + sample [for 2.5-3 h at 37 ºC in test samples/standard]

4.3 Results and discussion

The synthesized compounds are crystalline, colored, non-hygroscopic, insoluble in water, soluble in ethanol, acetone, DMF and DMSO.

In vitro antioxidant activity of all the synthesized compounds were evaluated by DPPH assay, Antioxidant activity of the compounds in different solvents is shown in Figure 4.1- 4.6 and their corresponding IC_{50} values are depicted in Table 4.1. A lower IC_{50} value is indicate of greater antioxidant activity. All the compounds inhibit DPPH radical in a concentration-dependent manner and show comparable free radical-scavenging activity to standard synthetic antioxidant BHA. The methyl substituted derivatives of TA and PA (TMA and PMA) showed lower IC_{50} values whereas the corresponding nitro substituent PNA and TNA showed higher IC_{50} values. The general trend in the order of antioxidant activity of synthesized compounds was PMA > TMA > PA > TA > PNA > TNA.

Table 4.1 DPPH Scavenging capacities (IC_{50} in µg/mL) of synthesized compounds in different solvents

Compound	Methanol	Chloroform	Acetonitrile	Acetone	Ethyl acetate
TA	1.85	2.94	23.2	33.3	150
TNA	4.08	6.01	43.2	90.3	206
TMA	1.67	2.77	18.5	26.0	134
PA	1.66	2.80	26.0	32.0	123
PNA	2.26	4.15	42.1	52.9	150
PMA	1.50	2.31	22.0	26.1	120
BHA	3.35	5.34	41.9	56.0	170

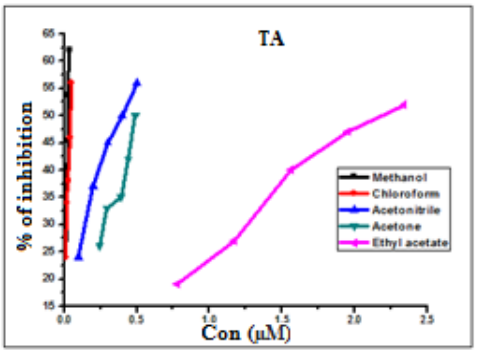

Figure 4.1 Antioxidant activity of TA.

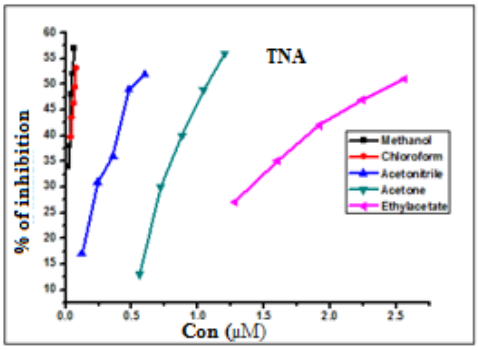

Figure 4.2 Antioxidant activity of TNA.

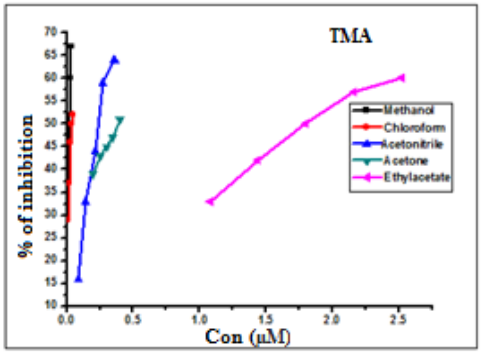

Figure 4.3 Antioxidant activity of TMA.

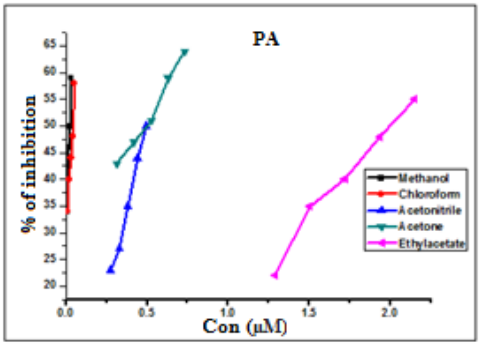

Figure 4.4 Antioxidant activity of PA.

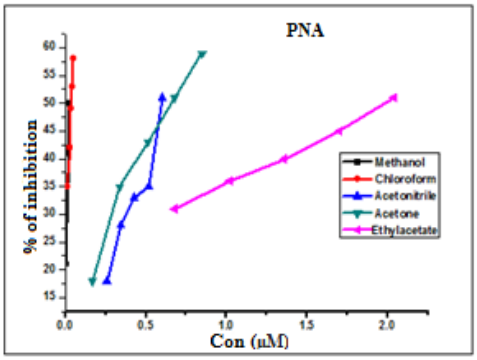

Figure 4.5 Antioxidant activity of PNA.

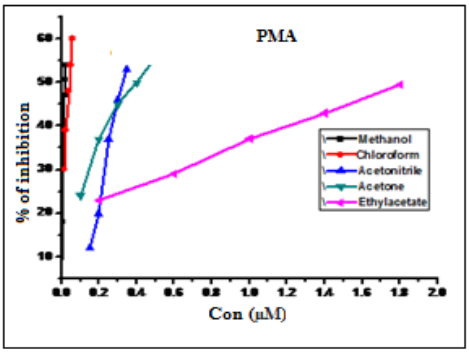

Figure 4.6 Antioxidant activity of PMA.

The IC_{50} values obtained from fixed reaction time-30 min was compared with that obtained from the steady state kinetic method (Figures for TA, TNA, TMA, PA, PNA and PMA in methanol solvent were given in Figures 4.7- 4.12). In steady state method measurement of the percentage of [DPPH radical] remaining at steady state was determined [Figure 4.7 a- 4.12 a] and it was plotted against the molar ratio of antioxidant to DPPH radical [Figure 4. 7 b- 4.12 b]. From the graph, effective concentration (EC_{50}) value was determined for each of the compounds. By using this method, Antiradical power (ARP), that is the inverse of EC_{50} value and stoichoimetry which gives the theoretical efficient concentration of each antioxidant needed to reduce 100% of the DPPH radical were also determined [13] [Table 4.2].

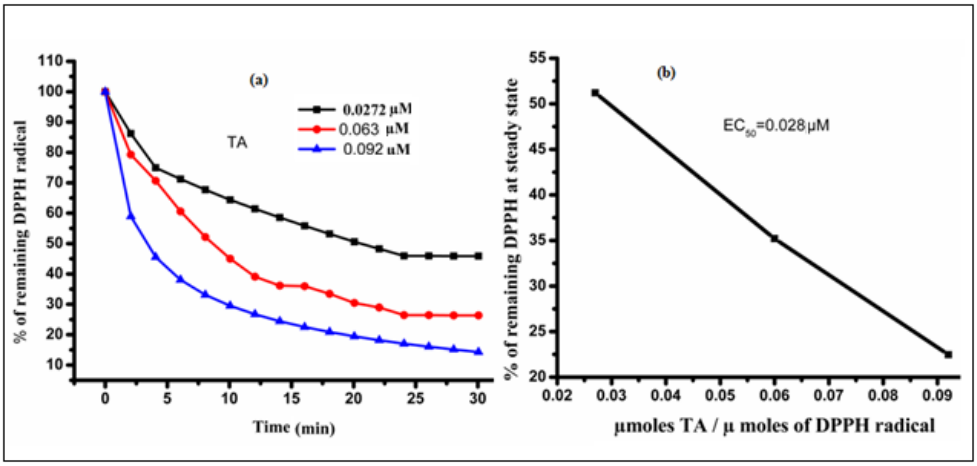

Figure 4.7 (a) Kinetic behavior of TA (b) The disappearance of DPPH radical as a function of the number of µ moles of TA/ µ mole DPPH.

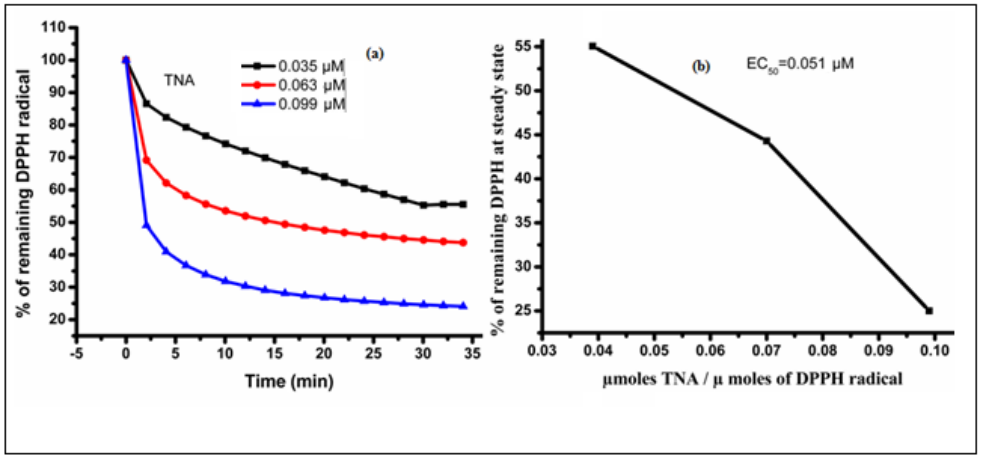

Figure 4.8 (a) Kinetic behavior of TNA (b) The disappearance of DPPH radical as a function of the number of µ moles of TNA/ µ mole DPPH.

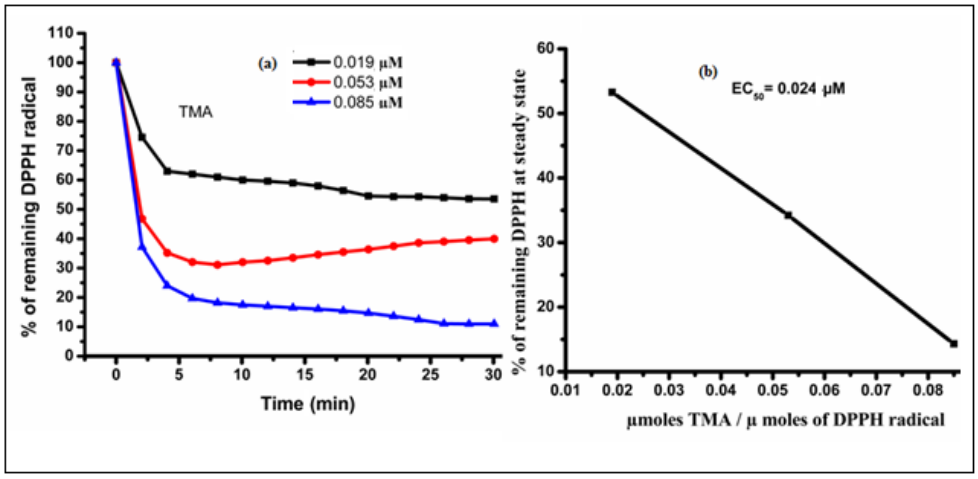

Figure 4.9 (a) Kinetic behavior of TMA (b) The disappearance of DPPH radical as a function of the number of µ moles of TMA/ µ mole DPPH.

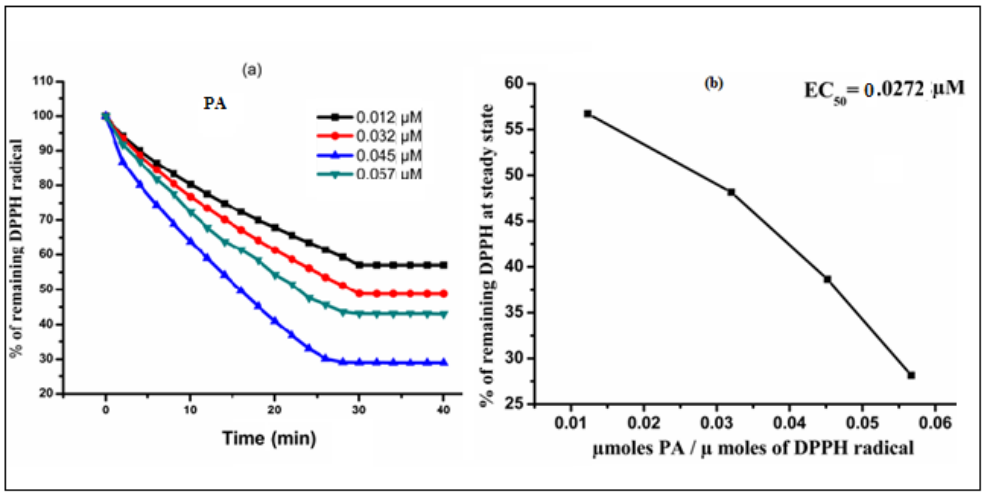

Figure 4.10 (a) Kinetic behavior of PA (b) The disappearance of DPPH radical as a function of the number of µ moles of PA/ µ mole DPPH.

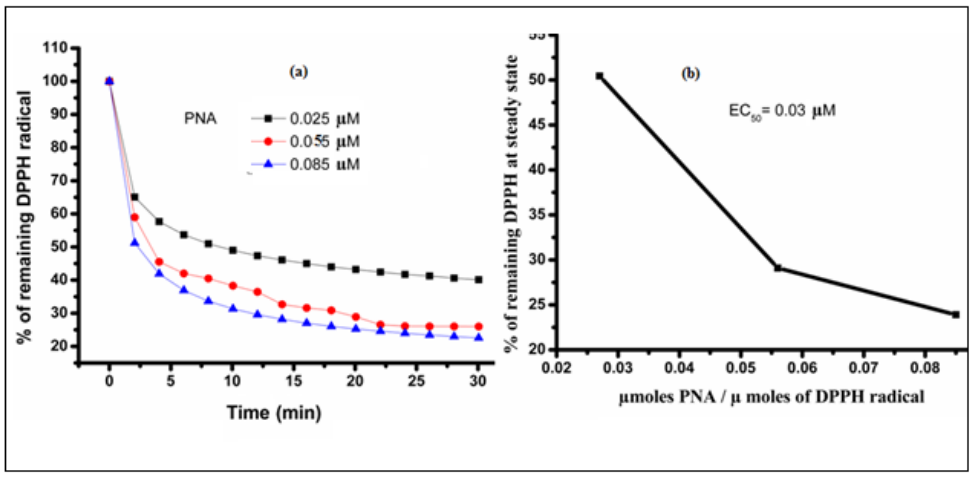

Figure 4. 11 (a) Kinetic behavior of PNA (b) The disappearance of DPPH radical as a function of the number of µ moles of PNA/ µ mole DPPH.

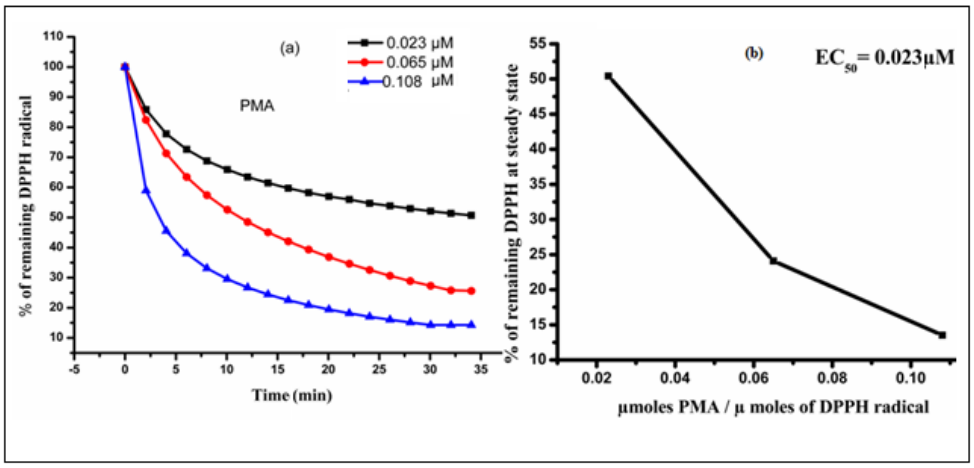

Figure 4.12 (a) Kinetic behavior of PMA (b) The disappearance of DPPH radical as a function of the number of µ moles of PMA/ µmole DPPH.

Table 4.2 Comparison of antiradical parameters: The antioxidant concentration (EC_{50}) that caused 50% decrease in DPPH radical estimated at steady state and fixed reaction time, antiradical power ($1/EC_{50}$), stoichiometry (EC_{50} x2)

Compound	IC_{50} (µM) in methanol (Fixed reaction time, 30 min)	EC_{50} (µM)in methanol (Steady state)	ARP ($1/EC_{50}$)	Stoichiometry (2 x EC_{50})
TA	0.028 ± 0.003	0.028 ± 0.003	35.71	0.056 ± 0.006
TNA	0.050 ± 0.004	0.051 ± 0.004	20.00	0.102 ± 0.008
TMA	0.024 ± 0.001	0.024 ± 0.001	41.66	0.048 ± 0.002
PA	0.027 ± 0.005	0.027 ± 0.005	37.03	0.054 ± 0.010
PNA	0.030 ± 0.001	0.034 ± 0.001	33.33	0.060 ± 0.002
PMA	0.023 ± 0.003	0.023 ± 0.003	43.47	0.046 ± 0.006

Brand-Williams, Cuvelier, and Berset suggested that IC_{50} and EC_{50} values are similar in the case of antioxidant with fast and medium reaction

kinetics with DPPH radical whereas for antioxidants under slow reaction kinetics, these values are different [13]. In the present work, synthesized Schiff bases showed approximately same IC_{50} and EC_{50} values (Table 4.2) which indicate a rapid radical scavenging activity in DPPH method.

The antioxidant potentials of the synthesized Schiff bases were further confirmed by testing their ABTS radical scavenging activity. ABTS radical assay is a conventional and excellent model for assessing the antioxidant activities of hydrogen-donating and chain breaking antioxidants. In this assay, at 734 nm, the absorbance of active ABTS radical solution obviously declined upon the addition of different concentration of synthesized Schiff base compounds. Results are shown in Figure 4.13. All the compounds are effective scavengers of the ABTS radical. All these compounds except TNA exhibited higher radical scavenging activities than the synthetic commercial antioxidant BHA (IC_{50} in methanol 4.22 µg/mL) TA, TNA, TMA, PA, PNA and PMA have IC_{50} values 2.12, 5.42, 1.76, 1.87, 3.45 and 1.65 µg/mL respectively**.** The ABTS radical scavenging ability of tested compounds can be ranked in the order PMA > TMA > PA > TA > PNA >TNA. It can be concluded that the synthesized Schiff bases showed same trend in radical scavenging for DPPH and ABTS radicals.

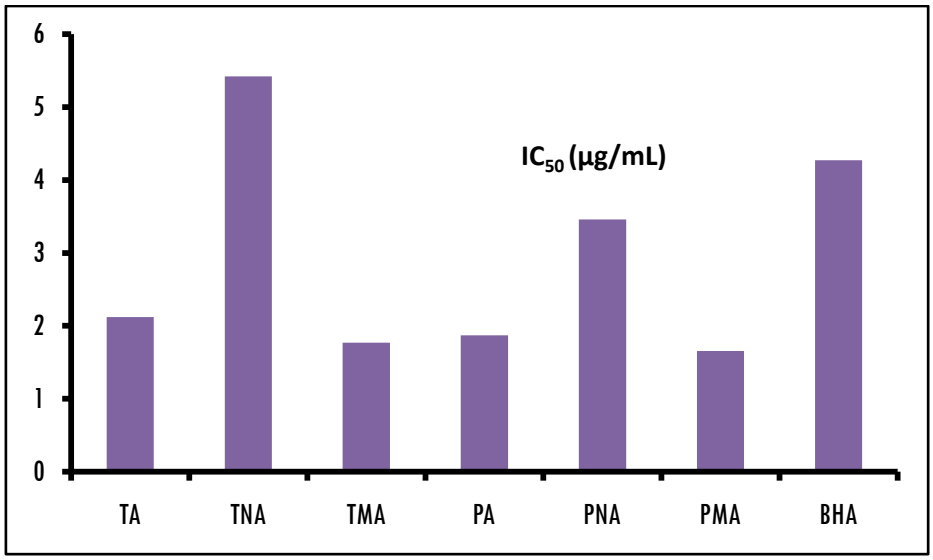

Figure 4.13 ABTS Scavenging capacities (IC_{50}) of synthesized compounds in methanol.

4.3.1 Solvent effect in DPPH assay and mechanism of action

Solvent effect on antioxidant activity of synthesized phenolic Schiff bases was studied in five different solvents having varying polarity (Table 4.1). Solvents used were polar protic solvent - methanol, polar aprotic solvents - acetonitrile, ethyl acetate and acetone, and non polar solvents – chloroform.

Antioxidants (ArX–H) may scavenge free radicals ( ) by H atom transfer through one of the three mechanisms [14-16]:

(i) Hydrogen atom transfer (HAT)

$$ArX\text{-}H + \dot{R} \longrightarrow Ar\dot{X} + R\text{-}H$$

The rate of reaction depends on Bond Dissociation Enthalpy (BDE)

ii) Electron Transfer–Proton Transfer (ET–PT)

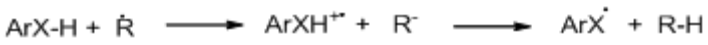

This mechanism involves two-steps; in the first step an electron is abstracted by the radical creating a cationic radical species of the phenol. In the second step the H^+ is removed from the cationic radical species of the phenol which is abstracted by the R- to form a neutral species. The rate of the reaction depends on Adiabatic Ionization Potential (AIP) for its first step and Proton Dissociation Enthalpy (PDE) for the second step [17-19].

iii Sequential Proton-Loss-Electron-Transfer (SPLET)

In the two step mechanism, the first step is the dissociation of phenolic antioxidant to an anionic species by the release of a proton. In the second step, the ions formed then react with free radicals. In this reaction, a radical form of the phenolic antioxidant and a neutral molecule appear. The rate of reaction depends on Proton affinity (PA) for first step and Electron Transfer Enthalpy (ETE) for the second step. The sequential proton loss electron transfer mechanism (SPLET) which is supported predominantly by polar protic solvents like methanol and ethanol [20-22]. In ET-PT and SPLET mechanism charge less substrate (phenol) is converted to a charged species the stabilization of transition state take place in polar medium. However in HAT this effect is reduced and H-bonding present in the transition state decide the solvent effect.

In the present study the influence of polar solvents on rate and mechanism of H atom donation by radicals are high, and are expected to form PhO – solvent bond which negatively influence the hydrogen atom donation phenol to radicals. All synthesized phenolic compounds showed higher antioxidant activity in polar protic solvent (methanol) in comparison to polar aprotic solvents (Table 4.1). The intermolecular hydrogen bond among the methanol molecules are stronger than that with the phenol moiety of the compounds with the solvent methanol, thus the lack of phenol–solvent hydrogen bond enhances the hydrogen abstraction by the DPPH radical as shown in SPLET mechanism (Figure 4.14). Among the polar aprotic solvents all compounds possesses greater activity in acetonitrile compared to that in acetone and ethyl acetate. This is due to weaker electronegative nature of nitrogen atom (Figure 4.14). The intermolecular H–O–hydrogen bond with the phenol moiety of studied compounds with acetone and ethyl acetate is stronger than C–N–H hydrogen bond with the solvent acetonitrile resulting easy liability for the hydrogen in acetonitrile solvent. Thus the hydrogen bond forming ability is the deciding factor rather than the polarity of the solvent. In HAT mechanism the antioxidant property depends mainly on solvent polarity but in SPLET mechanism it is controlled by hydrogen bonding ability [23-24]. As a result the scavenging activity of phenolic Schiff bases increases in this order, ethyl acetate < acetone < acetonitrile < methanol (Figure 4.14). This is also confirmed by steady state method by taking one fixed concentration of all test samples (Figure 4.15). Percentage of [DPPH radical] remaining was determined from the graph, and the result showed that scavenging activity of tested compounds were higher in methanol and lower in ethyl acetate.

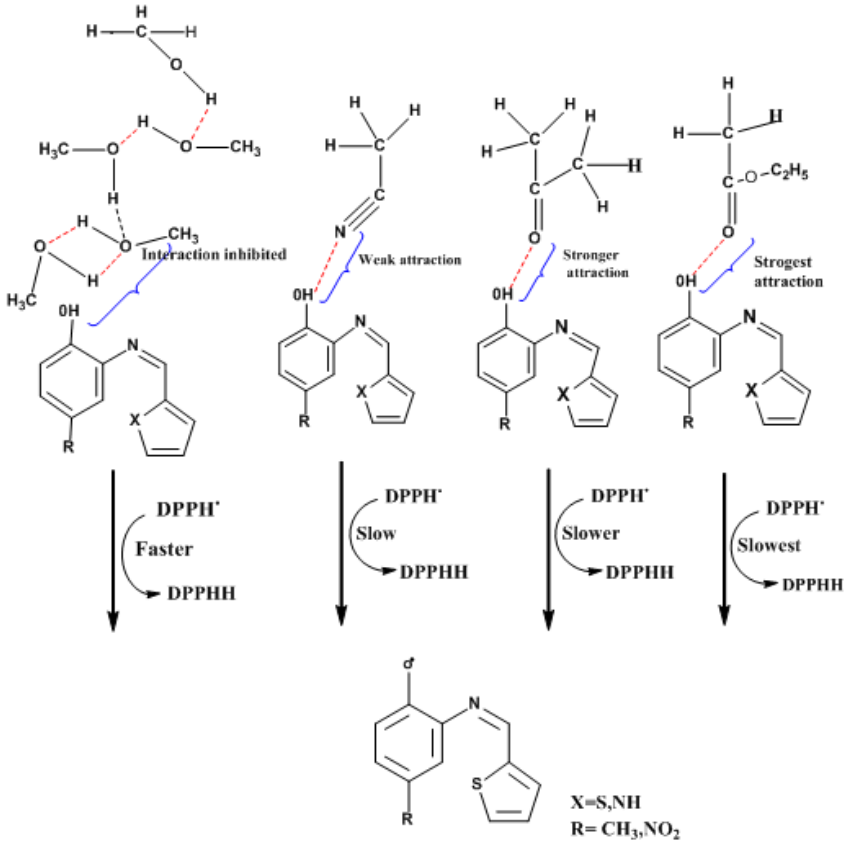

Figure 4.14 Solvent effects of synthesized Schiff bases in different solvents.

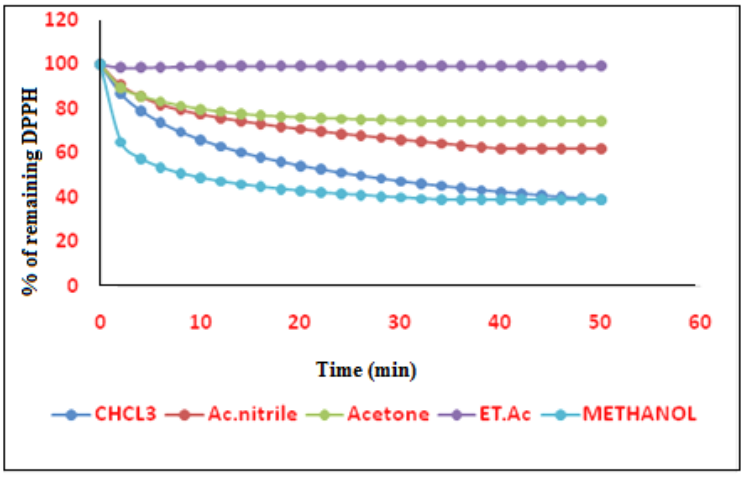

Figure 4.15 Kinetic behavior of PMA (100 µM) in DPPH assay in different solvent.

To find out the exact mechanism of radical scavenging of synthesized compounds, the antioxidant activity of these compounds were carried out in polar (eg. methanol) and non polar (eg. chloroform) solvents. Similar structure activity relationship was observed in both solvents. All the compounds have lower IC_{50} values in methanol than in chloroform. This can be explained in terms of dielectric constants of solvents. Phenolic compounds may ionize in methanol due to high dielectric constant of methanol (33). Solvents with high dielectric constant support ionization of phenols by abstraction of H^+ forming phenoxide ion (ArO^-). The phenoxide ion is strong electron donor than phenol (PhOH) and can rapidly transfer one of its electrons to the DPPH radical [25]. The partial dissociation of phenol in methanol and relatively high reduction potential of DPPH free radical suggest sequential proton loss electron transfer mechanism (SPELT) for radical scavenging activity of antioxidant in polar protic solvents (Figure 4.16). In polar aprotic solvents hydrogen bonding with hydrogen of phenol moiety is possible but with lesser extends and the antioxidant property also reduces in the same order indicating that SPLET mechanism is possible in these solvents. On the other side, chloroform has less ability to ionize phenols due to its low dielectric constant (4.8). The radical scavenging activity is however found to be similar to that in methanol indicating that the mechanism is different. In this case the interactions of phenol with DPPH occur by hydrogen atom transfer (HAT) mechanism (Figure 4.16). This shows that the antioxidant compounds interact with DPPH radicals by different pathway and have different activity in different solvents. Both SPELT and HAT mechanism results in the formation same phenoxyl radicals. The stability of this phenoxyl radical depends on the different substitution group on ortho or para position of phenyl ring.

Radical scavenging activity of synthesized Schiff bases (TA, TNA, TMA, PA, PNA and PMA) was also studied by ABTS method. ABTS is more reactive than DPPH radicals, therefore the antioxidants react with ABTS radical cation by very fast electron transfer followed by proton transfer mechanism [25] (Figure 4.16).

Figure 4.16 Proposed mechanism of reaction of Schiff bases with DPPH and ABTS radicals (SPLET in protic polar and aprotic polar solvents, HAT in aprotic less polar or non polar solvents).

4.3.2 Structure-activity relationship

Result in Table 4.1 indicates that all the Schiff bases except TNA have lower IC_{50} values than that of standard BHA [26-28]. Schiff base TMA and PMA having electron donating methyl substituent at para position of the phenol ring showed higher activity than Schiff base TA and PA (without any substituent). On the other hand Schiff base TNA and PNA which having electron withdrawing NO_2 group at para position of the phenol ring showed low activity due to their –I effect, which destabilizes the radical.

The two aldehydes, thiophene-2-carboxaldehyde and pyrrole-2-carboxaldehyde did not show any radical scavenging activity. However the phenols showed mild activities. In methanol, 2-aminophenol (IC_{50} in methanol = 2.5 µg/mL), 2-amino-4-nitrophenol (IC_{50} = 4.95 µg/mL), 2-amino-4-methylphenol (IC_{50} = 2.03 µg/mL) showed radical scavenging activity which was enhanced when the Schiff bases are formed from the aldehydes. The imine group increases free radical stabilization by conjugation. The absence of radical scavenging activity of aldehydes showed OH group is crucial for the antioxidant property of these compounds. The OH group is present ortho to the imine group, the lone pair of the nitrogen atom overlap with the phenolic radical at ortho position and provide electron supplementation which in turn increases radical scavenging activity by stabilization of radicals [29]. Brand-Williams, Cuvelier, and Berset suggestion for antiradical efficiencies of the different monophenolic compounds [14] were applicable to the present study. The donation of first hydrogen from OH group scavenges one DPPH radical converting the phenol to a phenoxide radical, which stabilizes by resonance as shown in Figure 4.17. In para substituted compounds the hydrogen donation from para methyl group scavenges the second DPPH molecule resulting in a stoichiometry 2, which applies to TMA and PMA, which possess hydrogens on the carbon in the para-position of the aromatic ring. The first hypothesis involves the donation of second hydrogen following electron delocalization

onto the para-substituted group as shown in reaction [1] of Figure 4.17. The dimerization between two phenoxyl radicals (reaction [2] of Figure 4.17) as described by Pokorny for phenols with free para- and ortho- positions [30]. After the dimerization, two hydroxyl groups would be regenerated by an intramolecular transfer of H radical and could again interact with the DPPH radical. The phenol radical can complexes with one DPPH radical as indicated in reaction [3] of Figure. 4.17. Reaction 2 and 3 apply to all molecules TA, TNA, TMA, PA, PNA, PMA and BHA.

Figure 4.17 Potential reactions of DPPH radical with synthesized compounds; Reaction [I], donation of second hydrogen; Reaction [2], dimcnzation; Reaction [3], complcxation.

4.4 Conclusion

Radical scavenging activity of Schiff bases (TA, TNA, TMA, PA, PNA and PMA) have been investigated using DPPH and ABTS methods. The antioxidant activity was in the order PMA > TMA > PA > TA > PNA > TNA and the influence of solvent in the activity are in the order methanol > chloroform > acetonitrile > acetone > ethyl acetate. Antioxidant studies of phenolic Schiff bases demonstrated that the position of the OH functional group and the presence of electron donating and withdrawing substituent's significantly influences the radical scavenging activity of phenolic Schiff bases. The rate of the radical scavenging reaction of phenols is also affected by the nature of the solvent and the strength of the phenolic OH– solvent interaction. The intermolecular hydrogen bonding between methanol molecules prevents methanol– phenolic OH interaction, which ensures that more phenolic OH groups are available for scavenging the free radical the polarity and protic nature of solvent play vital roles in the radical scavenging ability.

References

[1] H Yin, L. Xu and N. A. Porter, Chem. Rev., 111, (2011), 594-599.

[2] L. X. Cheng, J. J. Tang, H. Luo, X. L. Jin, F. Dai, J. Yang, Y. P. Qian, X. Z. Li and B. Zhou, Bioorg. Med. Chem. Lett., 20, (2010), 2417-2420.

[3] K. P. Srivastava, A. Kumar and R. Singh, J .Chem. Pharm. Res., 2, (2010), 68-77.

[4] S. K. Sridhar, M. Saravanan and A. Ramesh, Eur. J. Med. Chem., 36, (2001), 615-625.

[5] M. S. Karthikeyan, D. J. Prasad, B. Poojary, K. S. Bhat, B. S. Holla and N.S. Kumari. Bioorg. Med. Chem., 14, (2006), 7482-7489.

[6] P. Panneerselvam, R. R. Nair, G. Vijayalakshmi, E. H. Subramanian and S. K. Sridhar, Eur. J. Med. Chem., 40, (2005), 225-229.

[7] N. Soltani, H. Salavati, N. Rasouli, M. Paziresh and A. Moghadasi, Chem. Eng. Commun., 203, (2016), 840-854.

[8] A. A. Shanty, J. E. Philp, E. J. Sneha, M. R. P. Kurup, S. Balachandran and P. V. Mohanan, Bioorg. Chem., 70, (2017), 67-73.

[9] Y. Harinath, D. Harikishore Kumar Reddy, B. Naresh Kumar, C. Apparao and K. Seshaiah, Spectrochim. Acta A. Mol. Biomol. Spectrosc., 101, **(**2013), 264-267.

[10] K. Mishra, H. Ojha and N. K. Chaudhury, Food Chem., 130, (2012), 1036-1043.

[11] S. Mathew and T. E. Abraham, Food Chem. Toxicol., 44, (2006), 198-206.

[12] N. Nikolaos, W. Lan-fen, T. Maria and Z. Hong-yu, J. Agric. Food. Chem., 5, (2004), 4669-4674.

[13] W. Brand-Williams, M. E. Cuvelier and C. Berset, Lebenson Wiss Technol., 28, (1995), 25-30.

[14] M. Leopoldini, N. Russo and M. Toscano, Food Chem., 125, (2011), 288-306.

[15] M. C. Foti, C. Daquino and C. Geraci, J. Org. Chem., 69, (2004), 2309-2314.

[16] G. Litwinienko and K. U. Ingold, J. Org. Chem., 69, (2004), 5888-5896.

[17] M. Musialik and G. Litwinienko, Org. Lett., 7, (2005), 4951-4954.

[18] I. Nakanishi, T. Kawashima, K. Ohkubo, H. Kanazawa, K. Inami, M. Mochizuki, K. Fukuhara, H. Okuda, T. Ozawa, S. Itoh, S. Fukuzumi and N. Ikota, Org. & Biomolecular Chem., 3, (2005), 626-629.

[19] G. Litwinienko and K. U. Ingold, Acc Chem. Res., 40, (2007), 222-230.

[20] M. Leopoldini, N. Russo and M. Toscano, J. Agric. Food Chem., 54, (2006), 3078-3085.

[21] G. Mazzone, A. Galano, J. R. Alvarez-Idaboy and N. Russo, J. Chem. Inf. Model., 56, (2016), 662-670.

[22] A. Galano, G. Mazzone, R. Alvarez-Diduk, T. Marino, J. R. Alvarez-Idaboy and N. Russo, Annu. Rev. Food Sci. Technol., 7, (2016), 335-352.

[23] T. Velmurugan, A. B. Ryan Phillip and P.L. Lai, J. Phy. Chem. A., 113, (2009), 3068-3077.

[24] G. Litwinienko and K. U. Ingold, J. Org. Chem., 68, (2003), 3433-3438.

[25] L. Jing, L. Chang, C. Yun-Fen, Y. De-Yu and S. Cui-Rong, Bioorg. Med. Chem. Lett., 22 (2012), 5744-5747.

[26] E. I. Hassane Anouar, R. Salwa, B. Imene, T. Muhammad, S. B. Mohd, D. M. Florent, H. H. Mizaton, A. Aishah, I. N. Hadiani, F.W. Jean-Fre´de´ric and T. Patrick, J. Comput. Aided. Mol. Des., 27, (2013), 951-964.

[27] D. K. Beena and S. R. Diwan, Bioorg. Med. Chem. Lett., 23, (2013), 641-645.

[28] H. Vijay Kumar and N. Nagaraja, Eur. J .Med. Chem., 45, (2010), 2-10.

[29] C. Yohann, A. Felix and P. Roman, J. Am. Oil. Chem. Soc., 89, (2012), 55-66.

[30] J. Pokorny, Major factors affecting the autoxidation in lipids. In: Autoxidation of Unsaturated Lipids, ed. H. W-S Chan, Academic Press, London, (1987).

Chapter 5

DNA BINDING STUDIES OF SCHIFF BASES AND THEIR Ni(II), Cu(II) AND Zn(II) COMPLEXES

Contents

5.1 Introduction

Recent years have seen an increased interest in the study of molecules which are able to bind the deoxyribonucleic acid (DNA) in efforts to find agents that regulate gene expression and cell processes and to create new drugs with improved biological activity against cancer cells [1]. DNA plays a main role in the life process because it carries heritage information and instructs the biological synthesis of proteins and enzyme through the process of replication and transcription of genetic information [2]. As DNA is an important target for studies with small molecules such as steroids, carcinogens and several classes of drugs, investigation of small molecule-DNA interaction is very important [3].

Metal-based pharmaceuticals emerging from interface of inorganic chemistry and biology have witnessed spectacular successes [4]. Metal-imine complexes have been widely investigated due to antitumor and herbicidal

utilization. They can work as models for biologically important species. The chelating ability and biological implementations of metal complexes have attracted remarkable attention [5-6]. Transition metal complexes bind to DNA by both covalent and non-covalent interactions. Covalent binding involves the coordination of the nitrogenous base or the phosphate moiety of the DNA to the central metal ion. The three different non-covalent interactions are intercalation; which involves the stacking of the molecule between the base pairs of DNA, groove binding; which comprises the insertion of the molecule into the major or minor grooves of DNA and electrostatic or external surface binding [7]. The effective mode of the drugs targeted to DNA is intercalative binding, which is related to antitumor activity [8]. Intercalating drugs possess flat, hetero aromatic ring systems that can insert between two adjacent base pairs in a helix [9]. Upon binding to DNA, the small molecules are stabilized through a series of weak interactions such as π- stacking interactions of aromatic heterocyclic groups between the base pairs, hydrogen bonding and van der Waals interactions of functional groups bound along the groove of the DNA helix [10]. Shape, planar area, size and electron density of the interacting aromatic rings may affect the binding mode. Therefore, a systematic study of the influence of varying parameters on the interaction of metal complexes with DNA would be important in the rational design of new drugs and therapeutic reagents targeted to DNA [11-12].

Several classes of metal complexes have been synthesized using various ligands and metal ions, and their anticancer activity has been successfully evaluated both in vitro and in vivo. Among the non-platinum complexes for metal based chemotherapy, copper, nickel and zinc

complexes have been much explored due to the fact that all the metals are bio essential elements responsible for numerous bioactivities in living organism [13]. Cu(II) ion plays an important role in the development of connective tissue, nerve coverings and bone in humans. It also acts as a reductant in enzymes cytochrome oxidase, superoxide dismutase, lysil oxidase, dopamine hydroxylase [14]. In biological systems, it is a substantial catalytic co–factor for a variety of metabolic reactions, electron transfer and oxygen transport proteins such as azurin, plastocyanin, laccase and hemocyanin [15]. The biological behaviour of Cu(II) complexes has been subjected to intense investigation for DNA binding and cleavage activities [16]. Copper accumulates in tumors due to the selective permeability of cancer cell membranes to copper compounds. Thus, a number of copper complexes have been screened for anticancer activity, and some of them were found to be active both in vitro and in vivo [17].

Nickel is an important transition metal, its coordination compounds display interesting binding and cleavage reactivity with nucleic acids [18]. Nickel is present in the active sites of several important classes of metalloproteins, as either a homodinuclear or a heterodinuclear species. Many biological activities of Ni(II) Schiff base complexes have been reported in the literature [19]. Furthermore depending upon the electronic and steric factors of the Schiff base ligands, Ni(II) form four, five and six coordinate complexes [20].

Zn is the second most abundant essential metal for the growth and repair of our body tissues and it serves an important structural role in DNA binding proteins and stabilizing the acceptable binding sites. Mei-Ju Niu *et al.*

reported synthesis and characterization of novel chiral and achiral Zn(II) complexes based on *o*-vanillin Schiff base ligand [21]. Their interactions with CT-DNA were also investigated. The results showed that the chiral complex exhibited more efficient DNA interaction with respect to achiral. Also, the chiral Zn(II) complex showed more potent cytotoxic activity on selected cancerous cell lines. Therefore, the chiral and nuclearity of zinc complexes have large influence on the anticancer activities and fluorescent emission.

Having all the above facts in mind, the present work stems from our interest to study the DNA binding activities of heterocyclic Schiff bases and their Cu(II), Ni(II) and Zn(II) complexes.

5.2 Experimental

5.2.1 Materials

Deoxyribonucleic acid, Tris (Hydroxymethyl) Aminomethane, glacial acetic acid was obtained from S. D. FINE CHEM. LTd. Mumbai.

5.2.2 Methods

5.2.2.1 Preparation and characterization of ligands and their metal complexes are discussed in chapter 2 and chapter 3.

5.2.2.2 Preparation of DNA stock solution

The stock solution was prepared by dissolving Herring sperm DNA (HS-DNA) in the 50 mM Tris-HCl buffer (pH = 7.1). The DNA concentration was determined by UV-Vis. spectroscopy using the molar absorption coefficient 6600 $M^{-1}cm^{-1}$ at 260 nm [22]. The stock solution was stored at 4 °C.

5.2.3 DNA binding experiments

5.2.3.1 Absorption spectral studies

The UV-Visible absorption spectroscopic method is used to study the DNA binding nature of Schiff base ligands and their Ni(II), Cu(II), Zn(II) metal complexes. The DNA concentration per nucleotide was measured spectrophotometrically by using known molar extinction coefficient value 6600 $M^{-1}cm^{-1}$ at 260 nm. The absorption titrations were carried out in Tris–HCl buffer (5 mM Tris–HCl/50 mM NaCl, pH 7.1) at 25°C by keeping the concentration of ligands and complexes constant and varying the concentration of the HS-DNA while maintaining the total volume constant (3 mL). To measure the absorbance of complex and to eliminate the absorbance of HS-DNA itself, equal quantity of HS-DNA was added to both the complex solution and the reference solution. The magnitude of spectral perturbation is an evidence for extent of binding. From the absorption data, the intrinsic binding constant (K_b) was calculated by a plot made between [DNA] / (ε_a-ε_f) and [DNA] [23-25].

5.2.3.2 Voltammetric studies

Differential pulse voltammetric studies were performed on an Electrochemical Analyser (CH instrument, Austin, TX) which is a three electrode system with platinum electrode as the working electrode, a platinum wire as the auxiliary electrode and Ag/AgCl as the reference electrode. Platinum electrode was mechanically polished with aqueous slurries of alumina (50 nm) on a flat pad prior to surface modification. After polishing, it was rinsed ultrasonically with absolute ethanol to remove residual alumina particles from the surface and then cleaned with a piranha

solution (H_2O_2 : H_2SO_4 = 1:3v/v) for 10 minutes. Following this mechanical process, an electrochemical cleaning process was carried out using cyclic voltammetry performed from 0 to 1500 mV in a 0.5 M sulphuric acid solution at a scan rate of 100 mV/s until a stable cyclic voltammogram was obtained.

All the electrochemical measurements were carried out at room temperature in a 10 mL electrolytic cell by using 5 mM Tris–HCl/50 mM NaCl buffer (pH 7.1) as the supporting electrolyte. Solutions were deoxygenated by purging with N_2 prior to the measurements. The working electrode was cleaned after every electrochemical assay. The voltammogram of $1x10^{-5}$ M solution of complexes were recorded in the absence of DNA. The procedure was then repeated for systems of 10 mL of a mixture containing constant concentration of the complexes and varying the concentration of DNA [26].

5.2.3.3 Circular dichroism spectral studies

The circular dichroism (CD) spectrum has been utilized as a powerful tool for exploring the chiral aspect of compounds. CD spectra of HS-DNA in the presence and absence of metal complexes were obtained in Tris–HCl buffer (pH=7.1) containing 50 mM NaCl at room temperature by using a Jasco Circular Dichroism Spectropolarimeter (CS/PPG/CD/018) equipped with a Peltier temperature control device at 25 ± 0.1 °C with a 0.1 cm path length cuvette. The spectra of various concentrations of complexes were recorded in the range 220-320 nm by keeping the concentration of DNA at 1×10^{-5} M [27].

5.3 Results and Discussion

5.3.1. Electronic absorption studies

Absorption spectra of all the ligands and metal complexes were recorded (Figures 5.1 – 5. 24) in the absence and presence HS-DNA. The binding mode of the synthesized ligands and its complexes to DNA is characterized by the change in absorbance. The absorption spectra of ligands and its Ni(II), Cu(II) and Zn(II) complexes showed absorbance in the range 350-450 nm. All ligands and their metal complexes show a decrease in its absorbance as the concentration of HS-DNA is increased. This results in hypochromism indicating intercalative way of binding between DNA duplex and ligands or complexes [28-29].

Electronic absorption spectroscopy is an effective technique to study the binding mode and extent of binding of metal complexes with DNA [30]. "Hyperchromic" and "hypochromic" effects are the spectral features of DNA concerning its double helical structure [31]. The hyperchromic effect might be ascribed to external contact (electrostatic binding) or to partial uncoiling of the helical structure of DNA [32]. Hypochromism is usually observed when a complex binds to DNA through intercalation as a consequence of strong staking interaction between an aromatic chromophore and a base pair of DNA. The extent of the hypochromism commonly reflects the intercalative binding strength [33]. Hypochromism is observed due to the presence of aromatic chromophore which might facilitate the interaction of the complexes with the HS-DNA bases through noncovalent π-π^* interactions [34]. When the complexes intercalate to the base pairs of HS-DNA, the π^* orbital of the intercalated ligand in the complexes can

couple with π orbital of the DNA base pairs, and then decreasing the π-π* transition energies. The coupling π orbital was partially filled by electrons, thus decreasing the transition probabilities and concurrently resulting in hypochromism. Planar complexes containing aromatic heterocyclic ligands could stack among the DNA base pairs [35].

In order to elucidate the binding strengths of these ligands and complexes, the intrinsic binding constant K_b were calculated by monitoring the changes of absorbance in the ligand transfer bands with increasing amounts of HS-DNA. The K_b (intrinsic binding constant) is calculated from a plot of [DNA] / (ε_a-ε_f) Vs [DNA] using the equation:

$$[DNA] / (\varepsilon_a-\varepsilon_f) = [DNA] / (\varepsilon_b-\varepsilon_f) + 1/K_b (\varepsilon_b-\varepsilon_f),$$

Where [DNA] is the concentration of DNA in base pairs

ε_a = the apparent coefficient = Aobsd / [complex],

ε_f = the extinction coefficients of the free metal complexes,

ε_b = the extinction coefficients of the free metal complexes in the fully bound forms.

The binding constant K_b is calculated by the ratio of slope to the intercept. The magnitude of K_b value gives the extent of binding [36].

The absorption spectra of Schiff base ligands and metal complexes (1×10^{-5} M) in Tris-HCl buffer pH 7.1 in the absence (R = 0) and presence of increasing amount of DNA are represented in Figure 5.1 (a) - 5. 24 (a), A plot of [DNA] / (ε_a-ε_f) versus [DNA] for the titration of DNA with ligands and metal complexes for binding constant are represented in Figure 5.1 (b) - 5.24 (b). The binding constant values obtained for Schiff base ligands and its Ni(II), Cu(II), Zn(II) complexes are represented in Table 5.1

Table 5.1 Binding constant (k_b) M^{-1} for Schiff base ligands and complexes

Ligand	Binding constant (k_b) M^{-1}			
	Ligand	Ni(II) complex	Cu(II) complex	Zn(II) complex
TA	7.6×10^3	3.2×10^4	1.1×10^5	1.6×10^4
TNA	9.9×10^3	2.8×10^4	5.2×10^4	5.7×10^4
TMA	1.7×10^4	1.2×10^4	4.2×10^4	1.5×10^4
PA	2.3×10^4	5.9×10^4	4.1×10^4	4.8×10^4
PNA	7.7×10^3	3.5×10^4	2.1×10^4	2.5×10^4
PMA	6.5×10^4	2.5×10^4	6.6×10^4	1.5×10^4

The binding constant values fall in the range 10^4-10^5 for all ligand and complexes and they are comparable with but still lower than that of standard intercalator ethidium bromide (1×10^7 M^{-1}) [37].

These results indicate that all the synthesized compounds strongly interact with DNA by intercalation. This also shows that metal complexes have high DNA affinity than the corresponding ligands.

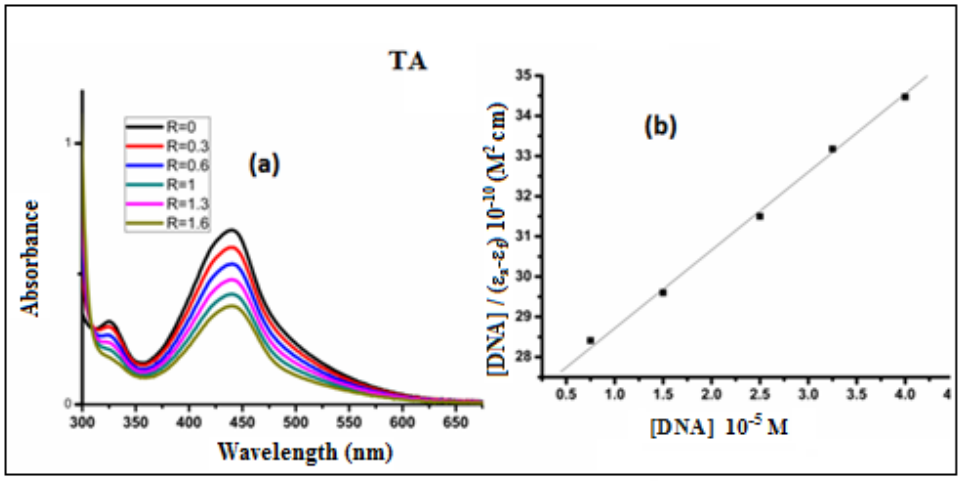

Figure 5.1 (a) Absorption spectra of TA (1.5×10^{-5} M) in Tris-HCl buffer of pH 7.1 in the absence (R = 0) and presence (R = 0. 3, 0. 6, 1, 1.3 & 1.6) of increasing amount of DNA, R= [DNA] / [Complex] (b) A plot of [DNA]/ (ε_a-ε_f) Vs [DNA].

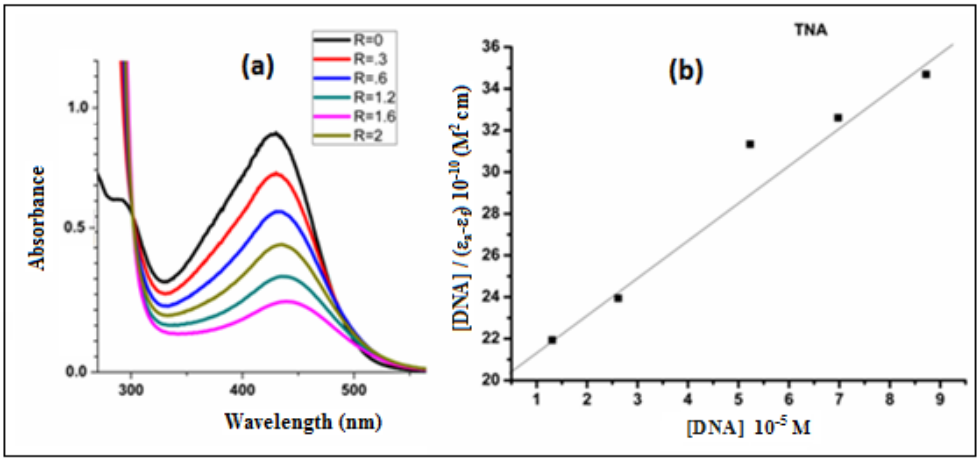

Figure 5.2 (a) Absorption spectra of TNA (1.5 x 10^{-5} M) in Tris-HCl buffer of pH 7.1 in the absence (R = 0) and presence (R = 0. 3, 0. 6, 1.2, 1.6 & 2) of increasing amount of DNA, R= [DNA] / [Complex] (b) A plot of [DNA]/ (ε_a-ε_f) Vs [DNA].

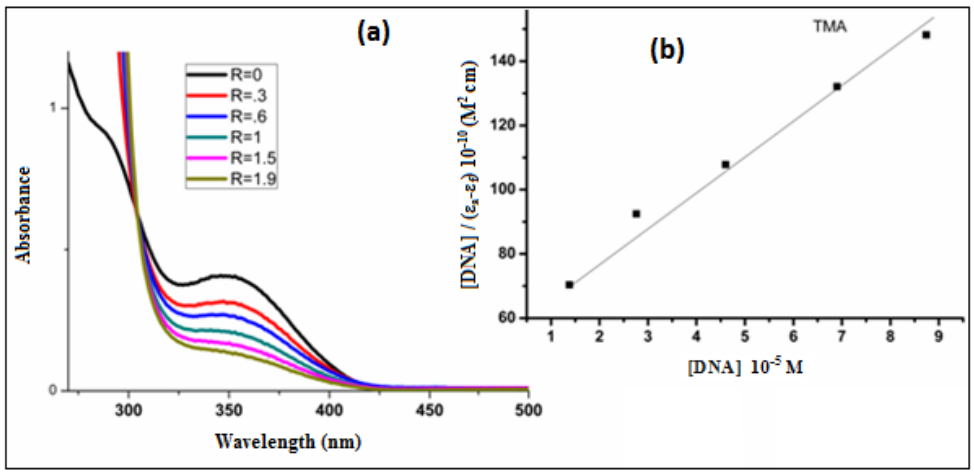

Figure 5.3 (a) Absorption spectra of TMA (1.5 x 10^{-5} M) in Tris-HCl buffer of pH 7.1 in the absence (R = 0) and presence (R = 0. 3, 0. 6, 1, 1.5 & 1.9) of increasing amount of DNA, R = [DNA] / [Complex] (b) A plot of [DNA]/ (ε_a-ε_f) Vs [DNA].

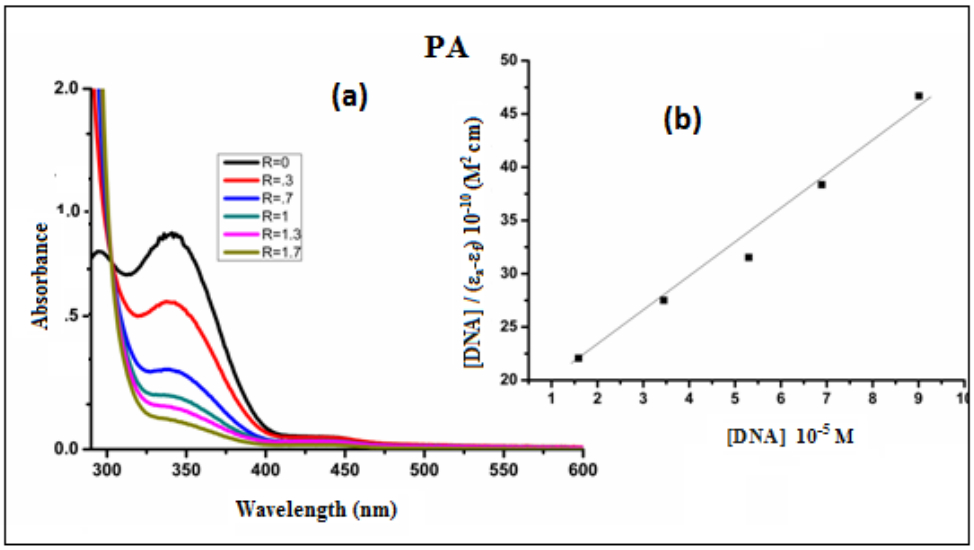

Figure 5.4 (a) Absorption spectra of PA (1.5 x 10^{-5} M) in Tris-HCl buffer of pH 7.1 in the absence (R = 0) and presence (R = 0. 3, 0. 7, 1, 1.3 & 1.7) of increasing amount of DNA, R = [DNA] / [Complex] (b) A plot of [DNA]/ (ε_a-ε_f) Vs [DNA].

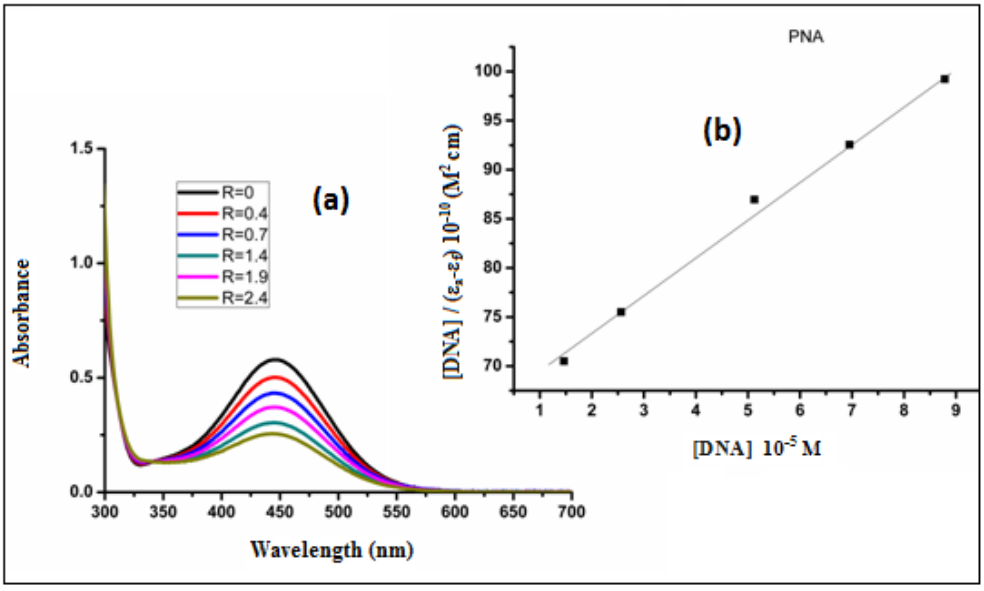

Figure 5.5 (a) Absorption spectra of PNA (1.5 x 10^{-5} M) in Tris-HCl buffer of pH 7.1 in the absence (R = 0) and presence (R = 0. 4, 0. 7, 1.4, 1.9 & 2.4) of increasing amount of DNA, R = [DNA] / [Complex]. (b) A plot of [DNA] / (ε_a-ε_f) Vs [DNA].

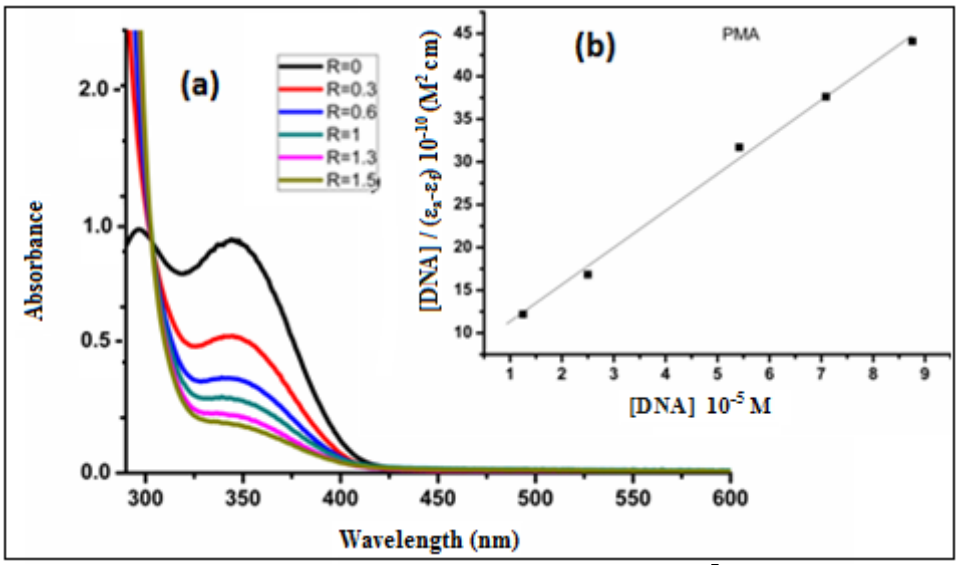

Figure 5.6 (a) Absorption spectra of PMA (1.5 x 10^{-5} M) in Tris-HCl buffer of pH 7.1 in the absence (R = 0) and presence (R = 0. 3, 0. 6, 1, 1.3 & 1.5) of increasing amount of DNA, R= [DNA] / [Complex] (b) A plot of [DNA]/ (ε_a-ε_f) Vs [DNA].

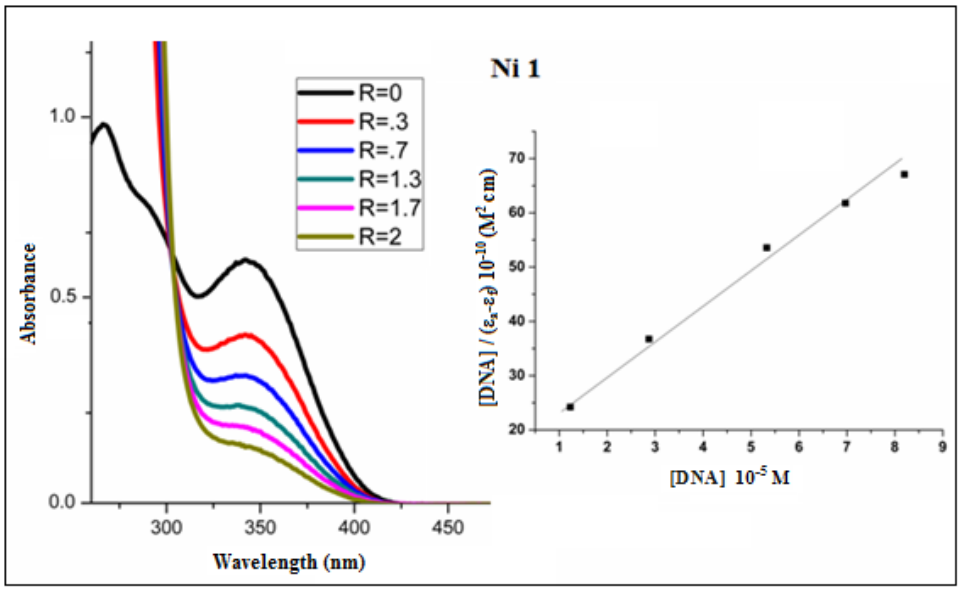

Figure 5.7 (a) Absorption spectra of $[Ni(TA)_2(H_2O)_2]$ (1.5 x 10^{-5} M) in Tris-HCl buffer of pH 7.1 in the absence (R = 0) and presence (R = 0. 3, 0. 7, 1.3, 1.7 & 2) of increasing amount of DNA, R= [DNA] / [Complex] (b) A plot of [DNA]/ (ε_a-ε_f) Vs [DNA].

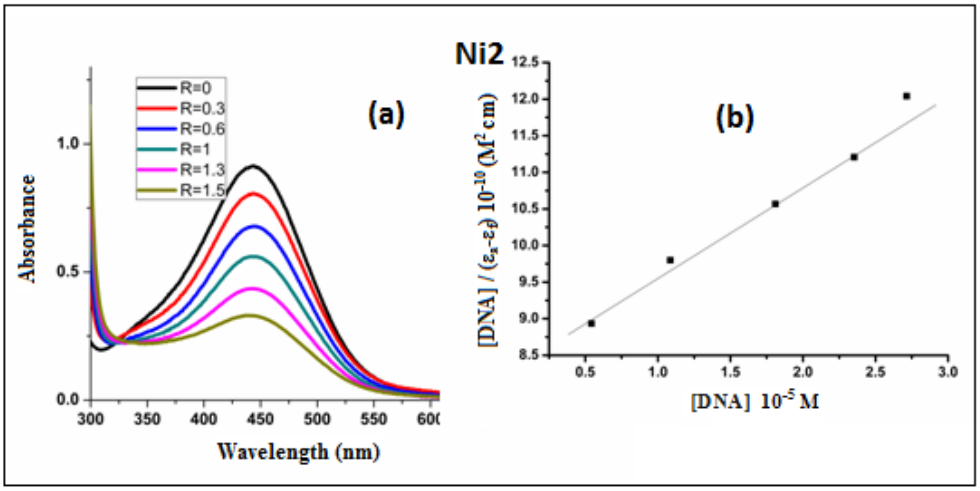

Figure 5.8 (a) Absorption spectra of $[Ni(TNA)_2(H_2O)_2]\cdot 2H_2O$ (1.5 x 10^{-5} M) in Tris-HCl buffer of pH 7.1 in the absence (R = 0) and presence (R = 0. 3, 0. 6, 1, 1.3 & 1.5) of increasing amount of DNA, R= [DNA] / [Complex], (b) A plot of [DNA]/ (ε_a-ε_f) Vs [DNA].

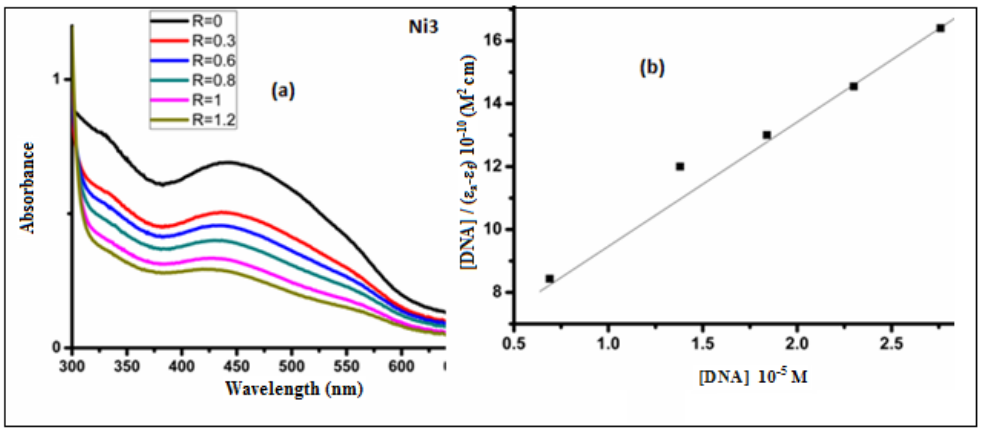

Figure 5. 9 (a) Absorption spectra of $[Ni(TMA)_2]\cdot 3H_2O$ (1.5 x 10^{-5} M) in Tris-HCl buffer of pH 7.1 in the absence (R = 0) and presence (R = 0. 3, 0. 6, 0.8, 1 & 1.2) of increasing amount of DNA, R= [DNA] / [Complex], (b) A plot of [DNA]/ (ε_a-ε_f) Vs [DNA].

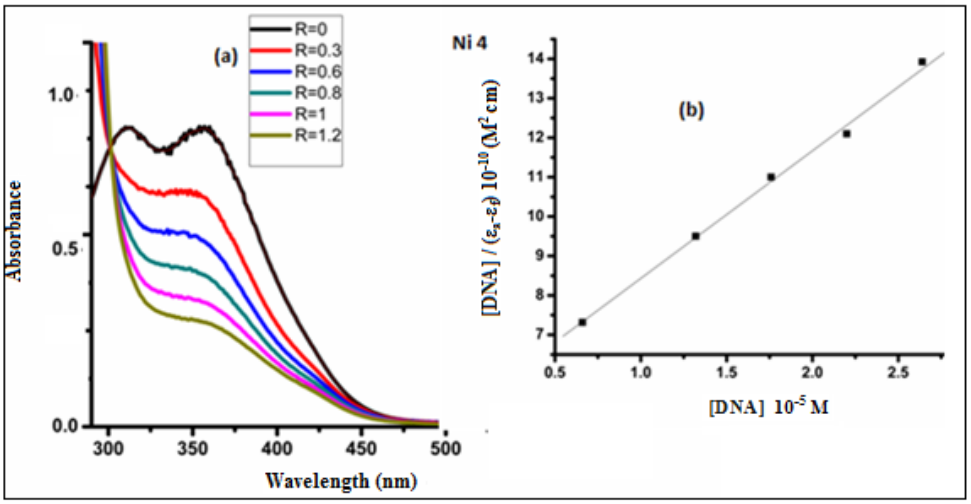

Figure 5.10 (a) Absorption spectra of [Ni $(PA)_2$]·H_2O (1.5 x 10^{-5} M) in Tris-HCl buffer of pH 7.1 in the absence (R = 0) and presence (R= 0. 3, 0. 6, 0.8, 1, & 1.2) of increasing amount of DNA, R= [DNA] / [Complex], (b) A plot of [DNA]/ (ε_a-ε_f) Vs [DNA].

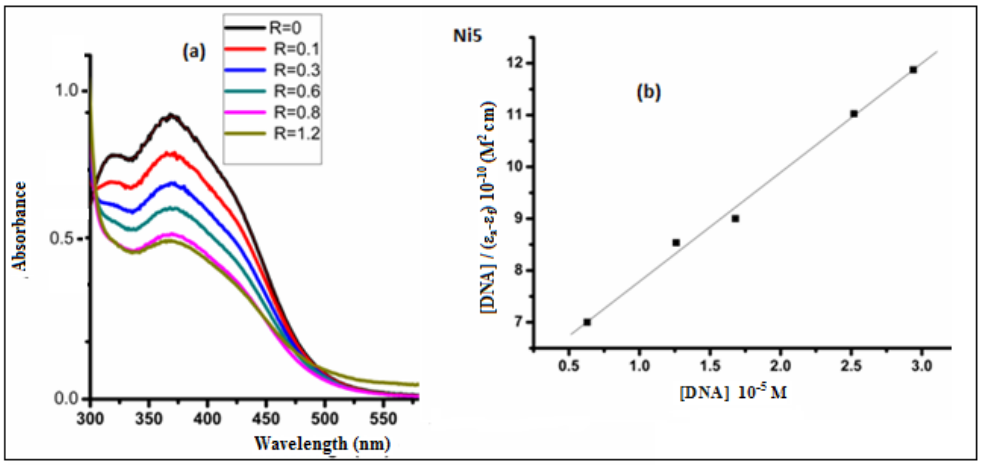

Figure 5.11 (a) Absorption spectra of [Ni $(PNA)_2$]·$2H_2O$ (1.5 x 10^{-5} M) in Tris-HCl buffer of pH 7.1 in the absence (R = 0) and presence (R = 0. 1, 0. 3, 0. 6, 0.8 & 1.5) of increasing amount of DNA, R = [DNA] / [Complex], (b) A plot of [DNA]/ (ε_a-ε_f) Vs [DNA].

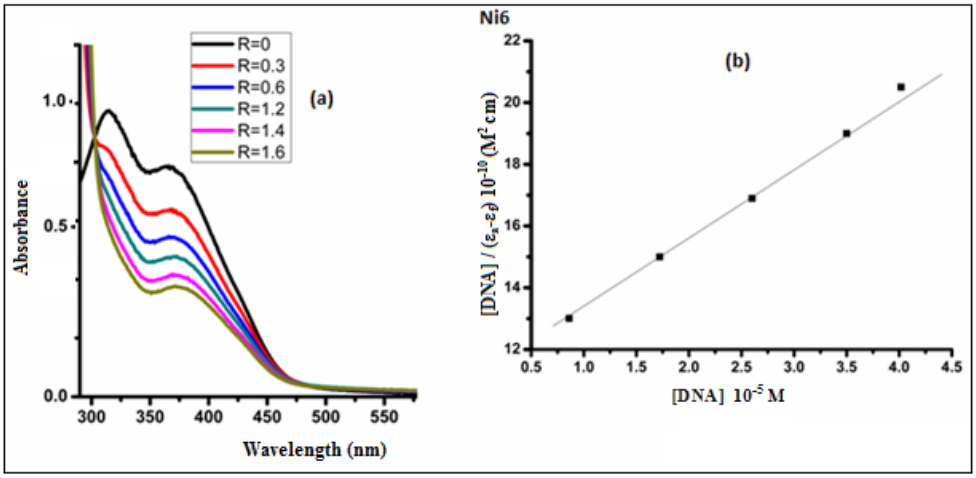

Figure 5.12 (a) Absorption spectra of [Ni $(PMA)_2$] (1.5 x 10^{-5} M) in Tris-HCl buffer of pH 7.1 in the absence (R = 0) and presence (R = 0. 3, 0. 6, 1, 1.3 & 1.5) of increasing amount of DNA, R = [DNA] / [Complex],(b) A plot of [DNA]/ (ε_a-ε_f) Vs [DNA].

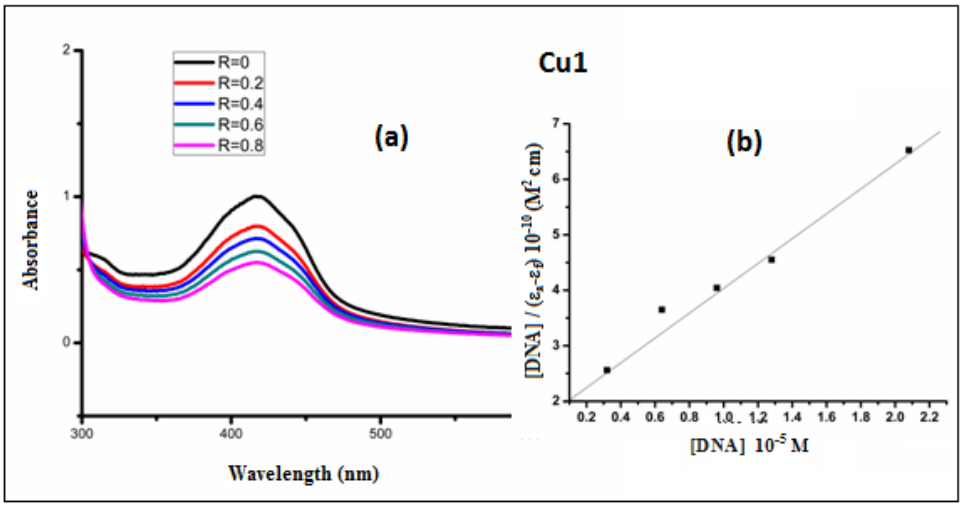

Figure 5.13 (a) Absorption spectra of [$Cu(TA)_2 H_2O]\cdot H_2O$] (1.5 x 10^{-5} M) in Tris-HCl buffer of pH 7.1 in the absence (R = 0) and presence (R = 0. 2, 0. 4, 0.6, & 0.8) of increasing amount of DNA, R= [DNA] / [Complex], (b) A plot of [DNA]/ (ε_a-ε_f) Vs [DNA].

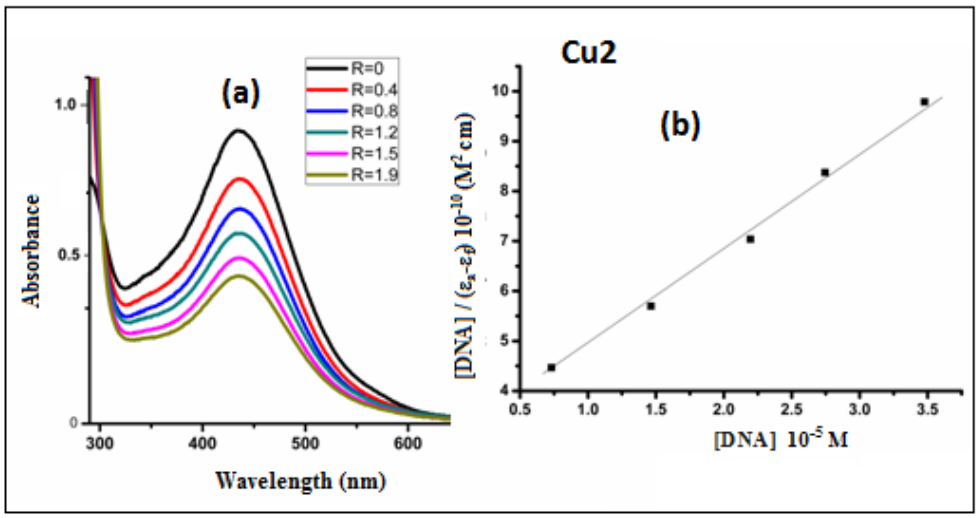

Figure 5.14 (a) Absorption spectra of $[Cu(TNA)_2]\cdot 2H_2O$ (1.5×10^{-5} M) in Tris-HCl buffer of pH 7.1 in the absence (R = 0) and presence (R = 0. 4, 0. 8, 1.2, 1.5, & 1.9) of increasing amount of DNA, R = [DNA] / [Complex] (b) A plot of [DNA]/ (ε_a-ε_f) Vs [DNA].

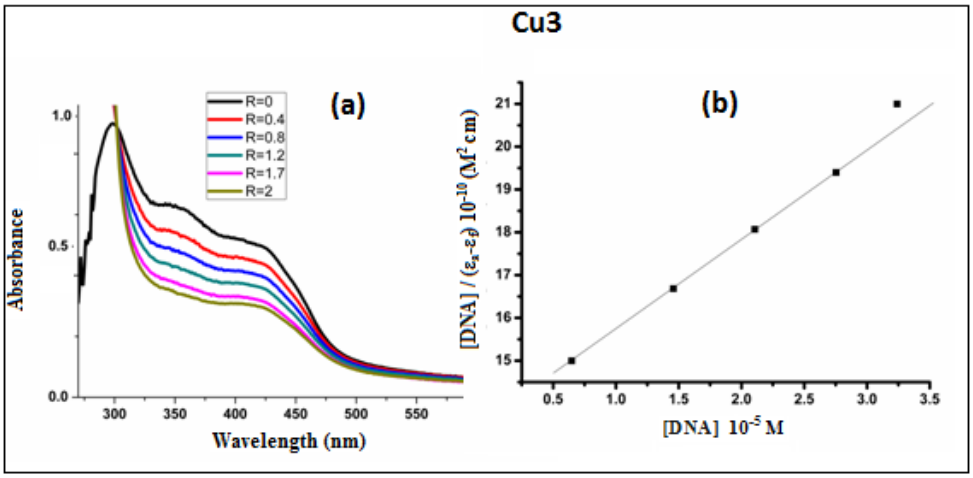

Figure 5.15 (a) Absorption spectra of $[Cu(TMA)_2]\cdot H_2O]$ (1.5×10^{-5} M) in Tris-HCl buffer of pH 7.1 in the absence (R = 0) and presence (R = 0. 2, 0. 4, 0.8, 1.2, 1.7 & 2) of increasing amount of DNA, R = [DNA] / [Complex], (b) A plot of [DNA]/ (ε_a-ε_f) Vs [DNA].

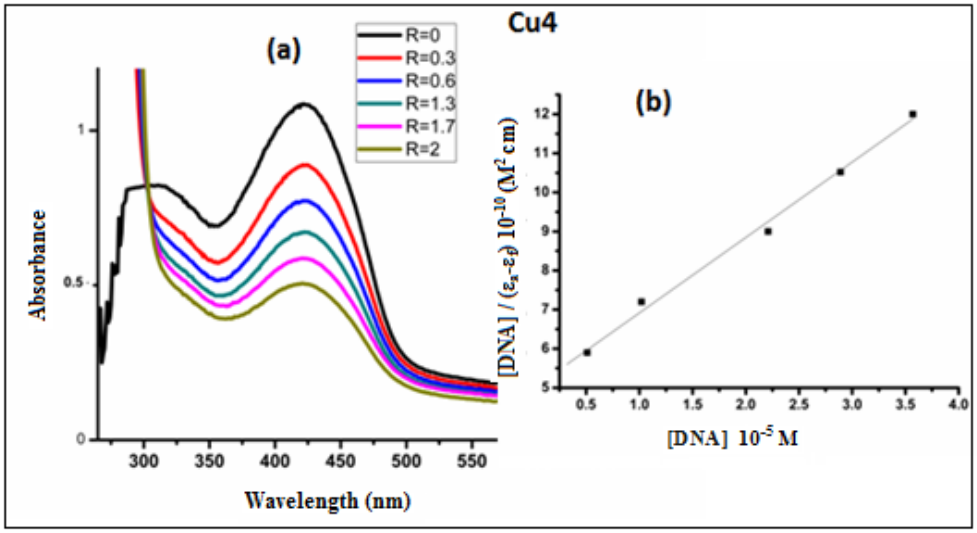

Figure 5.16 (a) Absorption spectra of $[Cu(PA)_2H_2O]\cdot 2H_2O$ (1.5 x 10^{-5} M) in Tris-HCl buffer of pH 7.1 in the absence (R = 0) and presence (R = 0. 2, 0. 3, 0.6, 1.3, 1.7 & 2) of increasing amount of DNA, R= [DNA] / [Complex], (b) A plot of [DNA]/ (ε_a-ε_f) Vs [DNA].

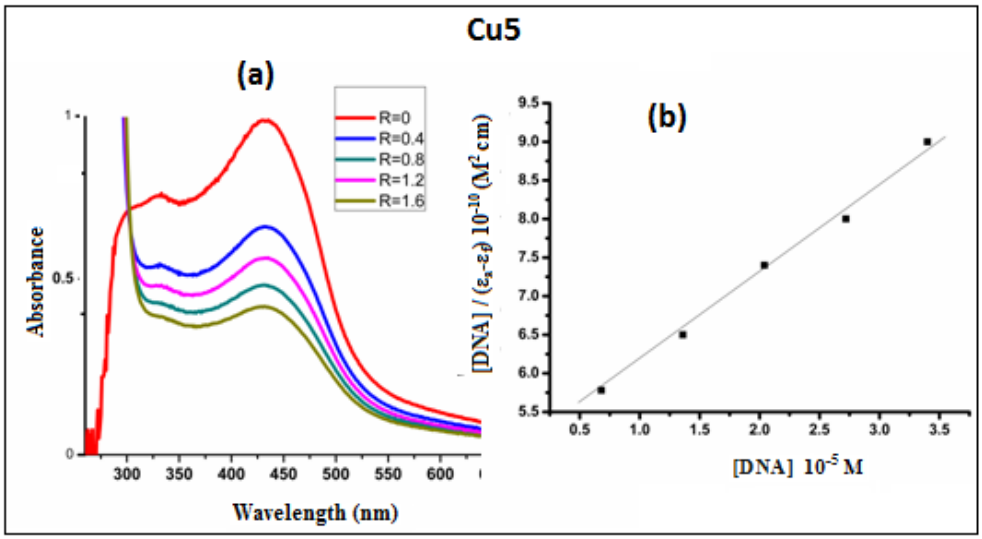

Figure 5.17 (a) Absorption spectra of $[Cu(PNA)_2]\cdot 3H_2O$ (1.5 x 10^{-5} M) in Tris-HCl buffer of pH 7.1 in the absence (R = 0) and presence (R = 0. 4, 0. 8, 1.2 & 1.6) of increasing amount of DNA, R= [DNA] / [Complex] (b) A plot of [DNA]/ (ε_a-ε_f) Vs [DNA].

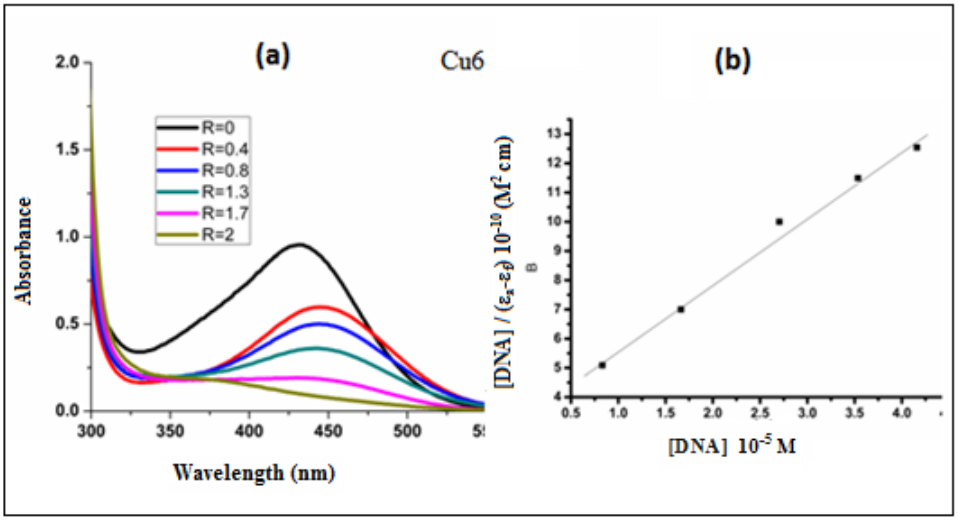

Figure 5.18 (a) Absorption spectra of $[Cu(PMA)_2]\cdot H_2O$ (1.5 x 10^{-5} M) in Tris-HCl buffer of pH 7.1 in the absence (R = 0) and presence (R = 0. 4, 0. 8, 1.2 & 1.6) of increasing amount of DNA, R = [DNA] / [Complex] (b) A plot of [DNA]/ (ε_a-ε_f) Vs [DNA].

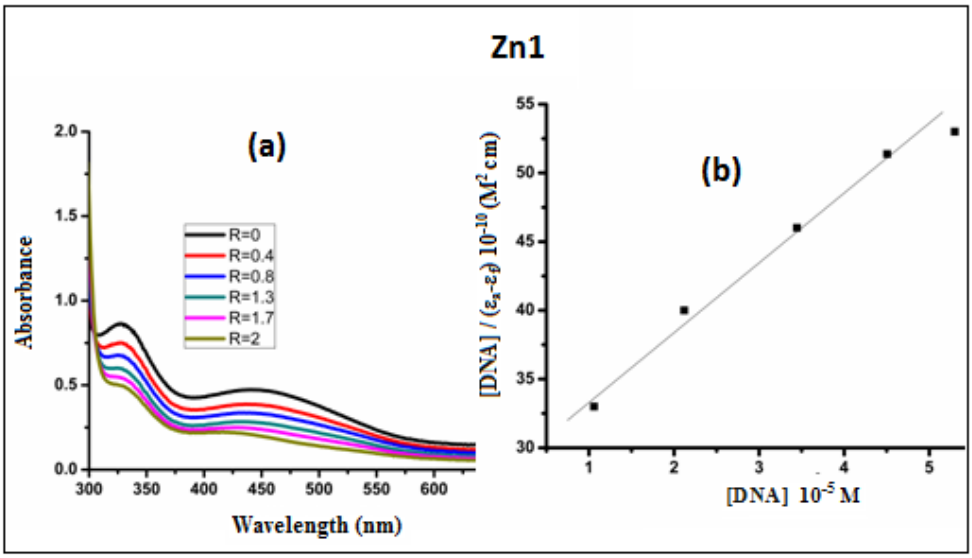

Figure 5.19 (a) Absorption spectra of $[Zn(TA)_2]$ (1.5 x 10^{-5} M) in Tris-HCl buffer of pH 7.1 in the absence (R = 0) and presence (R = 0. 2, 0. 4, 0.8, 1.3,1.7 & 2) of increasing amount of DNA, R= [DNA] / [Complex] (b) A plot of [DNA]/ (ε_a-ε_f) Vs [DNA].

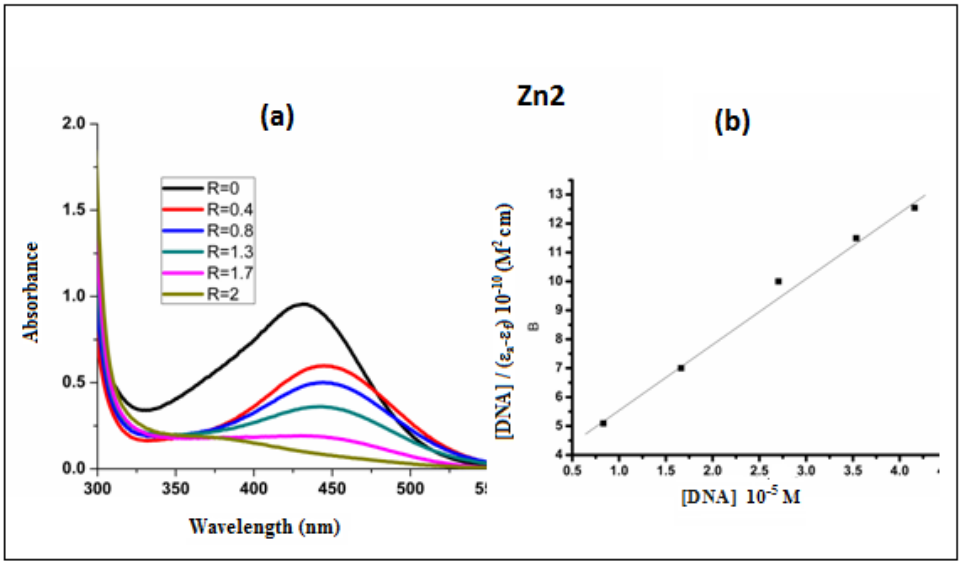

Figure 5.20 (a) Absorption spectra of $[Zn(TNA)_2]$ (1.5 x 10^{-5} M) in Tris-HCl buffer of pH 7.1 in the absence (R = 0) and presence (R= 0. 2, 0. 4, 0.8, 1.3, 1.7 & 2) of increasing amount of DNA, R = [DNA] / [Complex] (b) A plot of [DNA]/ (ε_a-ε_f) Vs [DNA].

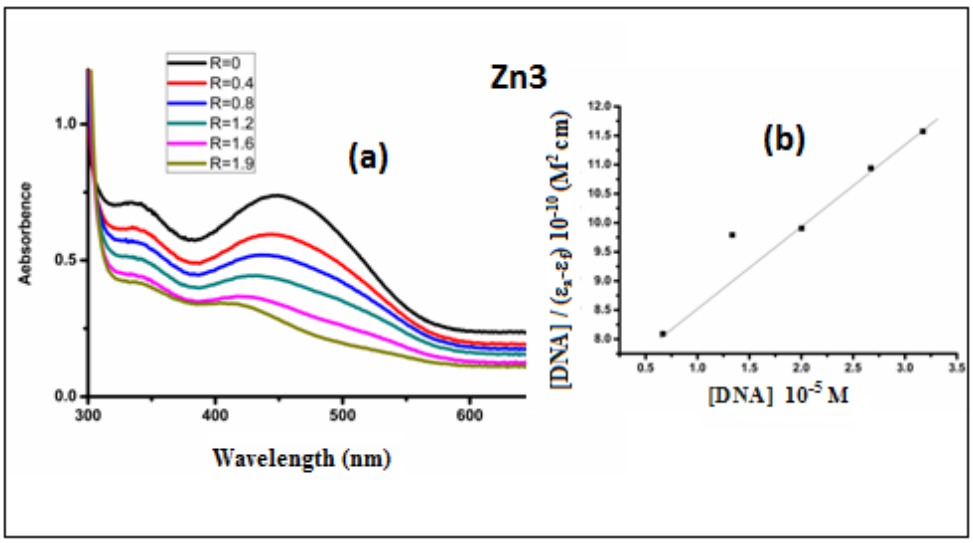

Figure 5.21 (a) Absorption spectra of $[Zn(TMA)_2]$ (1.5 x 10^{-5} M) in Tris-HCl buffer of pH 7.1 in the absence (R = 0) and presence (R = 0. 2, 0. 4, 0.8, 1.2, 1.6 & 1.9) of increasing amount of DNA, R= [DNA] / [Complex] (b) A plot of [DNA]/ (ε_a-ε_f) Vs [DNA].

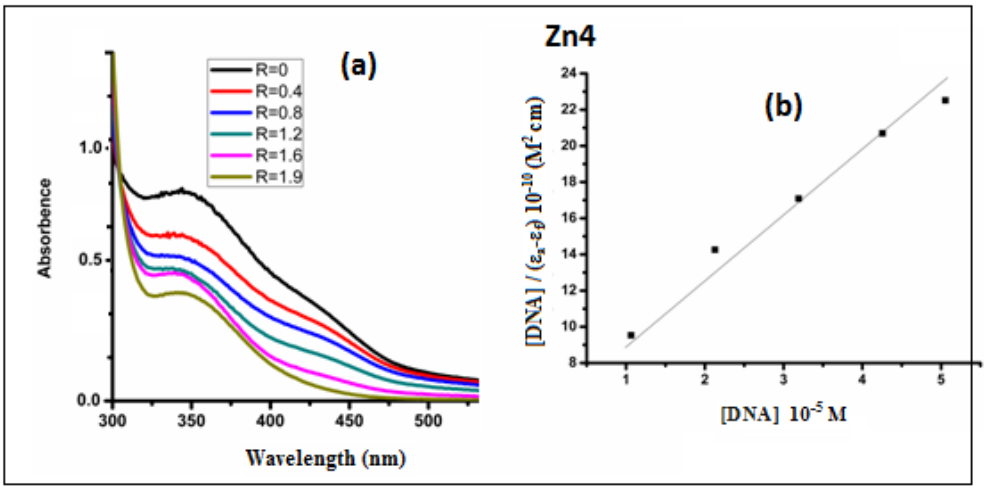

Figure 5.22 (a) Absorption spectra of $[Zn(PA)_2]$ (1.5 x 10^{-5} M) in Tris-HCl buffer of pH 7.1 in the absence (R=0) and presence (R = 0. 4, 0. 8, 1.2, 1.6 & 1.9) of increasing amount of DNA, R = [DNA] / [Complex] (b) A plot of [DNA]/ (ε_a-ε_f) Vs [DNA].

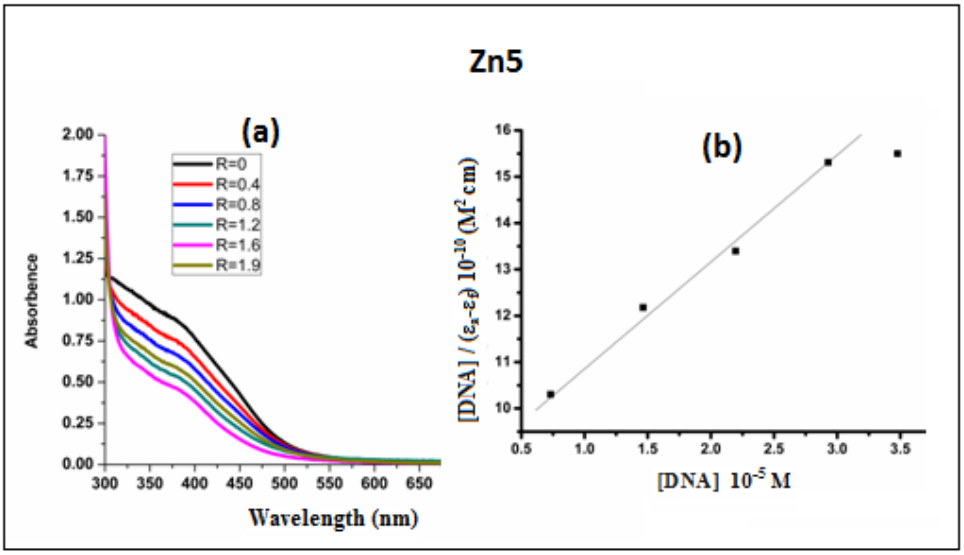

Figure 5.23 (a) Absorption spectra of $[Zn(PNA)_2]$ (1.5 x 10^{-5} M) in Tris-HCl buffer of pH 7.1 in the absence (R = 0) and presence (R = 0. 4, 0. 8, 1.2, 1.6 & 1.9) of increasing amount of DNA, R= [DNA] / [Complex] (b) A plot of [DNA]/ (ε_a-ε_f) Vs [DNA].

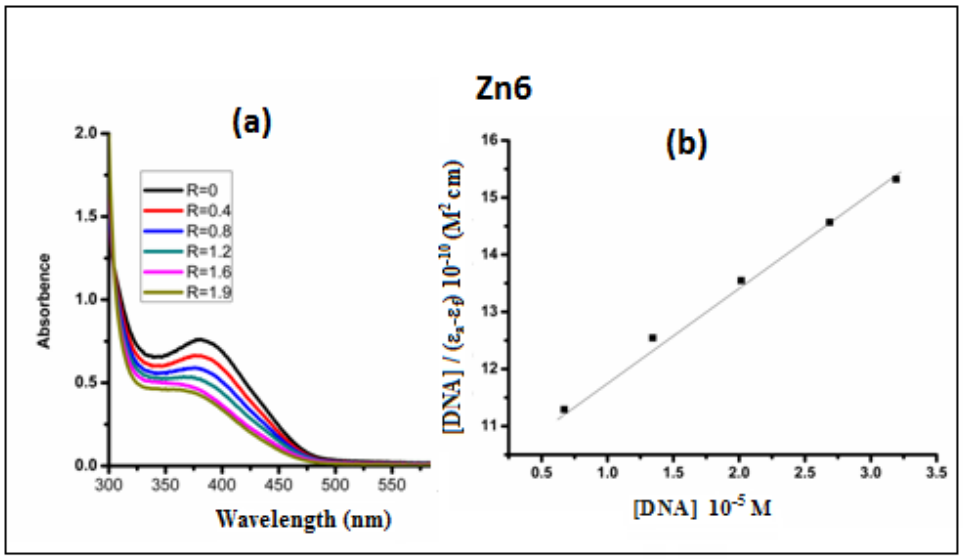

Figure 5.24 (a) Absorption spectra of [Zn (PMA) $_2$] (1.5 x 10^{-5} M) in Tris-HCl buffer of pH 7.1 in the absence (R = 0) and presence (R = 0. 4, 0. 8, 1.2,1.6 & 1.9) of increasing amount of DNA, R= [DNA] / [Complex] (b) A plot of [DNA]/ (ε_a-ε_f) Vs [DNA].

5.3.2 Voltammetric studies

Electrochemical techniques were used for further evidence about the DNA interaction with ligands and their metal complexes. The application of voltammetry to the study of binding of small molecules to DNA provides a useful complement to UV–Vis. spectroscopy [38]. One of the advantages of using this technique is that the simultaneous determination of multiple oxidation states of same species as well as mixtures of several interacting species. Differential pulse voltammogram (DPV) technique provides the needed high current sensitivity and good peak resolution for the investigation of the interaction between different molecule and DNA [39].

DPV techniques are considered to be the sensitive analytical instruments to determine the changes in oxidation state of the metallic species in the presence of biomolecules [40-41]. DPV experiments were performed to observe the changes in the formal potential as well as the current density during the addition of DNA to the experimental solution of Schiff base ligands and their Ni(II), Cu(II) and Zn(II) complexes.

Differential pulse voltammogram of ligands and its Ni(II), Cu(II) and Zn(II) complexes have been collected both in absence and presence of DNA. The effect of increasing concentration of DNA on voltammograms of the studied compounds is presented in Figure 5.25.-5.36. The parameters received from DPV study of compounds both in presence and absence of DNA are given in Table 5.2 - 5.5.

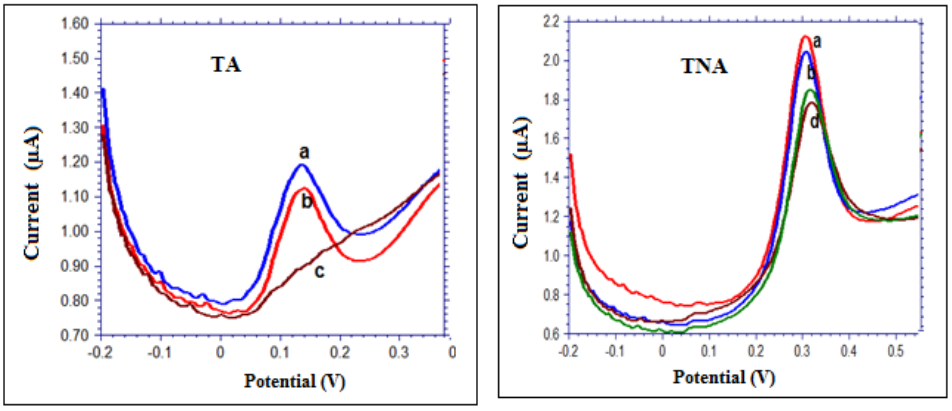

Figure 5.25 Differential pulse voltammogram of TA and TNA (1.5×10^{-5} M) in Tris-HCl buffer of pH 7.1 in the absence (a) and presence (b, c and d) of increasing amount of DNA.

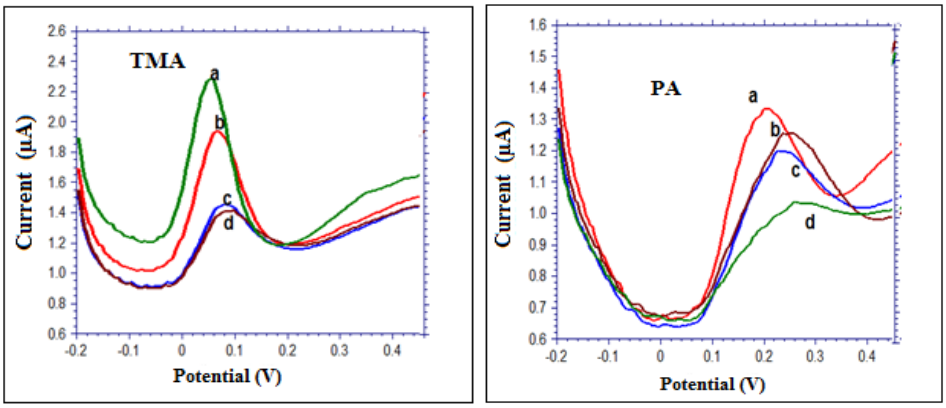

Figure 5.26 Differential pulse voltammogram of TMA and PA (1.5×10^{-5} M) in Tris-HCl buffer of pH 7.1 in the absence (a) and presence (b, c and d) of increasing amount of DNA.

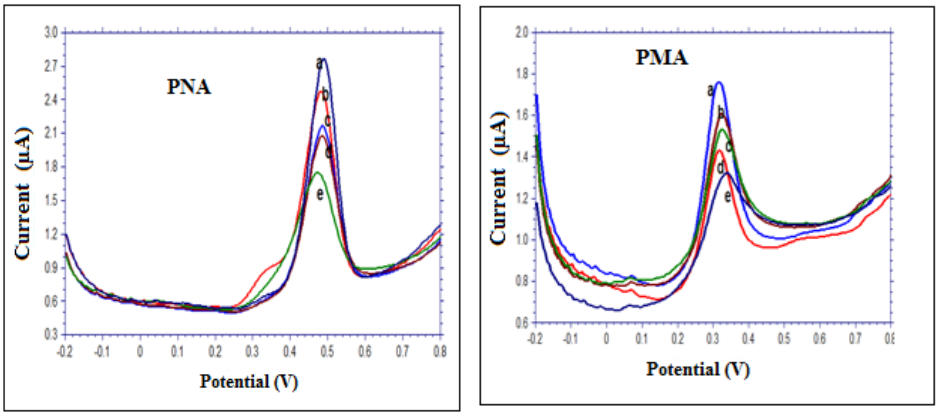

Figure 5.27 Differential pulse voltammogram of PNA and PMA (1.5×10^{-5} M) in Tris-HCl buffer of pH 7.1 in the absence (a) and presence (b, c and d) of increasing amount of DNA.

Table 5.2 Differential Pulse voltammetric data of ligands in the presence of different concentration of DNA in Tris-Hcl buffer pH 7.1

Ligand	R=[DNA] / [Complex]	Ep (V)	Ip (μA)
TA	0	0.144	2.87
	0.3	0.136	2.62
	0.6	0.128	2.35
TNA	0	0.308	2.02
	0.3	0.304	1.84
	0.6	0.302	1.53
TNA	0	0.072	3.67
	0.3	0.070	2.92
	0.6	0.064	2.56
PA	0	0.208	4.02
	0.3	0.204	3.56
	0.7	0.202	3.04
PNA	0	0.488	3.79
	0.3	0.485	3.43
	0.6	0.480	3.02
PMA	0	0.354	2.97
	0.3	0.352	2.53
	0.6	0.350	2.34

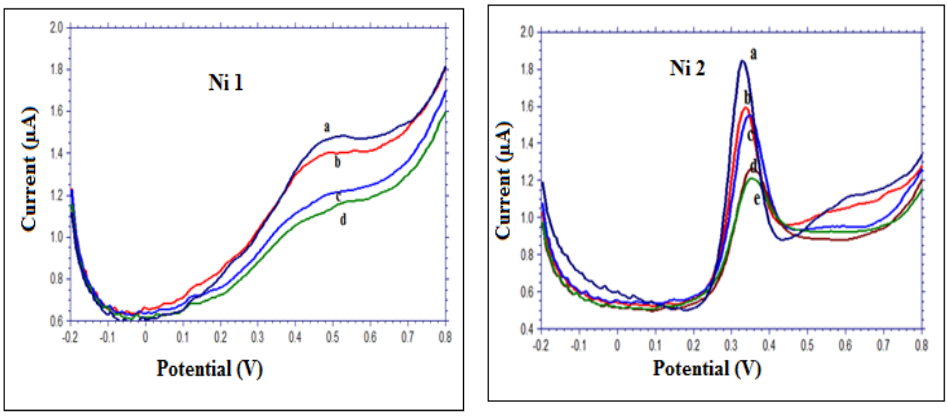

Figure 5.28 Differential pulse voltammogram of Ni 1 = $[Ni(TA)_2(H_2O)_2]$ and Ni 2 = $[Ni(TNA)_2(H_2O)_2]\cdot 2H_2O$ (1.5×10^{-5} M) in Tris-HCl buffer of pH 7.1 in the absence (a) and presence (b, c and d) of increasing amount of DNA.

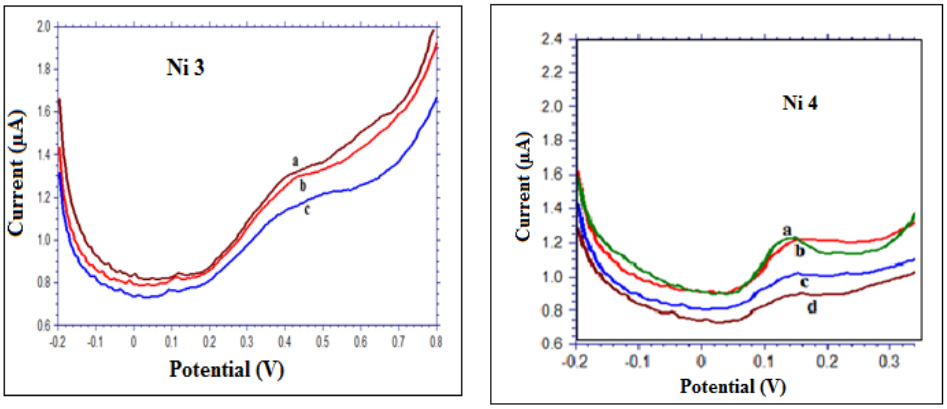

Figure 5.29 Differential pulse voltammogram of Ni 3 = $[Ni(TMA)_2]\cdot 3H_2O$ and Ni 4 = $[Ni(PA)_2]\cdot H_2O$ (1.5×10^{-5} M) in Tris-HCl buffer of pH 7.1 in the absence (a) and presence (b, c and d) of increasing amount of DNA.

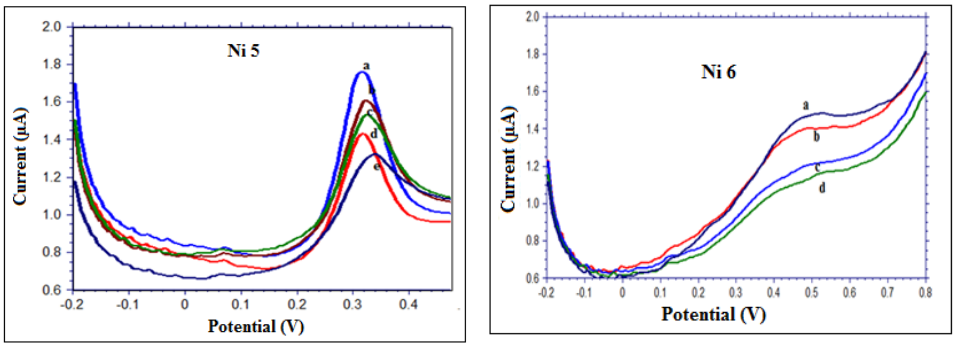

Figure 5.30 Differential pulse voltammogram of Ni 5 = $[Ni(PNA)_2]\cdot 2H_2O$ and Ni 6 = $[Ni(PMA)_2]$ (1.5×10^{-5} M) in Tris-HCl buffer of pH 7.1 in the absence (a) and presence (b, c and d) of increasing amount of DNA.

Table 5.3 Differential Pulse voltammetric data of nickel complexes in the presence of different concentration of DNA in Tris-Hcl buffer (pH 7.1)

Complex	R=[DNA] / [Complex]	Ep (V)	Ip (µA)
$[Ni(TA)_2(H_2O)_2]$	0	0.472	2.97
	0.3	0.467	2.72
	0.6	0.452	2.55
$[Ni(TNA)_2(H_2O)_2]\cdot 2H_2O$	0	0.348	2.08
	0.3	0.344	1.94
	0.6	0.342	1.63
$[Ni(TMA)_2]\cdot 3H_2O$	0	0.428	2.67
	0.3	0.426	2.32
	0.6	0.425	2.16
$[Ni(PA)_2]\cdot H_2O$	0	0.156	1.48
	0.3	0.154	1.23
	0.7	0.154	1.01
$[Ni(PNA)_2]\cdot 2H_2O$	0	0.328	2.45
	0.3	0.324	2.21
	0.6	0..322	1.98
$[Ni(PMA)_2]$	0	0.526	2.96
	0.3	0.523	2.73
	0.6	0..520	2.34

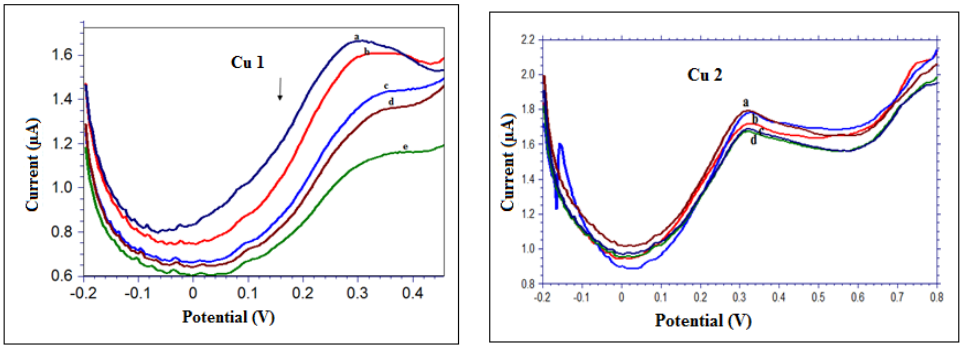

Figure 5.31 Differential pulse voltammogram of Cu1 = $[Cu(TA)_2H_2O]\cdot H_2O$ and Cu2 = $[Cu(TNA)_2]\cdot 2H_2O$ (1.5×10^{-5} M) in Tris-HCl buffer of pH 7.1 in the absence (a) and presence (b, c and d) of increasing amount of DNA.

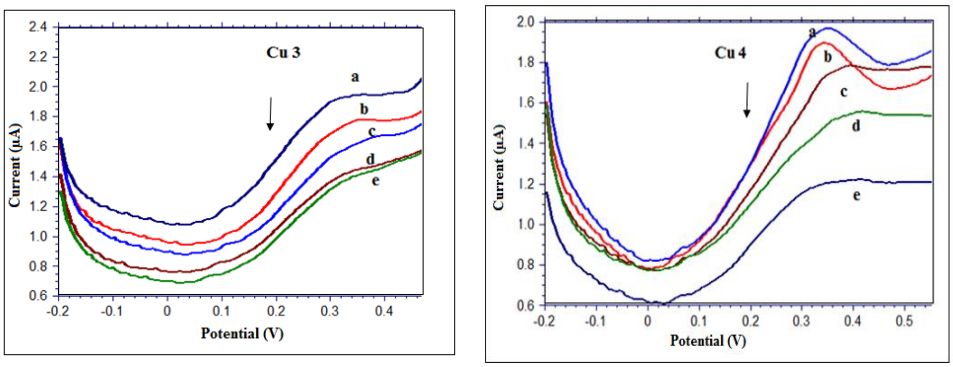

Figure 5.32 Differential pulse voltammogram of Cu3 = $[Cu(TMA)_2]\cdot H_2O$ and Cu4 = $[Cu(PA)_2H_2O]\cdot 2H_2O$ (1.5×10^{-5} M) in Tris-HCl buffer of pH 7.1 in the absence (a) and presence (b, c and d) of increasing amount of DNA.

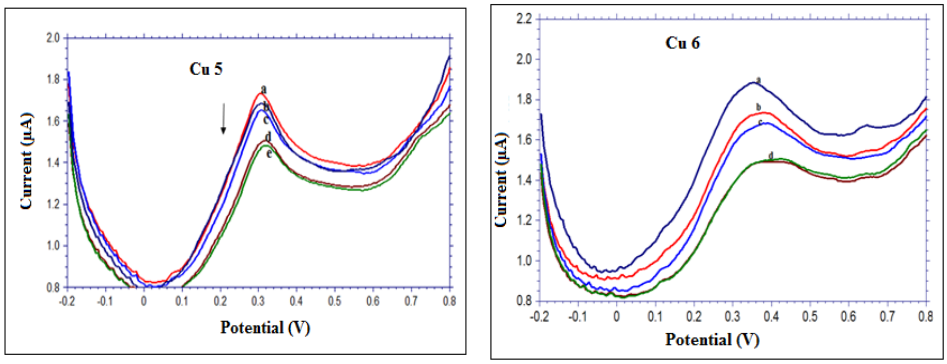

Figure 5.33 Differential pulse voltammogram of Cu5 = $[Cu\ (PNA)_2]\cdot 3H_2O$ and Cu6 = $[Cu(PMA)_2]\cdot H_2O$ (1.5×10^{-5} M) in Tris-HCl buffer of pH 7.1 in the absence (a) and presence (b, c and d) of increasing amount of DNA.

Table 5.4 Differential Pulse voltammetric data of copper complexes in the presence of different concentration of DNA in Tris-Hcl buffer (pH 7.1)

Complex	R=[DNA] / [Complex]	Ep (V)	Ip (μA)
$[Cu(TA)_2H_2O]\cdot H_2O$	0	0.308	3.29
	0.3	0.292	2.78
	0.6	0.290	2.02
$[Cu(TNA)_2]\cdot 2H_2O$	0	0.324	5.07
	0.3	0.312	4.68
	0.6	0.308	3.87
$[Cu(TMA)_2]\cdot H_2O$	0	0.324	2.27
	0.3	0.314	1.68
	0.6	0.306	1.41
$[Cu(PA)_2H_2O]\cdot 2H_2O$	0	0.344	4.49
	0.3	0.342	3.15
	0.7	0..341	2.62
$[Cu(PNA)_2]\cdot 3H_2O$	0	0.310	6.45
	0.3	0.308	5.21
	0.6	0..304	4.62
$[Cu(PMA)_2]\cdot H_2O$	0	0.344	5.30
	0.3	0.340	4.35
	0.6	0..342	3.49

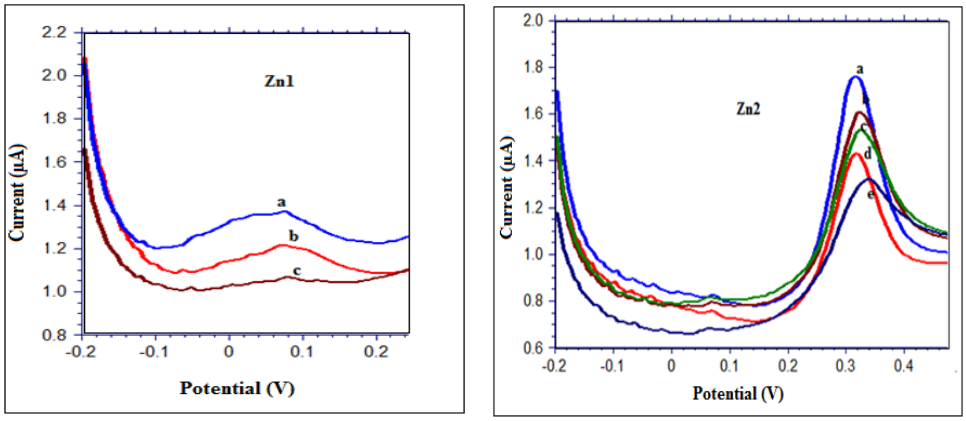

Figure 5.34 Differential pulse voltammogram of Zn1 = $[Zn(TA)_2]$ and Zn2 = $[Zn(TNA)_2]$ (1.5×10^{-5} M) in Tris-HCl buffer of pH 7.1 in the absence (a) and presence (b, c and d) of increasing amount of DNA.

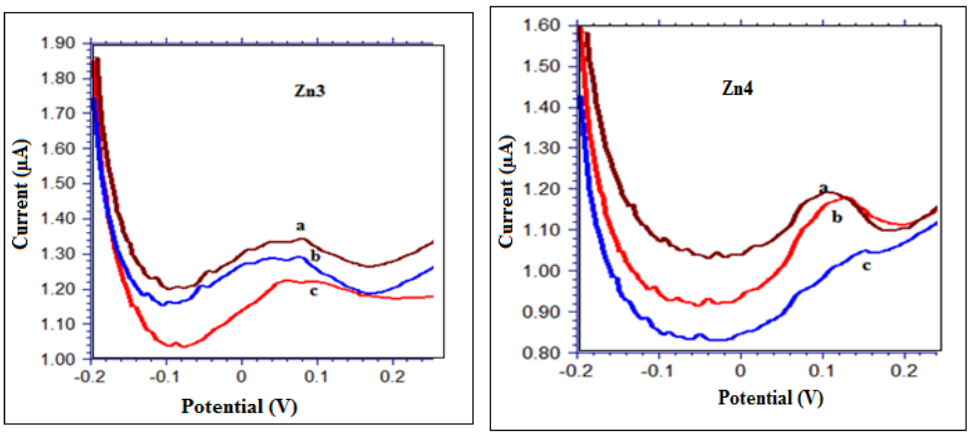

Figure 5.35 Differential pulse voltammogram of Zn3 = $[Zn(TMA)_2]$ and Zn4 = $[Zn(PA)_2]$ (1.5×10^{-5} M) in Tris-HCl buffer of pH 7.1 in the absence (a) and presence (b, c and d) of increasing amount of DNA.

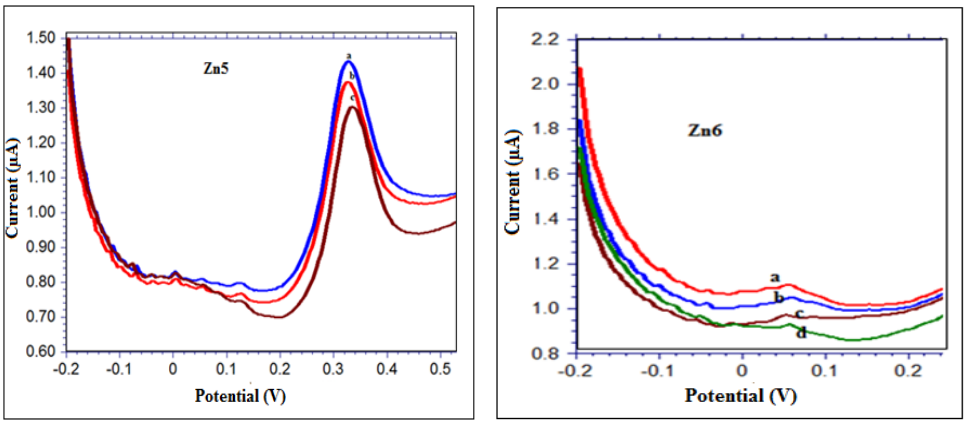

Figure 5.36 Differential pulse voltammogram of Zn5 = $[Zn\ (PNA)_2]$ and Zn6 = $[Zn(PMA)_2]$ (1.5×10^{-5} M) in Tris-HCl buffer of pH 7.1 in the absence (a) and presence (b, c and d) of increasing amount of DNA.

Table 5.5 Differential Pulse voltammetric data of zinc complexes in the presence of different concentration of DNA in Tris-Hcl buffer (pH 7.1)

Complex	R=[DNA] / [Complex]	Ep (V)	Ip (µA)
$[Zn(TA)_2]$	0	0.080	5.36
	0.3	0.076	4.65
	0.6	0.072	4.17
$[Zn(TNA)_2]$	0	0.324	6.85
	0.3	0.318	5.88
	0.6	0.316	5.36
$[Zn(TMA)_2]$	0	0.065	1.98
	0.3	0.062	1.48
	0.6	0..061	1.01
$[Zn(PA)_2]$	0	0.108	1.79
	0.3	0.106	1.35
	0.7	0.104	1.01
$[Zn(PNA)_2]$	0	0.336	2.89
	0.3	0.328	1.64
	0.6	0.324	1.52
$[Zn(PMA)_2]$	0	0.064	5.38
	0.3	0.062	4.45
	0.6	0.062	3.69

In all synthesized compounds, incremental addition of DNA effectively alters both potentials and currents of anodic peaks. Presence of DNA causes a considerable decrease in the voltammetric current. The drop of the voltammetric currents in the presence of DNA may be attributed to slow diffusion of the metal complexes bound to large and slowly diffusing HS- DNA. This in turn indicates the extent of binding affinity of the compounds to DNA. This result shows the interaction existing between the ligands and complexes with DNA. It can be concluded that all synthesized molecule binds to DNA through intercalation, with insertion of the molecule between the base pairs of the DNA strand.

5.3.3 Circular Dichroism studies

Additional evidence for DNA interaction was obtained from circular dichroism (CD) spectral studies. CD spectroscopy is an optical technique that measures the difference in the absorption of left and right circularly polarized light. This technique has been widely used in the studies of nucleic acids structures and the use of it to monitor conformational polymorphism of DNA. DNA may undergo conformational changes to B-form, A-form, Z-form, quadruplexes, triplexes and other structures as a result of the binding process to different compounds [42]. CD spectroscopy is extremely sensitive and relatively inexpensive, as compared with other techniques. CD shows extreme sensitivity for low concentrations of DNA (20 μg/mL). In addition, it is possible to detect as little as 25 μg oligonucleotides by using circular dichroism which made it a useful method for study low solubility samples. These studies show that CD spectroscopy is a powerful technique to monitor DNA conformational changes resulting from drug binding [43]. Circular dichoric studies are useful in diagnosing changes in the morphology of DNA during different compound-DNA interactions**.**

The CD spectrum of HS- DNA consists of a positive band at 275 nm that can be due to base stacking and a negative band at 245 nm that can be due to helicity and it is also characteristic of DNA in a right-handed B form [44]. CD spectra of HS-DNA in the UV region show a distinct change in the spectral band corresponding to the B-DNA conformation. Groove binding or electrostatic interaction between small molecules and DNA causes less or no perturbation on the base stacking and helicity bands, whereas a classical intercalation enhances both CD bands [45]. The observed decrease in the positive DNA dichroic signal is likely due to a transition from the extended nucleic acid double helix to the more denatured structure [46]. It should be

noted that hydrophobic base stacking in oligomers and polymers results in close contacts and coulombic interactions that give rise to intense CD bands corresponding to each base transition [47]. So the intercalated complexes which disrupt interactions between DNA bases and weaken base stacking and decrease the intensities of CD bands. Reductions in molar ellipticity in the negative band (245 nm) when complexes are present are related to destabilization and helix unwinding [48].

The conformational changes of HS-DNA induced by the synthesized Schiff base ligands and its Ni(II), Cu(II) and Zn(II) complexes were monitored by CD spectroscopy in Tris-buffer at pH = 7.1 at room temperature. The CD spectrum of HS-DNA exhibits two bands, a positive band at 275 nm due to base stacking and a negative band at 243 nm due to right-handed helicity. When the ligands (TA, TNA, TMA, PA, PNA and PMA) and their Ni(II), Cu(II) and Zn(II) complexes were incubated with HS-DNA, the CD spectra of HS-DNA undergo significant changes in both positive and negative bands represented in Figure 5.37- 5.52 and the data are given in Table 5.6 – 5.9.

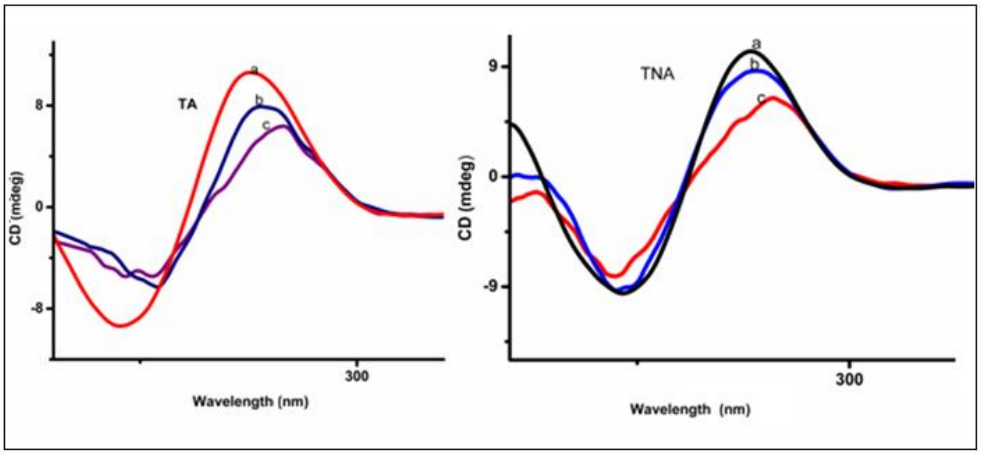

Figure 5.37 CD spectra of HS-DNA (1×10^{-5} M) in Tris-HCl buffer of pH 7.1 in the absence (a) and presence (b and c) of TA and TNA.

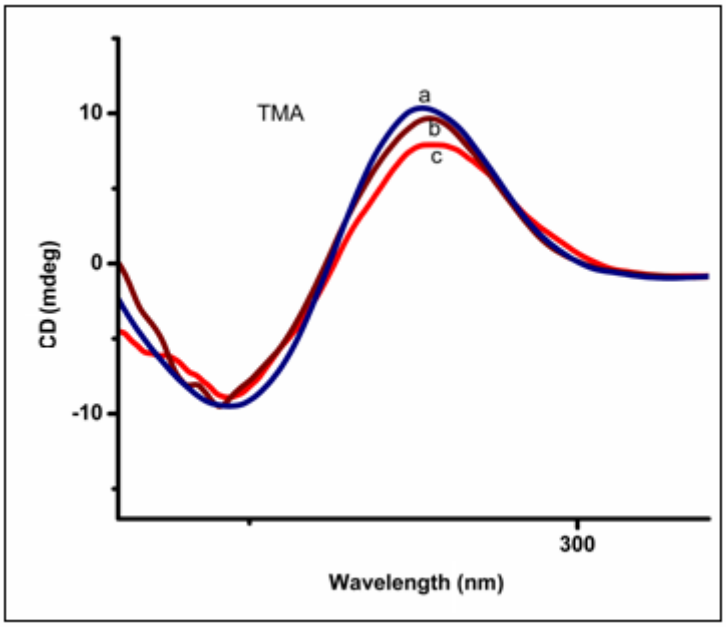

Figure 5.38 CD spectra of HS-DNA (1×10^{-5} M) in Tris-HCl buffer of pH 7.1 in the absence (a) and presence (b and c) of TMA.

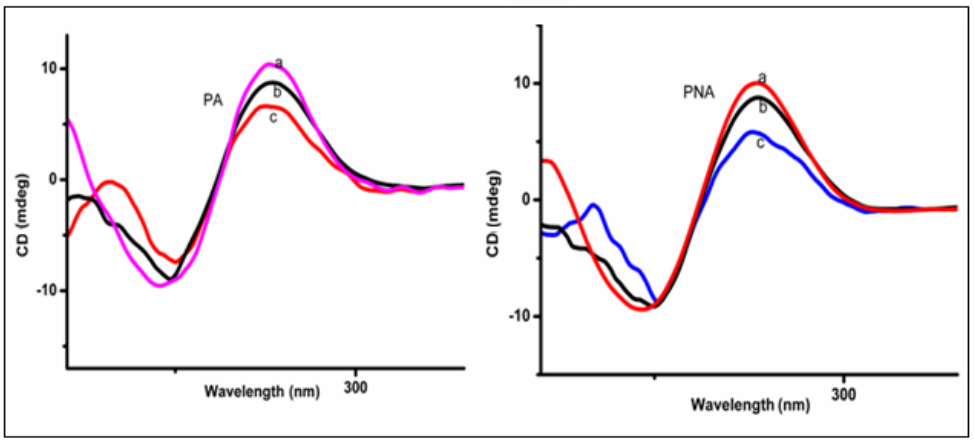

Figure 5.39 CD spectra of HS-DNA (1×10^{-5} M) in Tris-HCl buffer of pH 7.1 in the absence (a) and presence (b and c) of PA and PNA.

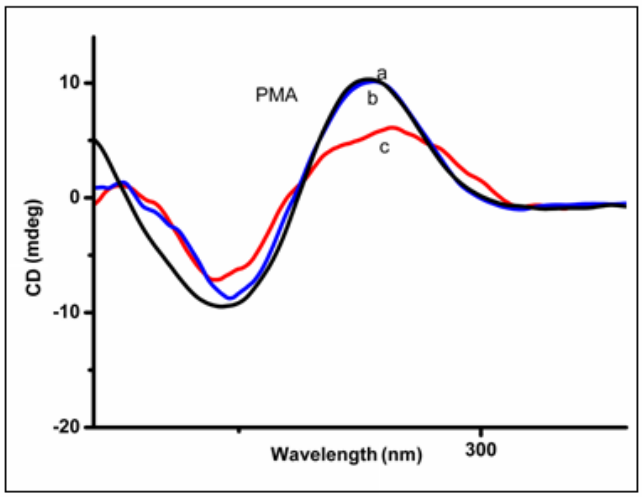

Figure 5.40 CD spectra of HS-DNA (1×10^{-5} M) in Tris-HCl buffer of pH 7.1 in the absence (a) and presence (b and c) of PMA.

Table 5.6 CD parameter for DNA-ligand interaction of Schiff bases

Complex	R=[DNA]/ [Complex]	Positive band		Negative band	
		λ_{max} (nm)	CD (mdeg)	λ_{max} (nm)	CD (mdeg)
TA	0	275	10.76	245	-9.133
	0.3	278	7.81	249	-5.837
	0.6	279	6.10	248	-4.588
TNA	0	275	10.50	245	-9.755
	0.3	277	8.46	246	-8.739
	0.6	278	5.91	245	-7.971
TNA	0	275	10.25	245	-9.696
	0.3	276	9.38	246	-8.960
	0.6	277	8.07	246	-8.089
PA	0	275	10.59	245	-9.743
	0.3	276	8.54	246	-8.238
	0.7	276	6.63	247	-6.734
PNA	0	275	10.01	245	-9.250
	0.3	276	8.69	245	-8.590
	0.6	275	5.79	245	-5.948
PMA	0	275	10.81	245	-9.609
	0.3	277	9.72	246	-8.064
	0.6	277	6.01	246	-6.670

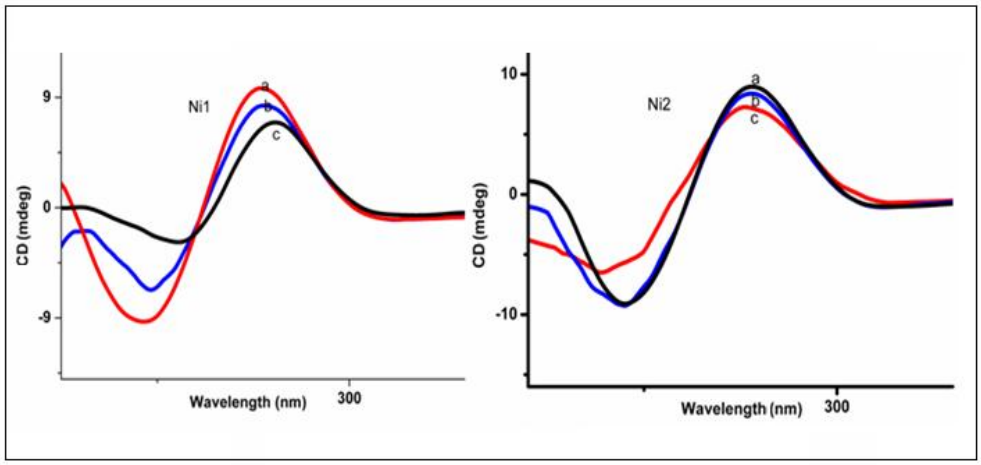

Figure 5.41 CD spectra of HS-DNA (1×10^{-5} M) in Tris-HCl buffer of pH 7.1 in the Absence (a) and presence (b and c) of of Ni1 = $[Ni(TA)_2(H_2O)_2]$ and Ni2 = $[Ni(TNA)_2(H_2O)_2]\cdot 2H_2O$.

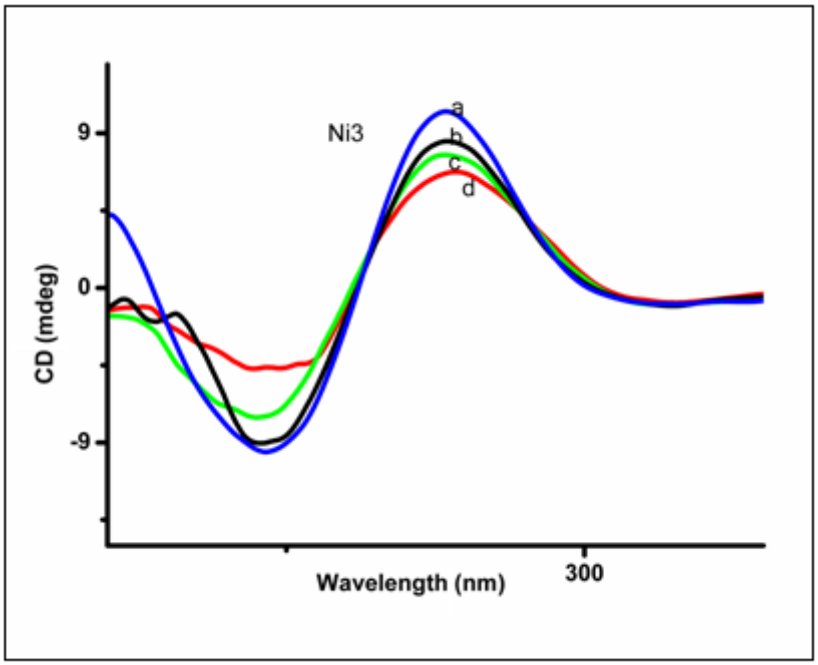

Figure 5.42 CD spectra of HS-DNA (1×10^{-5} M) in Tris-HCl buffer of pH 7.1 in the Absence (a) and presence (b and c) of of Ni3 = $[Ni(TMA)_2]\cdot 3H_2O$.

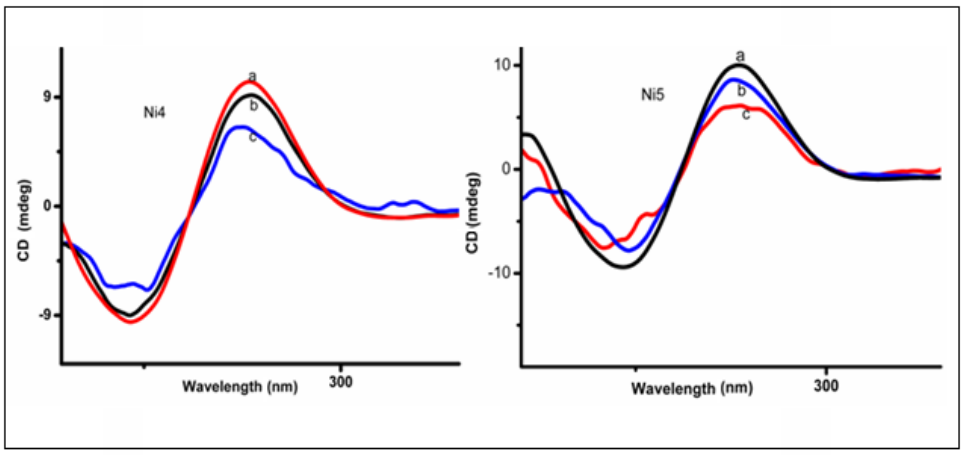

Figure 5.43 CD spectra of HS-DNA (1×10^{-5} M) in Tris-HCl buffer of pH 7.1 in the absence(a) and presence (b and c) of Ni4 = $[Ni(PA)_2]\cdot H_2O$ and Ni5 = $[Ni(PNA)_2]\cdot 2H_2O$.

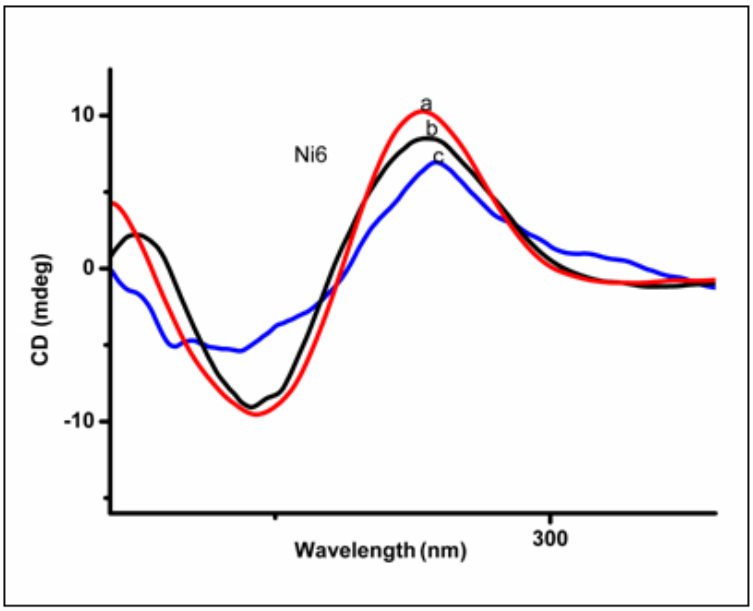

Figure 5.44 CD spectra of HS-DNA (1×10^{-5} M) in Tris-HCl buffer of pH 7.1 in the absence (a) and presence (b and c) of Ni6 = $[Ni(PMA)_2]$.

Table 5.7 CD parameter for DNA-complex interaction of nickel complexes

Complex	R=[DNA]/ [Complex]	Positive band		Negative band	
		λ_{max} (nm)	CD (mdeg)	λ_{max} (nm)	CD (mdeg)
$[Ni(TA)_2(H_2O)_2]$	0	275	9.85	245	-9.555
	0.3	277	8.01	247	-6.481
	0.7	279	6.54	249	-2.061
$[Ni(TNA)_2(H_2O)_2]\cdot 2H_2O$	0	276	8.83	245	-9.643
	0.3	277	8.03	243	-9.378
	0.6	278	6.84	245	-5.948
$[Ni(TMA)_2]\cdot 3H_2O$	0	275	10.50	245	-9.755
	0.3	277	8.46	246	-9.119
	0.6	276	7.57	246	-7.591
$[Ni(PA)_2]\cdot H_2O$	0	275	10.20	245	-9.901
	0.3	276	9.14	246	-8.958
	0.6	275	6.54	245	-6.473
$[Ni(PNA)_2]\cdot 2H_2O$	0	275	10.29	245	-9.510
	0.3	275	8.69	247	-8.201
	0.6	276	5.77	246	-6.445
$[Ni(PMA)_2]$	0	275	10.67	245	-9.378
	0.3	277	8.56	246	-8.723
	0.6	278	6.84	245	-5.152

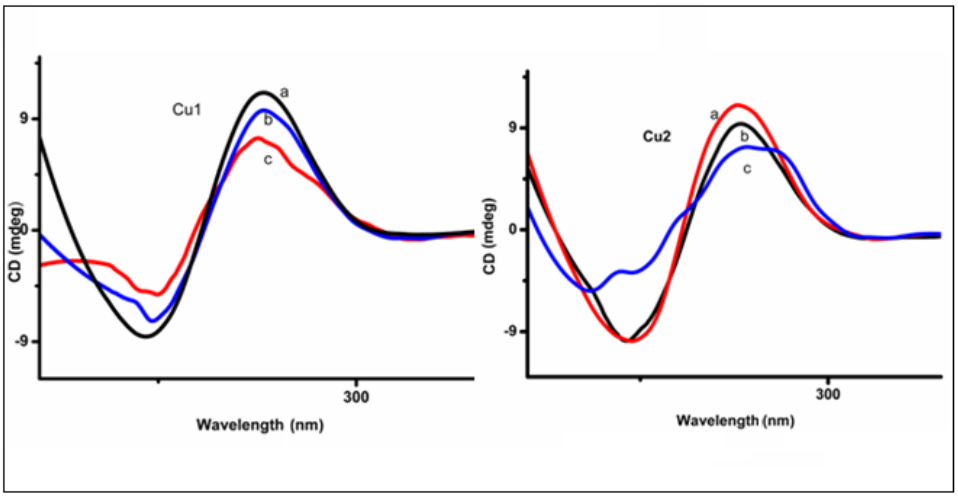

Figure 5.45 CD spectra of HS-DNA (1×10^{-5} M) in Tris-HCl buffer of pH 7.1 in the absence (a) and presence (b and c) of Cu1 = $[Cu(TA)_2H_2O]\cdot H_2O$ and Cu2 = $[Cu(TNA)_2]\cdot 2H_2O$.

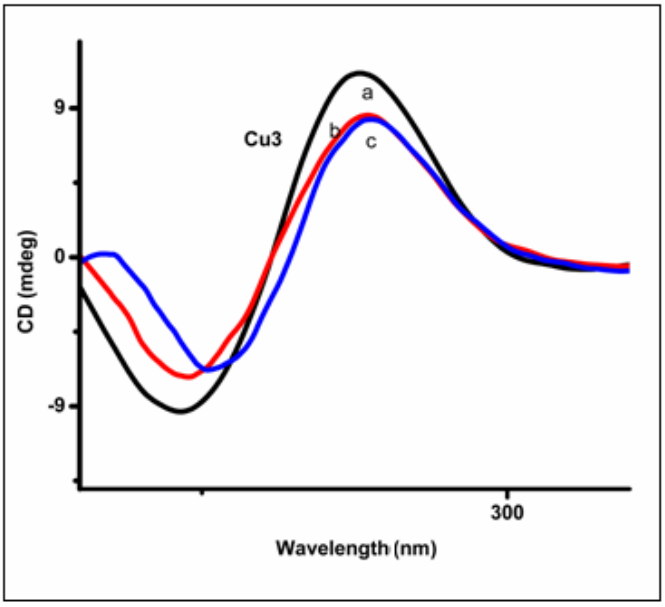

Figure 5.46 CD spectra of HS-DNA (1×10^{-5} M) in Tris-HCl buffer of pH 7.1 in the absence (a) and presence (b and c) of Cu3 = $[Cu(TMA)_2]\cdot H_2O$.

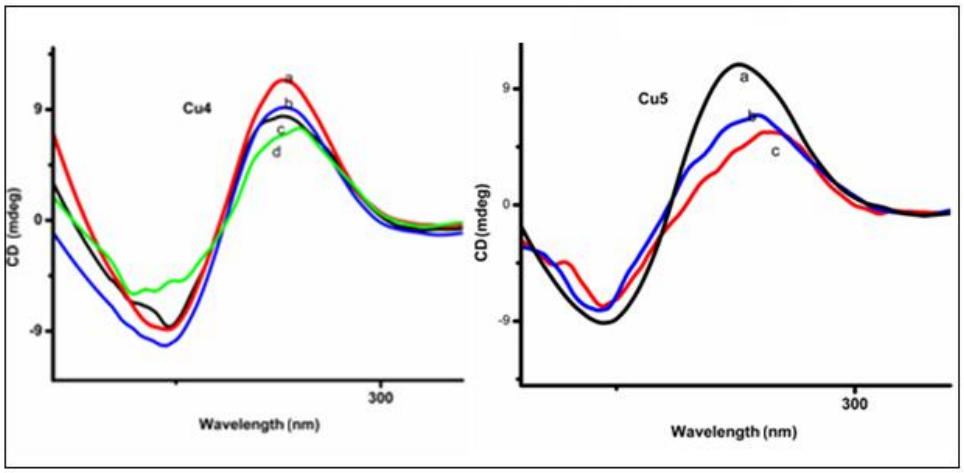

Figure 5.47 CD spectra of HS-DNA (1×10^{-5} M) in Tris-HCl buffer of pH 7.1 in theabsence (a) and presence (b and c) of Cu4 = $[Cu(PA)_2H_2O]\cdot 2H_2O$ and Cu5 = $[Cu(PNA)_2]\cdot 3H_2O$.

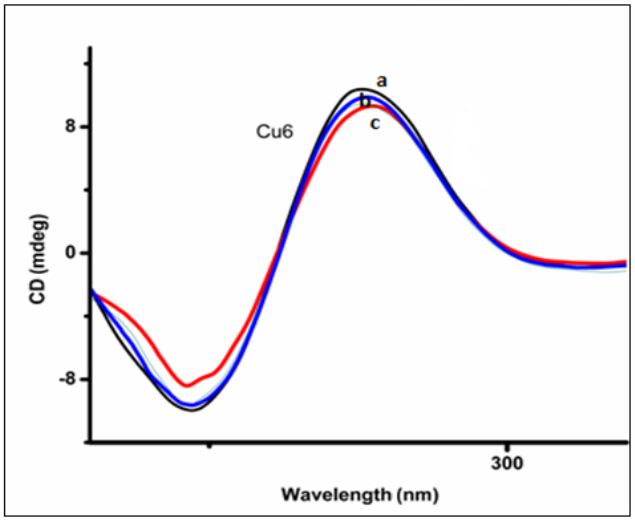

Figure 5.48 CD spectra of HS-DNA (1×10^{-5} M) in Tris-HCl buffer of pH 7.1 in the absence (a) and presence (b and c) of Cu6 = $[Cu(PMA)_2]\cdot H_2O$.

Table 5.8 CD parameter for DNA-complex interaction of copper complexes

Complex	R=[DNA]/ [Complex]	Positive band		Negative band	
		λ_{max} (nm)	CD (mdeg)	λ_{max} (nm)	CD (mdeg)
$[Cu(TA)_2H_2O]\cdot H_2O$	0	275	11.09	245	-8.548
	0.2	276	9.55	247	-7.244
	0.4	275	7.30	247	-4.997
$[Cu(TNA)_2]\cdot 2H_2O$	0	275	11.10	245	-10.154
	0.4	276	9.01	246	-9.296
	0.8	276	6.91	247	-5.242
$[Cu(TMA)_2]\cdot H_2O$	0	275	11.20	245	-9.312
	0.4	275	8.50	247	-7.218
	0.8	278	7.64	248	-6.113
$[Cu(PA)_2H_2O]\cdot 2H_2O$	0	276	11.34	245	-10.152
	0.3	276	9.00	247	-8.798
	0.6	279	7.16	248	-5.732
$[Cu(PNA)_2]\cdot 3H_2O$	0	275	11.34	245	-8.793
	0.4	279	6.78	246	-8.206
	0.8	280	5.32	246	-7.469
$[Cu(PMA)_2]\cdot H_2O$	0	275	10.20	245	-10.041
	0.4	275	9.74	247	-9.470
	0.8	277	9.06	247	-8.340

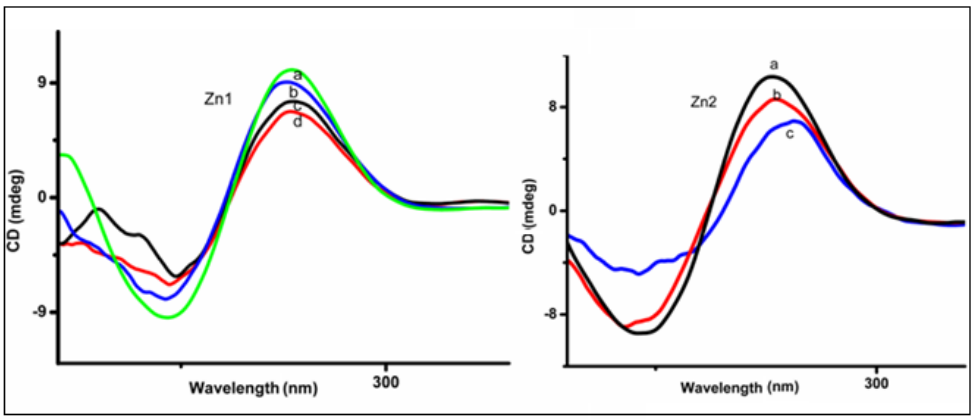

Figure 5.49 CD spectra of HS-DNA (1×10^{-5} M) in Tris-HCl buffer of pH 7.1 in the absence (a) and presence (b and c) of Zn1 = $[Zn(TA)_2]$ and Zn2 = $[Zn(TNA)_2]$.

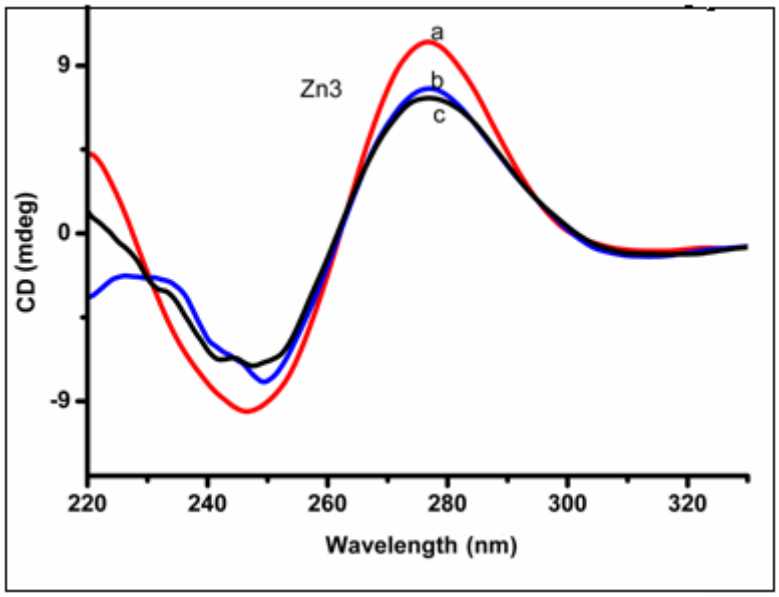

Figure 5.50 CD spectra of HS-DNA (1×10^{-5} M) in Tris-HCl buffer of pH 7.1 in the absence (a) and presence (b and c) of Zn3 = $[Zn(TMA)_2]$.

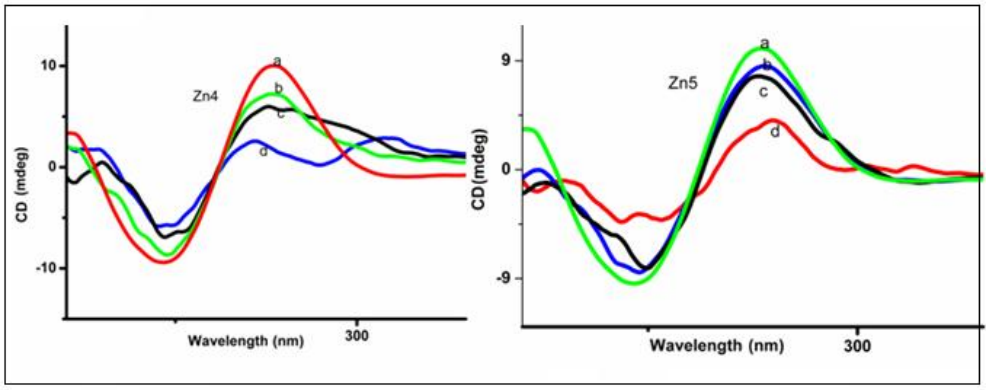

Figure 5.51 CD spectra of HS-DNA (1×10^{-5} M) in Tris-HCl buffer of pH 7.1 in the absence (a) and presence (b and c) of Zn4 = $[Zn(PA)_2]$ and Zn5 = $[Zn(PNA)_2]$.

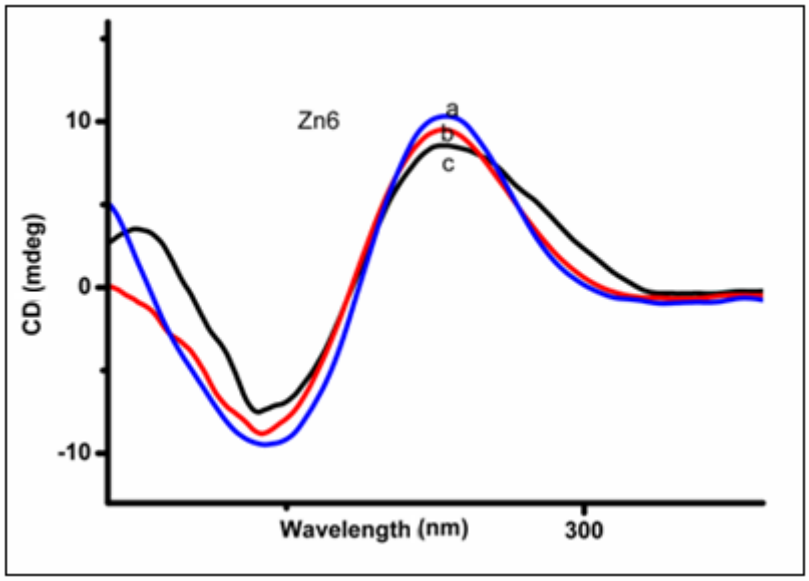

Figure 5.52 CD spectra of HS-DNA (1×10^{-5} M) in Tris-HCl buffer of pH 7.1 in the absence (a) and presence (b and c) of Zn6 = $[Zn(PMA)_2]$.

Table 5.9 CD parameter for DNA-complex interaction of zinc complexes

Complex	R=[DNA]/ [Complex]	Positive band		Negative band	
		λ_{max} (nm)	CD (mdeg)	λ_{max} (nm)	CD (mdeg)
$[Zn(TA)_2]$	0	275	9.97	246	-9.545
	0.4	275	8.90	246	-8.129
	0.8	276	7.48	245	-7.485
$[Zn(TNA)_2]$	0	275	10.42	245	-9.474
	0.4	276	8.61	247	-8.347
	0.8	279	6.78	247	-4.588
$[Zn(TMA)_2]$	0	275	10.32	245	-9.433
	0.4	276	7.96	246	-8.129
	0.8	276	7.01	246	-6.825
$[Zn(PA)_2]$	0	275	10.09	245	-9.567
	0.4	276	7.45	246	-8.643
	0.8	275	6.13	246	-6.924
$[Zn(PNA)_2]$	0	275	9.82	246	-9.407
	0.4	276	8.68	246	-8.267
	0.8	276	7.65	246	-6.607
$[Zn(PMA)_2]$	0	275	10.11	245	-9.543
	0.4	275	9.58	246	-8.885
	0.8	276	8.53	246	-7.302

In all ligands and metal complexes , the intensity of the positive band decreased and that of negative band increased. The decreased intensity in the positive band may be due to the intercalation of the complexes has effect on the π-π stacking of DNA base pairs. The increased intensity in the negative band suggests that the complexes can unwind the DNA helix and lead to some loss of helicity, which induces a more A-like conformation in DNA .This result remarks a loss of the typical chirality of HS-DNA after its interaction with synthesized compounds, in agreement with helix unwinding after intercalation. These changes also suggest that the stacking mode and the orientation of base pairs in DNA were disturbed with the binding of the

complexes, and certain conformational changes, such as the conversion from a more B-like to a more A-like structure within the DNA molecules. These observations clearly indicate that the binding mode of all the compounds should be intercalative.

5.4 Conclusion

The binding behavior of the ligands and metal complexes toward HS-DNA was determined by electronic absorption spectroscopy, CD spectral studies and voltammetric techniques. Upon electronic absorption spectral titrations, all the synthesized Schiff bases and their metal complexes showed hypochromism. Observed intrinsic binding constant (ranging from 10^3 - 10^5 M^{-1}) is comparable to other intecalaters. DNA-binding studies with HS-DNA indicate that ligands and metal complexes bind to DNA by intercalation modes. Result from DPV and CD clearly reveals that binding of DNA with ligands and metal complexes is through intercalation. Results also showed that metal complexes have stronger binding affinity than ligands.

References

[1] T. Alessio, D. Cosimo, M. Louise, B. Giampaolo and J. H. Michael, Dalton Trans., 42, (2013), 11220- 11226.

[2] L. Xiaoquan, W. Lan, L. Hongde, W. Rui and C. Jing, Talanta., 73, (2007), 444-450.

[3] G. W. Zhang, Y. Li and Y.T. Hu, J. Agric. Food Chem., 61, (2013), 2638-2647.

[4] C. Mala, B. Kakoli and A. Farukh, Inorg. Chem., 46, (2007), 3072-3082.

[5] A. M. Ahmed and M. A. M. Ibrahim, J. Basic and Appl. Sci., 4, (2015), 119-133.

[6] L. H. Abdel Rahman, A. M. Abu-Dief, N. A. Hashem and A. A. Seleem, Int. J. Nano. Chem., 2, (2015), 79 -95.

[7] A. T. Tarushi, C. P. Raptopoulou, V. Psycharis, A. Terzis, G. Psomas and D. P. Kessissoglou, Bioorg. Med. Chem., 18, (2010), 2678-2685.

[8] Y. J. Liu, C. H. Zeng, H. L. Huang, L. X. He and F. H. Wu, Eur. J. Med. Chem., 45, (2010), 564-571.

[9] S. Sreelatha, P. R. Padma and M. Umadevi, Food Chem. Toxicol., 47, (2009), 702-708.

[10] D. Arish and M. Sivasankaran Nair, Spectrochim. Acta Mol. Biomol. Spectrosc., 82, (2011), 191-199.

[11] H. Y. Liu, Q. Guo, J. F. Dong, Q. Wei, H. Zhang, X. B. Sun, C. C. Liu and L. Z. Li, J. Coord. Chem., 68, (2015), 1036-1040.

[12] L. Z. Li, Z. H. Guo, Q. F. Zhang, T. Xu and D. Q. Wang, Inorg. Chem. Commun., 13, (2010), 1161- 1166.

[13] A. Patra, B. Sen, S. Sarkar, A. Pandey, E. Zangrando and P. Chattopadhyay, Polyhedron., 51, (2013), 156-163.

[14] S. Shobana, J. Dharmaraja and S. Selvaraj, Spectrochim. Acta A: Mol. Biomol. Spectrosc., 107, (2013), 117-132.

[15] T. Stringer, B. Therrien, D. T. Hendricks, H. Guzgay and G. S. Smith, Inorg. Chem. Comm., 14, (2011), 956-960.

[16] C. Rajarajeswari, M. Ganeshpandian, M. Palaniandavar, A. Riyasdeen and M. A. Akbarsha, J. Inorg. Biochem., 140, (2014), 255-268.

[17] Q. Zhang, F. Zhang, W. Wang and X. Wang, J. Inorg. Biochem., 100, (2006), 1344-1352.

[18] C. N. Sudhamani, H. S. Bhojya Naik, T. R. Ravikumar Naik and M.C. Prabhakara, Spectrochim. Acta A: Mol. Biomol. Spectrosc., 72, (2009), 643-647.

[19] A. B. Hoda, M. A Abdel Nasser, A. Alaghazand, A. S, Mutlak, Int. J. Electrochem. Sci., 8, (2013), 9399- 9413.

[20] D. Pucci, A. Bellusci, A. Crispini, M. Ghedini and M. La Deda, Inorg. Chim. Acta, 357 (2004), 495-504.

[21] N. Mei-Ju, L. Zhen, C. Guo-Liang, K. Xiang-Jin, H. Min and Z. Qingfu, PLoS ONE, 10(6):e0130922. doi:10.1371/ journal.pone.0130922.

[22] R. Starosta, M. Puchalska, J. Cybińska, M. Barys and A.V. Mudring, Dalton Trans., 40, (2011), 2459-2468.

[23] L. H. Abdel Rahman, A. M. Abu-Dief, N. A. Hashem and A. A. Seleem, Int. J. Nano. Chem., 2, (2015), 79 -95.

[24] V. Narendrula, K. P. Marri, T. Somapangu and R. Aveliand Shivaraj, J. Fluoresc., 26, (2016), 1317-1329.

[25] L. H. Abdel-Rahman, A. M. Abu-Dief, E. F. Newair and S. K. Hamdan, J. Photochem. Photobiol. B: Biology, 160, (2016), 18-31.

[26] M. D. A. Maria, S. P. Iyyam, C. Joel, R. B. Biju, S. Subramanian and S. K. Damodar Kumar, J. Chem. Pharm. Res., 11, (2015), 105-116.

[27] A. Patra, B. Sen, S. Sarkar, A. Pandey, E. Zangrando, and P. Chattopadhyay, Polyhedron, 1, (2013), 156-163.

[28] V. Uma, V. G. Vaidyanathan and B. U. Nair, Bull. Chem. Soc., 78, (2005), 845-850.

[29] N. Z. Tian, Y. Zhou, S. G. Sun, Y. Ding and L. W. Zhong, Sci., 5825, (2007), 732-735.

[30] P. J. Cox, G. Psomasgand, C. S. Bolos, Bioorg. Med. Chem., 16, (2009), 6054-6062.

[31] R. F. Pasternack and E. J. Gibbs and J. Villafranca, Biochem., 22, (1983), 2406-2414.

[32] M. D. A. Mariya, S. P. Iyyam, S. Subramanian, S. Pradeepa and S. K. Damodar, Int. J. Inorg. Bioinorgan. Chem., 4, (2014), 61-67.

[33] B. Anupama, M. Padmaja and C. GyanaKumari, J. Chem., 1, (2012), 389-400.

[34] S. Kashanian, Z. Shariati, H. Roshanfekr and S. Ghobadi, DNA Cell Biol., 31, (2012), 1314-1348.

[35] A. Terenzi, R. Bonsignore, A. Spinello, C. Gentile, A. Martorana, C. Ducani, B. Högberg, A. M. Almerico, A. Lauria and G. Barone, RSC Adv., 4, (2014), 33245-33256.

[36] N. H. Campbell, N. H. A. Karim, G. N. Parkinson, M. Gunaratnam, V. Petrucci, A. K. Todd, R. Vilar and S. Neidle, J. Med. Chem., 55, (2011), 209-222.

[37] V. Rajendirn, R. Karthik, M. Palaniandavar, H. Stoeckli-Evans, V. S. Periasamy, M. A. Akbarsha, B. S. Srinag, H. Krishnamurty, Inorg. Chem., 46, (2007), 8208-8221.

[38] E. M. Boon and J. K. Barton, Bioconjugate Chem., 14, (2003), 1140-1147.

[39] M. T. Carter and A. J. Bard, J. Am. Chem. Soc., 109, (1987), 7528-7530.

[40] G. M. Blackburn and M. J. Gait, Nucleic acid in chemistry and biology, ed. 2nd, Oxford University Press, New York, (1996).

[41] N. Shahabadi, S. Kashanian and F. Darabi, DNA Cell Biol., 28, (2009), 1-8.

[42] A. Rodger and B. Nordén, ed. 3rd, Oxford University Press, Oxford; New York, (1997).

[43] J. Kypr, I. Kejnovská, D. Renčiuk and M. Vorlíčková, Nucleic Acids Res., 37, (2009), 1713-1725.

[44] Yu-Ming Chang, K. Cammy, M. Chen and Ming-Hon Hou, Int. J. Mol. Sci., 13, (2012), 3394-3413.

[45] Z.-H. Xu, F. J. Chen, P.X. Xi, X. H. Liu and Z. Z. Zeng, J. Photochem. Photobiol., A, 196, (2008), 77-83.

[46] L. Milne, P. Nicotera, S. Orrenius and M. J. Burkitt, Arch. Biochem. Biophys., 304, (1993), 102-109.

[47] B. Macıas, M. V. Villa, B. Gomez, J. Borrás, G. Alzuet, M. González-Alvarez and A. Castiñeiras, J. Inorg. Biochem., 101, (2007), 441-451.

Chapter 6

HIV-RT INHIBITORY ACTIVITY STUDIES OF SCHIFF BASES AND THEIR Ni(II), Cu(II) AND Zn(II) COMPLEXES

Contents

6.1 Introduction

Acquired immune deficiency syndrome (AIDS) is a formidable pandemic that is still wreaking havoc worldwide. There are two different species of HIV: HIV-1 and HIV-2. HIV-1 (Human Immunodeficiency Virus Type-1) is the pathogenic retrovirus (lentivirus family) and causative agent of AIDS or AIDS- related complex (ARC). HIV-2 is endemic and is mostly found in West Africa [1-3]. Currently the World Health Organization estimates that some 33 million people are infected with HIV-1, constituting a global pandemic illness with significant social and economic impact [4]. HIV infects humans, and the progression of its infection leads to AIDS. HIV can destroy entire "families" of CD4 cells. CD4 cells are a type of white blood cell that fights infection. Another name for them is T-helper cells. CD4 cells are made in the spleen, lymph nodes, and thymus gland, which are part of the lymph or infection-fighting system. For HIV negative person a normal CD4 count is in the range 460 – 1600 /μL. CD4 cells move throughout body, helping to identify and destroy germs such as bacteria and viruses [5].

HIV is spread when an infected body fluid is introduced directly into the blood stream of a non infected individual. It also transmitted through unprotected sex, shared needles, mother to child, birth, breast feeding and blood transfusions. At the final stage of this disease, the immune system of an infected person becomes severely damaged; as a result, this person becomes susceptible to a number of opportunistic infections (typically rare in people with healthy immune systems) and eventually dies [6-8]. Some opportunistic infections (CD4 Count 200-500/μL) are pneumonia (usually caused by bacteria), tuberculosis in the lungs, oral or vaginal yeast infections, shingles (viral skin infection), oral hairy leukoplakia and Kaposi's sarcoma [9-11].

6.1.1 Structure of HIV-1

The HIV-1 genome consists of cone-shaped nucleocapsid (core) which contains the genomic RNA molecules. There are three viral enzymes namely reverse transcriptase (RT), protease (PR), and integrase (IN) encoded by the gag and gag-pol genes of HIV play an important role in the virus replication cycle. Among them, viral reverse transcriptase (RT) catalyzes the formation of proviral DNA from viral RNA, the key stage in viral replication [12]. HIV-1 is an enveloped virus with roughly spherical virions of variable size. The envelope is studded with ten trimeric envelope (Env) proteins and various host membrane proteins. Assembly of the virus is largely driven by the viral Gag protein. Gag is a multi-domain polyprotein with the three folded domains matrix (MA), capsid (CA) and nucleocapsid (NC) and the three shorter peptides SP1, SP2 and p6 (Figure. 6.1) [13-19].

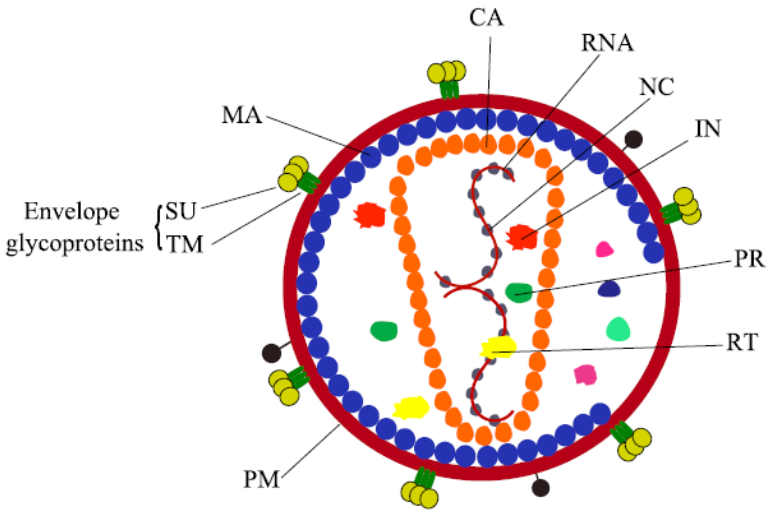

Figure 6.1 Structure of a mature HIV-1 virion. IN – integrase, PR – protease, RT – reverse transcriptase PM – virion envelope derived from the plasma membrane of an infected cell, SU – surface unit protein, TM – transmembrane protein, CA – capsid protein, MA – matrix protein, NC –nucleocapsid protein [Ref.13].

6.1.2 HIV-1 replication

When HIV infects a cell, RT copies the viral single stranded RNA genome into a double-stranded proviral DNA (Figure 6.2). The viral DNA is then integrated into the host chromosomal DNA. This insertion (integration) is catalyzed by the HIV-encoded enzyme – integrase (IN) which then allows host cellular processes, such as transcription and translation. The proviral DNA is transcribed by the cellular RNA polymerase. The mRNAs are translated by the cellular polysomes. Viral proteins and genomic RNA are transported to the cellular membrane. Immature virions are released. Polypeptide precursors are processed by the viral PR to produce mature viral particles. Viral protease (PR) initiates the essential process of virion maturation. That means transcription of the viral genome and of the viral

genes followed by translation, packaging, fusion and maturation supply the molecular components for the release of the new infectious viral particles [20-23].

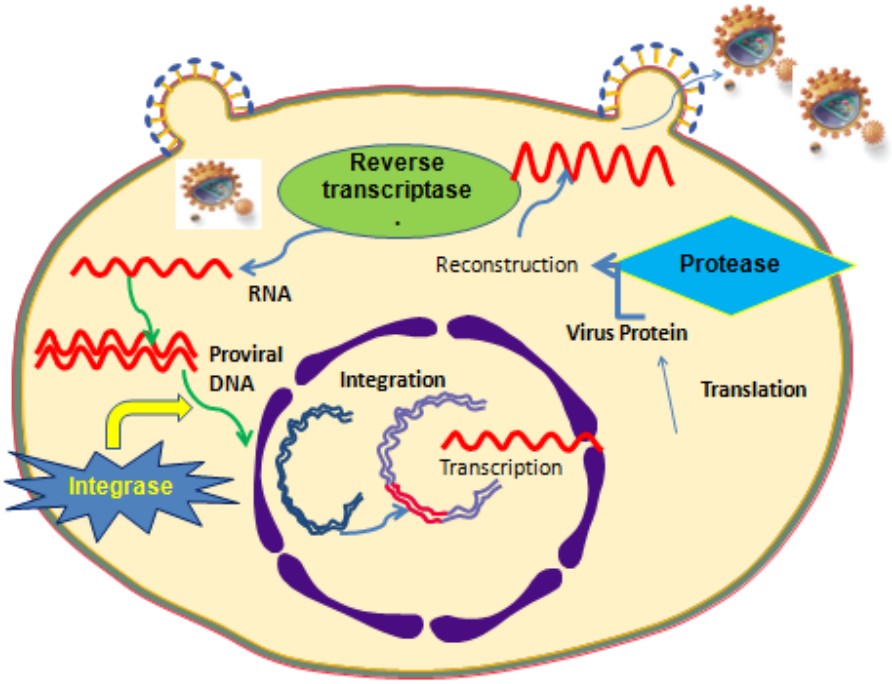

Figure 6.2 Steps in the replicative cycle of HIV (i) adsorption and cell fusion, (ii) reverse transcription, (iii) proviral DNA integration, (iv) proviral DNA transcription to viral mRNA, (v) viral mRNA translation to viral proteins and (vi) maturation and budding.

HIV-1 RT performs an integral role in virus replication and thus is a main target of current antiretroviral treatment. RT is a multifunctional enzyme that contains both polymerase and RNaseH activities to convert the single-stranded viral RNA genome into a double-stranded DNA (dsRNA) product ready for integration [24].

6.1.3 The HIV-1 RT enzyme

The HIV-1 RT is an asymmetric heterodimer, comprising of p66 subunit (560 amino acids) and a p51 subunit (440 amino acids) [25]. Both subunits are encoded by the same sequence in the viral genome. The p66 subunit is the larger of the two subunits within HIV-1 RT. This subunit contains the finger, palm, thumb, and connection sub domains as well as the RNaseH sub domain (Figure 6.3). The palm domain contains the polymerase active site with its three aspartic acids (110, 185 and 186) and the YMDD characteristic motif [26]. The p51 subunit is the smaller of the two subunits in HIV-1 RT**.** The p66 subunit assumes a flexible and open structure, whereas the p51 subunit is rather compact, and seems to play a structural role, devoid of catalytic activity, with the three aspartic acids buried inside**.** The p51 subunit is a product of the same gene as the p66 subunit, however, the RNaseH domain is absent in the p51 subunit as a result of proteolytic cleavage [27].

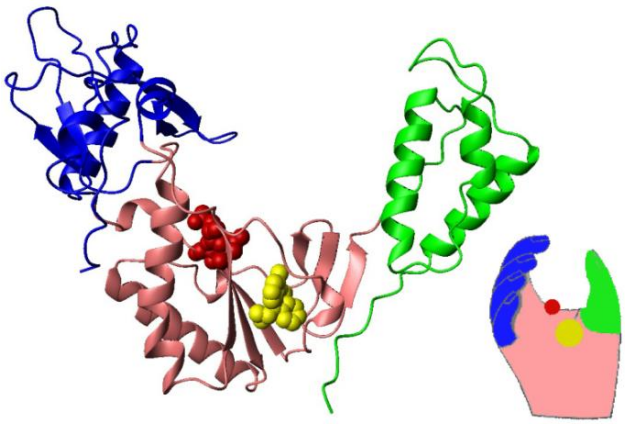

Figure 6.3 Ribbon representation of the active domain of RT (p66 monomer) illustrates its hand-like structure, showing fingers (blue), palm (pink) and thumb (green). DNA is elongated in the active site (red) which is in palm region, NNRTI binding pocket (yellow) [Ref.27].

RT Inhibitors block reverse transcriptase's enzymatic function and prevent completion of synthesis of the double-stranded viral DNA, thus preventing HIV from multiplying. The RT can be inhibited by two classes of drug belonging either to the nucleoside (or nucleotide) reverse transcriptase inhibitors (NRTIs and NtRTIs) or to the non-nucleoside reverse transcriptase inhibitors (NNRTIs). HIV-1 NNRTIs have become key components in the combination regimens of anti-HIV therapy [28]. Three NNRTIs are licensed for use in antiretroviral therapy: nevirapine, delavirdine, and efavirenz. Among those, efavirenz was the first NNRTI to demonstrate clinical efficacy in patients with NNRTI-resistant HIV-1 infection, and was approved by the FDA in 2008. Other NNRTIs with an improved resistance profile are currently being developed.

NRTIs and NtRTIs compete with the natural deoxynucleoside triphosphate (dNTP) for DNA incorporation by HIV-1 RT. After incorporation, they act as chain terminators. Non-nucleoside reverse transcriptase inhibitors (NNRTIs) bind to an allosteric site termed the NNRTI-binding pocket (NNRTI-BP) approximately 10 Å from the polymerase active site and disrupt RT polymerase function [29]. This binding site is located in the palm domain of the p66 subunit of the heterodimeric protein, between the β6–β10–β9 and β12–β13–β14 sheets, and at the basis of the β4–β7–β8 sheet, at a distance of approximately 10 Å from the catalytic site of the enzyme. This pocket is hydrophobic in nature and is lined by the aromatic (Y181, Y188, F227, W229, and Y232), hydrophobic (P59, L100, V106, V179, L234, and P236), and hydrophilic (K101, K103, S105, D132, and E224) amino acids of the p66 subunit, and two amino acids of the p51 subunit (I135 and E138) [30-33]. NNRTI binding to RT induces conformational changes in the enzyme that affect

key elements of the polymerase active site and also the association between the two protein subunits [34-35].

Huang *et al.* reported anti-HIV activity of Dicamphanoyl khellactone (DCK), a coumarin derivative [36]. Due to the potent anti-HIV activity, many DCK derivatives were synthesized and were shown to have improved anti-HIV activity [37-38]. Rao *et al.* reported 2-(2, 6-Dihalophenyl)-3-(pyrimidin-2-yl)-1,3-thiazolidin-4-ones as non-nucleoside HIV-1 RT inhibitors. Structure–activity relationship studies revealed that the nature of the substituents at the 2 and 3 positions of the thiazolidinone nucleus had a significant impact on the in vitro anti-HIV activity of this class of potent antiretroviral agents [39]. A series of 2-(2,6-dibromophenyl)-3-heteroaryl-1,3-thiazolidin-4-ones were designed, synthesized and evaluated as selective human immunodeficiency virus type-1 reverse transcriptase (HIV-1 RT) enzyme inhibitors by Ravindra *et al.* [40]. The results of the HIV-1 RT kit and in vitro cell based assay showed that compounds effectively inhibited HIV-1 replication at 20-320 nM concentrations with minimal cytotoxicity in MT-4 as well as in CEM cells. Ma *et al.* performed a comparative molecular field analysis (CoMFA) like 3D-QSAR and docking studies with the objective of understanding pharmacophore properties of styrylquinoline derivatives and to design inhibitors of HIV-1 integrase [41]. Yu'ning *et al.* discovered novel pyridazinylthioacetamides as potent HIV-1 NNRTIs using a structure-based bioisosterism approach [42].

The treatment for HIV faces many limitations like the production cost, metabolic instability and has several side-effects. Transition metal-based drugs are better alternatives for HIV treatment. Some of the attractive features of metal based therapeutics include synthetic simplicity, solubility control, redox capability, expansion of coordination number and topography matching of the complex to the protein's active site. Building asymmetry

into the complex, which may offer better discrimination between host and rogue cell, can readily be achieved through coordination of chiral ligands to the metal centre [43-44]. The variability of the d-block metals, coupled with the availability of designer organic ligands, augers well for the future development of clinical metallo-drugs for deployment against protease-associated fatal diseases [45]. Metal complexes that interfere with the viral glycoprotein and/or cell receptors are currently based on polyanionic ligands. Metal complexes have also been found to target other sensitive parts of the viral cycle like HIV RT, IN or PR [46].

The use of metal-organic complexes is a potentially fruitful approach for the development of novel enzyme inhibitors [47]. Copper is a bio-essential element and copper complexes have been extensively utilized in metal mediated DNA cleavage for the generation of activated oxygen species [48]. Copper can be potential for anti-HIV, as copper has inhibitor activity for HIV-protease. Copper can interact with donor atoms on a biological target via the formation of coordinate bonds rather than a combination of weaker intermolecular force such as H-bonding [49]. Metal complexes hold the attractive promise of forming stronger attachments with the target by combining the co-ordination ability of metals with the unique stereoelectronic properties of the ligand [50].

This chapter deals with the HIV-1 RT inhibitory activity of heterocyclic Schiff bases and their transition metal complexes by determining their percentage inhibition of HIV-1 RT activity in HIV-1 RT kit.

6.2 Experimental

6.2.1 Methods

In vitro HIV-RT kit assay

The HIV-RT inhibition assay was performed by using an RT assay kit (Roche), and the procedure for assaying RT inhibition was performed as described in the kit protocol [51]. Briefly, the reaction mixture consists of template/primer complex, 20-deoxy-nucleotide-50-triphosphates (dNTPs) and RT enzyme in the lysis buffer with or without inhibitors. After 1 h incubation at 37°C the reaction mixture was transferred to streptavidine-coated microtitre plate (MTP). The biotin labeled dNTPs that are incorporated in the template due to activity of RT were bound to streptavidine. The unbound dNTPs were washed using buffer and antidigoxigenin- peroxidase (DIG-POD) was added in MTP. The DIG-labeled dNTPs incorporated in the template was bound to anti-DIG-POD antibody. The unbound anti-DIG-POD was washed and the peroxide substrate (ABST) was added to the MTP. A colored reaction product was produced during the cleavage of the substrate catalyses by a peroxide enzyme.

The absorbance of the sample was determined at optical density (OD) 405 nM using ELISA reader. The resulting color intensity is directly proportional to the actual RT activity. The percentage inhibitory activity of RT inhibitors was calculated by comparing to a sample that does not contain an inhibitor. Pictorial representation of test principle was shown in Figure 6.4.

The percentage inhibition was calculated by formula as given below

$$\% \text{ Inhibition} = 100 - \frac{\text{OD 405 nm with inhibitor}}{\text{OD 405 nm without inhibitor}} \text{X} 100$$

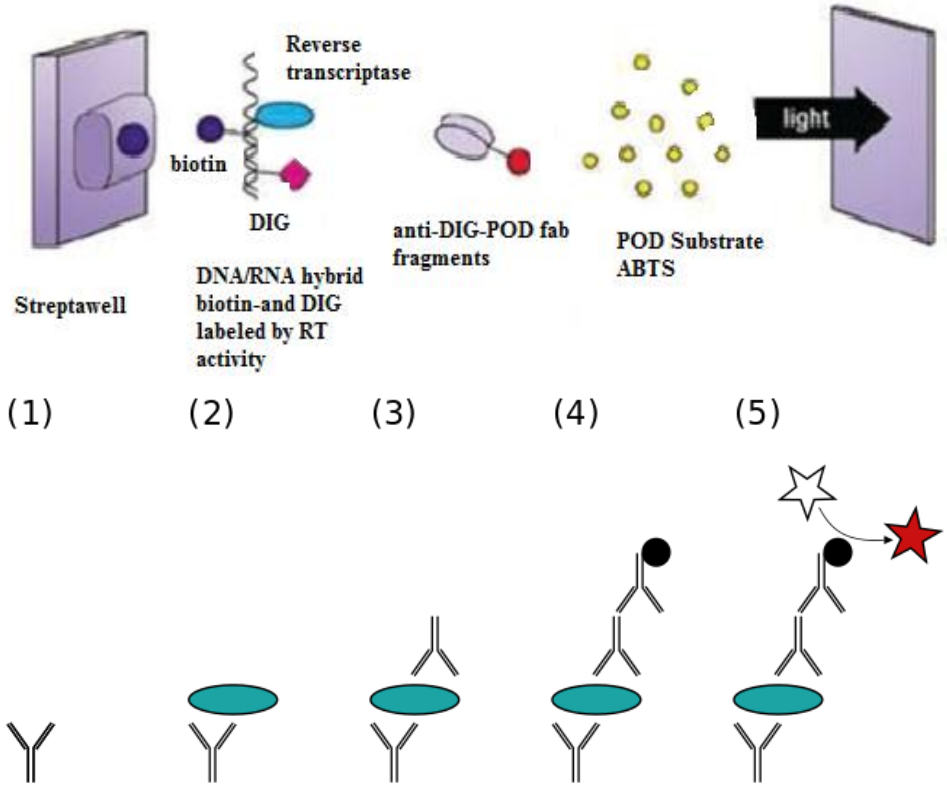

Figure 6.4 Pictorial representation of test principle – (1) Plate is coated with a capture antibody; (2) Addition of sample, and any antigen present binds to capture antibody; (3) Addition of detecting antibody and binds to antigen; (4) Addition of enzyme-linked secondary antibody and binds to detecting antibody; (5) Addition of substrate and is converted by enzyme to detectable form.

6.3 Results and discussion

The reverse transcriptase inhibitory activity of the synthesized Schiff bases and its Ni(II), Cu(II), Zn(II) complexes were studied by reverse transcriptase colorimetric assay kit (Roche). Nevirapine was used as reference drug. It has been observed from in vitro screening (Table 6.1-6.2) that, newly synthesized ligands and its Zn(II) complexes did not show any anti HIV activity. $[Ni(TA)_2(H_2O)_2]$, $[Ni(TNA)_2(H_2O)_2]\cdot 2H_2O$, $[Ni(PA)_2]\cdot H_2O$ and

$[Ni(PNA)_2]\cdot 2H_2O$ showed mild activity. But other two nickel complexes, $[Ni(TMA)_2]\cdot 3H_2O$ and $[Ni(PMA)_2]$ are inactive against reverse transcriptase. RT inhibitor activity of the tested compounds revealed that the complex formation had great positive effect on the bioactivity.

Table 6.1 Anti HIV results of Ni(II) complexes

Compound	% inhibition at 10 µg/ml	% inhibition at 50 µg/ml	% inhibition at 100 µg/ml
$[Ni(TA)_2(H_2O)_2]$	11.4	20.6	31.2
$[Ni(TNA)_2(H_2O)_2]\cdot 2H_2O$	13.5	18.3	29.3
$[Ni(TMA)_2]\cdot 3H_2O$	0	0	0
$[Ni(PA)_2]\cdot H_2O$	2.8	7.9	15.9
$[Ni(PNA)_2]\cdot 2H_2O$	22.6	30.3	35.9
$[Ni(PMA)_2]$	0	0	0

Table 6.2 Anti HIV results of Zn(II) complexes

Compound	% inhibition at 10 µg/mL	% inhibition at 50 µg/mL	% inhibition at 100 µg/mL
$[Zn(TA)_2]$	0	0	0
$[Zn(TNA)_2]$	2.0	0	7.8
$[Zn(TMA)_2]$	0	0	0
$[Zn(PA)_2]$	0	0	0
$[Zn(PNA)_2]$	0	0	0
$[Zn(PMA)_2]$	0	0	0

Cu(II) complexes possess potent RT inhibitory activity (Table 6.3). IC_{50} was calculated by drawing a graph with concentration against % inhibition (Figure 6.5 and 6.6). Among the synthesized copper(II) complexes, $[Cu(TA)_2H_2O]\cdot H_2O$ showed higher RT inhibitory activity with IC_{50} = 0.080 µM followed by $[Cu(TNA)_2]\cdot 2H_2O$ (IC_{50} = 0.087 µM), $[Cu(PA)_2H_2O]\cdot 2H_2O$ (IC_{50} = 0.092 µM) and $[Cu(PNA)_2]\cdot 3H_2O$ (IC_{50} = 0.11 µM). The HIV-1 RT inhibitory activity showed that all of the tested copper complexes showed

significant potency but none of them showed higher activity than nevirapine. The square planar geometry of Cu(II) complexes allows hydrogen bonding in the active site of RT thereby increasing their inhibitory activity. Another factor responsible for activity of Cu(II) complexes against reverse transcriptase is their hydrophilicity. Anti-HIV activity was also affected by different heteroaryl moiety with/or without an appropriate lipophilic substitution. Results showed that the new copper complexes effectively inhibited HIV-1 replication. Among them heterocyclic Schiff base complex with thiophene moiety showed higher anti-HIV activity than pyrole moiety. Result also indicates that the presence of electron donating group ie, methyl group decreases anti-HIV activity. Compared to Schiff bases, metal complexes (mainly copper complexes) were found to exhibit anti HIV activity (Figure 6.7).This is probably due to their greater lipohilic nature.

Table 6.3 Anti HIV results of Cu(II) complexes

Compound	% inhibition at 10 µg/mL	% inhibition at 50 µg/mL	% inhibition at 100 µg/mL	IC_{50} (µM)
$[Cu(TA)_2H_2O]\cdot H_2O$	1.9	63.3	85.1	0.080
$[Cu(TNA)_2]\cdot 2H_2O$	14.4	48.8	85.6	0.087
$[Cu(TMA)_2]\cdot H_2O$	0	0	8.2	-
$[Cu(PA)_2H_2O]\cdot 2H_2O$	2.1	46.5	70.2	0.092
$[Cu(PNA)_2]\cdot 3H_2O$	10.8	46.5	67.5	0.112
$[Cu(PMA)_2]\cdot H_2O$	6.3	35.2	48.4	-
Nevirapine	-	-	100	

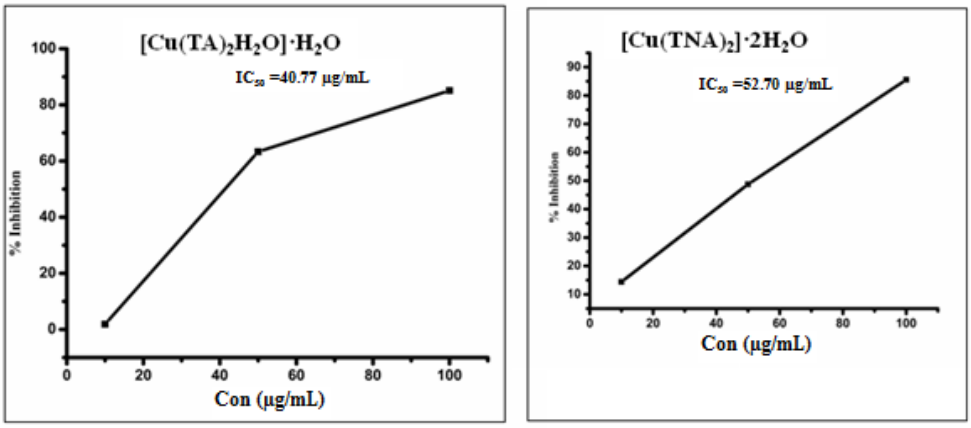

Figure 6.5 Anti HIV activity of $[Cu(TA)_2H_2O]\cdot H_2O$ and $Cu(TNA)_2]\cdot 2H_2O$

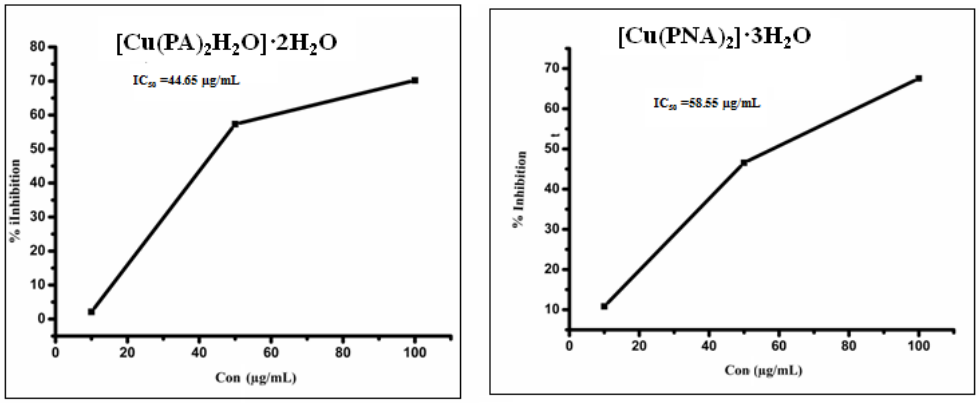

Figure 6.6 Anti HIV activity of $[Cu(PA)_2H_2O]\cdot 2H_2O$ and $[Cu(PNA)_2]\cdot 3H_2O$

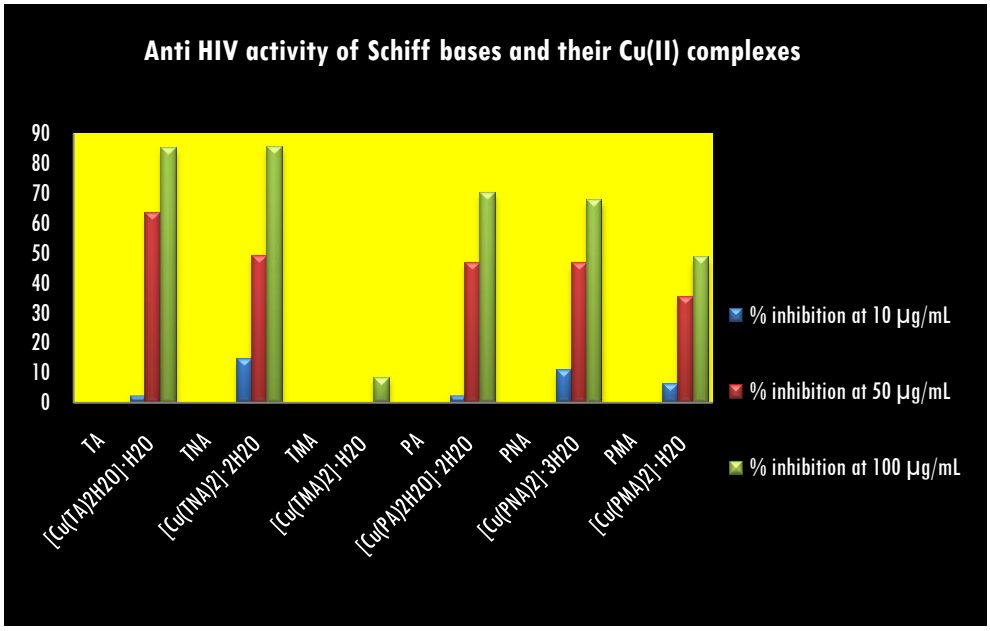

Figure 6.7 Graphical representation of the anti HIV activity of Schiff bases and their Cu(II) complexes

6.4 Conclusion

HIV-1 RT kit assay was used for testing the RT inhibition of Schiff base ligands and their Ni(II), Cu(II) and Zn(II) complexes. Reference drug used was Nevirapine. Results showed that the new copper complexes effectively inhibited HIV-1 replication. Among them heterocyclic Schiff base complex with thiophene moiety showed higher anti-HIV activity than pyrole moiety. Synthesized ligands and their complexes with nickel or zinc have not shown any RT inhibition activity.

References

[1] V. Ravichandran and R. K. Agrawal, Bioorg. Med. Chem. Lett., 17, (2007), 2197-2202.

[2] R. C. Gallo, S. Z. Salahuddin, M. Popovic, G. M. Shearer, M. Kaplan, B. F. Haynes, T. J. Palker, R. Redfield, J. Oleske and B. Safai, Science, 4, (1984), 500-503.

[3] F. Barre-Sinoussi, J. C. Chermann, F. Rey, M. T. Nugeyre, S. Chamaret, J. Gruest, C. Dauguet, C. Axler-Blin, F. Vezinet-Brun, C. Rouzioux, W. Rozenbaum and L. Montagnier, Science, 20, (1983), 868-871.

[4] http:// www.who. int/hiv/data/en.

[5] E. J. De Clercq, Med. Chem., 14, (1995), 2491-2517.

[6] J. Milton, M. J. Slater, A. J. Bird, D. Spinks, G. Scott, C. E. Price, S. Downing, D. V. S. Green, S. Madar, R. Bethell and D. K. Stammers, Bioorg. Med. Chem. Lett., 8, (1998), 2623- 2628.

[7] Y. Pommier, A. A. Johnson and C. Marchand, Nat. Rev. Drug Discovery, 4, (2005), 236-248.

[8] H. S. Lucianna, S. F. Rafaela and R. C. Ernesto, Mem. Inst. Oswaldo Cruz., 110, (2015), 847-864.

[9] S. Distinto, F. Esposito, J. Kirchmair, M. C. Cardia, M. Gaspari, E. Maccioni S. Alcaro, P. Markt, G. Wolber, L. Zinzula and E. Tramontano, Eur. J. Med. Chem., 50, (2012), 216-229.

[10] Z. Xuan, Y. Liu-Meng, L. Guang-Ming, L. Ya-Juan, Z. Chang-Bo, L. Yong-Jun, L. Hao-Zhi and Z. Yong-Tang, Molecules, 17, (2012), 6916-6929.

[11] E. Robert, R. Jingshan, R. Carl, J. Yvonne, S. David and S. David, Nat. Struct. Mol. Biol., 2, (1995), 303-308.

[12] S. Saleta, K. Bernd and K. Rolf, J. Clin. Virol., 34, (2005), 233-244.

[13] J. A. G. Briggs and, H. G. Kräusslich, J. Mol. Biol., 410, (2011), 491-500.

[14] E. Chertova, J. W. Bess, B. J. Crise, I. R. Sowder, T. M. Schaden and J. M. Hilburn, J. Virol. 76, (2002), 5315-5325.

[15] P. Zhu, E. Chertova, J. Bess, J. D. Lifson, L. O. Arthur and J. Liu, Proc. Natl Acad. Science, 100, (2003), 15812-15817.

[16] D. E. Ott, Rev. Med. Virol., 18, (2008), 159-175.

[17] B. K. Ganser-Pornillos, M. Yeager and W. Sundquist, Curr. Opin. Struct. Biol., 18, (2008), 203-217.

[18] C. M. Swanson and M. H. Malim, Cell, 133, (2008), 742-746.

[19] J. Wang, Z. W. Xu, S. Liu, R. Y. Zhang, S. L. Ding and X. M. Xie, World J. Gastroenterol., 21, (2015), 954-956.

[20] H. Ebina, N. Misawa, Y. Kanemura and Y. Koyanagi, Science, 339, (2013), 823-826.

[21] A. T. Das, A. Harwig and B. Berkhout, J. Virol., 85, (2011), 9506-9516.

[22] R. Viswanath, X. Wang, T. Ji, D. Krishnakumar, G. Yemmi and H. Indira, J. Mol. Endocrinol., 5, (2016), 1165-1174.

[23] N. D. Pritam, Chem. Bio. Phy. Science, 4, (2014), 1152-1170.

[24] L. A. Kohlstaedt, J. M. Wang, P. A. Friedman and T. A. Steitz, Science, 256, (1992), 1783-1790.

[25] G. S. Stefan, M. Bruno, D. Kalyan, H. Daniel, A. P. Michael, H. Stephen and A. Eddy, J. Mol. Biol., 3, (2009), 693-713.

[26] W. Huang, W. J. Feaver, A. E. Tomkinson and E. C. Friedberg, Mutat. Res., 3, (1998), 183-194.

[27] http://www.psc.edu/science/Madrid/getting a grip on aids.htm.

[28] Z. Peng, L. Xinyong, Z. Junjie, F. Zengjun, L. Zhenyu, P. Christophe and D. C. Erik, Bioorg. Med. Chem., 17, (2009), 5775-5781.

[29] X. Qing, R. Jessica, S. A. Karen and S. Nicolas–Cremer, Protein Sci., 16, (2007), 1728-1737.

[30] W. M. Kati, K. A. Johnson, L. F. Jerva and K. S. Anderson, J. Biol. Chem., 267, (1992), 25988-25997.

[31] J. E. Reardon, Biochem., 31, (1992), 4473-4479.

[32] L. A. Kohlstaedt, J. Wang, J. M. Friedman, P. A. Rice and T. A. Steitz, Sci., 256, (1992), 1783-1790.

[33] J. Ding, K. Das, Y. Hsiou, S. G. Sarafianos, A. D. Clark, M. A Jacobo, C. Tantillo, S. H. Hughes and E. Arnold, J. Mol. Biol., 284, (1998), 1095-1111.

[34] S. Liu, E. A. Abbondanzieri, J. W. Rausch, S. F. Le Grice and X. Zhuang, Science, 322, (2008), 1092-1097.

[35] E. A. Abbondanzieri, G. Bokinsky, J. W. Rausch, J. X. Zhang, S.F. Le Grice and X. Zhuang, Nature, 453, (2008), 184-189.

[36] L. Huang, Y. Kashiwada, L. M. Cosentino, S. Fan, C. H. Chen, A. T. McPhail, T. Fujioka, K. Mihashi, K.H. Lee, J. Med. Chem., 37, (1994) 3947- 3955.

[37] L. Xie, Y. Takeuchi, L. M. Cosentino and K. H. Lee, J. Med. Chem., 42, (1999), 2662- 2672.

[38] D. Yu, A. Brossi, N. Kilgore, C. Wild, G. Allaway and K. H. Lee, Bioorg. Med. Chem. Lett., 13, (2003), 1575- 1576.

[39] A. Rao, J. Balzarini, A. Carbone, A. Chimirri, E. De Clercq, A. M. Monforte, P. Monforte, C. Pannecouque, M. Zappalà Antiviral Res., 63, (2004), 79-84.

[40] K. R. Ravindra, T. Rajkamal and S. B. Katti, Eur. J. Med. Chem., 43, (2008), 2800-2806.

[41] X. H. Ma, X.Y. Zhang, J. J. Tan, W. Z. Chen and C. X. Wang, Acta Pharmacol. Sin., 25, (2004), 950-958.

[42] S. Yu'ning , Z. Peng, K. Dongwei, L. Xiao, T. Ye, L. Zhenyu, C. Xuwang, C. Wenmin, P. Christophe, D. C. Erik, and L. Xinyng, Med. Chem. Commun., 4, (2013), 810-816.

[43] A. Kellett, A. Prisecaru, C. Slator, Z. Molphy and M. McCann, Curr. Med. Chem., 20, (2013), 3134-3151.

[44] A. G. Shadia, S. AmiraAbd El-Alla, H. H. Khaled, A. M. Asmaa -El-Dina, S. Y. Nabil, I. Hoda and E. El-Diwan, J. Med. Chem., 7, (2010), 3035-3046.

[45] H. Lautre, T. Hadda, S. Das and A. Pillai, Curr. Chem. Lett., 4, (2015), 7-20.

[46] G. Sandra–Gallego, M. S. Jesús, A. Eduardo, D. Laura, M. Angeles Muñoz-Fernández, G. Pilar -Sal, M. O. Francesca, G. Rafael and F. Javier de la Mata, Eur. J. Inorg. Chem., 11, (2011), 1657-1665.

[47] Z. Peng, P. Christophe, D. C. Erik and L. Xinyong, J. Med. Chem., 59, (2016), 2849-2878.

[48] L. Cao, W. Song, E. De Clercq, P. Zhan and X. Liu, Curr. Med. Chem., 21, (2014), 1956-1967.

[49] H. S. Teguh and M. Fahimah, Indo. J. Trop. Infect. Disease., 6, (2016), 169-175.

[50] L. Florence, B. Nicole, L. Marie Ledecqa, D. François, B. Zohra, S. Sames, L. René, K. Olivier, M. Ange-Mickalade, D. Ginette – Duponte and R. Michèle-Ravauxb, Biochem. Pharmacol., 63, (2002), 1863-1873.

[51] K. R. Ravindra, T. Rajkamal, S. B. Katti, P. Christophe and D. C. Erik, Eur. J. Med. Chem., 43, (2008), 2800-2806.

Chapter - 7

ANTIBACTERIAL ACTIVITY STUDIES OF SCHIFF BASES AND THEIR Ni(II), Cu(II) AND Zn(II) COMPLEXES

Contents

7.1 Introduction

Schiff bases play an important role in the development of coordination chemistry as they can easily form stable complexes with most of the transition metals [1]. Schiff-base complexes are considered to be among the most important stereo chemical models in main group and transition metal coordination chemistry due to their preparative accessibility and structural variety [2]. One of the major advantage of the transition metal complexes is their medical testing as antibacterial and antitumor agents aiming toward the discovery of an effective and safe therapeutic regimen for the treatment of bacterial infections and cancers [3-4]. There are several biologically active molecules which contain various hetero atoms such as nitrogen, sulphur and oxygen, for perpetuity drawn the attention of chemist over the years mainly because of their biological consequence [5]. Moreover sulfur and nitrogen containing heterocyclic compounds represent an important group of compounds that are promising on practical application

[6-7]. Aminophenol based Schiff base complexes have wide applications in biological field, as antidepressants, antimicrobial, antitumor and also have good catalytic role in many reactions [8].

The main aim of the production and synthesis of any antimicrobial compound is to inhibit the causal microbe without any side effects on the patients. Bacteria can grow in different materials that are in close contact with humans, foods, etc. So, it is very important to control growth of microorganism in order to prevent risk of infections [9]. Biological metal ions play key roles in the structural organization and activation of certain enzymes, which are involved in the transfer of genetic information from DNA, leading to the synthesis of specific proteins [10]. Transition metal complexes have attracted attentions of inorganic, metallo-organic as well as bio-inorganic chemists because of their extensive applications in wide ranging areas from material to biological sciences [11]. Universal distribution of disease causing pathogens terrorizes human health due to microbial resistance. To overcome the alarming problem of microbial resistance to antibiotics, some novel active compounds with high efficacy was developed [12].

In general, the following five principal factors may affect the antimicrobial activity of metal complexes

i. The chelate effect, i.e. bidentate ligands, show higher antimicrobial efficiency than complexes with monodentate ligands.

ii. The nature of the ligands.

iii. The total charge of the complex; generally the antimicrobial efficiency decreases in the order cationic > neutral > anionic complex.

iv. The nature of the counter ion in the case of the ionic complexes.

v. The nuclearity of the metal center in the complex; binuclear centers are more active than mononuclear ones. The antimicrobial activities of metal complexes depended more on the metal center itself than on the geometry around the metal ion [13-15].

In order to appreciate the mechanisms of resistance, the action of antimicrobial agents is very important. Antimicrobial agents act selectively on vital microbial functions with minimal effects or without affecting host functions. Different antimicrobial agents act in different ways. The understanding of these mechanisms as well as the chemical nature of the antimicrobial agents is crucial in the understanding of the ways how resistance against them develops. The mechanism of action of antimicrobial agents can be characterized based on the structure of the bacteria or the function that is affected by the agents. These include generally the following [16-17]:

- Inhibition of the cell wall synthesis
- Inhibition of ribosome function
- Inhibition of nucleic acid synthesis
- Inhibition of folate metabolism
- Inhibition of cell membrane function

Microorganisms were increasingly becoming resistant to ensure their survival against the arsenal of antimicrobial agents to which they were being bombarded. They achieved this through different means but primarily based on the chemical structure of the antimicrobial agent and the mechanisms through which the agents acted.

Metal complexes of Schiff base derived from 2-thiophene carboxaldehyde and 2-aminobenzoic acid (HL) and Fe(III) or Co(II) or Ni(II) or UO_2(II) showed a good antibacterial activity against *Escherichia coli*, *Pseudomonas aeruginosa* and *Staphylococcus pyogenes* [18]. Bibhesh *et al.* have developed a new Schiff base 2-aminophenol-pyrrole-2- carboxaldehyde and its Zn(II), Cd(II), Sn(II) and Pb(II) complexes. The bio-efficacy of the ligand and their complexes has been examined against the growth of bacteria *in vitro* to evaluate their antimicrobial potential. The ligand and complexes exhibited high activity against *E. coli* (100 ppm) and *S. aureus* (100 ppm) bacteria. The zinc complex showed better activity than other metal complexes for both microorganisms [19]. Radhika *et al.* prepared terephthalaldehyde on reaction with 2-aminophenol and 2- aminothiophenol and it yielded a new series of polydentate Schiff's base ligands (H_2La and H_2Lb). They also reported antibacterial activity of these compound [20]. Co(II), Ni(II), Cu(II) and Mn(II) complexes of Schiff bases have been prepared and characterized by Pratibha *et al*. The newly synthesized metal complexes having a composition [M $(LX)_2Y_2$] where M = Co(II), Ni(II), Cu(II) and Mn(II), LX= bidentate ligand (derived from pyridine-2-aldehyde, furfuraldehyde or thiophene-2-carboxaldehyde with vinyl aniline). These Schiff-bases and their metal complexes have been screened for antibacterial and antifungal activity against bacterial species like- *Escherichia coli, Staphylococcus aureus, Klebsiella Psuedomonas* etc as well as fungal species like- *Candida albicans* or *Candida krusei.* All these synthesized compounds exhibited good antimicrobial activity [21].

Nair *et al.* reported antibacterial activity of Schiff base complexes of Co(II), Ni(II), Cu(II) and Zn(II) incorporating indole-3-carboxaldehyde and m-aminobenzoic acid. The order of antibacterial activity of the synthesized

compounds is as follows: Cu(II) > Co(II) > Ni(II) > Zn(II) > Ligand. The higher activity of the metal complexes may be due to the effect of metal ions on the normal cell membrane. Metal chelates bear polar and non polar properties together; this makes them suitable for permeation to the cells and tissues [22].

7.1.1 Bacterial species used for study

The microorganisms used in the present work included -*Bacillus coagulans, Bacillus pumills, Bacillus circulans, Clostridium, Staphylococcus aureus, Entrococcus faecalis, Salmonella typhi, Escherichia coli, Pseudomonas, proteus vulgaris* and *Klebsilla pneumonia.*

Bacillus species are gram positive rods often arranged in pairs or chains with rounded or square ends and usually have a single endospore. The endospores are generally oval or sometimes round or cylindrical and are very resistant to adverse conditions [23]. *Klebsiella pneumoniae* is a bacterium that normally lives inside human intestines, where it doesn't cause disease. However, if *K. pneumoniae* gets into other areas of the body, it can cause a range of different illnesses. These include: pneumonia, bloodstream infections, wound infections, surgical site infections, meningitis, urinary tract infections etc [24]. *Proteus vulgaris* is a rod-shaped, nitrate-reducing, indole and catalase-positive, hydrogen sulfide-producing, gram-negative bacterium that inhabits the intestinal tracts of humans and animals. It can be found in soil, water, and fecal matter. It is grouped with the *Enterobacteriaceae* and is an opportunistic pathogen of humans. It is known to cause wound infections and other species of its genera are known to cause urinary tract infections. *Enterococci* can cause urinary tract, wound, and soft tissue infections [25]. They are also associated with bacteremia which can lead to

endocarditic in previously damaged cardiac valves. E. faecalis is the most frequent species isolated from human intestine samples. *Clostridium difficile* infection (CDI) is a symptomatic infection due to the spore-forming bacterium, *Clostridium difficile*. Symptoms include watery diarrhea, fever, nausea, and abdominal pain [26].

Bacterial of the genus *Salmonella* are capable of causing a large number of human infections, including typhoid fever, systemic infections, septicemia, and gastroenteritis varying clinically from watery diarrhea to dysentery [27]. Typhoid fever is caused by microorganisms Salmonella enterica subspecies enterica serotype typhi (abbreviated as *Salmonella typhi*). The gram-negative rod shaped *Pseudomonas* is facultative anaerobic pathogen and causes lungs infection and other infections associated with urinary tract, and kidneys. *Staphylococcus aureus* is found in soft tissue, skin, endovascular, bone joint, and wound infections. Life-threatening diseases like pneumonia, toxic shock syndrome and sepsis are also caused by *Staphylococcus aureus* along with a number of illnesses as minor skin infections like cellulitis folliculitis and scalded skin syndrome. The gram negative non-sporulating bacterium *Escherichia coli* are frequently found in warm-blooded organisms, especially in the area of lower intestine. Several serotypes are the major cause of bacterial infections including cholecystitis, pneumonia, cholangitis, bacteremia, urinary tract infection (UTI), vomiting, bloody diarrhea and food poisoning but most of them are harmless [28].

This chapter deals with antibacterial studies of heterocyclic Schiff bases and their Ni(II), Cu(II) and Zn(II) complexes.

7.2 Experimental

7.2.1Materials

The bacterial strains used in the study were purchased from NCIM, Pune, India. *Bacillus coagulans* (NCIM 2030), *Bacillus pumills* (NCIM 2189), *Bacillus circulans* (NCIM 2107), *Clostridium* (NCIM 2677), *Staphylococcus aureus* (NCIM 2127), *Entrococcus faecalis, Salmonella typhi* (NCIM 2501), *Escherichia coli* (NCIM 2343), *Pseudomonas* (NCIM 2863), *proteus vulgaris* (NCIM 2027) and *Klebsilla pneumonia* (NCIM 2957) were used for the study. The strains were grown in nutrient broth medium overnight at 37°C and used for assay. All the media used in the study were purchased from Himedia, India. Mueller Hinton agar media was used for well diffusion.

7.2.2 Methods– Antibacterial studies

7.2.2.1 Agar Diffusion method

Synthesized compounds were evaluated for antibacterial activity by agar diffusion method. Test organism was inoculated onto a nutrient agar plate and incubated at 37 °C for 24 h to obtain the primary culture. Several discrete colonies were picked from the culture to make a bacterial suspension (10 mL) in a test tube using saline water. The turbidity of the suspension was compared with 0.5 Mc Farland standards to obtain 10^6-10^8 CFUs. The plates were dried for 15 minutes and then used for the sensitivity test. The discs which had been impregnated with (10 µL) the compounds and were placed on the Mueller-Hinton agar surface. The plate was then incubated at 37 °C for 18 to 24 hours depending on the species of bacteria used in the test. Ampicillin was used as standard antibacterial drug and control solvent respectively. All the tests were performed in triplicates for

those compounds that showed activity of more than 6.5 mm and their activity was recorded as average zone of inhibition [29].

7.2.2.2 Minimum Inhibitory Concentration (MIC)

Resazurin based Microtiter Dilution Assay (RMDA)

The quantitative antimicrobial activity of the test compounds was evaluated using Resazurin based Microtiter Dilution Assay (RMDA). Under aseptic conditions, 96 well microtitre plates (HiMedia) were used for Resazurin based Microtitre Dilution Assay. The first row of microtiter plate was filled with 100 µL of test materials dissolved in sterile water. All the wells of microtitre plates were filled with 50 µL of Luria broth. Two fold serial dilution (throughout the column) was achieved by transferring 50 µL test material from first row to the subsequent wells in the next row of the same column and so that each well has 50 µl of test material in serially descending concentrations. 2 µL of resazurin solution as indicator was added in each well. Finally, a volume of 10 µL was taken from bacterial suspension and then added to each well to achieve a final concentration of 5×10^6 CFU/mL. To avoid the dehydration of bacterial culture, each plate was wrapped loosely with cling film to ensure that bacteria did not become dehydrated. Each microtitre plate had a set of 3 controls: (a) a column with ampicillin as positive control, (b) a column with all solutions with the exception of the test material and (c) a column with all solutions except bacterial solution replaced by 10 µL of Luria broth. The plates were incubated at 37 °C for 24 h. The color change in the well was then observed visually. Any color change observed from purple to pink or colorless was taken as positive. The pink color is due to the formation of resorufin (Figure 1). The lowest concentration of the sample at which no color change occurred

was recorded as the MIC value. All the experiments were performed in triplicates. The average values were calculated for the MIC of test material [30].

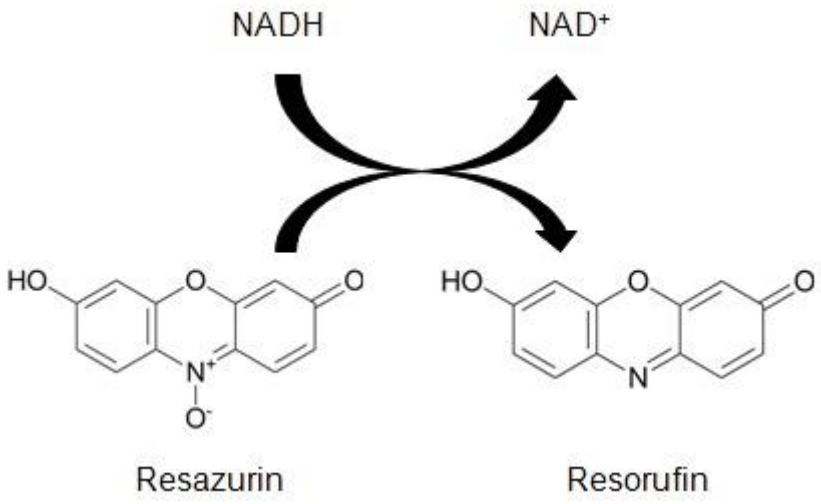

Figure 7. 1 Structure of resazurin substrate and the product pink fluorescent resorufin.

7.3 Results and discussion

The antibacterial activity of synthesized Schiff bases as well as their metal(II) complexes was tested on against gram positive and gram negative microorganisms using disc diffusion method. The microorganisms used in the present investigations included -*Bacillus coagulans, Bacillus pumills, Bacillus circulans, Clostridium, Staphylococcus aureus, Entrococcus faecalis, Salmonella typhi, Escherichia coli, Pseudomonas, proteus vulgaris* and *Klebsilla pneumonia*. Minimum inhibitory concentration (MIC) was evaluated for compounds which showed higher antibacterial activity. *Ampicillin* was used as standard antibiotics. The diameter of zone of inhibition and the MIC results for the Schiff bases and their metal complexes are presented in Tables 7.1-7.2 and Tables 7.3-7.4. Graphical representation of antibacterial activity of synthesized Schiff bases and their

metal complexes against tested organism are shown in Figure 7.2-7.11. Zone of inhibition and MIC of all compounds is illustrated in Figure 7-12-7.13. The Schiff base TA shows moderate activity on the bacteria *Salmonella typhi, Bacillus coagulans, Bacillus pumills, Clostridium;* good activity against *Bacillus circulans* and no activity against *Escherichia coli, Pseudomonas* and *Klebsilla pneumonia.* Schiff bases TNA and PNA did not exhibit any significant effect against these bacterial strains. Compound PA shows good or fairly good activity against *Salmonella typhi, Bacillus coagulans, Bacillus pumills, Pseudomonas* and did not show activity against *Escherichia coli, Bacillus circulans, Clostridium* and *Klebsilla pneumonia.* The compounds TMA and PMA show activity only against *Entrococcus faecali, Salmonella typhi* and *Escherichia coli*.

$[Ni(TA)_2(H_2O)_2]$ shows good activity against *Bacillus circulans* and moderate activity against *Bacillus pumills, Clostridium* and *Entrococcus faecalis.* $[Ni(TNA)_2(H_2O)_2]\cdot 2H_2O$ shows moderate activity only against *Clostridium* and inactive against all other tested organism. $[Ni(TMA)_2]\cdot 3H_2O$ exhibited activity against *Escherichia coli, Bacillus circulans and Entrococcus faecalis.* $[Ni(PA)_2]\cdot H_2O$ did not show any antibacterial activity. $[Ni(PNA)_2]\cdot 2H_2O$ is active against *Bacillus coagulans, Bacillus pumills, Bacillus circulans and Entrococcus faecali.* $[Ni(PMA)_2]$ showed activity against *Salmonella typhi, Entrococcus faecalis* and *Escherichia coli.*

$[Cu(TA)_2H_2O]\cdot H_2O$ exhibited higher activity against *Bacillus circulans* and moderate activity against *Bacillus coagulans, Bacillus pumills, Pseudomonas* and *Entrococcus faecalis.* $[Cu(TNA)_2]\cdot 2H_2O$ showed moderate activity against *Bacillus coagulans, Bacillus pumills, Bacillus circulans, Clostridium, Salmonella typhi, Pseudomonas* and *Staphylococcus aureus.* $[Cu(TMA)_2]\cdot H_2O$ showed fairly good activity against *Bacillus coagulans,*

Bacillus pumills, Bacillus circulans, Clostridium, Entrococcus faecali, Escherichia coli, proteus vulgaris, Pseudomonas, and *Staphylococcus aureus.* $[Cu(PA)_2H_2O]\cdot 2H_2O$ inactive against *Entrococcus faecali, Escherichia coli, proteus vulgaris* and *Staphylococcus aureus* and active against all other tested bacteria. $[Cu(PNA)_2]\cdot 3H_2O$ exhibited activity against *Bacillus coagulans, Bacillus pumills, Bacillus circulans* and *Entrococcus faecali.* $[Cu(PMA)_2]\cdot H_2O$ active against *Salmonella typhi, Bacillus coagulans, Bacillus circulans, proteus vulgaris, Entrococcus faecalis* and *Escherichia coli.*

$[Zn(TA)_2]$ showed higher activity against *Bacillus circulans,* moderate activity against *Bacillus pumills, Pseudomonas, Clostridium* and inactive against *Salmonella typhi, Bacillus coagulan, Entrococcus faecali, Escherichia coli, Klebsilla pneumonia, proteus vulgaris, Staphylococcus aureus.* $[Zn(TNA)_2]$ exhibited mild activity against *Salmonella typhi, Bacillus pumills, Entrococcus faecalis* and *Staphylococcus aureus.* $[Zn(TMA)_2]$ active against *Bacillus coagulans, Bacillus pumills, Bacillus circulans, Staphylococcus aureus, Entrococcus faecalis, Salmonella typhi, Escherichia coli and proteus vulgaris*. $[Zn(PA)_2]$ exhibited activity against *Bacillus coagulans, Bacillus pumills, Bacillus circulans, Staphylococcus aureus, Entrococcus faecalis, Salmonella typhi and Escherichia coli.* $[Zn(PNA)_2]$ showed mild activity against *Bacillus pumills, Entrococcus faecalis* and inactive against all other tested bacterial species. $[Zn(PMA)_2]$ active against *Bacillus coagulans, Bacillus pumills, Bacillus circulans, Staphylococcus aureus, Entrococcus faecalis, Salmonella typhi Escherichia coli* and inactive against *Staphylococcus aureus, Klebsilla pneumonia, Clostridium, Pseudomonas.*

Table 7.1 Antibacterial activities of Schiff bases TA, TNA, TMA and their metal complexes

	COMPOUNDS											
Bacteria	**TA**	**Ni**	**Cu**	**Zn**	**TNA**	**Ni**	**Cu**	**Zn**	**TMA**	**Ni**	**Cu**	**Zn**
Salmonella typhi[b]	08	-	-	-	-	-	08	07	09	-	-	10
Bacillus coagulans[a]	08	-	09	-	-	-	09	-	-	-	13	13
Bacillus pumills[a]	07	08	09	12	-	-	08	07	-	-	12	11
Escherichia coli[b]	-	-	-	-	-	-	-	-	10	12	12	11
Bacillus circulans[a]	16	22	19	17	-	-	10	-	-	10	14	12
Pseudomonas[b]	-	-	09	07	-	-	09	08	-	-	-	-
Clostridium[a]	08	12	-	11	-	07	10	-	-	-	-	-
Klebsilla pneumonia[b]	-	-	-	-	-	-	-	-	-	-	-	-
Entrococcus faecali[a]	07	08	08	-	-	-	-	-	14	15	16	13
proteus vulgaris[b]	-	-	-	-	-	-	-	-	-	-	13	11
Staphylococcus aureus[a]	-	-	-	-	-	-	07	07	-	-	12	10

'–' No activity.
a - Gram positive bacteria
b - Gram negative bacteria

Table 7.2 Antibacterial activities of Schiff bases PA, PNA, PMA and their metal complexes

	COMPOUNDS											
Bacteria	**PA**	**Ni**	**Cu**	**Zn**	**PNA**	**Ni**	**Cu**	**Zn**	**PMA**	**Ni**	**Cu**	**Zn**
Salmonella typhi[b]	17	-	-	18	-	-	-	-	09	10	10	11
Bacillus coagulans[a]	12	-	13	13	-	08	09	-	-	-	11	10
Bacillus pumills[a]	12	-	14	13	-	09	09	07	-	-	-	11
Escherichia coli[b]	-	-	-	11	-	-	-	-	10	11	11	10
Bacillus circulans[a]	-	-	18	11	-	08	08	-	11	-	12	11
Pseudomonas[b]	09	-	10	-	-	-	-	08	-	-	-	-
Clostridium[a]	-	-	11	-	-	-	-	-	-	-	-	-
Klebsilla pneumonia[b]	-	-	08	-	-	-	-	-	-	-	-	-
Entrococcus faecali[a]	-	-	-	20	-	07	08	07	12	16	12	16
proteus vulgaris[b]	07	-	-	15	-	-	-	-	-	-	11	10
Staphylococcus aureus[a]	-	-	-	-	-	-	-		-	-	-	-

'–' No activity.
a - Gram positive bacteria
b - Gram negative bacteria.

Table 7.3 MIC values (mg/mL) for the Schiff bases TA, TNA, TMA and their metal complexes

	COMPOUNDS												
Bacteria	**TA**	**Ni**	**Cu**	**Zn**	**TNA**	**Ni**	**Cu**	**Zn**	**TMA**	**Ni**	**Cu**	**Zn**	**Ampiciline**
Salmonella typhi[b]	0.04	-	-	-	-	-	0.08	0.16	0.17	-	-	0.03	0.05
Bacillus coagulans[a]	0.08	-	0.04	-	-	-	-	-	-	-	0.08	0.08	0.10
Bacillus pumills[a]	-	0.16	0.16	0.09	-	-	0.08	0.08	-	-	0.05	0.08	0.10
Bacillus circulans[a]	0.04	0.02	0.02	0.02	-	-	0.08	-	-	-	0.08	0.16	0.05
Pseudomonas[b]	-	-	0.16	-	-	-	0.16	-	-	-	-	-	-
Clostridium[a]	-	0.16	-	0.08	-	-	0.08	-	-	-	-	-	-
Entrococcus faecali	-	-	-	-	-	-	-	-	0.08	0.04	0.05	0.05	-
proteus vulgaris	-	-	-	-	-	-	-	-	-	-	0.03	0.03	0.05

Table 7.4 MIC values (mg/mL) for the Schiff bases PA, PNA, PMA and their metal complexes.

	COMPOUNDS											
Bacteria	**PA**	**Ni**	**Cu**	**Zn**	**PNA**	**Ni**	**Cu**	**Zn**	**PMA**	**Ni**	**Cu**	**Zn**
Salmonella typhi[b]	0.02	-	-	0.01	-	-	-	-	0.01	0.02	0.02	0.05
Bacillus coagulans[a]	0.04	-	0.01	0.01	-	0.16	0.08	-	-	-	0.16	0.16
Bacillus pumills[a]	0.08	-	0.02	0.02	-	0.08	0.08	-	-	-	-	0.08
Escherichia coli[b]	-	-	-	0.16	-	-	-	-	0.16	0.08	0.08	0.08
Bacillus circulans[a]	-	-	0.01	0.06	-	-	-	-	0.16	-	0.08	0.08
Pseudomonas[b]	0.16	-	0.08	-	-	-	-	-	-	-	-	-
Clostridium[a]	-	-	0.16	-	-	-	-	-	-	-	-	-
Entrococcus aecali[a]	-	-	-	0.01	-	-	-	-	0.16	0.04	0.08	0.04
proteus vulgaris[b]	-	-	-	0.04	-	-	-	-	-	-	0.03	0.03

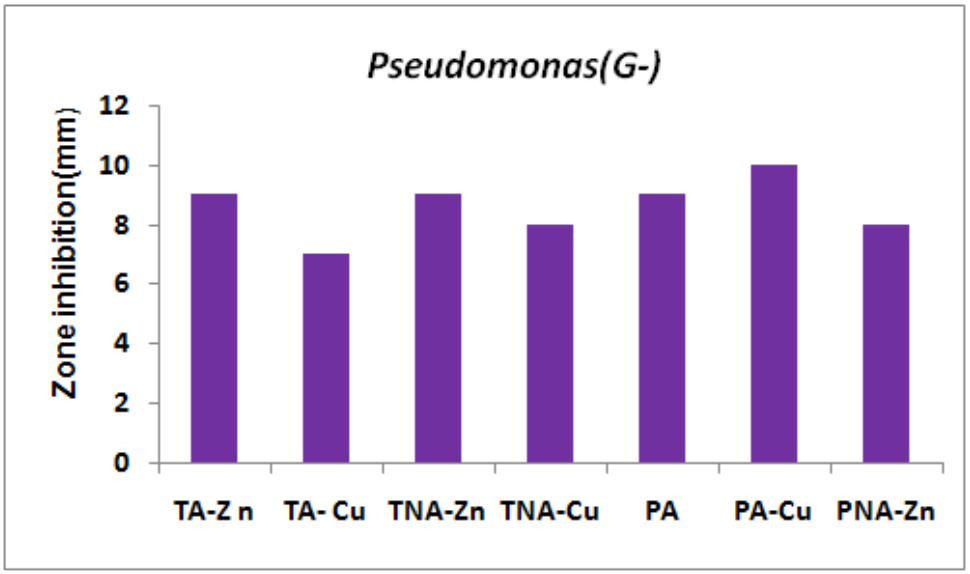

Figure 7.2 Graphical representation of the antibacterial activity of compounds against *Pseudomonas.*

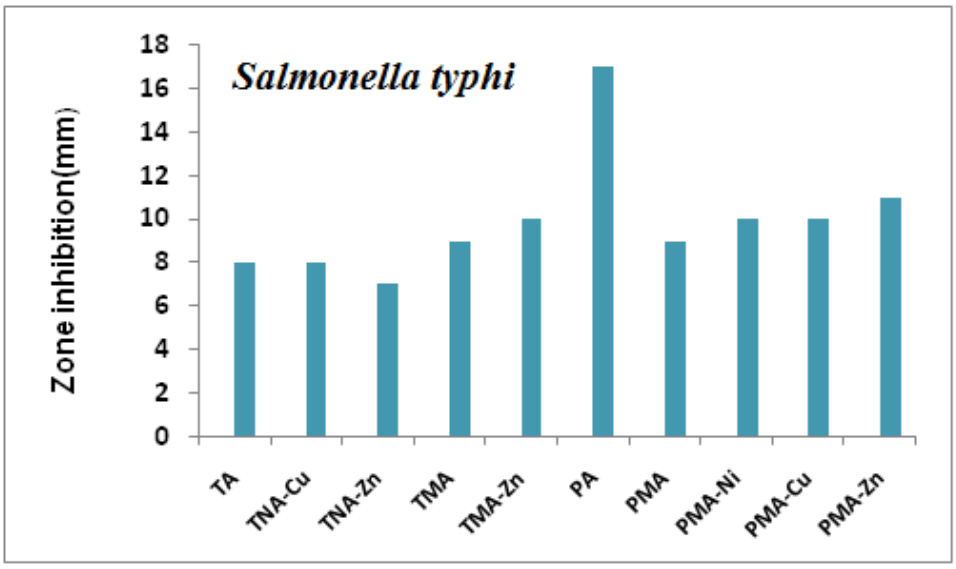

Figure 7.3 Graphical representation of the antibacterial activity of compounds against *Salmonella typhi.*

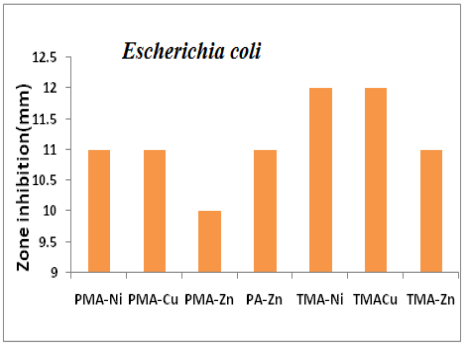

Figure 7.4 Graphical representation of the antibacterial activity of compounds against *Escherichia coli*

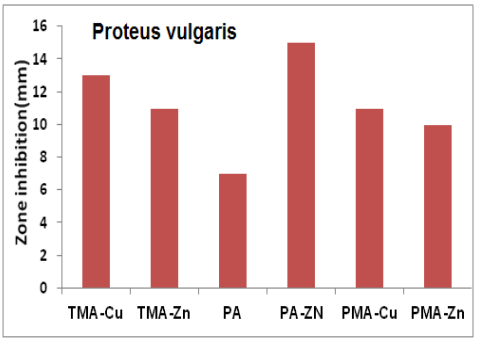

Figure 7.5 Graphical representation of the antibacterial activity of compounds against *Proteus vulgaris.*

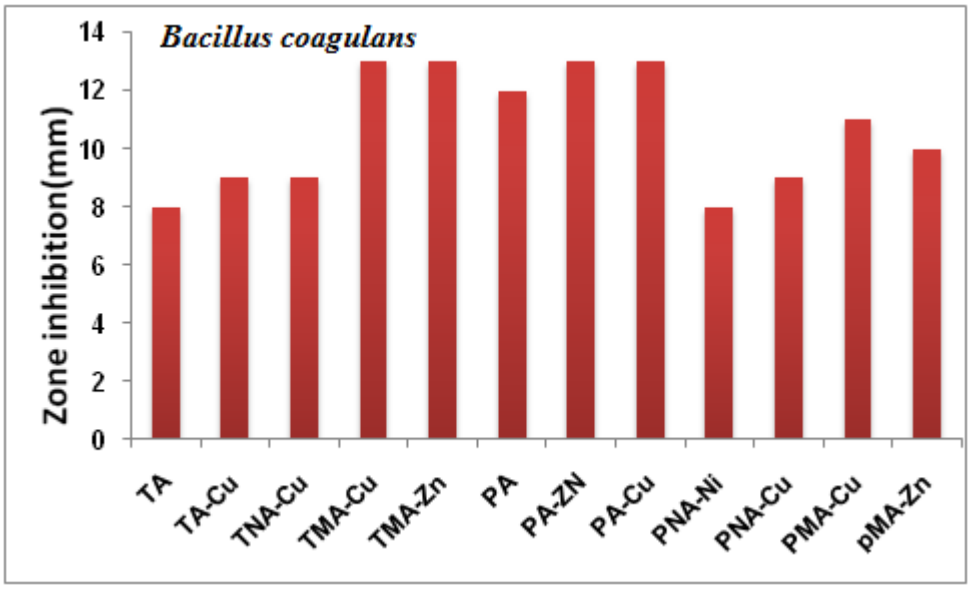

Figure 7.6 Graphical representation of the antibacterial activity of compounds against *Bacillus coagulans.*

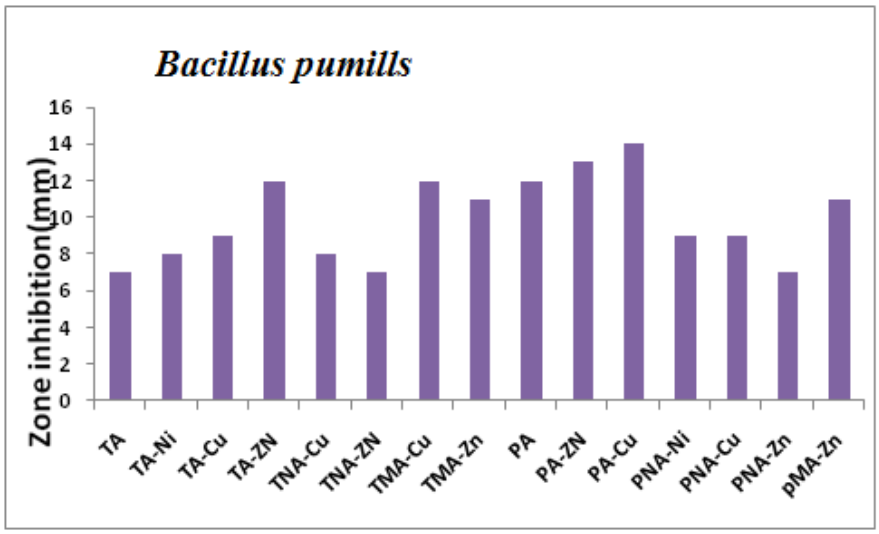

Figure 7.7 Graphical representation of the antibacterial activity of compounds against *Bacillus pumills.*

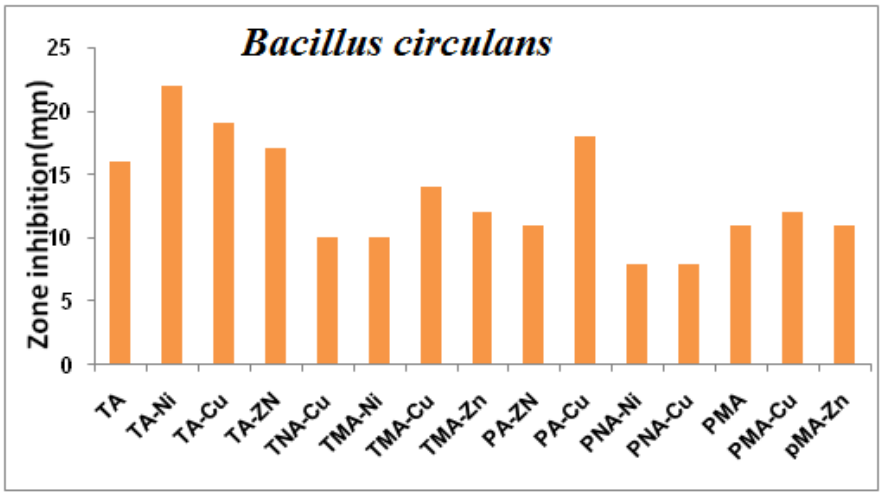

Figure 7.8 Graphical representation of the antibacterial activity of compounds against *Bacillus circulans.*

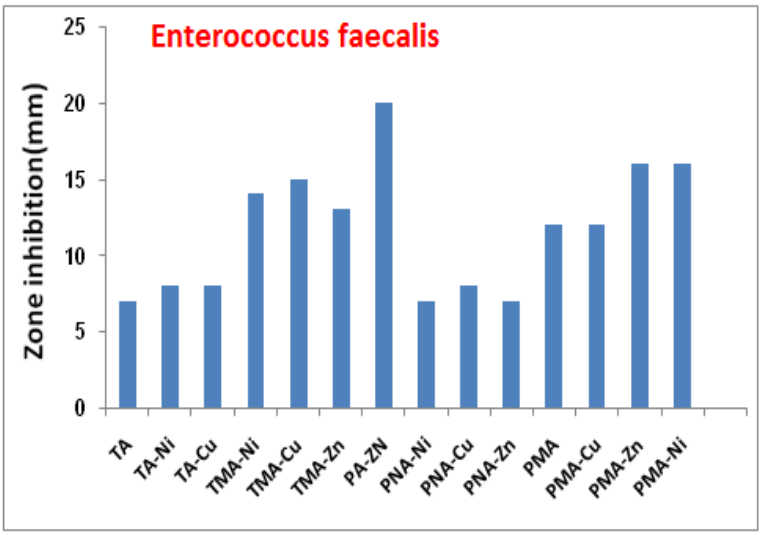

Figure 7.9 Graphical representation of the antibacterial activity of compounds against *Enterococcus faecalis.*

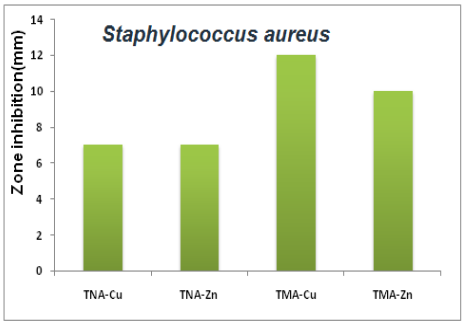

Figure 7.10 Graphical representation of the antibacterial activity of compounds against *Staphylococcus aureus*

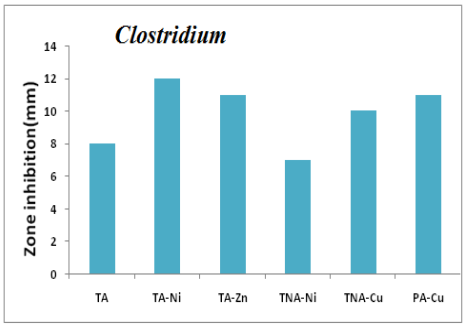

Figure 7.11 Graphical representation of the antibacterial activity of compounds against *Clostridium.*

The results shows that Ni(II), Cu(II) and Zn(II) metal complexes are more active than the free ligands. The higher activity of the metal complexes may be due to the effect of metal ions on the normal cell membrane and also due to the lipophilic nature of the metal ions in complexes [31].

The variation in the activity of different metal complexes against tested micro organisms depends on either the impermeability of cells of the microbes or difference in ribosomes of microbial cells [32]. The higher biological activity of metal complexes than that of the ligands can be explained on the basis of Overtone's concept and Tweedy's chelation theory [33]. On chelation, metal ion polarity is reduced to a greater extent due to the overlapping of the ligand orbital and partial sharing of positive charge of metal ion with donor groups [34]. Further, the delocalization of the π-electrons is increased over the whole chelate sphere and enhances the lipophilicity of the complex. The lipophilic nature of the central metal atom is also increased upon chelation, which subsequently favors the permeation through the lipid layer of cell membrane [35]. The normal cell process may be affected by the formation of hydrogen bond through the azomethine nitrogen atom with the active centers of cell constituents leading to interference with the cell wall synthesis [36]. There are other factors which also increase the activity is solubility, conductivity and bond length between the metal and ligand [37]. The difference in antimicrobial activity is due to the nature of metal ions and also the cell membrane of the microorganisms. It may be concluded that antibacterial activity of the compounds is related to cell wall structure of the bacteria. It is possible because the cell wall is essential to the survival of many bacteria and some antibiotics are able to kill bacteria by inhibiting a step in the synthesis of peptidoglycan [38].

Compared to gram positive bacteria, Schiff bases and its metal complexes showed moderate activity against the gram negative bacteria. This can be explained by considering the effect on lipopolysaccharide (LPS), a major component of the surface of gram negative bacteria [39]. LPS is an important entity in determining the outer membrane barrier function and the virulence of gram negative pathogens. The Schiff base can penetrate the bacterial cell membrane by coordination of metal ion through oxygen or nitrogen donor atom to LPS which leads to the damage of outer cell membrane and consequently inhibits growth of the bacteria [40].

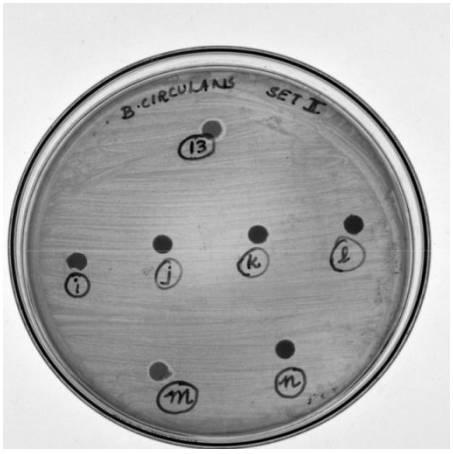
B·CIRCULANS SET I
13
i
j
k
l
m
n

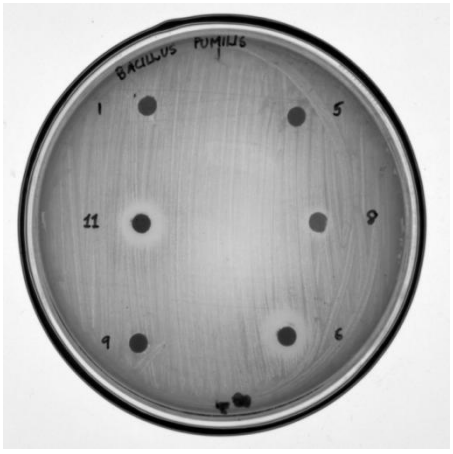
BACILLUS PUMILIS
1
5
11
9
9
6

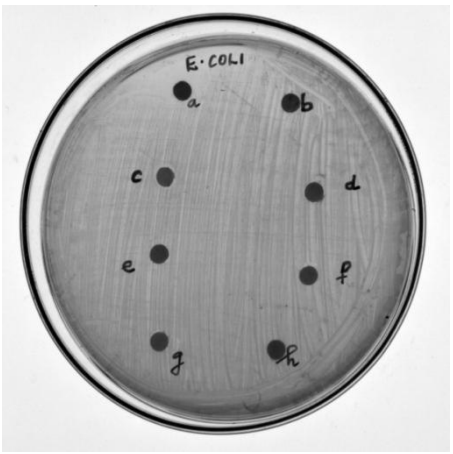
E·COLI
a
b
c
d
e
f
g
h

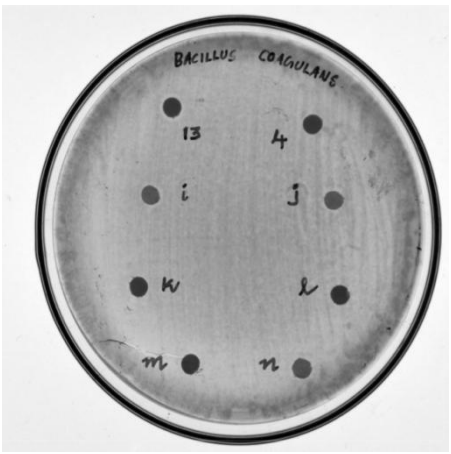
BACILLUS COAGULANS
13
4
i
j
k
l
m
n

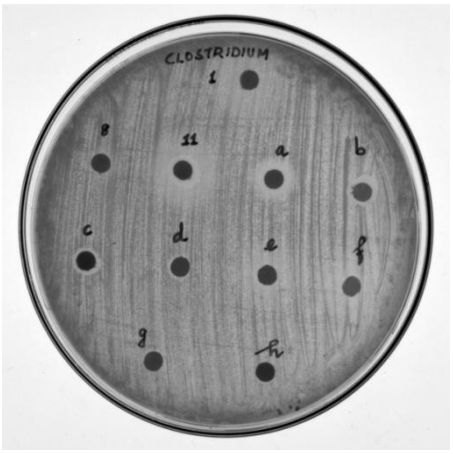
CLOSTRIDIUM
1
8
11
a
b
c
d
e
f
g
h

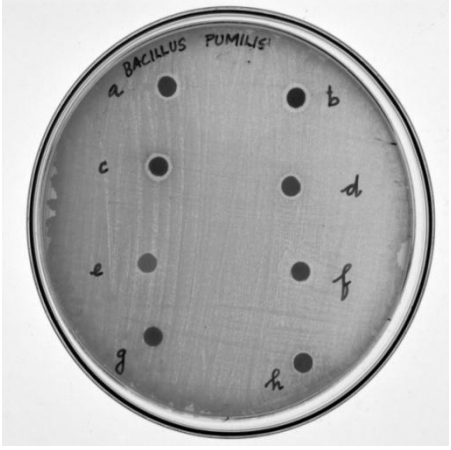
BACILLUS PUMILIS
a
b
c
d
e
f
g
h

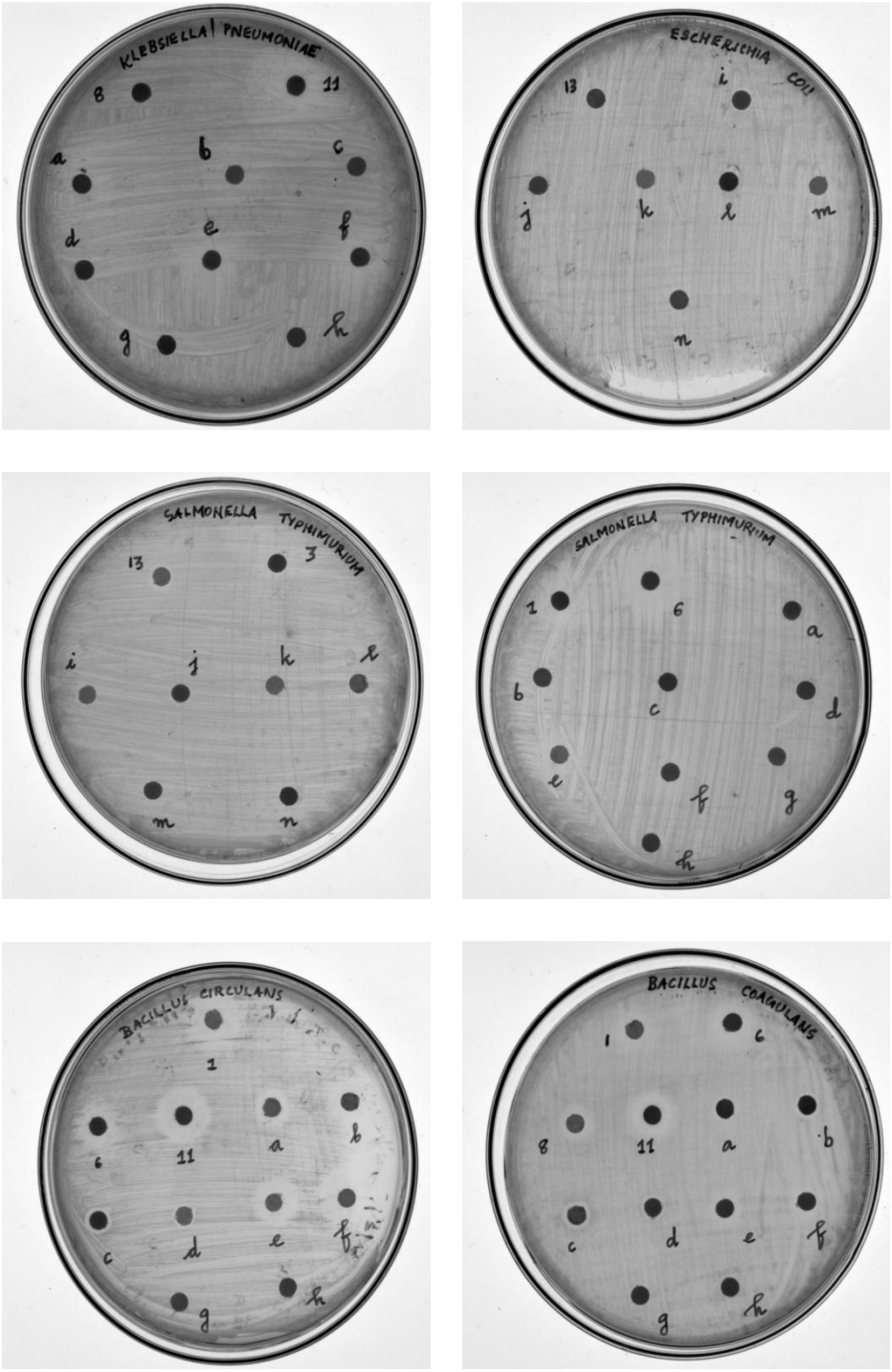
KLEBSIELLA PNEUMONIAE
8
11
a
b
c
d
e
f
g
h
ESCHERICHIA COLI
13
i
j
k
l
m
n
SALMONELLA TYPHIMURIUM
13
3
i
j
k
l
m
n
SALMONELLA TYPHIMURIUM
1
6
a
b
c
d
e
f
g
h
BACILLUS CIRCULANS
1
6
11
a
b
c
d
e
f
g
h
BACILLUS COAGULANS
1
c
8
11
a
b
c
d
e
f
g
h

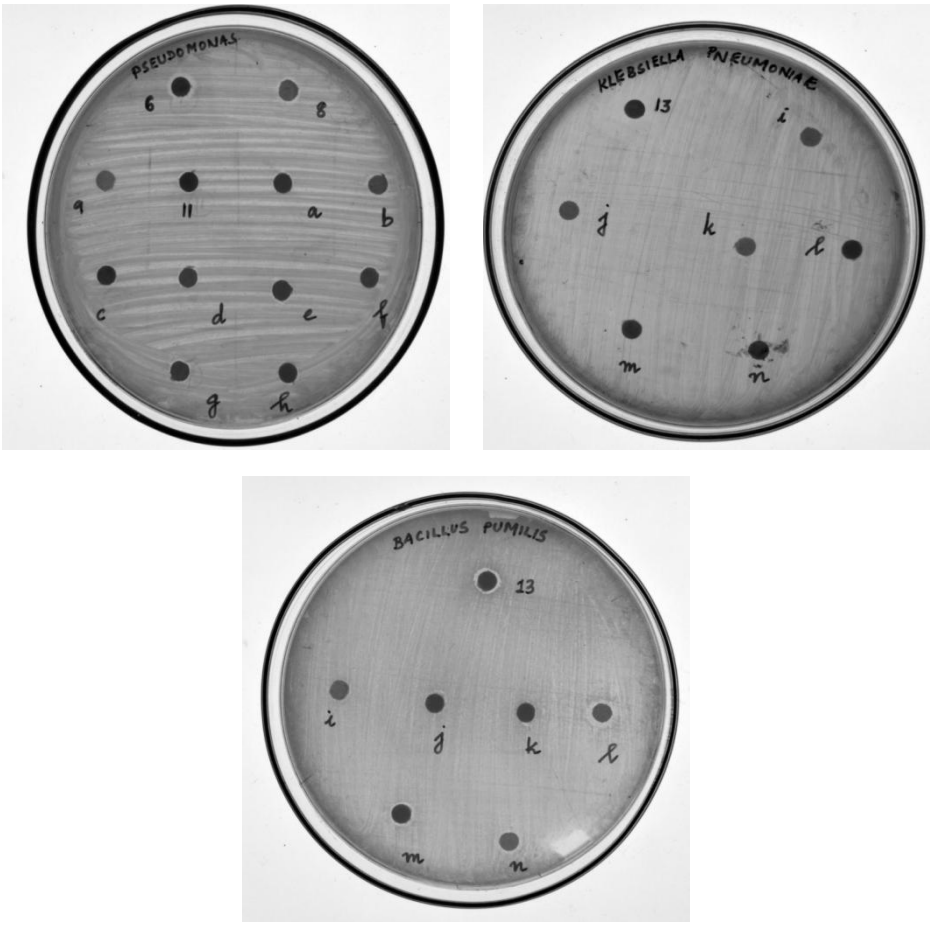

Figure 7.12 Antibiogram of TA, TNA, PA, PNA and their Ni(II), Cu(II), Zn(II) complexes.

1 = TA,	f = $[Ni(TA)_2(H_2O)_2]$,	a = $[Cu(TA)_2H_2O]\cdot H_2O$,	I = $[Zn(TA)_2]$
2 = TNA,	j = $[Ni(TNA)_2(H_2O)_2]\cdot 2H_2O$,	c = $[Cu(TNA)_2]\cdot 2H_2O$,	9 = $[Zn(TNA)_2]$
6 = PA,	n = $[Ni(PA)_2]\cdot H_2O$,	b = $[Cu(PA)_2H_2O]\cdot 2H_2O$,	10 = $[Zn(PA)_2]$
5 = PNA,	g = $[Ni(PNA)_2]\cdot 2H_2O$	d = $[Cu(PNA)_2]\cdot 3H_2O$	h = $[Zn(PNA)_2]$

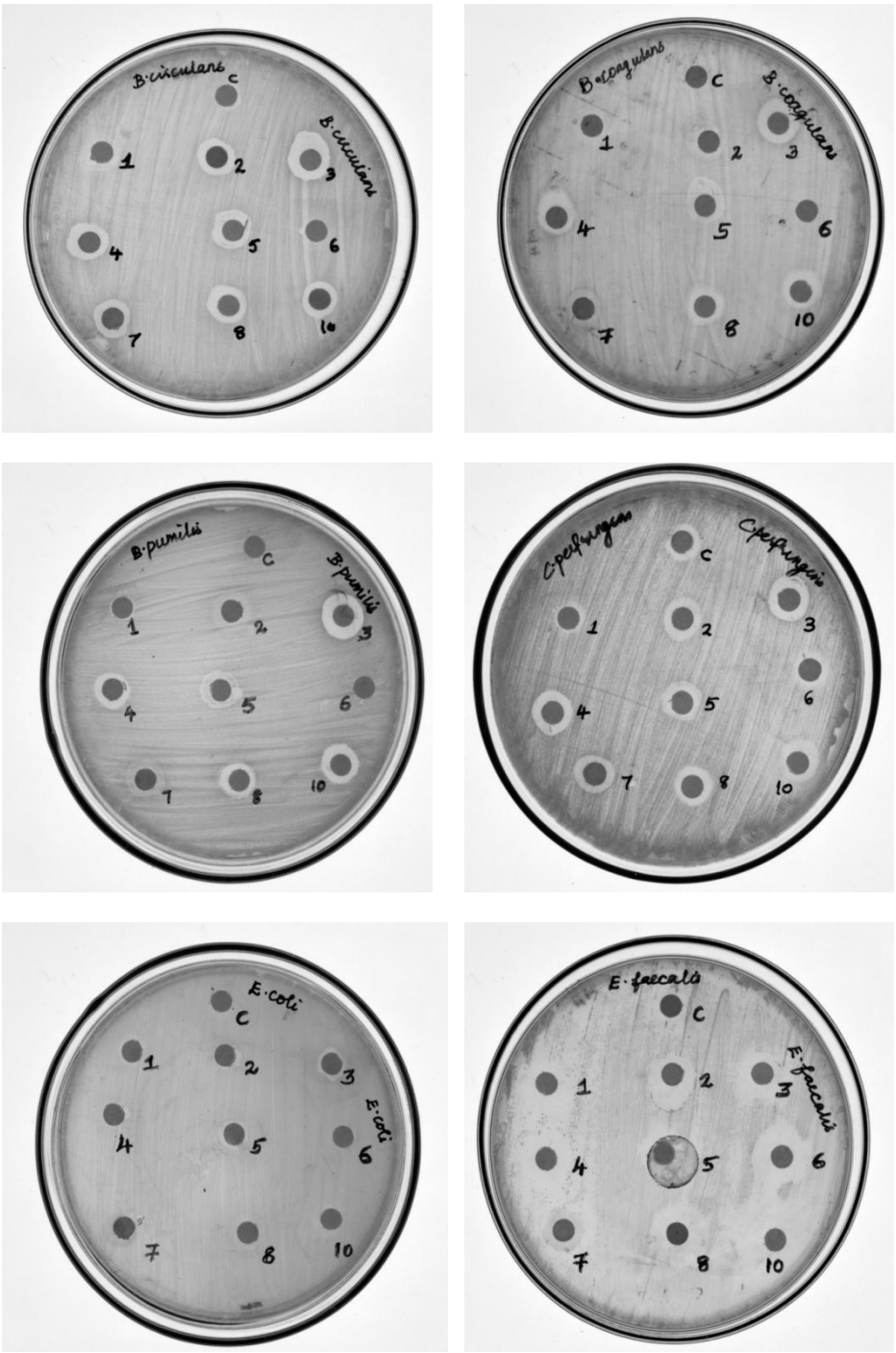
B.circulans
C
1
2
3
4
5
6
7
8
10
B.coagulans
B.pumilis
C.perfringens
E.coli
E.faecalis

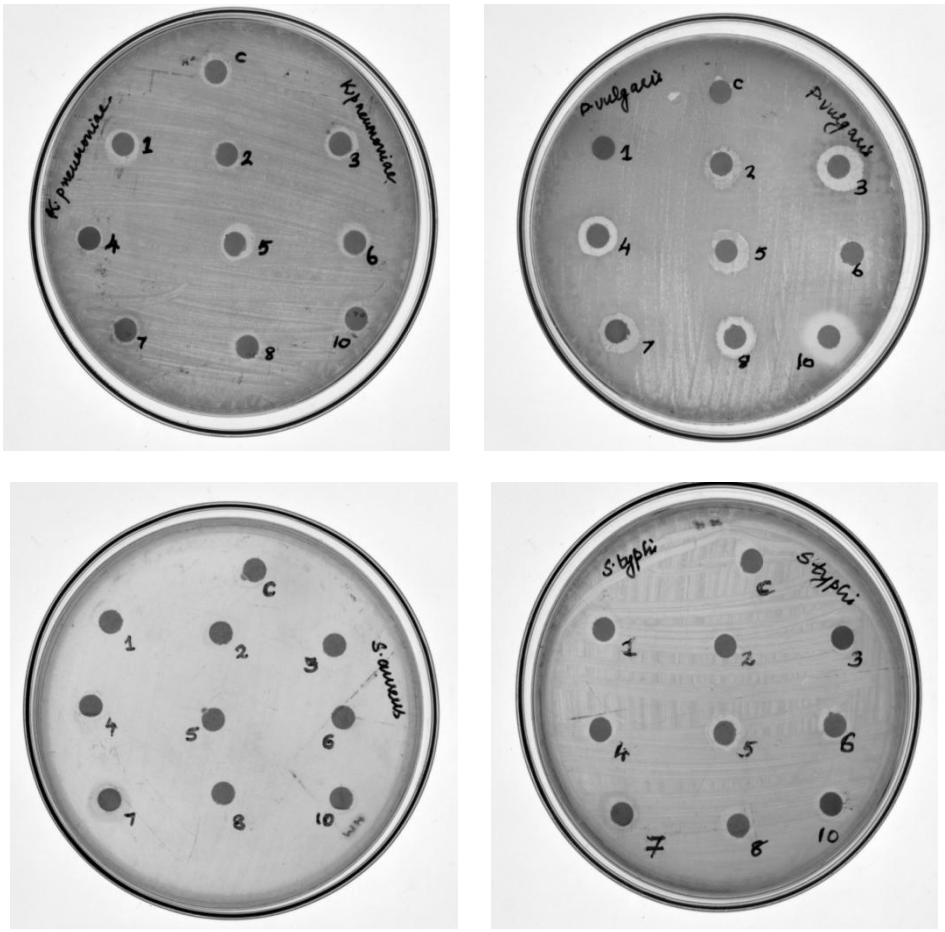

Figure 7.13 Antibiogram of TMA, PMA and their Ni (II), Cu (II), Zn (II) complexes.

1 = TMA, 2 = $[Ni(TMA)_2]\cdot 3H_2O$, 3 = $[Cu(TMA)_2]\cdot H_2O$, 4 =$[Zn(TMA)_2]$
5 = PMA, 6 = $[Ni(PMA)_2]$, 7 = $[Cu(PMA)_2]\cdot H_2O$, 8 = $[Zn(PMA)_2]$
10 = $[Zn(PA)_2]$, c = $[Cu(TNA)_2]\cdot 2H_2O$

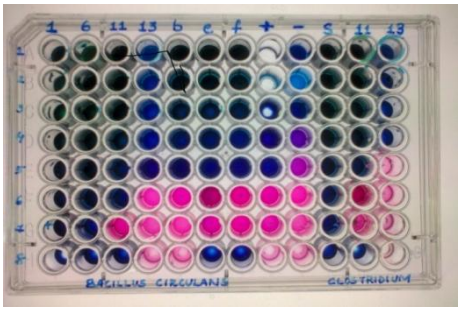
BACILLUS CIRCULANS
CLOSTRIDIUM


BACILLUS CIRCULANS
CLOSTRIDIUM

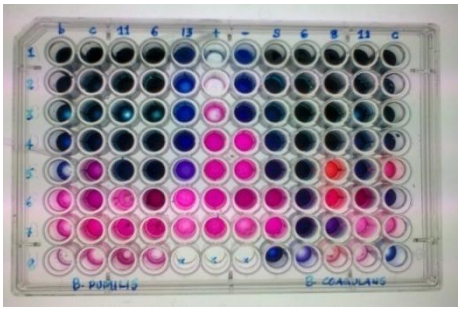
B. PUMILIS
B. COAGULANS

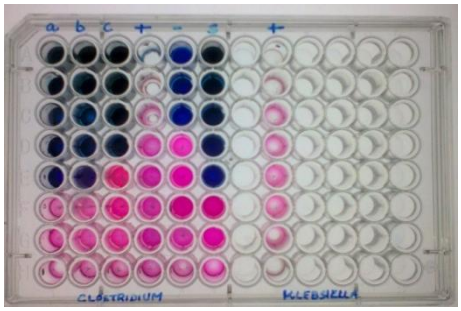
CLOSTRIDIUM
KLEBSIELLA

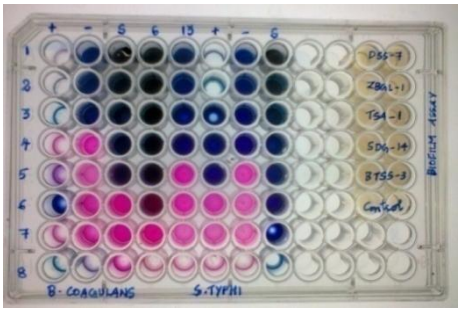
B. COAGULANS
S. TYPHI
BIOFILM ASSAY


B. Coagulans
Staphi
S. aureus

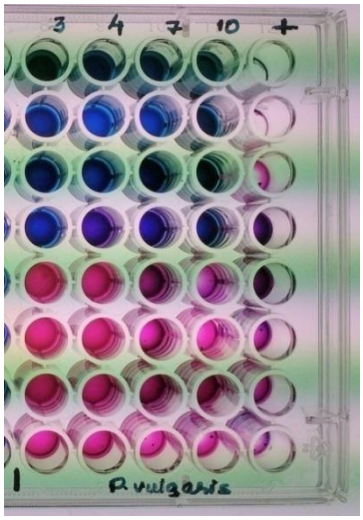
P. vulgaris

7.4 Conclusion

The antibacterial activity of synthesized Schiff bases as well as their metal complexes was tested against gram positive and gram negative bacteria using disc diffusion method. The quantitative antimicrobial activity of the test compounds was evaluated using resazurin based microtiter dilution assay. Ampicillin was used as standard antibiotics. Schiff bases and their metal complexes individually exhibited varying degrees of inhibitory effects on the growth of the tested bacterial species. Metal complexes exhibited higher antimicrobial activity than the free ligands. Antibacterial activity difference is due to the nature of metal ions and also the cell membrane of the microorganisms.

References

[1] N. K. Chaudhary, World J. Pha. Pha. Sci., 2, (2013), 6016-6025.

[2] H. Keypour, M. Rezaeivala, L. Valencia, P. Perez-Lourido and H. R. Khavasi, Polyhedron, 28, (2009), 3755-3758.

[3] R. Mahalakshmi and N. Raman, Int. J. Curr. Pharm. Res., 8, (2016), 1-6.

[4] R. E. Mewis and S. J. Archibald, Coord. Chem. Rev., 254, (2010), 1686-712.

[5] A. S. Patil, H. V. Naika, D. A. Kulkarnia and S. P. Badami, Spectrochim. Acta Mol. Biomol. Spectrosc., 75, (2010), 347-354.

[6] B. S. Holla, B. Veerendra, M. K. Shivananda and B. Poojary, Eur. J. Med. Chem., 38, (2003), 759-767.

[7] J. Wu, X. Liu, X. Cheng, X, Y. Cao, D. Wang, Z. Li, W. Xu, C. Pannecouque, M. Witvrouw and E. DeClercq, Molecules, 12, (2007), 2003-2016.

[8] M. H. Abu-Shawish, M. S. Saadeh, K. Hartani and M. H. Dalloul, J. Iran. Chem. Soc., 6, (2009), 729-737.

[9] S. Malladi, A. M. Isloor, I. Shrikrishna, D. S. Akhila and F. Hoong-Kun, Arab. J. Chem., 6, (2013), 335-340.

[10] C. Sridevi, J. Mol. Biol., 4, (2015), 363-366.

[11] G. G. Mohamed, M. A. Zayed and S. M. Abdallah, J. Mol. Struct., 979, (2010), 62-71.

[12] M. D. Lazimo, A. Luayen, B. Z. Birol and M. Bedrettin, Int. J. Drug Dev. & Res., 2, (2010), 102-107.

[13] J. V. Holtje, Microbiol. Mol. Biol., 62, (1998), 181-203.

[14] O. Espeli and K. J. Marians, Mol. Microbiol., 52, (2004), 925-931.

[15] K. Drlicaand and M. Snyder, J. Mol. Biol., 120, (1978), 145-154.

[16] A. S. Said, A. E. Amr, H. A. El-Sayed, M. A. Al-Omar and M. M. Abdalla, Int. J. Pharm., 11, (2015), 502-507.

[17] G. G. Mohamed, M. M. Omar and A. M. M. Hindy, Spectrochim. Acta, Part A., 62, (2005), 1140-1150.

[18] K. S. Bibhesh, A. Prakash, K. R. Hemant, N. Bhojak and D. Adhikari, 76, (2010), 376-383.

[19] P. Radhika, M. B. Ummathur and K. Krishnankutty, Arch. Appl. Sci. Res., 4, (2012), 2223-2227.

[20] M. Pratibha, J. Sunil, P. Vatsala, V. Uma, Int. J. Chem.Tech. Research., 1, (2009), 225-232.

[21] M. N. Uddin, D. A. Chowdhury, R. Moniruzzman H. Ershad, Mod. Chem., 2, (2014), 6-14.

[22] M.S. Nair, D. Arish and R. S. Joseyphus, J. Saud. Chem. Soc., 16, (2012), 83-88.

[23] E. C. Nannin and B. E. Murray, Principles and Practice of Clinical Bacteriology ed. 2nd, John Wiley & Sons, U.K., (2006).

[24] L. M. Teixeira, Carvalho, Maria da Gloria Siqueira and R. R. Facklam, Manual of Clinical Microbiology, ed. 9th, Government of Canada (2007).

[25] D. A. Leffler and J. T. Lamont, N. Engl. J. Med., 372, (2015), 1539-48.

[26] A. T. Utami, P. Bogi and Noorhamdan, J. Med. Surg. Pathol., 7, (2008), 10-14.

[27] M. Aslam, I. Anis, N. Afza, H. Ajaz, I. Lubna, I. Jamshed, I. Zaitoon, S. Iqbal, A. Hanif Chaudhry and N. Muhammad, Int. J. Curr. Pharm. Res., 4, (2012), 42-46.

[28] M. Aslam, I. Anis, N. Afza, M. T. Hussain, Rashadmehmood, A. Hussain, S. Yousuf, L. Iqbal, S. Iqbal and Inamullah Khan, J. Chil. Chem. Soc., 58, (2013), 1867-1871.

[29] E. A. Elzahany, K. H. Hegab, S. K. H. Khalil, N. S. Youssef, Aust J. Basic and Appl. Sci., 2, (2008), 210-222.

[30] K. Shanker, R. Rohini, V. Ravinder, P. M. Reddy and Y. P. Ho, Spectrochim. Acta Mol. Biomol. Spectrosc., 73, (2009), 205-211.

[31] A. Juan, P. Yaricruz, B. Alina and C. Juan, Med. Chem., 6, (2016), 467-473.

[32] C. Sridevi, J. Med. Biol. Eng. 4, (2015), 363-365.

[33] S. Syed Tajudeen and K. Geetha, I. J. A. C. S., 4, (2016), 40-48.

[34] P. Ejidike and P.A. Ajibade, Molecules, 20, (2015), 9788-9802.

[35] A. M. Abu-Dief, M. A. Ibrahim and Mohamed beni-suef, J. Basic Appl. Sci., 4, (2015), 119-133.

[36] M. Shoaib, G. Rahman, S. W. Ali Shah and M. Naveed Umar, J. Pharmacol., 10, (2015), 332-336.

[37] M. Alias, H. Kassum and C. Shakir, J. Assn. Arab. Univ. Basic Appl. Scien., 15, (2014), 28-34.

[38] G. G. Mohamed, M. A. Zayed and S. M. Abdallah., J. Mol. Struct., 979, (2010), 62-71.

[39] S. S. Tajudeen and K. Geetha, Indian. J. Adv. Chem. Sci., 4, (2016), 40-48.

[40] W. M. Al Momani, Z. A.Taha, A. M.Ajlouni, Q. M.Abu Shaqra and M. Al Zouby, Asian Pac. J. Trop. Biomed., 3, (2013), 367-370.

Chapter 8

α- AMYLASE ACTIVITY STUDIES OF HETEROCYCLIC SCHIFF BASES AND THEIR Ni(II), Cu(II) AND Zn(II) COMPLEXES

Contents

8.1 Introduction

Diabetes Mellitus (DM) is a pathological condition, characterized by hyperglycemia due to relative or absolute deficiency of insulin, and associated with severe physiological imbalances [1]. DM is classified as either insulin-dependent type 1 or non-insulin-dependent type 2, by the World Health Organization [2]. Insulin-dependent DM is characterized by the absence of insulin synthesis and secretion in the pancreas. Pathogenic processes involved in the development of diabetes are destruction of the β cells of the pancreas due to inadequate insulin secretion and/or diminished tissue responses to insulin at one or more points in the complex pathways of hormone action. Deficient supply of insulin causes abnormalities in carbohydrate, fat, and protein metabolism and these results in disability and premature cell death [3]. Therefore a therapeutic approach to treat diabetes is to decrease postprandial hyperglycemia. This can be achieved by the inhibition of carbohydrate hydrolyzing enzymes like α-amylase.

Amylases are one of the important hydrolase enzymes. Amylase can be classified into three types: α-amylase, β-amylase, and γ-amylase [4]. Among amylases, α-amylase is important due to its wide range of applications in the medicinal and industrial field. α-amylase is the major form of amylase found in humans and other mammals. Amylase enzymes randomly cleave internal glycosidic linkages in starch molecules to hydrolyze them and yield dextrins and oligosaccharides. α-amylase belongs to endo-amylases family, which catalyze the initial hydrolysis of starch into shorter oligosaccharides through the cleavage of α-D-(1-4) glycosidic bonds [5]. The products of α-amylase action are oligosaccharides with varying length with an α-configuration and α-limit dextrins which constitute a mixture of maltose, maltotriose, and branched oligosaccharides of 6–8 glucose units that contain both α-1,4 and α-1,6 linkages [6-7]. The structure of α-amylase is three-dimensional and is capable of binding to substrate. The human α-amylase is a classical calcium-containing enzyme [8].

8.1.1 Importance of α-amylase enzyme in human body

α-amylase catalyses the first stage in the metabolism of starch, a main source of carbohydrate in the human diet. Within the human body, amylase is found in two primary places and they are classified into two types (salivary amylase and pancreatic amylase) according to where they are found. Salivary amylase is a component obtained when saliva breaks starch into glucose and dextrin. It hydrolyzes the bonds between long-chain polysaccharides found in food, breaking compounds such as glycogen and starch into their useful monomers, glucose and maltose. Pancreatic amylase is added to the small intestine to further digest starches; amylase is denatured in the acidic stomach. Amylase is also present in blood where it digests dead white blood cells [9].

Amylases have a wide range of application in the industrial field due to its starch hydrolyzing properties. They can be used in food, textile, fermentation, detergent, paper, and pharmaceutical industries. Bacterial and fungal amylases could be potentially used in the pharmaceutical and fine-chemical industries. However, with the advances in biotechnology, the amylase application has expanded in several fields such as medicinal, clinical, and analytical chemistry [10-12].

Schiff bases and their metal complexes play a key role in modifying the pharmacological properties of known drugs. The imine group of Schiff base ligands leads to various biological activities including antidiabetic, antitumor, antibacterial, antifungal and herbicidal activities. Upon coordination to metal atom, all these activities are found to be enhanced [13]. There are many reported works on insulin-mimetic activity, α-glucosidase and α-amylase inhibition with different co-ordination of different ligands with transition metals. A number of transitional and other metal compounds like chromium, manganese, molybdenum, copper, cobalt, zinc, tungsten and vanadium have been proposed as possible adjuncts in the treatment of diabetes mellitus *in vitro* and *in vivo* [14-15]. Vanco *et al.* reported in vivo antidiabetic activity of Cu(II) and Zn(II) complexes derived from N-salicylidene-β-alanine [16]. Kannan *et al.* reported enzyme inhibition effects of N_2O_2 Schiff base Zn complex. This complex showed strong inhibition towards α-amylase and α-glucosidase with an IC_{50} value of 0.18 and 0.23 µg. The inhibition mechanism was analyzed with Lineweaver– Burk and Dixon plots. Mode of inhibition of zinc complex is found to be non competitive [17].

Two mixed-ligand complexes, [Cu(L)(2imi)](1) and [Ni(L)(2imi)]·MeOH (2) [L=2-(((5-chloro-2-oxyphenyl)imino)methyl) phenolato) and 2imi = 2-methyl

imidazole], have been prepared by the reaction of appropriate metal salts with H_2L and 2-methyl imidazole. α- amylase activities of these compounds have also been investigated by Yousef *et al*. The experimental data showed that α-amylase was inhibited by Ni(II) complex and Cu(II) complex. The reciprocal plot related to the reversible inhibitory effect of inhibitor showed mixed inhibition patterns [18].

8.2 Experimental

8.2.1 Materials

All reagents used were of analytical grade. Dinitrosalicylic acid (DNS) was purchased from Sigma Aldrich. α-amylase procured from Hi-media chemicals. The materials used for the preparation of Schiff bases and their metal complexes are presented in Chapter 2.

8.2.2 Method

8.2.2.1 α-amylase inhibition assay

α -amylase inhibitory activity was determined by dinitrosalicylic acid (DNS) method as reported earlier with slight modification [19]. The total assay mixture composed of 500 µL of 0.5 mg/mL amylase (in 0.05 M sodium phosphate buffer (pH = 6.9) and test compounds (at different concentrations of 50-200 µM) was incubated at 37 °C for 10 min. After pre-incubation 500 µL of 1% starch solution from the above buffer was added to each tube and again incubated at 37 °C for 15 min. The reaction was stopped by adding 1.0 mL DNS reagent. The test tubes were then incubated in a boiling water bath for 5 min and cooled to room temperature. The reaction mixture was then diluted by adding 10 mL of distilled water and the absorbance was measured at 540 nm. The control amylase represented 100% enzyme activity and did

not contain sample. Acarbose was used as a standard inhibitor and it was assayed at above mentioned test sample concentrations. The maltose liberated was determined with the help of standard maltose curve and the activities were calculated according to the following equation [20]

$$\text{Activity} = \frac{\text{Conc. of maltose liberated x enzyme used in mL}}{\text{Mol. Wt. of maltose x time}(\text{min}) \text{ x dilution factor}}$$

The IC_{50} values were determined from plots of percent inhibition versus log inhibitor concentration and were calculated by non linear regression analysis from the mean inhibitory values. For IC_{50} values the above procedure was used with different concentration of test samples (50 µM - 200 µM). All tests were performed in triplicate. The % inhibition was calculated according to the formula [21].

$$\% \text{ Inhibition} = \frac{\text{Abs } 540(\text{control}) - \text{Abs } 540(\text{sample})}{\text{Abs } 540(\text{control})} \text{X} 100$$

8.2.2.2 Kinetics of inhibition

The mode of inhibition of α-amylase by the samples was determined by Michaelis-menten and Lineweaver– Burk plots. For study, 200 µL of the sample was incubated with 0.5mg/mL α-amylase. Concentration of starch (substrate) was varied from 0.2 to 5 mg/mL. The mixture was then incubated for 10 min at 37°C and then boiled for 5 min after the addition of 1.0 mL of DNS to stop the reaction. The amount of reducing sugars released was determined spectrophotometrically using a maltose standard curve and converted to reaction velocities. A double reciprocal plot (1/V versus 1/[S]) where V is reaction velocity and [S] is substrate concentration was plotted and the type (mode) of inhibition of the samples on α-amylase activity was determined [22].

8.3 Results and discussion

α-amylase activity of the synthesized compounds was evaluated *in vitro* by amylase inhibition assay using DNSA method. The results of the α-amylase activity studies of ligands and their Ni(II), Cu(II) and Zn(II) complexes are given in Table 8.1-8.4. In the case of synthesized compounds, Schiff base TMA, PMA and their nickel and copper complexes shows amylase inhibition activity. These compounds showed lower amylase inhibition activity than that of standard amylase inhibitor acarbose (IC_{50} value - 0.13 µM). In the action media, salvation behavior of synthesized compounds and acarbose are different. This may be a reason why Schiff bases TMA, PMA and their nickel and copper complexes showed lesser amylase inhibition activity compared to that of acarbose [23]. All other Schiff bases, TA, TNA, PA, PNA and their nickel, copper and zinc complexes have induced the amylase activity. Zinc complexes of TMA and PMA also enhance α-amylase activity. Amylase inhibition of TMA is 49.9% and that of PMA is 53.5% at 200 µM. Amylase inhibition increases when these ligands are complexed with nickel and copper. In each case, concentration of maltose liberated is shown in Table 8.1.-8.4.

Table 8.1 α- amylase inhibitory activity of heterocyclic Schiff base ligands (200 µM)

Compound	OD at 540 nm	Conc.of Maltose liberated (mg)	Activity (µmoles/mL/min)	% Activity	% Inhibition
Control	0.2068	0.140	0.0013	100.0	0.00
TA	0.3456	0.235	0.0022	167.9	-67.9
TNA	0.3501	0.240	0.0022	171.5	-71.5
TMA	0.1034	0.070	0.0006	50.0	49.9
PA	0.3891	0.270	0.0025	192.9	-92.9
PNA	0.3654	0.253	0.0023	180.8	-80.8
PMA	0.0956	0.065	0.0006	46.4	53.6

Table 8.2 α- amylase inhibitory activity of Ni(II) complexes (200 µM)

Compound	OD at 540 nm	Conc.of Maltose liberated (mg)	Activity (µmoles/mL/min)	% Activity	% Inhibition
Control	0.2068	0.140	0.0013	100.0	0.0
$[Ni(TA)_2(H_2O)_2]$	0.3671	0.260	0.0024	185.8	-85.8
$[Ni(TNA)_2(H_2O)_2]\cdot 2H_2O$	0.2625	0.180	0.0017	128.6	-28.6
$[Ni(TMA)_2]\cdot 3H_2O$	0.1234	0.045	0.0004	32.2	67.9
$[Ni(PA)_2]\cdot H_2O$	0.3794	0.267	0.0025	190.8	-90.8
$[Ni(PNA)_2]\cdot 2H_2O$	0.3080	0.210	0.0019	150.0	-50.0
$[Ni(PMA)_2]$	0.0904	0.063	0.0006	45.3	54.7

Table 8.3 α- amylase inhibitory activity of Cu(II) complexes (200 µM)

Compound	OD at 540 nm	Conc.of Maltose liberated (mg)	Activity (µmoles/mL/min)	% Activity	% Inhibition
Control	0.2068	0.140	0.0013	100.0	0.0
$[Cu(TA)_2H_2O]\cdot H_2O$	0.3768	0.260	0.0024	185.8	-85.8
$[Cu(TNA)_2]\cdot 2H_2O$	0.3866	0.270	0.0025	192.9	-92.9
$[Cu(TMA)_2]\cdot H_2O$	0.1167	0.053	0.0005	37.9	62.1
$[Cu(PA)_2H_2O]\cdot 2H_2O$	0.3321	0.230	0.0021	164.3	-64.3
$[Cu(PNA)_2]\cdot 3H_2O$	0.2760	0.190	0.0018	135.8	-35.8
$[Cu(PMA)_2]\cdot H_2O$	0.0956	0.063	0.0006	45.0	54.9

Table 8.4 α- amylase inhibitory activity of Zn(II) complexes (200 µM)

Compound	OD at 540 nm	Conc. of Maltose liberated (mg)	Activity (µmoles/mL/min)	% Activity	% Inhibition
Control	0.2068	0.140	0.0013	100.0	0.0
$[Zn(TA)_2]$	0.2964	0.210	0.0019	150.3	-50.0
$[Zn(TNA)_2]$	0.2878	0.205	0.0019	146.5	-46.6
$[Zn(TMA)_2]$	0.3301	0.219	0.0020	156.5	-56.5
$[Zn(PA)_2]$	0.2354	0.169	0.0016	120.7	-20.7
$[Zn(PNA)_2]$	0.3960	0.276	0.0026	197.9	-97.1
$[Zn(PMA)_2]$	0.3767	0.260	0.0024	185.8	-85.8

IC_{50} values of those compounds which show inhibition were also determined. IC_{50} values of TMA, PMA and their nickel and copper complexes are depicted in Table 8.5. Lower IC_{50} value indicated greater inhibition activity. Inhibition of enzymes such as α-amylase involved in the hydrolysis of carbohydrates has been exploited as a therapeutic approach for controlling postprandial hyperglycemia [24]. The inhibition activity of α-amylase was extended and might be responsible for decreasing the rate of glucose absorption and concentration of postprandial serum glucose [25]. This effect would delay the degradation of starch and oligosaccharides, which would in turn cause a decrease in the absorption of glucose and consequently inhibit the increase in postprandial blood glucose. In the human species, α-amylase is present in both salivary and pancreatic secretions. This enzyme is responsible for cleaving large malto-oligosaccharides to maltose.

Table 8.5 IC_{50} (μM) values of Schiff bases and their metal complexes

Compound	IC_{50} (μM)
TMA	91.38
$[Ni(TMA)_2]\cdot 3H_2O$	88.89
$[Cu(TMA)_2]\cdot H_2O$	90.45
PMA	95.50
$[Ni(PMA)_2]$	87.18
$[Cu(PMA)_2]\cdot H_2O$	91.38
Acarbose	0.13

8.3.1 Mode of inhibition

Kinetic studies were carried out to identify the mode of inhibition of TMA, PMA and their metal complexes (nickel and copper) using Michaelis-menten and Lineweaver-Burk plot. Figures 8.1- 8.6 shows that in all these cases, the straight lines intercept at a single point in the second quadrant. This indicates that all these compounds inhibit α-amylase enzyme non

competitively. The non competitive mode of inhibition obtained from the Lineweaver-Burk plot points to the fact that the active components in TMA, PMA and their nickel and copper complexes do not compete with the substrate for binding to the active site rather the inhibitors bind to a separate site on the enzyme to retard the conversion of disaccharides to monosaccharides [26]. Kinetic parameters: Michaelis-Menten constant (K_m) and the maximum reaction velocity (V_{max}) for TMA, PMA and their nickel and copper complexes are presented in Tables 8.6 and 8.7. In all these compounds V_{max} decreases but K_m remained the same.

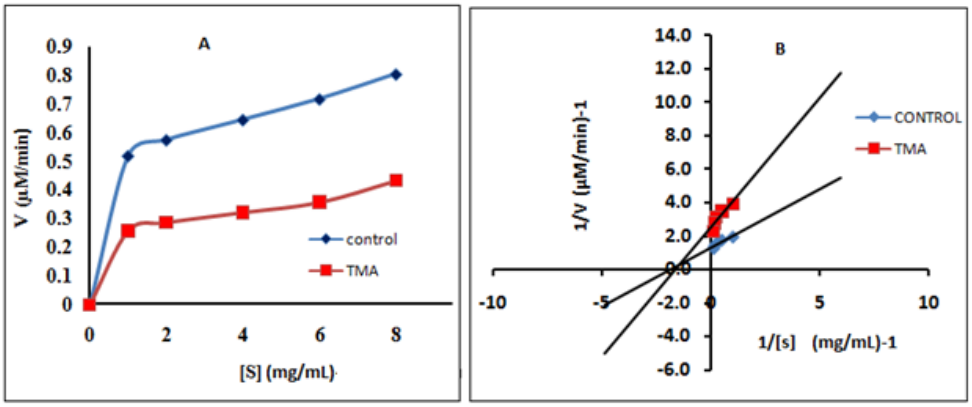

Figure 8.1 Mode of inhibition of α-amylase by TMA (A) Michaelis-Menten plot and (B) Lineweaver-Burk plot.

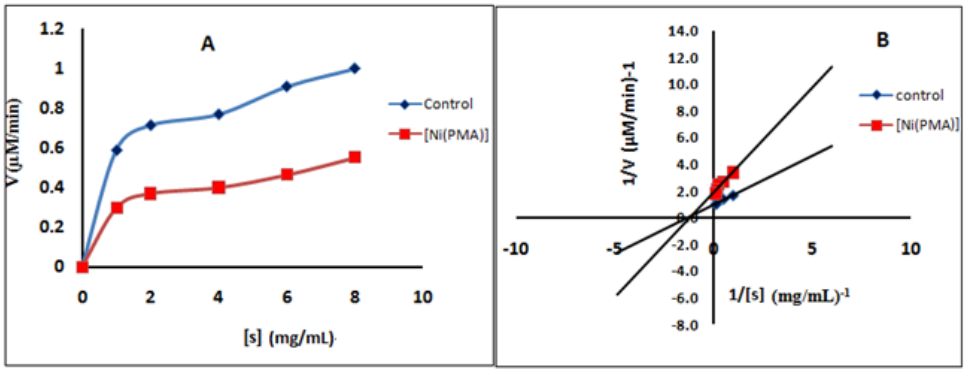

Figure 8.2 Mode of inhibition of α-amylase by $[Ni(TMA)_2]\cdot 3H_2O$ (A) Michaelis-Menten plot and (B) Lineweaver-Burk plot

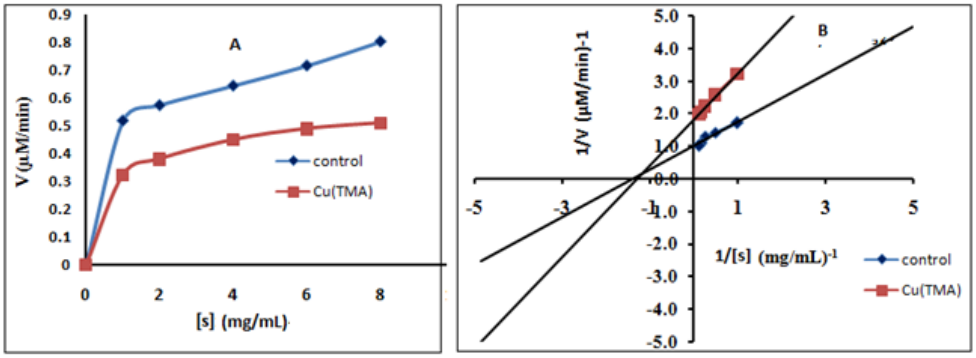

Figure 8.3 Mode of inhibition of α-amylase by $[Cu(TMA)_2]\cdot H_2O$ (A) Michaelis-Menten plot and (B) Lineweaver-Burk plot.

Table 8.6 Kinetic parameters K_m and V_{max} for Schiff base TMA and its complexes

Compound	K_M	V_{Max}
Control	0.6022	0.7788
TMA	0.6203	0.4014
Control	0.7012	0.9970
$[Ni(TMA)_2]\cdot 3H_2O$	0.7220	0.4297
Control	0.7279	0.9991
$[Cu(TMA)_2]\cdot H_2O$	0.7228	0.5509

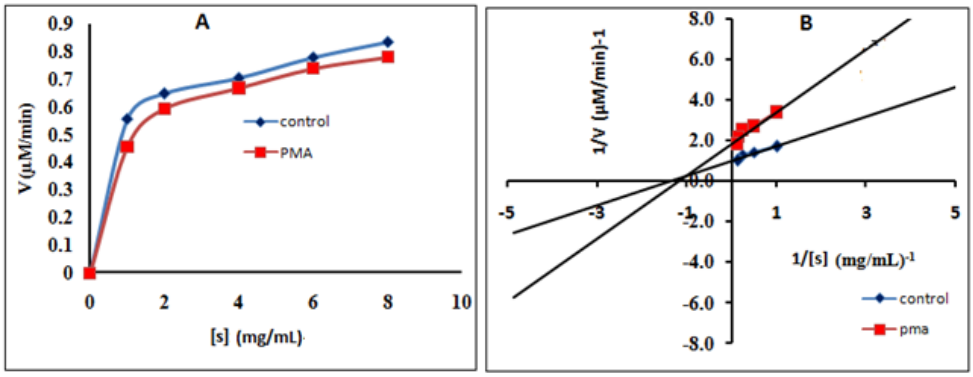

Figure 8.4 Mode of inhibition of α-amylase by PMA (A) Michaelis-Menten plot and (B) Lineweaver-Burk plot.

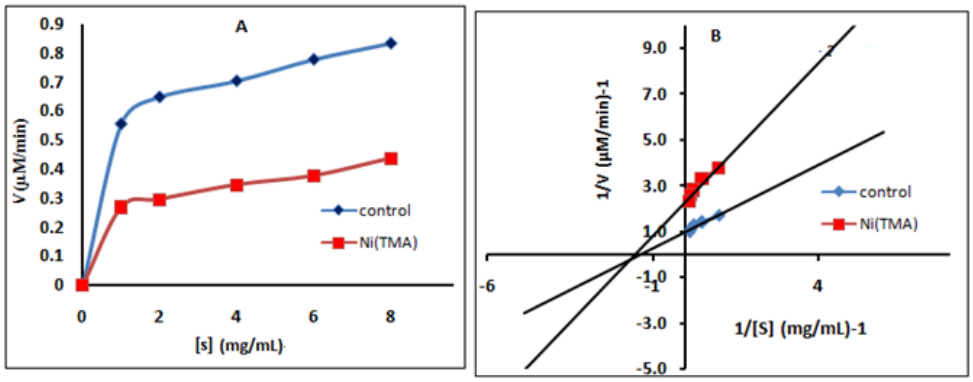

Figure 8.5 Mode of inhibition of α-amylase by $[Ni(PMA)_2]$ (A) Michaelis-Menten plot and (B) Lineweaver-Burk plot.

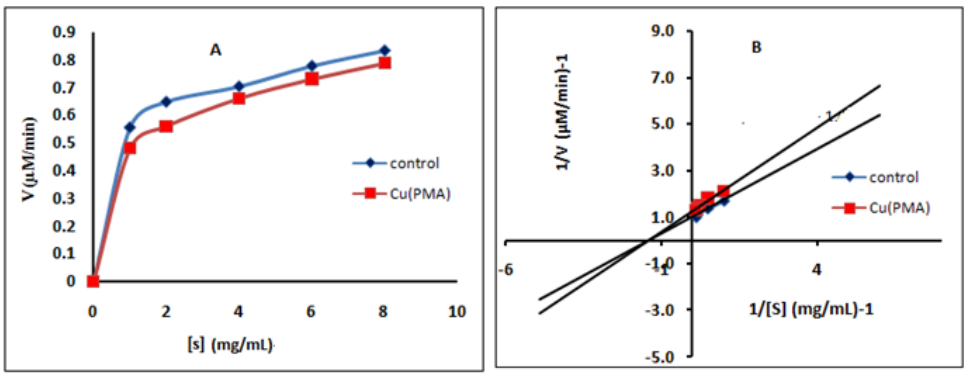

Figure 8.6 Mode of inhibition of α-amylase by $[Cu(PMA)_2]\cdot H_2O$ (A) Michaelis-Menten plot and (B) Lineweaver-Burk plot.

Table 8.7 Kinetic parameters K_m and V_{max} for Schiff base PMA and its complexes

Compound	K_m	V_m
Control	0.7342	0.9970
PMA	0.7228	0.5347
Control	0.7396	0.9991
$[Ni(PMA)_2]$	0.7278	0.5362
Control	0.7413	0.9970
$[Cu(PMA)_2]\cdot H_2O$	0.7379	0.7098

8.4 Conclusion

α-amylase inhibition activity of synthesized compounds has been studied by DNS method. Ligands TA, TNA, PA, PNA and their Ni(II), Cu(II) and Zn(II) complexes have enhanced α-amylase activity. Ligands TMA, PMA and their Ni(II), Cu(II) complexes exhibited inhibition of α-amylase. IC_{50} values of these compounds were also calculated. Results indicate that these compounds showed lesser amylase inhibition activity than that of standard acarbose. Kinetic studies were carried out to identify the mode of inhibition using Michaelis- Menten and Lineweaver-Burk plot. Results showed that ligands TMA, PMA and their Ni(II), Cu(II) complexes inhibit α-amylase non competitively**.**

References

[1] G. Kumar, D. Kumar, S. Devi, R. Verma and R Johari, Int. J. Eng. Sci. Technol., 3, (2011), 1630-1635.

[2] S. J. Folley and A. L. Greenbaum, Br. Med. Bull.,16, (1960), 228-232.

[3] American Diabetes Association (ADA), Diabetes Care, 27, (2004), 94-102.

[4] S. Ajita, P. Thirupathihalli and M. Krishna, J. Appli. Environ. Microbiol., 2, (2014), 166-175.

[5] G. D. Brayer, Y. Luo and S. G. Withers, Protein Sci., 4, (1995), 1730-1742.

[6] M. J. Van der Maarel, B. Van der Veen, J. C. Uitdehaag, H. Leemhuis and L. Dijkhuizen, J. Biotechnol., 94, (2002), 137-155.

[7] D. C. Whitcomb and M. E. Lowe, Dig. Dis. Sci., 52, (2007), 1-17.

[8] J. Iulek, O. L. Franco, M. Silva, C.T. Slivinski, C. Bloch Jr., D. J. Rigden and M. F. Grossi de Sa, Int. J. Biochem. Cell. Biol., 32, (2000), 1195- 1204.

[9] S. Sindhu. Nair, K. Vaibhavi and M. Anshu, Eur. J. Exp. Biol., 3, (2013), 128-132.

[10] R. Gupta, P. Gigras, H. Mohapatra, V. K. Goswami and B. Chauhan, Process Biochem., 38, (2003), 1599-1616.

[11] A. Upgade, A. Nandeshwar and L. Samant, J. Microbiol. Biotechnol. Res., 1, (2011), 45-51.

[12] M. S. Paula and O. M. Pérola, Braz. J. Microbiol., 41, (2010), 850-861.

[13] K. B. Pandeya, I. P. Tripathi, M. K. Mishra, N. Dwivedi, Y. Pardhi, A. Kamal, P. Gupta, N. Dwivedi and C. Mishra, Int. J. Org. Chem., 3, (2013), 1-22.

[14] S. K. Bharti and S. K Singh, Der. Pharmacia. Lettre., 1, (2009), 39-51.

[15] S. Rafique, M. Idrees, A. Nasim, H. Akbar and A. Athar, Biotech. Mol. Biol. Rev., 5, (2010), 38-45.

[16] J. Vanco, J. Marek, Z. Trávní ck, E. Racanská, J. Muselíkand and O. Švajlenová, J. Inorg. Biochem., 102, (2008), 595-602.

[17] B. Kannan, R. Periyasamy, P. V. Govindan, A. Sirichai and P. Thayumanavan, Arabian J. Chem., doi.org/10.1016/j. arabjc. 2014.07.002 (2015).

[18] E. Yousef, M. Maryam, C. Jesús, M. Nasrin, R. A. Hadi and S. Alessandro, J. Coord. Chem., 68, (2015), 632-649.

[19] G. L. Miller, Anal. Chem., 31, (1959), 426-428.

[20] P. Sudha, S. S. Zinjarde, S.Y. Bhargava and A. R. Kumar, BMC Complem. Altern. Med. 11, (2011), 11-15.

[21] A. V. Gusakov, E. G. Kondratyeva and A. P.Sinitsyn, Int. J. Anal. Chem., doi.org/10.1155/2011/283658 (2011).

[22] D. L. Nelson and M. M. Cox, Lehninger Principles of Biochemistry, ed. 5th, W. H. Freeman, NewYork, USA, (2008).

[23] R. A. Thesingu and R. Natarajan, Spectrochim. Acta Mol. Biomol. Spectrosc., 127, (2014), 292-302.

[24] Y. A. Lee, E. J. Cho, T. Tanaka and T. Yokozawa, J. Nutr. Sci. Vitaminol. 53, (2007), 287-292.

[25] N. Ramasubbu, C. Ragunath, P. J. Mishra, L. M. Thomas, G. Gyemant and L. Kandra, Eur. J. Med. Chem., 271, (2004), 2517-2529.

[26] I. A. Ogunwande, T. Matsui, T. Fujise, and K. Matsumoto, Food Sci. Technol. Res., 13, (2007), 169-172.

Chapter 9

CYTOTOXICITY STUDIES OF SCHIFF BASES AND THEIR Ni(II), Cu(II) AND Zn(II) COMPLEXES

Contents

9.1 Introduction

Schiff-base ligands are potential anti-cancer, anti-viral and anti-bacterial agents and their activities tend to increase in Schiff-base metal complexes. New strategies have been developed in synthesis of new therapeutic agents since most drugs used currently show many important side effects [1]. Approval of cisplatin as a chemotherapeutic drug triggered an enormous response in the chemical and medical research communities for the design of new complexes by metal-ligand bonding derivatives [2].

The cytotoxicity test is one of the important biological evaluation and screening tests, uses tissue cells in vitro to observe the cell growth, reproduction and morphological effects by medical devices [3]. According to the International Organization for Standardization (ISO) and national standards, medical devices must undergo rigorous testing to determine their

biocompatibility when they have contact with the body, regardless of their mechanical, physical and chemical properties [4-5].

Cell viability and cytotoxicity assays were used for drug screening and cytotoxicity tests of chemicals. These are widely used for measuring receptor binding and a variety of signal transduction events that may involve the expression of genetic reporters, trafficking of cellular components, or monitoring organelle function [6]. They are based on various cell functions such as enzyme activity, cell membrane permeability, cell adherence, ATP production, co-enzyme production, and nucleotide uptake activity. To measure cell viability, researchers typically use an MTT assay, Cell Titer Blue, Trypan blue exclusion, ATP, Colony Formation method or Crystal Violet method [7-8]. The MTT assay is currently the most commonly used method to test cell growth rate and toxicity of the culture.

9.1.1 Importance of MTT assay

The MTT (3-(4,5-dimethylthiazol-2-yl)-2,5-diphenyltetrazolium bromide) tetrazolium reduction assay was the first homogeneous cell viability assay developed for a 96-well format that was suitable for high throughput screening [9]. It is a sensitive, quantitative and reliable colorimetric assay. MTT assay, which uses tetrazolium salt known as [3-(4,5-dimethyl-2-thiazolyl)-2,5-diphenyl-2H-tetrazolium bromide)], has been a powerful biological tool to measure cell proliferation and cytotoxicity [10]. The assay is based on the capacity of mitochondrial dehydrogenase enzymes in living cells to convert the yellow water-soluble substrate 3-(4,5- dimethylthiazol-2-y1)-2,5-diphenyl tetrazolium bromide (MTT) into a dark blue formazan product that is insoluble in water [11]. Viable cells are able to reduce the yellow MTT under tetrazolium ring cleavage to a water-insoluble purple-blue

formation which precipitates in the cellular cytosol and can be dissolved after cell lysis, whereas cells being dead following a toxic damage, cannot transform MTT. This formation is proportionate to the viable cell number and inversely proportional to the degree of cytotoxicity. The reaction is mediated by dehydrogenases enzymes (Scheme 1) associated with the endoplasmatic reticulum and the mitochondria [12].

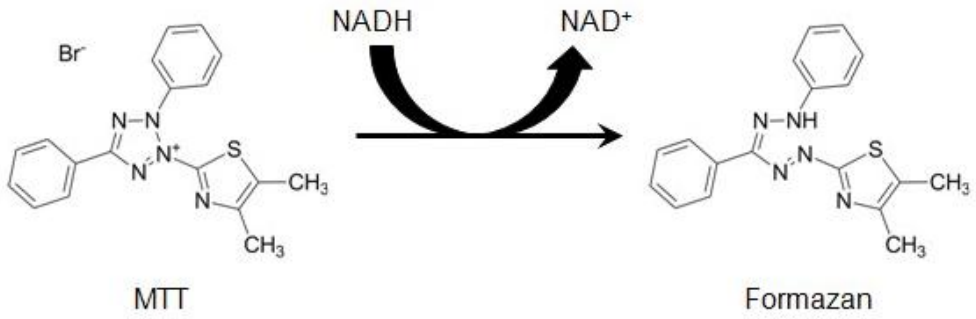

Scheme 1 Formation formazan

Schiff bases and their transition metal complexes derived from various heterocycles, were reported to possess anticancer, cytotoxic [13] and antifungal activities [14]. El-Sonbati *et al.* reported cytotoxic and antitumor activity with 3-[(2-hydroxy-3-methoxy-benzylidene)-hydrazono]-1,3-dihydro-indol-2-one and its metal [Cu(II), Co(II), Ni(II) and Cd(II)] complexes [15]. The cytotoxic study of Cu(II) Schiff base complex shows that it has best in-vitro anticancer activity against both MCF-7 (human breast adenocarcinoma) and HT-29 (colon carcinoma) [16]. Schiff base prepared from pyridine-2-carboxaldehyde were evolved as a cytotoxic agent against human cell T-lymphoblastic leukemia and human colon adrenocarcinoma cell [17]. Schiff base derived from 2-thiophenecarboxaldehyde and 2-aminobenzoic acid and their metal complexes have been recommended and/ or established as a new pathway for the development of newer antitumor agents [18]. Vijay Kumar *et al.* reported DNA

cleavage, cytotoxic activities, and antimicrobial studies of ternary Cu(II) complexes of Isoxazole Schiff base and heterocyclic Compounds [19].

9.2 Experimental

9.2.1 Materials

Mouse 3T3L1 preadipocytes from American Type Culture Collection, USA, were grown in Dulbecco's modified eagle's medium (DMEM) supplemented with 10% FCS and antibiotics (100 U/ml of penicillin and 100 µg/mL of streptomycin) under a humidified atmosphere with 5% CO_2 at 37 °C [3-(4,5-dimethyl-2-thia-zolyl)-2,5-diphenyl-2H-tetrazolium bromide)](MTT), and dimethyl sulfoxide (DMSO) were purchased from Sigma, St. Louis, MO, USA.

9.2.2 Methods

MTT Assay [20] 3T3L1 cells were grown in Dulbecco's Modified Eagle's Medium (DME) and spread in 96 well plates at a density of $5x10^3$ cells / well and incubated at 37 °C in presence of 5% CO_2 for 24 h prior to addition of complexes. The cells were then treated with different concentrations (10, 50, 100 and 150 µM) of compounds dissolved in DMSO and incubated at 37 °C in presence of 5% CO_2 for 24 h. Triplicate was maintained. After 24 h, MTT was added (after removal of media from the wells) at a concentration of 50 µg/well and incubated in a CO_2 incubator. The working solution of MTT was prepared in Hank's balanced salt solution (HBSS) without phenol red. After 2.5-3 h, the formazan crystals formed were viewed under the phase contrast microscope (Figure 9.1) The crystals were then solubilized by adding DMSO (after removal of MTT) and further incubated for 20 min at 37 ºC in the dark. After solubilization, the plate was read at an absorbance of 570 nm. Control samples

were cells without any treatment. The percentage cell viability of control cells were kept as 100%. The relative cell toxicity in percent was calculated as:

(100-Absorbance of treated / Absorbance of control) x 100

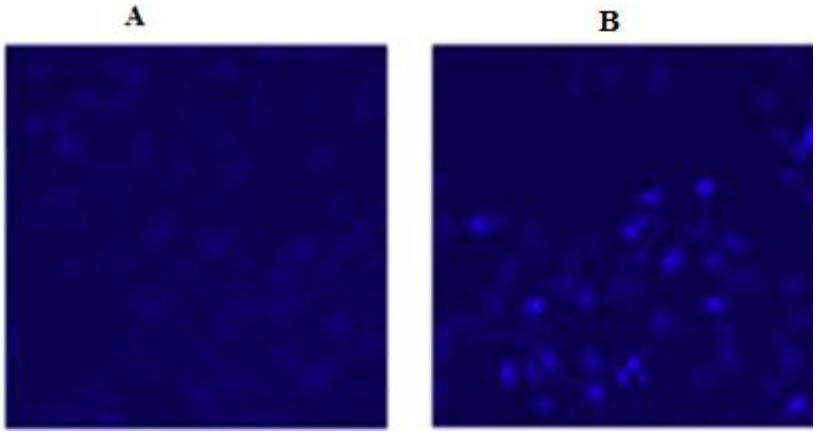

Figure 9.1. A. shows a field of 3T3L1 cells photographed immediately after addition of the MTT solution. B. shows a change in cell morphology and the appearance of formazan crystals after 4 hours of exposure to MTT.

9.3 Results and discussion

Cytotoxicity is a common limitation in terms of the introduction of new compounds into the pharmaceutical industry. The in vitro cytotoxicity of heterocyclic Schiff bases and their Ni(II), Cu(II) and Zn(II) was evaluated by MTT assay against normal 3T3L1 cells. The inhibitory effects of the compounds on the growth of cells were determined after 3T3L1 cells being incubated with different concentrations (10, 50, 100 and 150 µM) of compounds. The results were analyzed by means of cell viability. Viable cells with active metabolism convert MTT into a purple colored formazan product with an absorbance maximum near 570 nm. When cells die, they lose the ability to convert MTT into formazan, thus color formation serves as a useful and convenient marker for only the viable cells.

All the synthesized ligands, TA, TNA, TMA, PA, PNA and PMA exhibited 100% cell viability in 10, 50,100 and 150 µM (Table 9.1).

Table 9.1 The percentage cell viability of Schiff bases against 3T3L1 cells by MTT assay

Compounds	Cells	10 µM	50 µM	100 µM	150 µM
TA	3T3L1	100	100	100	100
TNA	3T3L1	100	100	100	100
TMA	3T3L1	100	100	100	100
PA	3T3L1	100	100	100	100
PNA	3T3L1	100	100	100	100
PMA	3T3L1	100	100	100	100

Cell viability results of nickel complexes (Table 9.2) indicates that $[Ni(PA)_2]\cdot H_2O$, $[Ni(PNA)_2]\cdot 2H_2O$ and $[Ni(PMA)_2]$ are nontoxic in 10, 50, 100 and 150 µM. $[Ni(TA)_2(H_2O)_2]$ shows toxicity at higher concentration (150 µM), whereas $[Ni(TNA)_2(H_2O)_2]\cdot 2H_2O$ and $[Ni(TMA)_2]\cdot 3H_2O$ shows very low toxicity at higher concentrations.

Table 9.2 The percentage cell viability of Ni(II) complexes against 3T3L1 cells by MTT assay.

Compounds	Cells	10 µM	50 µM	100 µM	150 µM
$[Ni(TA)_2 (H_2O)_2]$	3T3L1	99	97	59	26
$[Ni(TNA)_2(H_2O)_2]\cdot 2H_2O$	3T3L1	84	77	70	55
$[Ni(TMA)_2]\cdot 3H_2O$	3T3L1	98	90	82	74
$[Ni(PA)_2]\cdot H_2O$	3T3L1	100	100	100	100
$[Ni(PNA)_2]\cdot 2H_2O$	3T3L1	100	100	100	100
$[Ni(PMA)_2]$	3T3L1	100	100	100	100

Cytotoxicity results of Cu(II) complexes (Table 9.3) indicates that $[Cu(TNA)_2]\cdot 2H_2O$, $[Cu(PNA)_2]\cdot 3H_2O$ and $[Cu(PMA)_2]\cdot H_2O$ are nontoxic in

10, 50, 100 and 150 µM. $[Cu(TA)_2H_2O]\cdot H_2O$ shows high toxicity in all concentration against 3T3L1. $[Cu(TMA)_2]\cdot H_2O$ and $[Cu(PA)_2H_2O]\cdot 2H_2O$ also shows mild toxicity in 50, 100 and150 µM.

Table 9.3 The percentage cell viability of Cu(II) complexes against 3T3L1 cells by MTT assay

Compounds	Cells	10 µM	50 µM	100 µM	150 µM
$[Cu(TA)_2H_2O]\cdot H_2O$	3T3L1	10	0	0	0
$[Cu(TNA)_2]\cdot 2H_2O$	3T3L1	100	100	100	100
$[Cu(TMA)_2]\cdot H_2O$	3T3L1	56	21	15	10
$[Cu(PA)_2H_2O]\cdot 2H_2O$	3T3L1	38	32	25	20
$[Cu(PNA)_2]\cdot 3H_2O$	3T3L1	100	100	100	100
$[Cu(PMA)_2]\cdot H_2O$	3T3L1	100	100	100	100

Cell viability results of zinc complexes (Table 9.4) indicates that $[Zn(TA)_2]$, $[Zn(TNA)_2]$, $[Zn(PA)_2]$ and $[Zn(PNA)_2]$ exhibited 100% cell viability against normal 3T3L1cells. $[Zn(TMA)_2]$ and $[Zn(PMA)_2]$ showed mild toxicity at higher concentration.

Table 9.4 The percentage cell viability of Zn(II) complexes against 3T3L1 cells by MTT assay

Compounds	Cells	10 µM	50 µM	100 µM	150 µM
$[Zn(TA)_2]$	3T3L1	100	100	98	93
$[Zn(TNA)_2]$	3T3L1	100	100	100	100
$[Zn(TMA)_2]$	3T3L1	58	50	42	37
$[Zn(PA)_2]$	3T3L1	100	100	100	100
$[Zn(PNA)_2]$	3T3L1	100	100	100	100
$[Zn(PMA)_2]$	3T3L1	82	58	40	30

9.4 Conclusion

The cytotoxicity of Schiff bases and their metal complexes have been evaluated by MTT assay against normal 3T3L1 cells. All ligands exhibited 100% cell viability against normal 3T3L1cells. $[Ni(PA)_2]\cdot H_2O$, $[Ni(PNA)_2]\cdot 2H_2O$, $[Ni(PMA)_2]$, $[Cu(TNA)_2]\cdot 2H_2O$, $[Cu(PNA)_2]\cdot 3H_2O$, $[Cu(PMA)_2]\cdot H_2O$, $[Zn(TA)_2]$, $[Zn(TNA)_2]$, $[Zn(PA)_2]$ and $[Zn(PNA)_2]$ also showed 100% cell viability. $[Cu(TA)_2H_2O]\cdot H_2O$ showed high toxicity in all concentrations against 3T3L1 cells. Mild toxicity was observed for other complexes in concentration dependent manner.

References

[1] D. Pectasides, K. Kamposioras and G. Papaxoinis and E. Pectasides, Cancer Treat. Rev., 34, (2008), 603-613.

[2] M. T. Tarafder, A. Kasbollah, N. Saravan, K. A. Crouse, A. M. Ali and O. K. Tin, J. Biochem. Mol. Biol. Biophys., 6, (2002), 85-91.

[3] S. J. Soenen, B. Manshian, J. M. Montenegro, F. Amin, B. Meermann, T. Thiron, M. Cornelissen, F. Vanhaecke and S. Doak, W. J. Parak, ACS Nano, 6, (2012), 5767-5783.

[4] L. Weijia, Z. Jing and X. Yuyin , Biomed. Rep., 3, (2015), 617-620.

[5] V. P. Gundarov and G. I. Kavalerov, Med. Tekh., 35, (2001), 4-8.

[6] T. Mossman, J. Immunol. Methods**,** 65, (1983), 55-63.

[7] G. Repetto, A. del Peso and J. L. Zurita, Nat. Protoc., 3, (2008), 1125-1131.

[8] P. Nymark, J. Catalán, S. Suhonen, H. Jarventaus, R. Birkedal, P. A. Clausen, K. A. Jensen, M. Vippola, K. Savolainen, H. Norppa, Toxicology, 313, (2013), 38- 48.

[9] http://pubchem.ncbi.nlm.nih.gov/assay.

[10] G. Fotakis and J. A. Timbrell, Toxicol. Lett., 160, (2006) 171-177.

[11] D. T. Vistica, P. Skehan, D. Scudiero, A. Monks, A. Pittman and M. R. Boyd, Cancer. Res., 51, (1991), 2515-2520.

[12] P. Senthilraja and K. Kathiresan, J. Appl. Pharm. Sci., 5, (2015), 80-84.

[13] S. Bernadette, Creaven, D. Brian, A. E. Denise, K. Kevin, R. Georgina, R. T. Venkat and W. Maureen, Inorganica. Chim. Acta., 363, (2010), 4048-4058.

[14] R. Pignatello, A. Panico, P. Mazzane, M. R. Pinizzotto, A. Garozzo and P. M. Fumeri, Eur. J. Med. Chem., 29, (1974), 781-785.

[15] A. Z. El-Sonbati, M. A. Diaba, A. A. El-Bindarya, M. I. Abou-Dobara and H. A. Seyama J. Mol. Liquids., 218, (2016), 434 - 456.

[16] A. A. Osowole, Appl. Chem., 39, (2011), 4827-4831.

[17] A. Noureen, S. Saleem, T. Fatima, S. H. Masood and B. Mirza, Pak. J. Pharm. Sci., 1, (2013), 113-124.

[18] K. A. Crouse, Chew Kar-Beng, M. T. H. Tarafder, A. Kasbollah, M. B. Ali, B. M. Yamin and H. K. Fun, Polyhedron, 23, (2004), 161-168.

[19] K. C. Vijay, K. Sathish, M. Ramesh, T. Parthasarathy and Shivaraj, Bioinorg. Chem. Appl., 1, (2014), 11-18.

[20] F. A. Beckford, M. Shaloski Jr., G. Leblanc, J. Thessing, L. C. Lewis-Alleyne, A. A. Holder, L. Li and N. P. Seeram, Dalton Trans., 48, (2009), 10757-10764.

Chapter - 10

SUMMARY AND CONCLUSION

Coordination chemistry is dominated by the utilization of Schiff bases as ligands due to its chelating ability and complexing ability towards transition metal ions. Heterocyclic Schiff base complexes incorporating phenolic group as chelating moieties in the ligand are considered as models for executing important biological reactions and mimic the catalytic activities of metallo enzymes. Schiff-bases are every important material for inorganic chemists as these are widely used in medicinal inorganic chemistry due to their diverse biological, pharmacological, antitumor activities. Recently, there has been tremendous interest in studies related to the interaction of transition metal ions with nucleic acid because of their relevance in the development of new reagents for biotechnology and medicine.

The thesis is divided into ten chapters. Contents of various chapters are briefly described as follows:

Chapter 1

This chapter involves a general introduction to Schiff bases and their transition metal complexes. Brief discussion about the applications of Schiff bases and their metal complexes in various field, importance of heterocyclic Schiff base transition metal complexes, antioxidants and its relevance, enzyme and its kinetics are included in this chapter. A brief discussion about the structure of DNA and its interactions with small molecule are also discussed in this chapter. The scope of the present work is highlighted at the end of this chapter.

Chapter 2

Chapter 2 is broadly divided into two sections. Part A provides details of the reagents used and various analytical and physico-chemical techniques employed in the characterization and biological studies of ligands and its complexes. Part B gives the details of the preparation and spectral characterization of six new heterocyclic Schiff bases. Schiff bases have been synthesized by the condensation of 2-aminophenol, 2-amino-4-nitrophenol and 2-amino-4-methylphenol with thiophene-2-carboxaldehyde and pyrrole-2-carboxaldehyde. Single crystal X-ray studies of the Schiff bases also included in this part.

Chapter 3

Chapter 3 describes the synthesis and characterization of Ni(II), Cu(II) and Zn(II) complexes of synthesized Schiff bases. All metal complexes were synthesized by refluxing methanolic solution of metal salt with corresponding Schiff bases. Synthesized metal complexes were characterized by elemental analysis, FT-IR, UV-Visible, TG-DTG, EPR, AAS, conductance and magnetic susceptibility measurements. The analytical data suggest that all Ni(II), Cu(II) and Zn(II) complexes are mononuclear. Low molar conductance values indicates that all Ni(II), Cu(II) and Zn(II) complexes are non electrolytic in nature. All the complexes are found to be thermally stable. Ni(II) complexes with magnetic moment values ranging from 2.91-2.96 B.M. shows octahedral structure and that from 3.5-3.7 B.M. shows tetrahedral structure. Copper complexes exhibited square pyramidal and square planar geometry. All Zn(II) complexes are tetrahedral in nature.

Chapter 4

Chapter 4 deals with antioxidant activity of phenolic Schiff bases - solvent effect, structure activity relationship and mechanism of action. Radical scavenging activity of Schiff bases (TA, TNA, TMA, PA, PNA and PMA) have been investigated using DPPH and ABTS methods. The fixed reaction time and steady state measurement methods were used to find out antioxidant activity of these compounds in five different solvents (methanol, acetonitrile, acetone, ethyl acetate and chloroform) of varying polarity. BHA was used as standard. All Schiff bases exhibited higher antioxidant activity. Schiff bases with electron donating substituent at para position of the phenol ring showed higher activity than Schiff base without any substituent. On the other hand Schiff bases, which having electron withdrawing substituent at para position of the phenol ring showed lower activity. Influence of solvent in the activity are in the order methanol > chloroform > acetonitrile > acetone > ethyl acetate. The potent activity of the synthesized compounds was due to the presence OH groups in its structure. Polarity and protic nature of solvent play vital roles in the radical scavenging ability.

Chapter 5

This chapter describes DNA binding studies of Schiff bases and their metal complexes. The binding behavior of the ligands and metal complexes toward HS-DNA were investigated by electronic absorption spectroscopy, CD spectral studies and voltammetric techniques. Intrinsic binding constants were calculated. DNA binding studies with HS-DNA indicate that ligands and metal complexes bind to DNA by intercalation modes. Results also showed that metal complexes have stronger binding affinity than ligands.

Chapter 6

This chapter deals with the HIV-1 RT inhibitory activity of heterocyclic Schiff bases and their transition metal complexes. HIV-1 RT kit assay was used for testing the reverse transcriptase inhibition activity of the ligands and their metal complexes. Reference drug used was Nevirapine. Results showed that the new copper complexes effectively inhibited HIV-1 replication. Among them heterocyclic Schiff base complex with thiophene moiety showed higher anti-HIV activity than pyrrole moiety. Synthesized ligands and their complexes with nickel or zinc have not shown any reverse transcriptase inhibition activity.

Chapter 7

Chapter 7 deals with antibacterial studies of heterocyclic Schiff bases and their Ni(II), Cu(II), Zn(II) complexes. The antibacterial activity of synthesized Schiff bases as well as their metal complexes was tested against gram positive and gram negative bacteria using disc diffusion method. The bacteria used in the present investigations included -*Bacillus coagulans*, *Bacillus pumills, Bacillus circulans, Clostridium, Staphylococcus aureus*, *Entrococcus faecalis, Salmonella typhi, Escherichia coli, Pseudomonas, proteus vulgaris* and *Klebsilla pneumonia*. Minimum inhibitory concentration (MIC) was evaluated for compounds which showed higher antibacterial activity. *Ampicillin* was used as standard antibiotics. Compared to Schiff bases, metal complexes exhibited higher degrees of inhibitory effects on the growth of the tested bacterial species.

Chapter 8

This chapter describes α-amylase activity studies of heterocyclic Schiff bases and their Ni(II), Cu(II) and Zn(II) Complexes. α-amylase activity of the synthesized compounds were measured by DNS method.

Kinetic studies were carried out to identify the mode of inhibition using Michaelis- Menten and Lineweaver-Burk plot. Ligands TA, TNA, PA, PNA and their Ni(II), Cu(II) and Zn(II) complexes has enhanced α-amylase activity. Ligands TMA, PMA and their Ni(II), Cu(II) complexes exhibited α-amylase inhibition . IC_{50} values of these compounds were also calculated. Results indicates that ligands TMA, PMA and their Ni(II), Cu(II) complexes inhibit α-amylase non competitively.

Chapter 9

Chapter 9 describes cytotoxicity studies of heterocyclic Schiff bases and their Ni(II), Cu(II) and Zn(II) Complexes. The cytotoxicity of Schiff bases and their metal complexes have been evaluated by MTT assay against normal 3T3L1 cells. All ligands exhibited 100% cell viability against normal 3T3L1 cells. $[Ni(PA)_2]\cdot H_2O$, $[Ni(PNA)_2]\cdot 2H_2O$, $[Ni(PMA)_2]$, $[Cu(TNA)_2]\cdot 2H_2O$, $[Cu(PNA)_2]\cdot 3H_2O$, $[Cu(PMA)_2]\cdot H_2O$, $[Zn(TA)_2]$, $[Zn(TNA)_2]$, $[Zn(PA)_2]$ and $[Zn(PNA)_2]$ also showed 100% cell viability. $[Cu(TA)_2H_2O]\cdot H_2O$ showed high toxicity in all concentration against 3T3L1 cells. Mild toxicity was observed for other complexes in concentration dependent manner.

Future outlook

- Docking studies- Docking Studies have become nearly indispensable for study of macromolecular structures and interactions. Docking studies are computational techniques for the exploration of the possible binding modes of a substrate to a given receptor, enzyme or other binding site. Which allow us to characterize the behavior of small molecules in the binding site of target proteins as well as to elucidate fundamental biochemical processes. Docking studies provides most detailed possible view of small molecules drug-receptor interaction and has created a new rational approach to drug design where the structure of drug is designed based on its fit to three dimensional structures of receptor site, rather than by analogy to other active structures or random leads. This may help to increase ligand specificity and if the drug produces undesirable side effect by binding to another macromolecule, it may be possible diminish affinity for that competing site and thus may achieve a better therapeutic index.
- *In vivo* studies – Testing effects of synthesized biological entities on whole, living organisms or cells.
- Synthesis of new heterocyclic ligands and metal complexes with different substituent groups for enhancing the biological activity.
- Development of the pharmacophore in to commercially viable cells.

PUBLICATIONS

1. **A. A. Shanty**, E. P. Jessica, E. J. Sneha, M. R. P Kurup, S. Balachandran, P. V. Mohanan, Synthesis, characterization and biological studies of Schiff bases derived from heterocyclic moiety, Bioorganic Chemistry 70, (2017), 67-73.
2. **A. A. Shanty**, S. Balachandran and P.V. Mohanan, Synthesis, characterizations and biological evaluation of phenolic Schiff bases derived from pyrrole-2-carboxaldehyde, National Seminar 2015, S.H. College, Thevara, Kerala, India, (2015), ISBN: 978-81-930558-1-6.
3. **A. A. Shanty** and P.V. Mohanan, Synthesis, structural characterization and antioxidant properties of phenolic Schiff bases, International Conference MatCon-2016, Cochin University of Science and Technology, Kerala, India, (2016), ISBN: 978-93-80095-738.
4. **A. A. Shanty**, G. Raghu, R. Tripathi and P. V. Mohanan, Biological evaluation of Cu(II) heterocyclic Schiff base complexes as non-nucleoside HIV-1 RT inhibitors and antibacterial agent, (communicated).

PAPERS PRESENTED –Oral / poster (International/ National)

1. **A. A. Shanty** and P.V. Mohanan, HIV-RT inhibitory activity of heterocyclic Schiff base complex, Presented at international symposium on new trends in applied chemistry (NTAC-2017), S.H. College, Thevara, Kerala, India, (2017).

2. **A. A. Shanty** and P.V. Mohanan, Antioxidant activity of phenolic schiff bases- Solvent effect, structure activity relationship and mechanism of action, Presented at World Congress on Drug Discovery & Development, IISc Bengaluru, (2016).
3. **A. A. Shanty** and P.V. Mohanan, DNA binding and cytotoxicity studies of Zn(II) complex derived from heterocyclic Schiff base, Presented at National conference CTriC 2017, Cochin University of Science and Technology, Kerala, India, (2017).
4. **A. A. Shanty** and P.V. Mohanan, Synthesis and evaluation of Cu(II) Heterocyclic Schiff base Complexes as non-nucleoside HIV-1 RT inhibitors, Presented at Kerala science congress, Thiruvalla, (2017).
5. **A. A. Shanty** and P.V. Mohanan, Phenolic Schiff bases as antioxidant and antibacterial Agent, Presented at National conference on Organic synthesis 2016, St. Joseph's College, IJK, kerala, India, (2016).
6. **A. A. Shanty**, S. Balachandran and P. V. Mohanan, Antioxidant and antibacterial properties of phenolic Schiff bases, National Conference on resent trends in Bio-inorganic and Organometallic Chemistry-NCBOC-2015, Sri Shakthi Institute of Engineering and Technology, Coimbatore, India, (2015).
7. **A. A. Shanty**, S. Balachandran and P.V. Mohanan, Synthesis, characterizations, and biological evaluation of heterocyclic Schiff bases, Chemistry in Cancer Research-CCR 2015, St. Albert's College, Ernakulam, Kerala, India, (2015).

8. **A. A. Shanty**, S. Balachandran and P. V. Mohanan, Cu(II) and Zn(II) complexes derived from heterocyclic Schiff-Bases: Synthesis and structural characterisation, presented at National conference CTriC 2014, Cochin University of Science and Technology, Kerala, India, (2014).

Workshop attended

- Recent trends in inorganic-organic hybrid materials, Mahatma Gandhi University Kottayam, Kerala, (2015).

Other papers

1. **S. Shanty**, J. Theresa , R. Leena, K. Girish Kumar, Manganese Porphyrin Sensor for the Determination of Bromate, J. Food Sci. Technol. 53, (2016), 1561-1566.
2. **A. Shanty** and K. Girish Kumar, Voltammetric Determination of Bromate, Presented at Recent Advances in Surface Science (RASS-2013), Gandhigram Rural Institute, Dindigul, Tamil Nadu, India, (2013).
3. **A. Shanty** and K. Girish Kumar, Voltammetric determination of bromate using [5,10,15,20 tetrakis (4methoxyphenylporphyrinato] manganese(iii)chloride modified gold electrode sensor, Presented at 23rd Swadeshi Science Congress, Mahatma Gandhi University, Kottayam, (2013).

Abbreviations

ε	-	Molar absorptivity
µM	-	micro molar
ABTS	-	2,2'-Azinobis-3-ethylbenzothiazoline-6-sulfonic acid
AIDS	-	Acquired Immune Deficiency Syndrome
ARP	-	Antiradical Power
BDE	-	Bond Dissociation Enthalpy
BHA	-	Butylated Hydroxy Anisole
BHT	-	Butylated Hydroxyl Toluene
CA	-	Capsid Protein
Calc.	-	Calculated
CD	-	Circular Dichroism
Con.	-	Concentration
CT	-	Calf Thymus
Cu	-	Copper
CV	-	Cyclic Voltammetry
DIG-POD	-	Antidigoxigenin- Peroxidase
DM	-	Diabetes Mellitus
DMSO	-	Dimethylsulphoxide
DNA	-	Deoxyribonucleic acid
DNS	-	Dinitrosalicylic acid
dNTP	-	Deoxynucleoside Triphosphate
DPPH	-	2-Diphenyl-1-Pikryl-Hydrazyl
DPV	-	Differential Pulse Voltammogram
DTG	-	Differential Thermogravimetry
ELISA	-	Enzyme Linked Immunosorbent Assay
ET	-	Electron-transfer

ETE	-	Electron Transfer Enthalpy
FT-IR	-	Fourier Transform Infrared Spectroscopy
HAT	-	Hydrogen Atom Transfer
HIV	-	Human Immunodeficiency Virus
HS	-	Herring Sperm
IN	-	Integrase
IP	-	Ionization Potential
M	-	molar
MA	-	Matrix Protein
λ_{max}	-	Maximum Wavelength
mmol	-	millimolar
MTP	-	Microtitre Plate
MTT	-	(3-(4,5-dimethylthiazol-2-yl)-2,5-diphenyltetrazolium bromide)
NC	-	Nucleocapsid
Ni	-	Nickel
NNRTIs	-	Non nucleoside Reverse Transcriptase Inhibitors
NRTIs	-	Nucleoside Reverse Transcriptase Inhibitors
OD	-	Optical Density
PA	-	Proton Affinity
PA	-	Schiff base derived from pyrrole-2-carboxaldehyde and 2-aminophenol
PMA	-	Schiff base derived from pyrrole-2-carboxaldehyde and 2-amino-4-methyl phenol
PNA	-	Schiff base derived from pyrrole-2-carboxaldehyde and 2-amino-4- nitro phenol
PR	-	Protease

RNA	-	Ribonucleic Acid
ROS	-	Reactive Oxygen Species
RT	-	Reverse Transcriptase
SPLET	-	Sequential Proton Loss Electron Transfer
TA	-	Schiff base derived from thiophene-2-carboxaldehyde and 2-aminophenol
TBHQ	-	Tertiary Butylated Hydroxylquinine
TG	-	Thermogravimetry
TMA	-	Schiff base derived from thiophene-2-carboxaldehyde and 2-amino-4- methyl phenol
TNA	-	Schiff base derived from thiophene-2-carboxaldehyde and 2-amino-4- nitro phenol
UV-Vis	-	Ultra Violet –Visible
Zn	-	Zinc

Assurance of God Protection

If you dwell in the shelter of the Most High,
and rest in the shadow of the Almighty
you can say to the LORD, "My stronghold, my refuge, my God, in whom I trust."
Surely he will rescue you from the fowler's snare
and from the deadly pestilence.
He will cover you with his feathers,
and under his wings you will find refuge;
his faithfulness will be your shield and rampart.
You will not fear the terror of night,
nor the arrow that flies by day,
nor the pestilence that stalks in the darkness,
nor the plague that destroys at midday.
A thousand may fall at your side,
ten thousand at your right hand,
but it will not come near you.
You will only observe with your eyes
and see the punishment of the wicked.
If you say, "The LORD is my refuge,"
and you make the Most High your dwelling,
no harm will overtake you,
no disaster will come near your tent.
For he will command his angels concerning you
to guard you in all your ways;
they will lift you up in their hands,
so that you will not strike your foot against a stone.
You will tread on the lion and the cobra;
you will trample the great lion and the serpent.
"Because he clings to me in love, I will rescue him," says the LORD
"I will protect him, for he acknowledges my name.
He will call on me, and I will answer him;
I will be with him in trouble,
I will deliver him and honor him.
With long life I will satisfy him
and show him my salvation."

(The Holy Bible-Psalm 91/1-16)